PHYSICO-CHEMICAL STUDIES OF SOME BIOLOGICALLY IMPORTANT ORGANIC MOLECULES IN DIFFERENT MEDIA

Thesis Submitted for the Degree of Doctor of Philosophy (Science)

of the University of North Bengal

2006

by

Susanta Kumar Das

DEPERTMENT OF CHEMISTRY
University of North Bengal
Darjeeling, West Bengal
India

Acknowledgements

I take this opportunity to express my profound sense of gratitude to my supervisor, Prof. S. K. Saha, Department of Chemistry, University of North Bengal for his wise guidance, continued interest and incessant encouragement throughout the investigation.

I also acknowledge the help extended to me by the Director, Central Drug Research Institute, Lucknow, by providing NMR spectra of some viscoelastic micellar systems.

The co-operation and help from the Head of the Department, teachers, officers, research fellows and other staff members of the Department of Chemistry, University of North Bengal, are thankfully acknowledged. I am also thankful to Ratan Adhikari, Amitava Chakraborty, Bidyut Debnath, Subrata Chakraborty, Goutam Bit, Mrinmay Jha and Moazzam Ali for their kind co-operation. I am also thankful to Purok Das for his generous help.

I express my best regards to my parents and thanks to other family members for their inspiration. Finally, I would like to thank my wife, Madhumita, for her constant encouragement and moral support under all circumstances.

—

Susanta Kumar Das

Date: 08.08.2006 **(Susanta Kumar Das)**

University of North Bengal

Contents

CHAPTER – 1
INTRODUCTION

Introduction

The importance of interfacial region between aqueous and non-polar part of the self-assembled lipid phase is very well recognized in biological membranes. It is also well known that the characteristics of this region are different from those of bulk aqueous phase and interior of the lipid or micellar phase, which can mimic the properties of the lipid. Absorption and fluorescence spectroscopic probes are used to estimate the effective dielectric constants (D_{eff}),[1-9] microviscosities,[10-15] surface potentials[1,17-21] etc. One of the techniques involved in finding the above properties is to observe pK_a values of weak acid-base indicators. Such an indicator equilibrium provides the first example of the micellar induced effects upon chemical reactions in aqueous solution. The examples of micellar effects upon reactivity are the observations that the cationic micelles sometimes increase and anionic micelles decrease the deprotonation of the simple weak acids. Although Fernandez and Fromherz,[1] have shown that (using 4-Heptadecyl-7-hydroxycoumrin and 4-Octacycloxy-1-naphthoic acid as acid-base indicators) D_{eff} of ionic micelles can be equated to the D_{eff} of the interface of the nonionic micelles of surfactants with poly (ethylene oxide) head groups, but, more recent researchers,[11,13-16] have shown that, in many cases pK_a^{obs} of weak acid-base equilibrium in ionic micelles can be explained on the basis of the factors as mentioned above viz., dielectric constants, microviscosities, surface potentials etc.

Recently, it has also been reported that there is an effect of ionic and non-ionic detergents on the acid-base properties of some groups like –NH,[24,25] $-NH_2$[26-28] and –OH. The fluorescence spectra of the mono cations formed by the molecules containing the above groups viz., benzimidazols, have shown the tendency to form premicellar aggregates with sodiumdodecylsulfate (SDS) molecules,[29] indicating some kind of interaction with the sulfate group of SDS detergent molecules and proton of the cation of benzimidazols.[30]

Since a number of biologically important organic molecules exhibit either weak acid or weak base behaviour, there is an added incentive to investigate the acid base equilibria of weak acid and weak base at the lipid-water interface. For example, the apparent pK_a values of fatty acids, bile acids, an uncouplers of oxidative phosphorylation, phosphatidylserine, phosphate-dylethanolamine and some local anaesthetics located in the rudimentary model biological membranes, are all shifted negative to their pK_a values in pure water.

It is also well known that the spectral characteristics,[31] specially fluorescence spectra ,[32] are very sensitive to the environments around the systems. Due to this fact, the fluorescence spectroscopy[33] has become one of the fundamental methods for the study of the structure and dynamics of the microheterogeneous systems, e.g., micelles, reverse micelles, membranes, polymers and biological macromolecules. Large numbers of fluorophore molecules are available, where fluorescence spectra are very sensitive to the environments and can be used as probes. Although, there are certain class of molecules which are biologically important, but their spectral properties are not quite sensitive to the surroundings.[34-37] The other useful properties of the molecules which also depends on the nature of the solvents is the acid-base equilibrium as has already been mentioned. Thus, pK_a values for the different acid-base equilibria of indicators are found to be very useful to explore the characteristics of the microheterogeneous systems.[38,39,52,53]

Fluorescence characteristics of various fluorophores have been utilized to find out the polarity, dielectric constants, viscosities, etc. of the micelles, reverse micelles and other biologically active organic mcromolecules.[40-49] The quenching of the fluorophore present in the micelles has find its use to the determination of aggregation number of the micelles,[50] and confirmation of the Menger's model[51] that water molecules can penetrate to some extent into the core of the micelles.

Investigations of acid-base equilibria of amino acids, their interaction with metal ions in media of varied ionic strength, temperature and dielectric constant throw light on the mechanism of enzymes catalyzed reaction. Although it is known that the polarity of the active site cavities in proteins is lower than that of the bulk, a direct measurement of dielectric constant is not possible. A method wherein comparison of formation constants obtained from acid-base and/or metal complex equilibria with the corresponding values observed at the biological centre offers a way to estimate an effective dielectric constant or equivalent solution dielectric constant for the cavity has been invoked.

Solvent polarity and the local environment have profound effects on the emission spectra of polar fluorophores. These polar effects are the origin of the Stokes' shift. This is one of the earliest observations in fluorescence. Emission spectra are easily measurable, and as a result, there are numerous publications on emission spectra of fluorophores in different solvents and when bound to proteins, membranes, and different nucleic acids. One common use of solvent effects is to determine the polarity of the probe-binding sites on the macromolecule. This is accomplished by comparison of the emission spectra and/or quantum yields of the fluorophore when it is bound to the macromolecule and when it is dissolved in solvents of different polarity. However, there are many additional instances where the solvent effects are used extensively. Suppose a fluorescent ligand binds to a protein. Binding is usually accompanied by a spectral shift due to nature of the different environment for the bound ligand. Alternatively, fluorophores often display spectral shifts when they bind to membranes.

The effects of solvent and environment on fluorescence spectra are complex, and there is no single theory that can account for all these effects. Spectral shifts result from the general effects of solvent polarity whereby the energy of the excited state decreases with increasing solvent polarity. This effect can be accounted for by the Lippert equation. However spectral shifts

also occur due to the specific fluorophore-solvent interactions and also due to the charge separation in the excited state.

While fluorescence spectral shifts can be interpreted in terms of general solvent effects, this theory is often insufficient for explaining the detailed behaviour of fluorophores in a variety of environment. This is because the fluorophores often undergo specific interactions with the local environment which arises due to hydrogen bonding and also due to the formation of an internal charge transfer state or twisted internal charge transfer state.

The phenomenon of micellar growth as the preferred surface curvature decrease is quite general. Any change in the system that reduces the effective head group area will produce the effect, for example, as well as electrolyte addition, addition of a surfactant with a compact head group, changing the counter ion, changing the anion for cationic surfactants, changing the hydrophilicity of non-ionic head groups and changing the degree of protonation for zwitterionic surfactants.

When the average length of the micelles exceeds the mean distance between them, a very large increase in viscosity occurs. The overlapping micelles interact extensively and a transient network of randomly oriented rods is formed. When such a system is sheared, the fluid flow orients the rods and reduces the interaction between them. This orientation results in a reduction of the effective viscosity, that is, a shear thinning behaviour. This simple technology was used in some of the early formulations of shampoos, which contained an anionic surfactant and enough salt to produce the 'thickness' in the product. The addition of small amount of perfume would complete the very simple formula. Without the salt, the surfactant solution, even at 25% concentration, would be too watery to apply conveniently to the hair, to say nothing of its lack of aesthetic appeal.

A mixture of alkyl ethoxy sulfate and alkyl dimethyl amine oxide, that is, $R–(OCH_2CH_2)_nOSO_3Na$ and $R'–(CH_3)_2N\rightarrow O$, is typical of a mixed

surfactant system that has been used to provide shear thinning viscosity via long cylindrical micelles. The anionic surfactant has a bulky head group and the amine oxide a comparatively compact one. The viscosity, which is a function of micellar length, can be controlled by changing the ratio of the two surfactants, by choosing different alkyl chain lengths, R and R', or by changing the number of ethylene oxide groups in the anionic surfactant. This type of viscosity control works well in products at such extremes of pH and the surfactants provide the products with additional desirable properties such as surface wetting and detergency.

The study of bilayer membranes in the form of liposomes and vesicles has taken on a much wider perspective with the development of chemical routes to a greater range of artificial membrane-forming lipids.[54,55] Surfactant aggregates, either in the simplest form of monolayers or in the form of micelles, vesicles, liposomes and microemulsions, all provides unique opportunities to bring other molecules closer together, to orient them in specific ways and to alter their reactivities. This field, which has acquired the name 'membrane mimetic chemistry'[55] has understandably been the subject of considerable research interest.

Some applications of liposome dispersions are already established and others are in the process of being put into practice, such as the drug carriers. When dispersions of liposomes are injected intravenously, they travel around the circulatory system, have a long lifetime and can be shown to be taken up preferentially by certain organ in our body, such as the liver and spleen.[56] Knowledge of this behaviour has prompted many attempts to devise drug-carrier systems based on liposomes.[57] The notion is to dissolve the water-soluble or insoluble drug in the liposomes, inject intravenously and allow the drug to be carried to the target organ.

Liposomes can also be used as medium for enzyme reactions. Enzymes trapped within the liposomes occupy the aqueous region between the surfactant head groups and offer some interesting possibilities for novel catalysis.[55,58]

Certain sugars are used to preserve freeze-dried biological materials. When the water is removed, the sugar molecules hold the fragile structures apart and protect the system from collapse. The same technology can be applied to liposomes to allow dispersions containing suitable carbohydrates to be freeze-dried. Liposomes containing drugs could then be stored in a dry state without the need for refrigeration, and reconstituted prior to injection simply by adding water.

Adsorption of surfactants on solid surfaces plays important roles in two aspects of detergency. In the removal of oily soils from fibers, a mechanism known as 'roll-up' can occur. Adsorption of the surfactant at the solid/water and the oil/water interfaces causes a dramatic change in the contact angle, which the oil/water interface makes with the solid surface. The change is in direction to reduce the area of oil contact and the oil drop is then more easily removed from the solid by gentle agitation.

The second area is in the removal of particulate soil. Surfactants, especially anionics, can adsorb on the particles and stabilize them as a dispersion of discrete particles in the wash solution, thereby assisting in their removal from fibre surfaces. Redeposition onto the fibres during the wash cycle is hindered by the adsorbed anionic surfactants but is prevented more efficiently by the inclusion of small quantities of anionic co-polymers.

References

1. Fernandez, M. S., Fromherz, P., *J. Phys. Chem.*, **81**, 1755 (1977).
2. Kalyanasundram, K., Thomas, J. K., *J. Phys. Chem.*, **81**, 2176 (1977).
3. Mukerjee, P., Cardinal, J. R., Desai, N. R., *In Micellization, Solubilization and Microemulsions*, Mittal, K. L., Ed. Plenum Press: New York, Vol. **1**, p. 241 (1977).
4. Mukerjee, P., Cardinal, J. R., *J. Phys. Chem.*, **82**, 1620 (1978).
5. Zachariasse, K. A., Van Phua, N., Kozankiewcz, B., *J. Phys. Chem.* **85**, 2676 (1981).
6. Law, K. Y., *Photochem. Photobiol.*, **33**, 799 (1981).
7. Ramachandran, C., Pyter, R. A., Mukerjee, P., *J. Phys. Chem.*, **86**, 3198 (1982).
8. Lianos, P., Viriot, M. L., Zana, R., *J. Phys. Chem.*, **88**, 1098 (1984).
9. Handa, T., Matsuzaki, K., Nakagaki, M. J., *Colloid. Interface Sci.*, **116**, 50 (1987).
10. Blatt, E., Ghiggino, K. P., Sawyer, W. H., *J. Phys. Chem.*, **86**, 4461 (1982).
11. Drummond, C. J., Grieser, F., Healy, T. W., *J. Phys. Chem.*, **92**. 2604 (1988).
12. Drummond, C. J., Grieser, F., Healy, T. W., *Faraday Discuss. Chem. Soc.*, **81**, 95 (1986).
13. Drummond, C. J., Grieser, F., Healy, T. W., *J. Chem. Soc., Faraday Trans.*, **85**, 521, 537, 551, 561 (1989).

14. Mukerjee, P., *In Solution Chemistry of Surfactants*; Mittal, K. L., Ed.; Plenum Press: New York, Vol. **1**, p 153 (1979).

15. Turro, N. J., Aikawa, M., Yokta, A., *J. Am. Chem. Soc.*, **101**, 772 (1979).

16. Grieser, F., Drummond, C. J., *J. Phys. Chem.*, **92**, 5580 (1988) and references listed therein.

17. Lucas, S., *J. Phys. Chem.*, **87**, 5045 (1983).

18. Mukerjee, P., Banerjee, K., *J. Phys. Chem.*, **68**, 3567 (1964).

19. Moller, J. V., Kragh-Hansen, U., *Biochemistry*, **14**, 2317 (1975).

20. Castle, J. D., Hubell, W. L., *Biochemistry*, **20**, 2208 (1981).

21. Ehrenberg, B., Berezin, Y., *Biophys. J.*, **45**, 663 (1984).

22. Hartley, G. S., Roe, J. W., *Trans. Faraday Soc.* , **35**, 101 (1940).

23. Davies, J. T., *Ado. Carol.*, **6**, 56 (1954).

24. Nigam, S., Dogra, S. K., *J. Photochem. Photobiol.*, **54A**, 219 (1990).

25. Nigam, S., Dogra, S. K., *J. Phys. Chem.*, in press.

26. Sarpal, R. S., Dogra, S. K., *J. Chem. Soc., Faraday Trans.*1, **88,** 2715 (1992).

27. Sarpal, R. S., Dogra, S. K., *J. Photochem. Photochem. Photobiol.*, **69**, 1993 (1993).

28. Sarpal, R. *S.;* Dogra, S. K. *Indian J. Chem.*, **33A**, 111 (1984)

29. Nigam, S., Sarpal, R. S., Dogra, S. K., *J. Colloid. InterfaceSci.*, **163**, 152 (1994).

30. Saha, S. K., Tiwari, P. K., Dogra, S. K., *J. Phys. Chem.*, **98**, 5953 (1994).

31. Jaffe, H. H., Orchin, M., *Theory and application of ultraviolet spectroscopy*, John Wiley, New York, (1962).

32. Lakowicz, J. R., *Principles of fluorescence spectroscopy*, Plenum Press, New York, 189 (1980).

33. Lakowicz, J. R., *Topics in fluorescence spectroscopy*, **1-3**, Plenum Press, New York, (1992).

34. Lister, H., *Fused Pyridines*, Part-II, Wiley Interscience, New York, (1971).

35. Preston, P. N., *Benzimidazoles and congeneric tricyclic compounds*, Part-II, Wiley, New York, 531 (1981).

36. Preston, P. N., *Benzimidazoles and congeneric tricyclic compounds*, Part-I, Wiley Interscience, New York, (1981).

37. Tway, T. C., ClineLove, L. J., *J. Phys. Chem.*, **86,** 5223 (1982).

38. Bunton, C. A., Mong, Y. S., Romsted, L. S., *Solution behaviour of surfactants*, Edited by, Mittal, K. L., Fendler, E. J., **2**, 1137, Plenum Press, New York, (1982).

39. Bunton, C. A., Savelli, G., *Adv. Phys. Org. Chem.*, **22**, 213 (1986).

40. Kalyanasundaram, K., *Photochemstry in microheterogeneous systems*, Academic Press, New York, (1987).

41. Tomas, J. K., *ACS monograph*, **187**, Washington D. C., (1987).

42. Kalyanasundaram, K., Gratzel, M., *Kinetics and catalysis in micro-heterogeneous systems*, Surfactant Science series, Marcel Dekker, New York, **38**, (1991).

43. Kalyanasundaram, K., *Photochemistry in organized and constrained media*, Edited by Ramamurthy, V., VCS Publishers, New York, **39**, (1991).

44. Turro, N. J., Kuo, P. L., Somasundaram, P., Wong. K., *J. Phys. Chem.*, **90**, 288 (1986).

45. Cardinal, J. R., Mukherjee, P., *J. Phys. Chem.*, **82**, 14 (1978).

46. Keno, K., Veno, Y., Hasimoto, S., *J. Phys. Chem.*, **89**, 3161 (1985).

47. Grieser, F., Drummond, C. J., *J. Phys. Chem.*, **92**, 5580 (1988).

48. Law, K. Y., *Photochem. Photobiol.*, **33**, 799 (1981).

49. Grieser, F., Lay, M., Thistlethwayte, J., *J. Phys. Chem.*, **89**, 2065 (1985).

50. Bhattacharia, S. C., Das, H. T., Moulik, S. P., *Photochem. Photobiol.*, **71**, 257 (1993).

51. Encinas, M. V., Lissi, E. A., *Photochem. Photobiol.*, **42**, 491 (1985).

52. Mukherjee, P., Banerjee, K., *J. Phys. Chem.*, **68**, 3567 (1964).

53. Saha, S. K., Dogra, S. K., *Indian J. Chem.*, **35A**, 734 (1996).

54. Kunitake, T., Okahata, Y., *J. Amer. Chem. Soc.*, **99,** 3860 (1977).

55. Fendler, J. H., Wiley Interscience, New York, 1982.

56. Roerdink, F., Dijkstra, J., Hartman. G., Bolscher, B., Scherphof, G., *Biochim. Bio phys. Acta.*, **667**, 79 (1981).

57. Gregoriadis, G., *Comprehensive Biotechnology*, Moo-Yong, M. (ed.), Pergamon Press, London, **4**, 17 (1985).

58. Freeman, A., Lilly, M. D., *Appl. Microbiol. Biotechnol.*, **25**, 495 (1987).

CHAPTER – 2

SCOPE AND OBJECT

Scope and Object

Perhaps the most important feature of living organisms is the cell membrane. It serves many purposes simultaneously from a simple structural component to a complex element in biochemical process such as ion transport and immunological recognition.

A biological membrane consists of three main layers: glycocalix, protein-lipid bilayer and cytoskeleton. The glycocalix is responsible for, among other things, the surface recognition of cells and consists mainly of the oligosaccharide head groups of the glycoproteins and glycolipids that are incorporated into the membrane. On the inside of the cell, the cytoskeleton is a cross-linked network of protein molecules, which are anchored to bilayer proteins, and this provides some structural rigidity to the membrane. The main central layer is a mixture of lipids and proteins in different ratios depending on the function of the membrane.

The most common membrane lipids are double-chained phospholipids or glycolipids, with 16-18 carbons per chain, one of which is often unsaturated or branched. These properties of lipid molecules are important to the correct functioning of biological membranes because[2] :

1. They can pack readily into bilayer membranes;
2. They have extremely low cmc values so that the membranes remain intact in presence of large amounts of water; and
3. The unsaturation or branching ensures that the membranes are in a fluid state at physiological temperatures.

Much of the interesting physical chemistry of liposomes and vesicles has been established from studies of lipids, either from the natural sources or synthesized as pure lipids. However, the field has been greatly extended by the development of synthetic surfactants capable of mimicking the membrane-forming properties of lipids.

The study of bilayer membranes in the form of liposomes and vesicles has taken a much wider perspective with the development of chemical routes to a greater range of artificial membrane-forming lipids. The incentive of this type of study has been two-fold. Firstly, to build up a better understanding of the functioning of natural membrane lipids but, secondly, to create microenvironments that promote novel chemistry, which might otherwise not be readily achieved. Surfactant aggregates, either in the simplest form of monolayers or in the form of micelles, vesicles, liposomes and microemulsions, all provide unique opportunities to bring other molecules closer together, to orient them in specific way and to alter their reactivities. Thus, much of the impetus for the study of reactions in micelles, vesicles or microemulsions is that they model, to a limited extent, reactions in biological assemblies.

As has already been mentioned, the importance of interfacial region between aqueous and non-polar part of the self-assembled lipid phase is very well recognized in biological membranes. For the measurement of the electrical potential at the surface of a charged membrane or a similar interface one requires a probe of molecular size which does not disturb the system itself. It has been suggested the use of pH indicators adsorbed to charged micelles and attributed the "apparent" shift of pK_a detectable in the micellar solution, as compared to pure aqueous solutions, to a change of the "local interfacial" proton activity at the surface of charged micelles as compared to that in bulk water. The equilibrium of an indicator, bound to a surface, may be affected not only by an electrostatic potential, but in addition by a different local environment, e.g., by a lower dielectric constant as compared to bulk water and also by specific interactions of the indicator at the surface, if any. Although different types of organic indicator molecules have been applied as spectroscopic probes for studying above properties, surprisingly, two important uv active aromatic amino acids e.g., tyrosine and tryptophan have not been used so far. However, there are certain class of molecules which are biologically quite important but their spectral properties are quite insensitive to

the surroundings. It has been found that while the protonation-deprotonation equilibrium of hydroxy group of tyrosine and 5-Hydroxytryptophan influence their electronic spectra to a great extent, the spectral profile of tryptophan is insensitive to acid or base. Thus sometimes, the spectral characteristics, specially fluorescence spectra, are very sensitive to the environments of the systems. Because of this, fluorescence spectroscopy has become one of the fundamental methods for the study of the structure and dynamics of the microheterogeneous systems. The photophysics of probe molecules, therefore, are studied in those systems.

Physical gelation of surfactant micelles and their stimuli responsive behaviour are interesting from biology as well as chemical technology points of view. The most extensively studied system is the cetyltrimethylammonium bromide (CTAB) micelles in presence of a hydrotrope, sodium salicylate. Unlike simple halides, salicylate promotes sphere to worm-like micellar transition at much lower concentration viz., near the cmc of CTAB. The flexible and elongated worm-like micelles under dilute conditions show complex and unusual rheological phenomena, which includes strong viscoelasticity and shear induced structure (SIS) formation. Although it is generally believed that micellar entanglement and transient network formation are responsible for developing shear induced viscoelasticity, precise knowledge regarding the nature of interaction in micellar entanglement and SIS formation is still lacking. It is particularly interesting that while a wide variety of worm-like ionic micellar solution display identical rheological responses, a common element in all of these systems is the presence of salt anions like sodium salicylate. This limitation has perplexed the scenario to some extent and impeded the development of an acceptable theory which may explain micellar shape transition under dilute condition. It has been found in the present work that molecules like 1- and 2-Naphthols with a strong hydrophobic aromatic ring and a polar hydroxy group support shape transitions of surfactant micelles very efficiently.

Keeping the above aspects in view, a number of biologically important organic molecules and their hydroxy derivatives and also 1- and 2-Naphthols are chosen as indicator (probe) molecules for studying the protonation-deprotonation equilibria at the micellar surface of different ionic and non-ionic micelles as well as in aqueous-organic medium. These indicator molecules are, 5-Hydroxyindole, 5-Hydroxy-L-tryptophan, L-Tyrosine, L-Tyrosine-methylester, 1-Naphthol and 2-Naphthol. Fluorescence spectroscopic properties of these molecules have been studied in different solvents to understand the photo-physics of the systems.

Moreover, the role of 1- and 2-Naphthols in developing stimuli sensitive properties of surfactant solutions has been studied. The physicochemical aspects of micellar shape transition, rheological behaviour have been investigated and the microstructure of the system is proposed.

CHAPTER – 3

PROTONATION-DEPROTONATION EQUILIBRIUM OF OH GROUPS OF BIOLOGICALLY IMPORTANT INDICATOR MOLECULES IN MICELLAR MEDIA

3.1. Introduction and review of previous works

Surfactants, some times called surface active agents or detergents, are materials that contain both apolar, hydrophobic (lipophobic) and polar, hydrophilic (lipophobic) groups[1-8]. In solvents which have a strong three dimensional structure, for example water, hydrazine, 1,2-diols[9-12] or sulphuric acid[13] this dual character of the amphiphile leads to self association or micellization. In the small colloidal particles, or micelles, which result, the apolar groups tend to pack together away from the polar solvents, and the polar or ionic head groups tend to be at the surface of the micelle where they interact with the solvent. Water is the preferred solvent for study of this phenomenon and all the results discussed in this chapter relate to experiments in water unless otherwise specified. Micellization is a manifestation of the strong self – association of water and similar solvents and is an example of the hydrophobic or solvophobic effect (the term applies to the interactions in a variety of associated solvents other than water), which forces self-association of apolar materials.[14] Micelles are small, relative to the wavelength of light. Their solutions are therefore transparent, but they scatter light, and this properly provided compelling evidence for the formation or discrete micelles.[15,16]

Most studies of micellar systems have been carried out on synthetic surfactants where the polar or ionic head group may be cationic, e.g., an ammonium or pyridinium ion, anionic, e.g., a carboxylate, sulphate or sulfonate ion, non ionic, e.g., hydroxyl compound, or zwitterionic, e.g., an amine oxide or a carboxylate or sulfonate.[3] Some of surfactants used in the present study are listed in Table 1, together with values of critical micelle concentration, cmc. This is the surfactant concentration at the onset of micellization[17] and can therefore be taken to be the maximum concentration of monomeric surfactant in a solution.[18] Its value is related to the change of free energy on micellization.[3-5]

TABLE: 1

Synthetic surfactants	cmc/M
Cetyltrimethylammonium bromide (CTAB)	9.0×10^{-4}
Sodium dodecylsulfate (SDS)	8.0×10^{-3}
Sodium bis(2-ethylhexylsulfosuccinate), Aerosol-OT (AOT)	2.5×10^{-3}
Polyoxyethylenesorbitan monopalmitate (Tween – 40)	3.6×10^{-5}
Polyoxyethylenelauryl ether (Brij-35)	4.8×10^{-5}

Micellization depends upon a balance of forces and the cmc decreases with the increasing hydrophobicity of the apolar groups, and for ionic amphiphile also depends upon the nature and concentration of counter ions in solution. Added electrolytes decrease the cmc, and the effect increases with decreasing charge density of the counter ion. Divalent counter ions, however, lead lower values of cmc than do univalent ions because ion binding, of itself lead to a decrease in entropy.[19] Non-ionic and zwitterionic amphiphiles typically have lower values of the cmc than otherwise similar amphiphiles, because there is no formal coulombic repulsion between the head groups.

Ionic surfactants form approximately spherical micelle in water with ionic head groups at the surface and counter ions clustered around the micelle partially neutralizing the charges. Counter ions which are closely associated with the micelle can be assumed to be located in shell, the so called stern layer, the thickness of which should be similar to the size of the micellar head groups. The ionic head groups will repel monomeric co-ions. The hydrophobic alkyl groups pack randomly and parts of the chains are exposed to water at the surface.

The cmc is a key property, because it is related to free energy difference between monomer and micelles. The onset of micellization is detected by

marked changes in such properties as surface tension, refractive index and conductivity (for ionic micelles); light scattering also increases sharply on micellization, as does solubilization of hydrophobic solutes. To a first approximation the solution can be assumed to contain monomeric amphiphiles and fully formed micelles with sub-micellar particles playing a minor role. It has long been known that aqueous micelles can influence chemical rates and equilibrium,[1,20-22] and there are a number of related self assembling colloids which share this ability. Microemulsions generally contain water, an oil, a surfactant and a co-surfactant which is generally a medium chain length alcohol, amine or similar polar organic molecule.[23,24] Oil in water (o/w) microemulsions are formed when water is the bulk solvent. The droplets are larger than normal micelles in water[25,23] but the two structures have the common feature that the polar or ionic head groups are in contact with water. Water in oil (w/o) microemulsions are formed when oil is the bulk solvent. They are akin to the reverse microemulsions, which form when surfactants, usually with small amount of water, are dissolved in an apolar organic solvent.[3,26] The interiors of these droplets contain water and the apolar regions of the emulsions are in contact with the apolar solvent.[27] Micelles in water have long been known to influence acid-base indicator equillibria and the effects were rationalized in term of Hartley's Rules which related change in equilibrium constants to micellar charge.[1] These rules were subsequently applied to micellar effects upon the rates of attack of OH^- upon triarylmetheyl dye cations.[20,28] These early studies of micelles effects upon reaction rates and equilibrium are described in an extensive monograph.[3] The original work on ionic reactions was in normal micelles in water, but subsequently there has been extensive work on reactions in reverse micelles.[28-32] There has also been a great deal of work on photochemical and radiation induced reactions in a variety of colloidal systems, and microemulsions have been used as a media for a variety of thermal, electrochemical and photochemical reactions.[4,24,33]

Much of the impetus for the study of reactions in micelles is that they model, to a limited extent, reaction in biological assemblies. Synthetic vesicles and cyclodextrins are other model reaction media and the term "Bio-mimetic Chemistry" has been coined to describe this general area of study. Work in this area is reviewed in recent publications.[4,8]

Hartley showed that micellar effects upon acid-base indicator equilibrium could be related to the ability of anionic micelles to attract, and cationic micelles to repel hydrogen ions. More recently attempts have been made to qualify these ideas in terms of the behaviour of a micelle as a sub-microscopic solvent, together with an effect due to its surface potential.[34]

Unique property of micelles is that it is a microheterogeneous system possessing an interior organic solvent like phase and an exterior aqueous phase. This feature leads to the enhanced micelles solubilization of both nonpolar and polar compounds of wide variety. Even large bio-molecules, viz. DNA, RNA, proteins are soluble in micelles. Solubilization of the substrates in micellar media can modify their equilibrium and kinetic properties.[35-39] Inherited surface charge of ionic micelles under favourable conditions help their association with reacting substances. In the case of non-ionic micelles selective extraction by hydrophobic forces of the reagents may help their compartmentalization[40-44] in micelles. The micellar catalyzed reactions are explained in terms of lowering of activation energy,[45] fractal dimension[46-48] decreased in the degree of freedom of their reactants by way of their immobilization in the diffusion phase space of micelles.[45] The knowledge on the acid-base equilibrium of substrates in micellar media is required in relation to their potential for analytical application, as spectroscopic probes, as catalysts etc. The solubilisates in micelles are often analogically modeled as equivalent to membranes and enzymes.

As has already been mentioned, micelles have the ability to solubilize a wide range of inorganic and organic compounds. The water solubility of non-polar organic compounds can be remarkably increased in micelles media. The

water pools of reverse micelles can solubilize larger molecules like DNA, RNA etc. The different solubilization sites of micelles have been experimentally verified by using spectroscopic and other methods.[34,49-52] The solubilization sites have different micro-polarity. The solubilisates get adsorbed at the sites of micelles depending on their nature. The hydrocarbons having no polar groups, in small concentration get solubilized in micellar hydrocarbon core. In the stern layer, the solubilisates reside associated with the polar/charged head groups of the surfactants. The repulsive interaction between the surfactant head groups is reduced resulting in the increased stability of the organic compounds having polar/ionic group. Highly polar or charged molecules may reside just outside the stern layer. In organic ions as well as counter ions are found in this site. The site that is further away from the stern layer are generally occupied when water-soluble substrates are taken in excess and the capacities of the first three sites are full. The site for solubilization thus depends on the nature of both the solubilisate and the micelles.

The polarity of the micelles microenvironment has been investigated using various probes.[53-60] The hydrocarbon core of micelles has very low polarity, similar to hydrocarbon solvents (dielectric constant 2-4). However, the stern layer is much more polar due to the presence of charged or polar head groups of surfactants. For charged micelles the stern layer contains charged head groups as well as a fraction of counter ions attached to the head group and so is more polar than non-ionic micelles. Fluorescence studies with probe molecules have shown penetration of a significant amount of water molecules into the hydrocarbon. The polarity gradually decreases from stern layer to the interior hydrocarbon region. Outside the stern layer, the polarity rapidly reaches the value of the bulk solvent. For normal micelles this bulk solvent is water with dielectric constant 80; for reverse micelles it is the organic solvent of low dielectric constant.

Organic compounds are soluble in micellar media although they may or may not be soluble in water or organic solvent alone. This solubilization leads

to a change in the acid-base equilibrium. In general, two established models, viz, thermodynamic model and the pseudophase ion exchange model, explain the observed pK_a shifts of the acid-base equilibrium. The thermodynamic model qualitatively explains the pK_a shifts and is thus simple and the most widely used model. The pseudo-phase ion-exchange model although can explain the pK_a shifts both qualitatively and quantitatively, is less popular for its inherent complexity. Both models are discussed below, briefly.

1. Thermodynamic model:

The pK_a values of a substrate are expected to be different in the three different types of micelles (cationic, anionic and non-ionic) because the micellar surface charge influence the acid-base equilibrium. The shift in the acid-base equilibrium is mainly guided by two factors.

(i) Due to the change in the polarity of the slubilization site of the micelle compared to the bulk solvent. This is commonly known as micro-environment or medium effect.

(ii) Due to the influence of the electrostatic potential present at the micellar solubilization site, commonly known as potential effect.

The site of solubilization of the molecule has considerable influence on the shift of the acid-base equilibrium. At low concentration of the substrate, the strongest sites will be occupied, but at higher concentration, both the strong and weak sites will be occupied. Thus the observed shift of the acid-base equilibrium depends also on the substrate concentration.

The successive acid-base equilibria of a solubilisate can be represented by the following general equillibria :

$$A^{+n} = B^{+(n-1)} + H^{+} \qquad (1)$$

where n=0, 1,2 etc. For a titration experiment of a completely micelle bound solubilisate, one measures the proton activity in the bulk phase and the

concentration ratio of acidic and basic forms of the solubilisates and the micelles. Thus the apparent acid-base equilibrium K_a^A is characterized by

$$K_a^A = [B_m]\,[H_w]/[A_m] \qquad (2)$$

In other words, pK_a^A is the bulk pH for which the indicator (probe molecule) in the micelle will release 50% of its H^+ ion in water. Here $[A_m]$ and $[B_m]$ represents the concentrations of the micelle bound acidic and basic form of the indicator and $[H_w]$ are the bulk hydrogen ion concentration. If we consider that A and B forms of the solubilisate are completely micelle bound and then concentrations are so low that the activities can be replaced by concentrations, then we can write[34] :

$$pK_a^i - pK_a^w = \Delta pK_a^i = \{(\mu_B^m - \mu_A^w) - (\mu_A^m - \mu_A^w)\}\ 2.3RT \qquad (3)$$

and

$$pK_a^{mw} - pK_a^w = \Delta pK_a^{mw} = \Delta\, pK_a^i - F\psi/\ 2.3RT \qquad (4)$$

where K_a^w, K_a^i and K_a^{mw} are the dissociation constants of the solubilisate in water, in non-ionic micelle and charged micelle respectively. Here μ is the chemical potential, ψ is the electrical potential and R, T and F have their usual meaning.

Equation (3) can explain qualitatively the origin of shift of pK_a values in non-ionic micelle compared to water. There lie three possibilities about the charge of A and B in most cases:

i) A is charged and B is neutral.

ii) A is neutral and B is charged

iii) Both A and B are charged.

If A or B is charged, then it is more stable in water than in the organic phase like micellar sites and so, $(\mu^m - \mu^w)$ will be positive. However, uncharged organic solubilisate is more stable in micellar phase than in water and so

$(\mu^m - \mu^w)$ is expected to be negative. Thus a resultant positive ΔpK_a^i is expected when B is charged and A is uncharged, and a resultant negative ΔpK_a^i is expected when A is charged but B is uncharged. In other words, the equilibrium is shifted to right for (i) and the equilibrium will be shifted to left for (ii).

Case (iii) occurs generally for the successive dissociation of an acid or a base. In this case, B will have charge higher than A. In this case, $(\mu^m - \mu^w)$ will be positive for A and B but will be higher in magnitude for B, as higher charged solubilisate will be more unstable at the micellar interface. As a result, pK_a will be negative in most cases. However, above explanation can never be generalised.

2. Pseudophase Ion Exchange (PIE) model:

A major shortcoming of the thermodynamic model is that it does not account for the generally observed specific counter ion effect on the micelle induced pK_a shifts. PIE model successfully explain this fact by considering specific ion-exchange constants. This model is used to represent the acid-base equilibrium in ionic micelle. The basic assumptions of the model are as follows:

(i) Micelles act as a separate phase, homogeneously distributed throughout the solution and the medium property of this phase is independent of solution composition.

(ii) Ionization of micelle bound substrate is described by a intrinsic acidity constant that reflects the medium property of micelle.

(iii) Total concentration of counter ions at the micellar interface is constant and independent of the surfactant concentration and the type of counter ion.

(iv) The distribution of counter ions between micelles and water is described by an empirical ion-exchange constant that reflects the different specific interactions of the counter ions.

There are several reviews and papers dealing with the theory of PIE model and its application.[61-64] According to PIE model, the shift of pK_a values in charged micelles compared to pK_w is explained by considering the transfer of conjugate acid-base forms of the solubilisate and H^+/OH^- ion from large volume of water into the much smaller volume of micellar pseudo-phase. Addition of salt in anionic micelle results in the displacement of H^+ ion from micellar surface to water by the cations of the added salts. As a result, the H^+ ion concentration in micelle surface decreases with the addition of salt and so a decrease in pK_a is observed. Similarly, in cationic micelles, OH^- ions are replaced from the micellar interface by the anion of the added salts and thus OH^- concentration in micellar interface decreases compared to that in the bulk water.

For the last four decades a considerable amount of research effort has been directed toward determining the physicochemical properties of self-assembled surfactant aggregates, especially micelles and unilamellar vesicles. Although many reasons can be cited for the widespread interest in elucidating the physicochemical properties of micelles and vesicles, there are primarily three reasons. Firstly, one can consistently and easily prepare aqueous micellar and vesicular solutions which have aggregates of colloidal dimensions with characteristic size, shape and surface properties. Hence, micellar and vesicular systems have been employed as model systems in investigations concerned with understanding colloidal physicochemical phenomena.[35,65] Secondly, the similarities between self-assembled surface aggregates, such as micelles, vesicles and biological lipid membranes have been noted. Thus, in many studies, micelles and vesicles have served as rudimentary model systems for biological lipid membrane systems.[4,35] Thirdly, it has been found that micelles and vesicles can act as unique reaction media. Indeed, solubilization of reactants within self-assembled surfactant aggregates frequently leads to alter reaction rates, reaction routes and stereochemistry[4,35]. Obviously, micelles and

vesicles cannot be fully exploited as reaction media until all their physicochemical properties have been ascertained.

Spectroscopic techniques based on either the optical absorption or the emission of light from a specific aromatic probe molecule has been often used to determine certain physicochemical properties of micelles and vesicles.[66] In some cases, spectroscopic probe techniques provide the only means of ascertaining a particular physicochemical property, while in other cases, the simplicity of application has resulted in a spectroscopic probe technique being employed in preference to a more classical colloidal measurement, such as light scattering, osmometry or conductivity.

The majority of spectroscopic probes used in studying the physicochemical properties of self-assembled surfactant systems are aromatic derivatives. Data on the time averaged sites of solubilization in an amphiphilic aggregate are obtained mainly from fluorescence, uv/vis absorption and nmr spectroscopy[3,67,72]. However, from the literature, it appears that 'free' aromatic probes are solubilized on average at the water/hydrocarbon interface of most micelles, and may be present at either the water/hydrocarbon interface or in the interior of the hydrocarbon bilayer of vesicles. Mukerjee[68,69] has indicated that the main reasons for 'free' aromatic molecules residing on average at the micelle/water interface stems from (i) the pronounced surface activity of aromatic species at the hydrocarbon/water interface, (ii) the high Laplace pressure of the micelle cores, and (iii) the high effective interfacial volume of a micellar structure. Specific interactions between the aromatic molecules and surfactant headgroups may also play an important role. It is generally well established that such interactions exist if the head group is a quaternary ammonium group.[70-72]

Acid-Base Equilibria.

The acid-base equilibrium of an indicator, which has its prototropic moiety residing within the interfacial region of a self-assembled surfactant aggregate, can be represented as

$$HIN_i^z \rightleftharpoons^{K_a^i} H_i^+ + IN_i^{z-1} \quad (5)$$

and the thermodynamic acid-base equilibrium constant for this reaction, K_a^i, is given by

$$K_a^i = (a_{H^+}^i \, a_{IN}^i) / a_{HIN}^i \quad (6)$$

where superscript z is the charge on the protonated form of the indicator, subscript or superscript i denotes the interfacial region, and $a_{H^+}^i$, a_{IN}^i, and a_{HIN}^i are the activities of the various species involved in the equilibrium.

There is no direct experimental method for determining $a_{H^+}^i$, and as a result K_a^i cannot be determined by any direct means. Nevertheless, it is possible by experiment to study an apparent acid-base equilibrium for an interfacially located prototropic moiety of an indicator, i.e.

$$HIN_i^z \rightleftharpoons^{K_a^{obs}} H_w^+ + IN_i^{z-1} \quad (7)$$

and equilibrium constant of this reaction,

$$K_a^{obs} = (a_{H^+}^w \, [IN^{z-1}]_i) / [HIN^z]_i \quad (8)$$

where subscript or superscript w denotes the bulk aqueous solution and $[IN^{z-1}]_i$ and $[HIN^z]_i$ are the interfacial concentrations of the conjugate base and conjugate acid forms of the indicator, respectively. According to Boltzmann's law, the hydrogen ion activity at a point in the vicinity of a charged interface and the hydrogen ion activity in the bulk aqueous solution are related by

$$a_{H^+}^i = a_{H^+}^w \exp\left(\frac{-e\psi}{kT}\right) \quad (9)$$

where e is the unit electronic charge, k is the Boltzmann constant, T is the absolute temperature, and ψ is the electrostatic mean field potential at the point

being considered.[73] Therefore the apparent pK_a, pK_a^{obs}, is related to the thermodynamic intrinsic interfacial pK_a, pK_a^i, through the expression

$$pK_a^{obs} = pK_a^i + \log\frac{\gamma_{IN}^i}{\gamma_{HIN}^i} - \frac{e\psi}{2.303kT} \qquad (10)$$

where γ_{IN}^i and γ_{HIN}^i denote the activity coefficients of the conjugate base and conjugate acid forms of the indicator, respectively, referred to the interfacial phase at infinite dilution. Generally it is assumed that

$$pK_a^0 = pK_a^i + \log\frac{\gamma_{IN}^i}{\gamma_{HIN}^i} \qquad (11)$$

so that

$$pK_a^{obs} = pK_a^0 - \frac{e\psi}{2.303kT} \qquad (12)$$

where ψ is the mean field potential at the time-averaged location of the prototropic moiety of the indicator in the interfacial region. Note that if the prototropic moiety resides on average in the plane of the surface charge then the mean field potential in equation 12 is the surface potential, ψ_0. Fromherz and co-workers[34,74] have shown that there is also a thermodynamic route by which equation 12 can be derived.

Providing (i) there are no specific molecular interactions or "salt effects" which significantly interfere with the intrinsic interfacial acid-base equilibrium of an indicator, and (ii) the mean solvent characteristics of interfacial microenvironments can be mimicked by organic solvent/water mixtures, then there is a connection between the pK_a^0 values of the indicator situated in self-assembled surfactant aggregates and the pK_a values of the indicator in organic solvent/water mixtures.[34,75-78]

The acid-base equilibrium of an indicator in an organic solvent/water mixture (m) can be represented as

$$HIN_m^z \rightleftharpoons^{K_a^m} H_m^+ + IN_m^{z-1} \qquad (13)$$

with equilibrium constant in the mixture,

$$K_a^m = (a_{H^+}^m a_{IN}^m) / a_{HIN}^m \qquad (14)$$

To enable a thermodynamically correct comparison to be made between the results of organic solvent/water pH titrations and the pH titrations performed in self-assembled surfactant solution, it is necessary to convert the one-phase pK_a^m values into two-phase pK_a^0 values. This can be accomplished by making two main assumptions. The first assumption is that the concentration ratio $[IN^{z-1}]_i / [HIN^z]_i$ is equivalent to the activity ratio a_{IN}^m / a_{HIN}^m in an organic solvent/water mixture with the same dielectric constant as the interfacial dielectric constant (D_{eff}) value where the protonatable portion of the indicator resides on average. With this assumption

$$pK_a^0 = pK_a^m - \log {}_m\gamma_{H^+} \qquad (15)$$

where ${}_m\gamma_{H^+}$ is the medium effect on the proton. Since ${}_m\gamma_{H^+}$ is defined in terms of single ion activity coefficients it cannot be determined by thermodynamic means. Hence one makes the second assumption, namely that ${}_m\gamma_{H^+}$ values can be approximated by the values of the medium effect on HCl in organic solvent/water mixtures, ${}_m\gamma_{\pm}$. In this manner a reference pK_a^0 curve as a function of dielectric constant can be acquired from the pK_a^m values for an indicator. The reference pK_a^0 curve as a function of dielectric constant can then be used in conjunction with the pK_a^0 values obtained from the indicator in self-assembled surfactant aggregates to estimate D_{eff} values for the interfacial regions.

The pK_a^0 values of a number of acid-base indicators in some self-assembled surfactant aggregates are known to be influenced by specific

molecular interactions and/or interfacial "salt-effect".[75,83] The pK_a^0 values measured in these indicator/surfactant aggregate systems cannot validly be compared with a reference organic solvent/water pK_a^0 versus dielectric constant curve.[79]

In the present study, a few biologically important organic molecules viz., some aromatic amino acids and derivatives of amino acids and also naphthols are chosen for monitoring the protonation-deprotonation equilibria of the hydroxy groups in 1,4-dioxane-water mixture, as well as in non-ionic and charged micelles. These organic compounds are of biological relevance and the derivatives are, 5-Hydroxyindole, 5-Hydroxy-L-tryptophan, L-Tyrosine, L-Tyrosinemethylester, 1-Naphthol and 2-Naphthol.

Among the indicator molecules in the above list, first two posses similar structures, while the third and fourth are otherwise identical except the fact that the fourth one does not form carboxylate anion at high pH. The structures of these pH indicator molecules are given below:

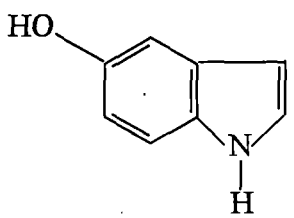

5-Hydroxyindole

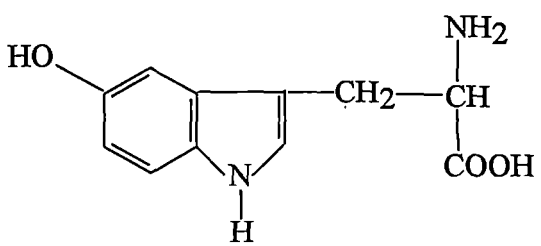

5-Hydroxy-L-tryptophan

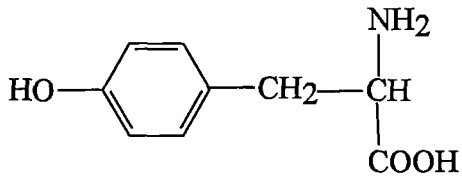

L-Tyrosine

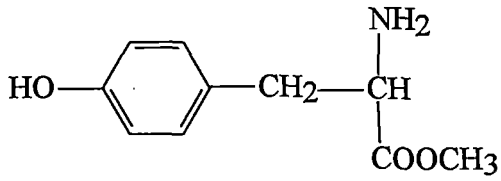

L-Tyrosinemethylester

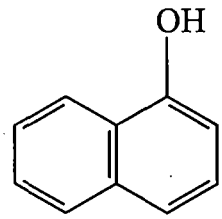

1–Naphthol

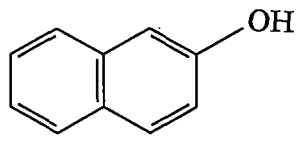

2–Naphthol

Apart from the biomolecules, and their derivatives, 1- and 2-Naphthols are also included in the above list as pH indicators because due to the presence of the hydrophobic aromatic moiety, these two compounds are solubilized more readily in micellar phase and that may cause pronounced effect on the acid-base equilibrium. Moreover, investigations of ground and excited state proton-transfer reactions in organized molecular assemblies (black bilayer membranes, vesicles, micelles monolayer aggregates etc.) are very important and provide unique information about the local structure and dynamics of such systems. These data are necessary to understand mechanism of the natural proton transport, which is of primary importance for bioenergetics and some other biological processes, and to design model and artificial systems for solar energy conversion etc. Perhaps the most widely studied excited state is the ionization of aromatic hydroxy compounds; and among them naphthols are most important molecules, which are appropriate for studies in micellar and vesicular solutions. Therefore, the effect of interfacial polarity on the acid-base equilibrium of naphthols in the ground state is very interesting aspect for investigation.

The primary objective of the present study is, therefore, to obtain a quantitative assessment of the factors, which are responsible for the difference between the apparent acid-base equilibrium constant of an interfacially located pH indicator molecule and its bulk aqueous pK_a value (pK_a^w). More specifically, following four points have been considered during the acid-base equilibrium study of indicator (probe) molecules in the present work.

(i) Variations of pK_a's, which appear in the study of an interfacial acid-base equilibrium, are characterized.

(ii) Titration of all indicators (molecular probe) in charged and uncharged micelles is described.

(iii) The observable shifts of "apparent" pK_a which is partitioned explicitly into a component due to the electrical potential and a

component caused by a change of polarity for a charged micelle is described.

(iv) By comparing the shift of the interfacial intrinsic pK_a^i to the pK_a shift measured in non-polar non-aqueous solvents, an attempt has been made to estimate the effective interfacial dielectric constant wherever possible, exhibiting the indicators as probes of interfacial polarity in same systems.

The pK_a values of OH groups of the present indicator molecules in aqueous medium are listed below:

TABLE: 2

Indicator Molecules	**Abbreviation used**	**pK_a^w**
5(OH) indole	HIn	11.04
5(OH)-L-Tryptophan	HTr	11.15
L-Tyrosine	Ty	10.05
L-Tyrosinemethylester	TyE	11.09
1-Naphthol	1 Nph	9.39
2-Naphthol	2 Nph	9.50

The acid-base equilibrium of the above indicator molecules is far more complex than that of a simple weak acid. As is apparent from the structures of

the molecules, several species could be postulated to be involved in the acid-base equilibrium.

However, one very important point worth mentioning is that ultraviolet spectra of all the above indicator molecules are influenced only on dissociation of hydroxy group attached to the aromatic ring. Therefore, acid-base equilibrium is monitored by the change of the ultraviolet spectra (figs. 3-20) by changing the solution pH. This gives rise to the required thermodynamic parameters.

3.2. Experimental

The indicator compounds applied for the present study, viz., L-Tyrosine was obtained from Himedia, India, L-Tyrosinemethylester, 5-Hydroxyindole, 5-Hydroxy-L-tryptophan were all Fluka products (USA) and were used as received. 1-Naphthol and 2-Naphthol were E. Merck, India products and were purified by vacuum sublimation (twice). The surfactants Cetyltrimethylammonium bromide (CTAB), Sodium dodecyl sulphate (SDS), Tween-40, Aerosol-OT (AOT) and Brij-35 were purchased from either Fluka, USA or Sigma Aldrich Chemical Co. USA and were used as received. 1,4-Dioxane (E. Merck, Germany) was further purified by distillation as mentioned in the literature.[80]

Stock solutions of the order of 10^{-3}M of all the pH indicators were prepared in pure water. The sample solutions of desired compositions of 1,4-dioxane-water mixtures and surfactant solutions were prepared from the stock solution with the help of micropipette. The pH of the solution was adjusted by adding small amount of dilute HCl or NaOH solutions and was measured with pH meter (model-Systronics:361, India). The uv spectra were recorded on a Shimadzu Spectrophotometer (model-UV 240, Japan). All the measurements were carried out at 298$\pm$1 K.

In pure water and aqueous micellar solutions, the negative logarithm of the hydrogen ion activity was taken as equal to the pH meter reading. However, for the organic solvent-water mixtures, the pH meter reading is not a direct measure of the negative logarithm of the hydrogen ion activity.[83] Van Uitert and Haas have shown that an empirical calibration can be made so that the pH meter reading can be converted into the stoichiometric hydrogen ion concentration.[81] The equation they derived for 1,4-dioxane-water mixtures was

$$-\log[H^+] = B + \log U_H^0 + \log \gamma_{\pm}^m \qquad (16)$$

where B is the pH-meter reading and $\log U_H^0$ is a correction factor which is independent of ionic strength and is attributable to two effects[81]: (i) the liquid junction potential being a function of the solvent composition, and (ii) the medium effect on the activity co-efficient of the hydrogen ion varying with solvent composition. $\gamma_{\pm}^m$ in equation (16), the mean ionic activity co-efficient for hydrochloric acid, referred to the particular 1,4-dioxane-water mixture at infinite dilution. The values for $\gamma_{\pm}^m$ can be obtained by interpolation of the values given by Harned and Owen[82] and taken in the present study from Drummond's work (Fig.1).[83]

The method generally applied to obtain the correction factor, $\log U_H^0$, was based on the dilution method, which has been described by Sanchez-Ruiz et al[84] and adopted by Drummond and co-workers.[83] The experimental procedure involves taking a 100% aqueous solution of known volume and hydrogen ion concentration and successively diluting this solution with known volumes of 1,4-dioxane. After each dilution and a sufficient time delay to allow for equilibration, the pH-meter reading B, is taken. The values of $\log U_H^0$ for each of the various 1,4-dioxane-water mixtures are then calculated on the basis of equation (16), and the tabulated $\gamma_{\pm}^m$ values. For the 100% aqueous solution – $\log [H^+]$ is assumed to be equal to the quantity $[pH - \log(1/ \gamma_{\pm}^m)]$. For each successive 1,4-dioxane-water mixture, the stoichiometric hydrogen ion

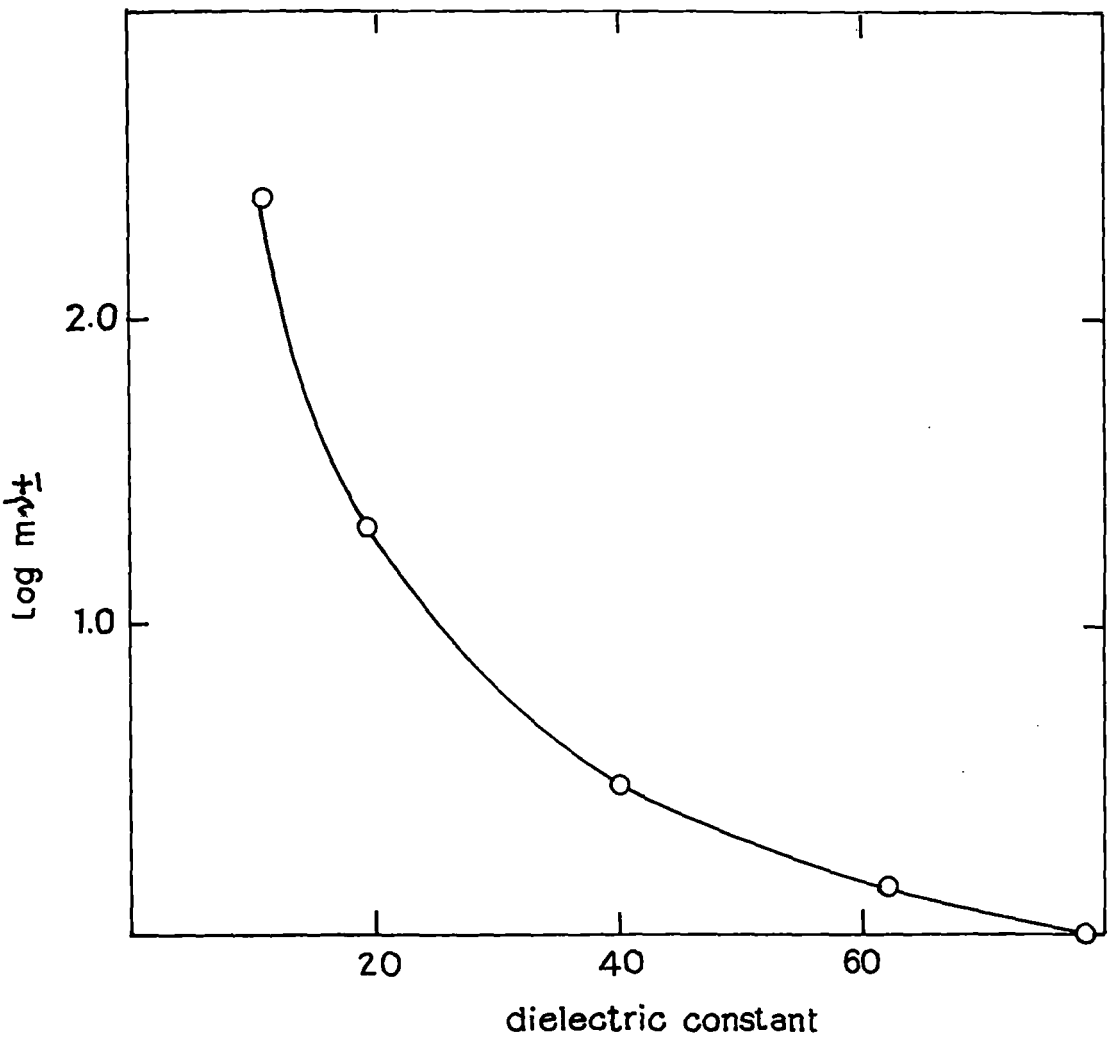

Fig. 1. log $_{m}\gamma_{\pm}$ values as a function of dielectric constant of 1,4-dioxane-water mixtures.

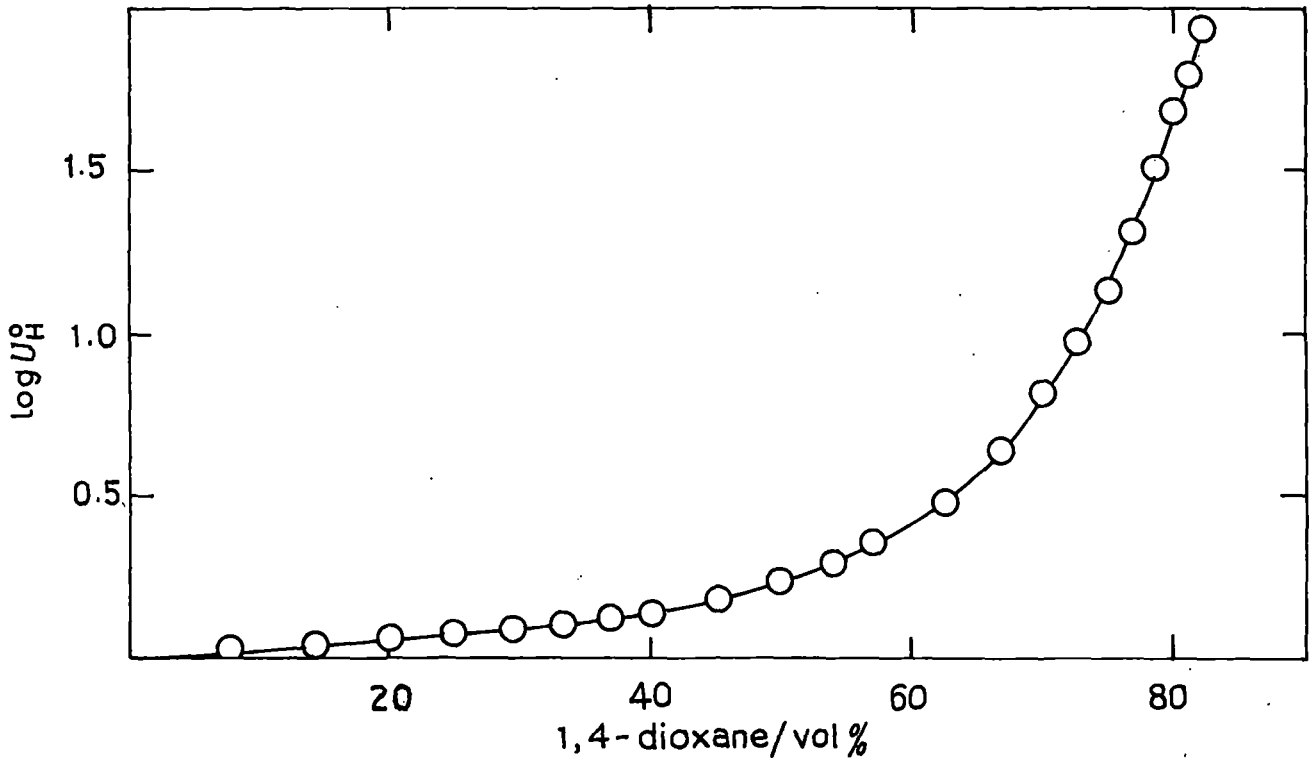

Fig. 2. The pH-meter correction factor, $\log U^0_H$, as a function of volume% 1,4-dioxane-water mixtures.

concentration is calculated by taking the dilution and the density of the solution into account. As no extra electrolyte is added to the solutions, the ionic strength is considered to be equal to the stoichiometric hydrogen ion concentration and the $\gamma_{\pm}^{m}$ values are calculated accordingly.

In figure 2, (adopted from ref.83), the values obtained for log U_H^0 are plotted as a function of the volume % of 1,4-dioxane in the 1,4-dioxane-water mixture.

When determining the various pK_a values, it may be assumed that the acid-base equilibrium of the present indicator molecules could be described by

$$HIN \overset{K_a}{\rightleftharpoons} H^+ + IN^- \text{ (Equation 7, with simplified notations)} \quad (17)$$

where HIN, IN, H^+ denote the protonated (acid), deprotonated (base) forms of the solute organic molecule and the proton respectively.

For the organic indicators in aqueous micellar solution, the apparent pK_a values were obtained from the change in the ultraviolet absorption spectrum of each indicator with bulk aqueous pH by means of the expression

$$pK_a^{obs} = pH - \log \frac{[IN]}{[HIN]} \quad (18)$$

with $$\frac{[IN]}{[HIN]} = \frac{\alpha}{1-\alpha} \quad (19)$$

and $$1-\alpha = \frac{A_{IN} - A}{A_{IN} - A_{HIN}}$$

where A represents the uv absorbance at the uv wave length band maximum of the deprotonated form of the indicator, λ_{max}, at a given pH, A_{HIN} the absorbance at λ_{max} when all the indicator molecules are protonated and A_{IN} the absorbance

at λ_{max} when all the indicator molecules are deprotonated. Representative ultraviolet absorption spectra for 5-Hydroxyindole, 5-Hydroxy-L-tryptophan, L-Tyrosine, L-Tyrosinemethylester, 1-Naphthol and 2-Naphthol, as a function of bulk aqueous pH are shown in figs. 3-20. Tables 3-7 gives the positions of the uv absorption band maximum of the indicator molecules in the media investigated.

The thermodynamic acid-base equilibrium constant for the reaction described by equation (17) in 1,4-dioxane-water mixtures is given by :

$$pK_a^m = B + \log U_H^o - \log \frac{[IN]}{[HIN]} - \log \frac{\gamma_{IN}^m}{\gamma_{HIN}^m} \qquad (20)$$

where γ_{IN}^m and γ_{HIN}^m denote the activity co-efficient of the base and acid forms of the indicators, respectively, referred to the particular 1, 4 dioxane-water mixture at infinite dilution. It is not completely clear how one should approximate the activity co-efficients of large complex organic ions such as the present indicator molecules. Consequently, the pK_a^m values given in this work neglect the activity co-efficient term.[83]

pH titrations in 1,4-dioxane-water mixtures were carried out with low indicator concentrations.(1.0×10^{-4}) mol dm^{-3}, and with no added electrolyte other than the HCl and NaOH required to perform the titrations. These HCl and NaOH additions were always kept to a minimum. The high pH and low pH spectra were always the final spectra to be taken in an experiment to determine a pK_a^m. At the background of low ionic strength, the interpolated magnitudes of the mean activity co-efficients of HCl in dioxane-water mixtures suggests that for the present composition of the mixtures, the activity co-efficient term in equation (20) is negligibly small. Hence the pK_a^m values of this work in the experimental mixtures are believed to approximate well the thermodynamic acid-base equilibrium constants.

3.3. Results and discussion

The theoretical background to the forthcoming analysis of the interfacial protonation-deprotonation equilibrium of the present indicator (probe) molecules has been given in pages 12 to 16 of the current chapter. Provided there is no significant contribution to the apparent acid-base equilibrium constant of an interfacially located organic molecules from specific solute-solvent interactions, the following relationship hold:

$$pK_a^i = pK_a^m - \log m\gamma_{H^+} \quad (21)$$

$$pK_a^0 = pK_a^i + \log \frac{\gamma_{IN}^i}{\gamma_{HIN}^i} \quad (22)$$

$$pK_a^0 = pK_a^{obs} + \frac{F\psi_0}{2.303RT} \quad (23)$$

where $m\gamma_{H^+}$ is the medium effect on the proton as discussed thoroughly by Drummond and co-workers.[83] γ_{IN}^i and γ_{HIN}^i denote the activity co-efficients of the deprotonated and protonated forms of the indicator molecules respectively, referred to the interfacial phase at infinite dilution, and F, R, T, Ψ_0 represent the Faraday constant, the universal gas constant, the absolute temperature and the electrostatic surface potential respectively. It may be recalled that while equation (21) describes equilibrium in 1,4-Dioxane-water medium, pK_a^i is related to pK_a^0 of the indicator molecule at the non-ionic micellar interface by the relation (22). However, the quantity log γ_{IN}/γ_{HIN} is negligibly small. Equation (23) is relevant for the acid-base equilibrium of the indicator molecule partitioned at the charged micellar interface.

In addition, it is convenient to define:

$$\Delta pK_a^m = pK_a^m - pK_a^w \quad (24)$$

$$\Delta pK_a^i = pK_a^i - pK_a^w \quad (25)$$

$$\Delta pK_a^0 = pK_a^0 - pK_a^w \qquad (26)$$

Figs 21 to 35 show the nature of variation of ΔpK_a^m and ΔpK_a^i as a function of the dielectric constant of 1,4 dioxane-water mixtures. The experimental data points refer to 0, 10, 20, 30, 50, 60 and 80 weight% of 1,4 dioxane in the mixtures. The dielectric constants were obtained from the work of Critchfield and co-workers[85]. As suggested by Drummond and co-workers,[83] the ΔpK_a^i values were derived from the ΔpK_a^m values with the aid of equation (21) above and by assuming that the $m\gamma_{H^+}$ can be approximated by the mean medium effect on HCl, $m\gamma_{\pm}$, in the same 1,4 dioxane in the mixtures. In calculating pK_a^0 for charged micelles, surface potential ψ of CTAB, SDS and AOT micelles were taken as +141 mv, -140 mv and, -140 mv respectively.[34]

3.3.1. Ultraviolet absorption spectra of 5-Hydroxyindole and 5-Hydroxy-L-tryptophan:

The uv spectra of 5-Hydroxyindole and 5-Hydroxy-L-tryptophan, as a function of the bulk aqueous pH in pure water as well as in different concentrations of cationic, anionic and non-ionic micellar solutions are shown in (figs. 3 to 20).

The spectral profile of 5-Hydroxyindole as a function of the bulk aqueous pH in pure in water is given in fig. 3. The spectral profile of the same probe in 0.02M CTAB (Fig.7), is representative of that obtained in 0.001M, 0.01M, 0.02M, 0.05M and 0.1M CTAB. Similarly, the spectral profile of 5-Hydroxyindole in 0.05M SDS solution (fig.8) is representative of those obtained in 0.001M, 0.01M, 0.02M, 0.05M and 0.1M of SDS. Similar spectra obtained for Tween-40 and Brij-35. The representative spectra of the above indicator molecule in Brij-35 is shown in fig. 9. The position of absorption band maximum λ_{max} for protonated and deprotonated forms of 5-

Hydroxyindole in each of the media investigated are given in table 3. The spectra exhibit a sharp isobestic point indicating the presence of an well defined protonation-deprotonation equilibrium.

Figs. 3-20 show the ultraviolet absorption spectrum of 5-Hydroxy-L-tryptophan as a function of the bulk aqueous pH in pure water and in different representative concentrations of CTAB, SDS, Tween-40, and Brij-35.

Since the molecular structure of 5-Hydroxyindole and that of 5-Hydroxy-L-tryptophan are similar, their uv spectral profile are also similar. Table-1 contains the λ_{max} values for the protonated and deprotonated forms of 5-Hydroxy-L-tryptophan in different media studied. These spectra also exhibit a sharp isobestic point.

As shown in figures 3 and 7-9 and as reported in table 3, micellar solubilization causes the λ_{max} of the protonated form of 5-Hydroxyindole to undergo a small blue shift in Tween-40 and dioxane-water mixtures. This can be ascribed to the effect that the different solvent properties of the micellar interfacial microenvironment has on energy of the π-π^* electronic transition. On the other hand, for the deprotonated form of 5-Hydroxyindole, λ_{max} is slightly red shifted in dioxane-water mixtures and SDS micelles while blue shift is observed in AOT micelles. In the case of 5-Hydroxy-L-tryptophan, as shown in figs 4, 10, 11, and as reported in table 4, the micellar solubilization causes the λ_{max} of the protonated form of the solute to undergo a very small blue shift in dioxane-water mixtures and registers no major change in the charged or uncharged micelles. The deprotonated form is, however, only slightly red shifted in dioxane-water mixtures with low dielectric constant and remain virtually unchanged in micellar interfaces. This indicates that there is little or no difference between the influence of the pure water and that of the micellar interfacial microenvironment on the energy of the π-π^* electronic transition.

Protonation-deprotonation equilibrium of OH groups of 5-Hydroxyindole and 5-Hydroxy-L-Tryptophan:

In 1,4 dioxane-water mixtures:

The pK_a^w values for protonation-deprotonation equilibrium of hydroxy groups of 5-Hydroxyindole and 5-Hydroxy-L-Tryptophan have been reported in tables 8 and 9. pK_a^m values for 5-Hydroxyindole and 5-Hydroxy-L-tryptophan as a function of 1,4-dioxane% in dioxane-water mixture as well as ΔpK_a^m a function of dielectric constants are shown in figures 21 to 23. Similarly, ΔpK_a^i values for 5-Hydroxyindole and 5-Hydroxy-L-tryptophan as a function of solvent dielectric constant in water-organic mixtures are shown in figures 24-26. pK_a^{obs} is found to vary from 11.041 to 16.213 for 5-Hydroxyindole for the variation of solvent composition from water to 80% dioxane in dioxane-water mixtures. Similarly, for 5-Hydroxy-L-tryptophan, a variation from 11.145 to 15.630 in pK_a^{obs} is registered.

In Micellar solutions:

The pH titration results for 5-Hydroxyindole and 5-Hydroxy-L-tryptophan in the aqueous micellar solutions investigated are summarized in tables 8 and 9 Also included in tables 18 and 19 are estimates of the effective interfacial dielectric constants, D_{eff} of the micelles for some systems. It is, however, possible to estimate the D_{eff} values if both of the protonated and deprotonated forms of the indicators have partitioned quantitatively into the interfacial micellar phase and if the micellar acid-base equilibrium are not influenced by specific molecular interactions or interfacial "salt effects".

It has been assumed that there is no contribution to pK_a^0 values due to the specific molecular interactions. Thus, by comparing a ΔpK_a^0 value with the plot of reference ΔpK_a^i values as a function of the solvent dielectric constant (Fig. 21-35), one can estimate the effective dielectric constant of the interfacial microenvironment of micelles. As the ΔpK_a^i values of the indicator molecules respond uniquely to changes in the solvent dielectric constant, these molecules

can provide unambiguous estimates of the interfacial D_{eff} at their average site of residence. For complex organic molecules, there will obviously be some ambiguity associated with the D_{eff} estimates.

For the charged micellar systems, the pK_a^0 values were determined from the known micellar surface potentials, the pK_a^{obs} values and equation (26), i.e.,

$$pK_a^{obs} = pK_a^{\circ} - \frac{F\psi}{2.303RT} \qquad (26)$$

The electrostatic surface potential of a CTAB micelle in the whole range of concentrations is considered to be +141 mV, whilst the surface potential of an SDS and AOT micelle are considered to be −140 mV in each case. Although, most of the indicator molecules applied in the present study are very little soluble in water, the possibility exists that the pK_a^{obs} value is a composite value comprising of the contributions from the species within the interfacial phase and the bulk aqueous phase. In this study, we attempted to avoid this occurrence by using high concentration of surfactants also. Nevertheless, the pK_a^{obs} results for Tween-40 and Brij-35 micelles suggest that a high percentage of the species in these systems may not have partitioned into the interfacial phase.

From table 8, it is observed that in the presence of non-ionic surfactant, viz., Tween-40 and Brij-35, pK_a^{obs} value is increased slightly compared to that in aqueous medium. This indicates that the deprotonated form of 5-Hydroxyindole is stabilized more in the non-ionic micellar media. On the other hand, in the presence of charged micelles, both CTAB and AOT micelles, pK_a^{obs} is decreased, indicating that the protonated form of the hydroxy derivative is stabilized. Like other surfactant micelles, SDS also registers a variation of pK_a values with concentration. At low concentration, (e.g., 0.01 M SDS) the pK_a^{obs} is smaller than that in water, but at higher concentrations, it gives larger values.

Protonation-deprotonation equilibrium of 5-Hydroxy-L-tryptophan also shows similar behaviour in micellar environment. This is not unexpected because of their structural similarities. The pK_a values are found to decrease significantly in CTAB and AOT micelles indicating stabilization of the deprotonated species. However, the changes in the pK_a^{obs} values are not very high but register an increasing trend in SDS and Brij-35 micelles. The negative ΔpK_a^0 values for SDS and AOT micelles are indicative of the fact that there are some specific interactions between the negatively charged head groups and the deprotonated anions of either 5-Hydroxyindole or 5-Hydroxy-L-tryptophan because ΔpK_a^i and ΔpK_a^m values for these indicator molecules are positive for organic-water media (Fig. 21 to 35).

On the other hand, the ΔpK_a^0 values of these indicators in Tween-40 and Brij-35 micelles are small. This indicates that the indicator molecules are not partitioned in non-ionic micellar interfaces efficiently. Although Fernandez and Formherz[34] using 4-Heptadecyl-7-hydroxy coumarin and 4-Octacycloxy-1-naphthoic acid as acid-base indicator, have shown that D_{eff} of ionic micelles can be equated to the D_{eff} of the interface of non-ionic micelles of surfactants with poly (ethylene oxide) head group, Drummond and co-workers[83] were of the opinion that this assumption is not valid in many cases and pK_a^{obs} value of weak acid-base equilibrium in ionic micelles can be explained on the basis of factors like low interfacial polarity, salt effect and specific interaction of the indicator species with the head groups of the surfactants. In the present study, the D_{eff} values determined for CTAB micellar interface by comparing the ΔpK_a^0 values with those of ΔpK_a^i values, shows that the effective dielectric constant varies from 38.8 to 52.2 yielding an average value of 43.1, while previous authors found a value of ~32 for interfacial polarity of CTAB micelle.[34] Further, observed variation of D_{eff} with CTAB concentrations indicates that the solubilization sites are different and depends on molar ratio of CTAB and the indicator. A locally varying dielectric constant as a function of distance from the charged surface of polyelectrolytes on lipid membranes has

been interpreted in many cases to justify experimental low dielectric constant values. In other words, it seems apparent that not all the 5-Hydroxyindole molecules are partitioned in the interfacial region but some must have been accumulated at a distance from the surface of the micelle and the estimated D_{eff} gives an average value for such a distribution. Moreover, to justify the observed variation of D_{eff} with CTAB concentration it may be argued that the population of the indicator molecules in the interfacial and surrounding regions is redistributed as the molar ratio of indicator and CTAB changes. However, comparison of the results of ΔpK_a^0 (Table 14) and ΔpK_a^i (Figs. 21-35) for 5-Hydroxy-L-tryptophan molecule yield an average D_{eff} value for interfacial polarity of CTAB micelle as ~55. At high concentration of CTAB micelle (0.1M), the D_{eff} value is found to be 47.

3.3.2. Ultraviolet absorption spectral study of protonation-deprotonation equilibrium of L-Tyrosine and L-Tyrosinemethylester

As depicted in figs. 3-20, the spectral feature of L-Tyrosine and L-Tyrosinemethylester are more complicated than those of 5-Hydroxyindole and 5-Hydroxy-L-tryptophan. The protonation-deprotonation equilibrium of hydroxy groups in L-Tyrosine and L-Tyrosinemethylester influences the corresponding uv spectra to a great extent and in each case three clear and well defined isobestic points are exhibited. The uv absorption spectra of both L-Tyrosine and L-Tyrosinemethylester have become complicated due to the presence of three isobastic points in the wave length region 220 to 300 nm. However, the absorbance of the conjugate base of hydroxy groups of the indicators were accessible from the λ_{max} at ~240 nm. While L-Tyrosine is found to be well behaved pH indicator to study micellar interfacial microenvironment, L-Tyrosinemethylester has been selected to examine the effect of carboxyl anionic charge, if any, present in L-Tyrosine molecule.. The spectral profile of L-Tyrosine in 0.02M CTAB solution (fig. 15) is

representative of that obtained in 0.001M, 0.01M, 0.02M, 0.05M and 0.1M CTAB. Similarly, the spectral profile of L-Tyrosine in 0.02M SDS, 0.001M Tween-40 and 0.001 Brij-35 are representative of those observed in other concentrations. The position of ultraviolet absorption band maximum λ_{max}, for the protonated and deprotonated forms of L-Tyrosine in each of the media investigated are given in tables 5 and 6.

As shown in figures 12-15 and as reported in table 5, the micellar solubilization causes the λ_{max} of the protonated form of L-Tyrosine to undergo blue shift in dioxane-water mixtures as well as in the presence of micellar interfacial microenvironment. Maximum shift has, however, been observed in SDS micelles. This can again be ascribed to the effect that the different solvent properties of the micellar interfacial microenvironment has on the energy of the π-π^* electronic transition. In contrast to this, the λ_{max} values for the deprotonated form of L-Tyrosine, figs 12-15 and table 5, is found to undergo a red-shift in dioxane-water mixture of low dielectric constant. However, this red-shift in presence of micellar interfacial microenvironment is most prominent in AOT micelles but less prominent in SDS micelles. It is unlikely that interfacial microenvironment of SDS micelles being more "aqueous like" in nature for the deprotonated form of L-Tyrosine and less so in case of protonated L-Tyrosine. On the other hand, it may be attributed to the fact that due to the existence of an isoelectric point of L-Tyrosine near 5.66, the protonated form remains more close to the SDS micellar interface than those of deprotonated form due to electrostatic repulsion at high pH. However, hydrophobic interaction of the amino acid with AOT micelles seems to be greater resulting in the quite large red shift of λ_{max} of deprotonated L-Tyrosine in presence of AOT micelles. As shown in figs 16-18 and as reported in table 5, the effect of micellar interfacial microenvironment or the medium effect (in presence of dioxane-water mixtures) on λ_{max} values of protonated and deprotonated forms of L-Tyrosinemethylester is more or less same as that of L-Tyrosine and the result does not indicate any large effect of estarification of carboxylic acid group of L-Tyrosine. This indicates that the effect of anionic

charge or the existence of isoelectric point (there is no isoelectric point in TyE) are once again not the dominating factors and the overall complex and nearly identical structure of the molecules determine their resultant properties with respect to electronic transition. Tables 10-11 show that, in the presence of non-ionic micelles, viz., Tween-40 and Brij-35 micelles, pK_a^{obs} values of both L-Tyrosine and L-Tyrosinemethylester are increased compared to those in aqueous medium. This indicates that the deprotonated forms of both the indicator molecules are stabilized more in the non-ionic micellar media. On the other hand, mostly in charged micelles (e.g., CTAB and SDS), pK_a^{obs} values are decreased indicating that the protonated forms are stabilized in CTAB and SDS micelles. However, unlike the results of 5-Hydroxyindole and 5-Hydroxy-L-tryptophan, AOT micelle stabilizes mostly the deprotonated forms of L-Tyrosine and L-Tyrosinemethylester. ΔpK_a^0 values (Tables 10 and 11) for the present indicator once again yield values which are negative for SDS and AOT micelles. This discrepancy may once again be interpreted as the result of strong electrostatic interaction between the deprotonated phenoxide ion and the carboxylate anion with that of micellar anionic head groups.

Values of ΔpK_a^i and ΔpK_a^m for both of the indicators are consistently positive in 1,4-Dioxane-water mixtures (Tables 15 and 16). Effect of carboxylate anion in L-Tyrosine is not very apparent if one compares the result of L-Tyrosine with that of its methyl ester counterpart. For the present indicator molecules, ΔpK_a^0 values are small but positive for Tween-40 and Brij-35 micelles. This indicates that these indicators are not efficiently partitioned in the interfacial region of the non-ionic micelles. However, both L-Tyrosine and L-Tyrosinemethylester are partitioned to a greater extent in CTAB micelles yielding larger positive ΔpK_a^0 values which is consistent with the ΔpK_a^i and ΔpK_a^m values in the organic-aqueous medium (Tables 20-21). D_{eff} values have been estimated by comparing ΔpK_a^0 values of L-Tyrosine and L-Tyrosinemethylester in CTAB micelles with those of ΔpK_a^i for 1,4-Dioxane-water mixtures. The effective dielectric constant values for CTAB micellar interface for above two indicators are more or less same, i.e., 49 ± 1. This value

once again shows that the indicator molecules are distributed in the interfacial region of the micellar surface upto a certain distance.[86]

3.3.3. Ultraviolet absorption spectral study of protonation-deprotonation equilibrium of 1-Naphthol and 2-Naphthol

The spectral profiles of 1-Naphthol in different media under investigation are shown in figs. 19 and 20 The position of ultraviolet absorption band maximum λ_{max} for protonated and deprotonated forms of 1-Naphthol in each of the media investigated is given in table 7. As shown in figs. 19 and 20 and as reported in table 7, the micellar solubilization causes the λ_{max} of both the forms blue shifted to some extent except AOT. In AOT, the deprotonated form of 1-Naphthol is red shifted to a greater extent. All the spectra gives well defined conjugate acid and conjugate base absorption bands which allow one to determine the pK_a of acid-base equilibrium of the probe molecules in aqueous as well as interfacially located regions.

The ultraviolet spectra of 2-Naphthol is unfortunately quite insensitive to solution pH as is observed from its spectral profiles as a function of bulk pH. Therefore, no attempt has been made to determine the dissociation constant value of 2-Naphthol in aqueous or micellar media from ultraviolet spectroscopic measurement.

Considering the simpler aromatic structure and the high hydrophobic nature, 1-Naphthol may be thought to be a well-behaved probe molecule for protonation-deprotonation equilibrium study at micellar interface. However, the results obtained in case of 1-Naphthol was found to be comparable with those of other indicator molecules under investigation. These results also justify the use of these indicators as probe molecules. Table 12 shows that except in CTAB micelles, pK_a^{obs} values of 1-Naphthol are positive in all the anionic and non-ionic micelles. Therefore, it may be argued that the

deprotonated form of the indicator is stabilized in interfacial region of the micelles. However, in CTAB micelles at comparatively lower concentrations (0.001M to 0.02M), the deprotonated form is stabilized. The ΔpK_a^0 still give negative values in SDS and AOT micelles showing a repulsive interaction between the deprotonated forms of the Naphthol with the surfactant head groups. As a result, 1-Naphthol is not partitioned effectively in the micellar core in spite of its strong hydrophobic aromatic ring. In Tween-40 and Brij-35 micelles, the indicator molecules are partitioned more effectively than other four indicators as is evident from the high ΔpK_a^0 values (Table 12). The interfacial polarity of CTAB micelles (D_{eff}) determined by comparing ΔpK_a^0 values in the interface with that of ΔpK_a^i in 1,4-Dioxane-water mixtures (Table 12) shows that at high concentration of CTAB, 1-Naphthol is partitioned more efficiently and D_{eff} value of ~ 45 is obtained (Table 22). Like other indicator molecules studied in the present work, distribution of 1-Naphthol in the interfacial region of CTAB micelles, however, probably changes upto a limited distance as a function of CTAB concentration.

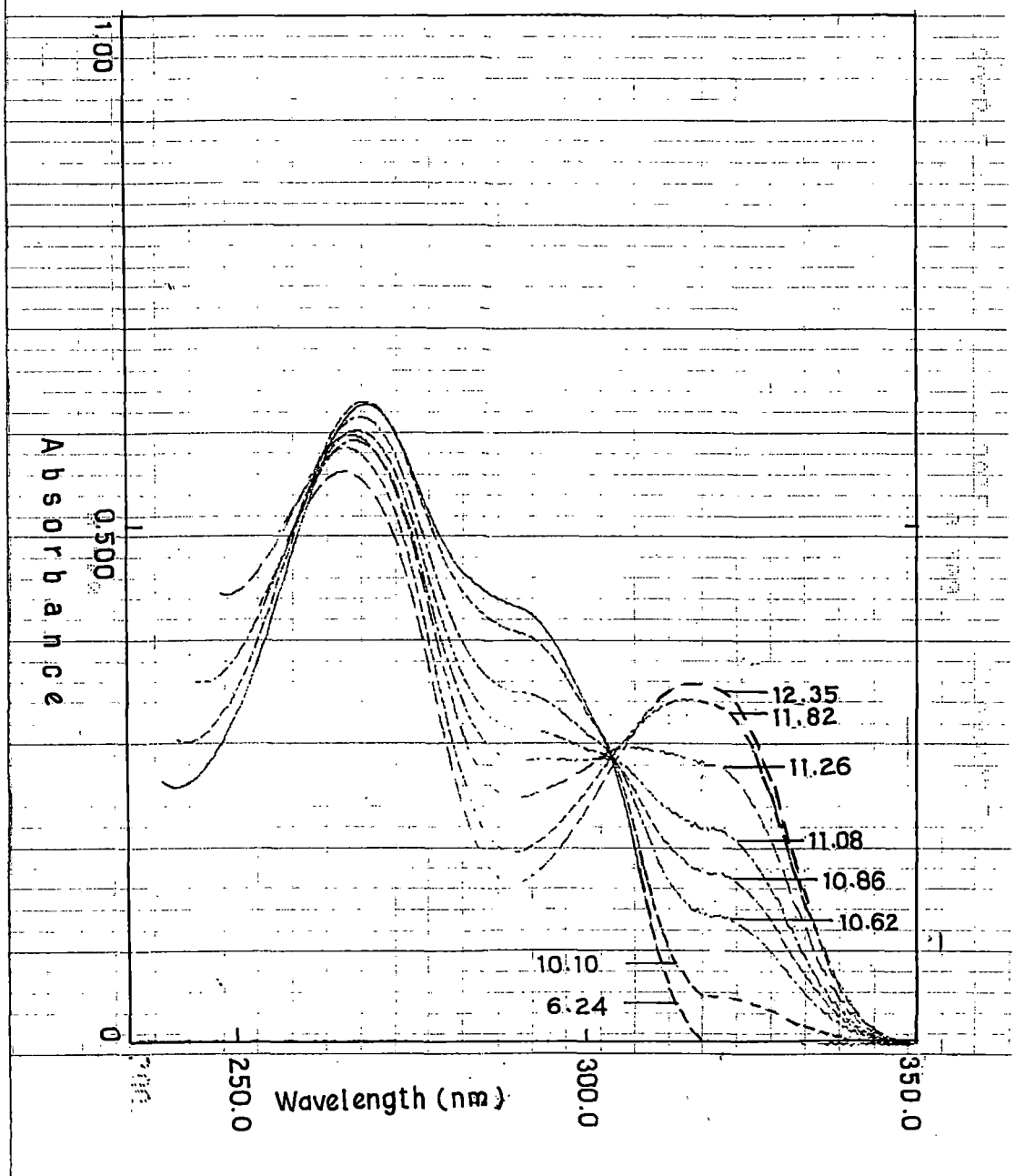

Fig. 3. Absorption spectrum of 5-Hydroxy indole ($1x10^{-4}M$) in water.

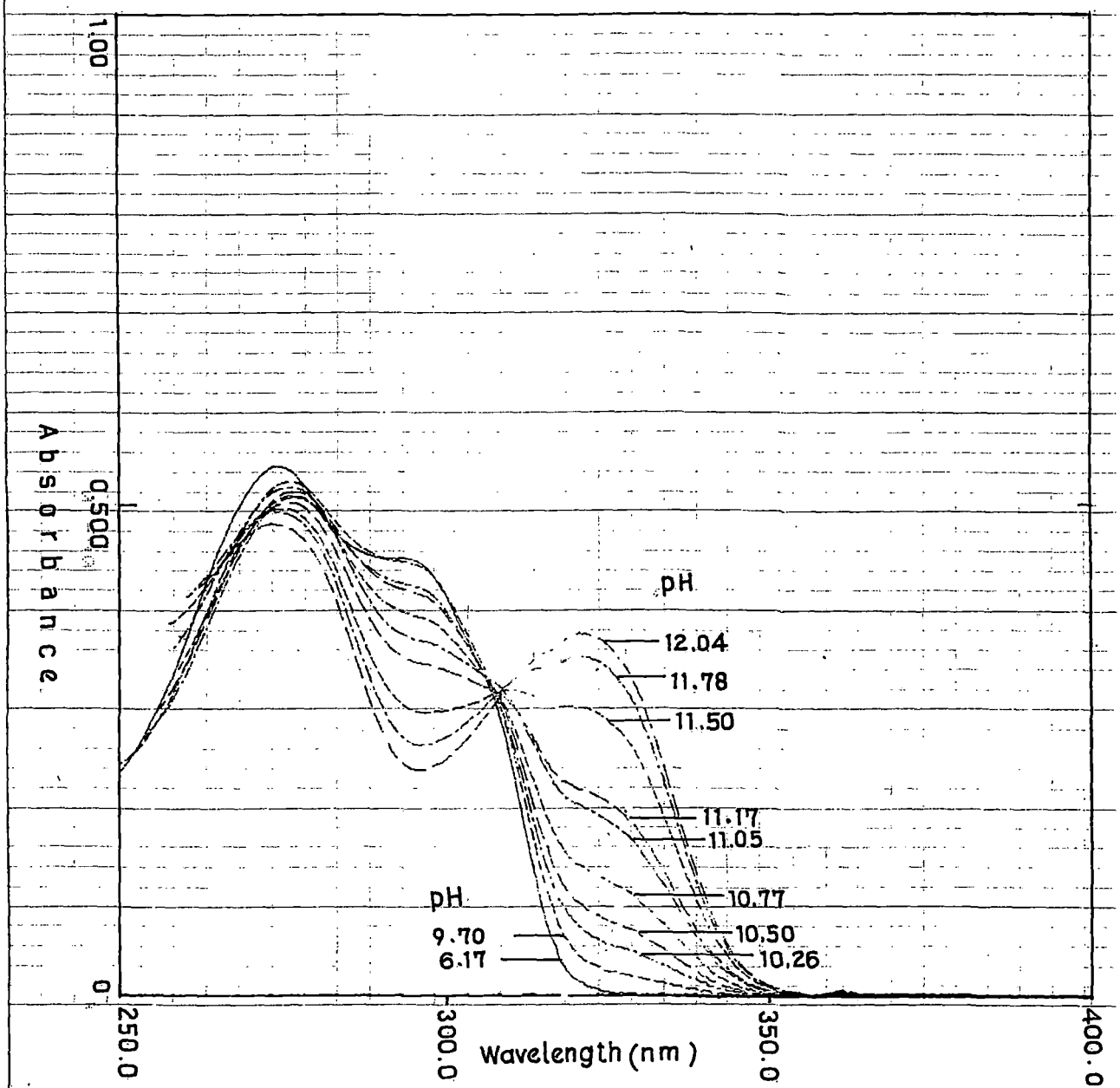

Fig. 4. Absorption spectrum of 5-Hydroxy-L-tryptophan ($1x10^{-4}M$) in water.

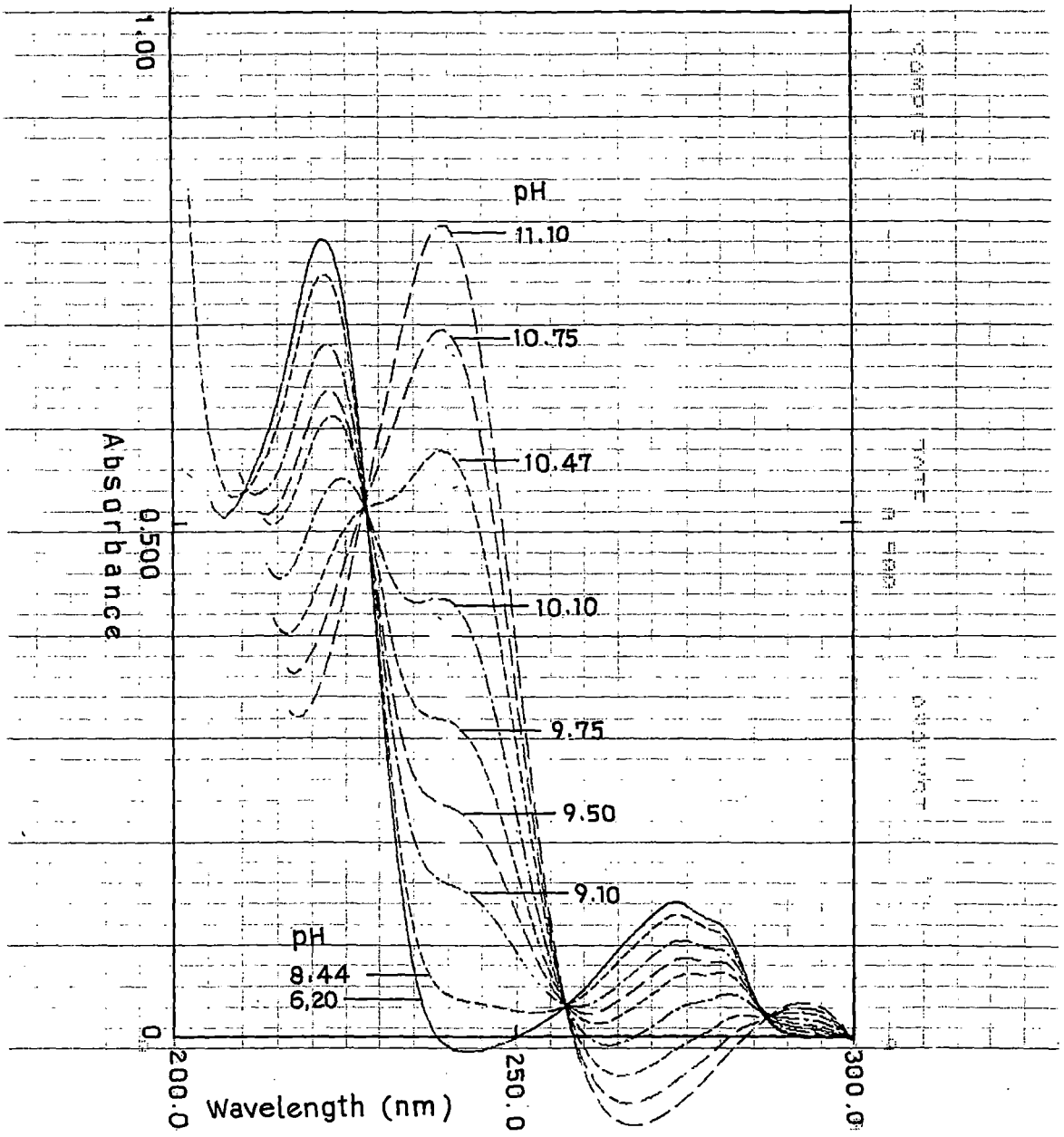

Fig. 5. Absorption spectrum of L-Tyrosine ($1x10^{-4}M$) in water.

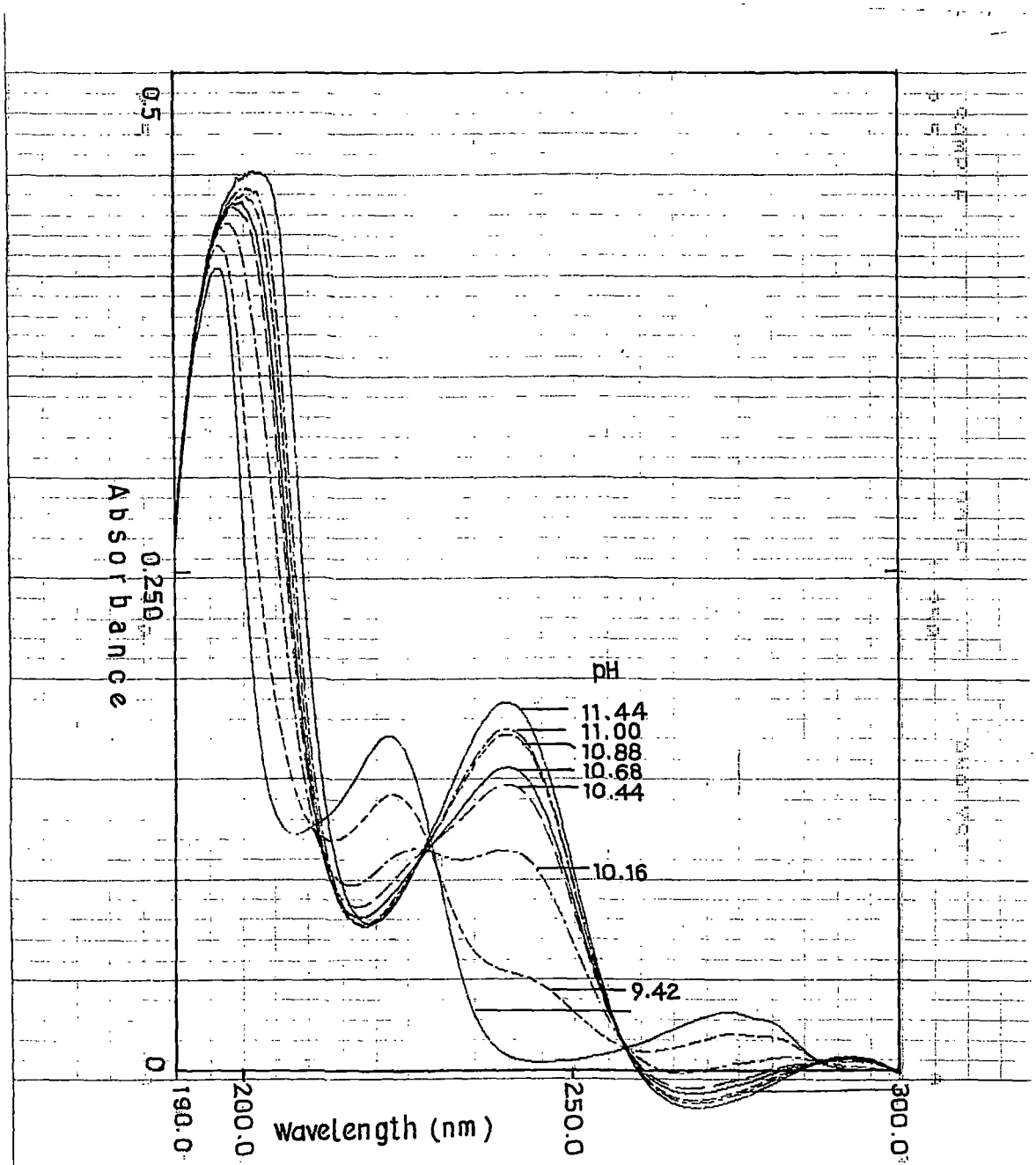

Fig. 6. Absorption spectrum of L-Tyrosine methyl ester(1×10^{-4}M) in water.

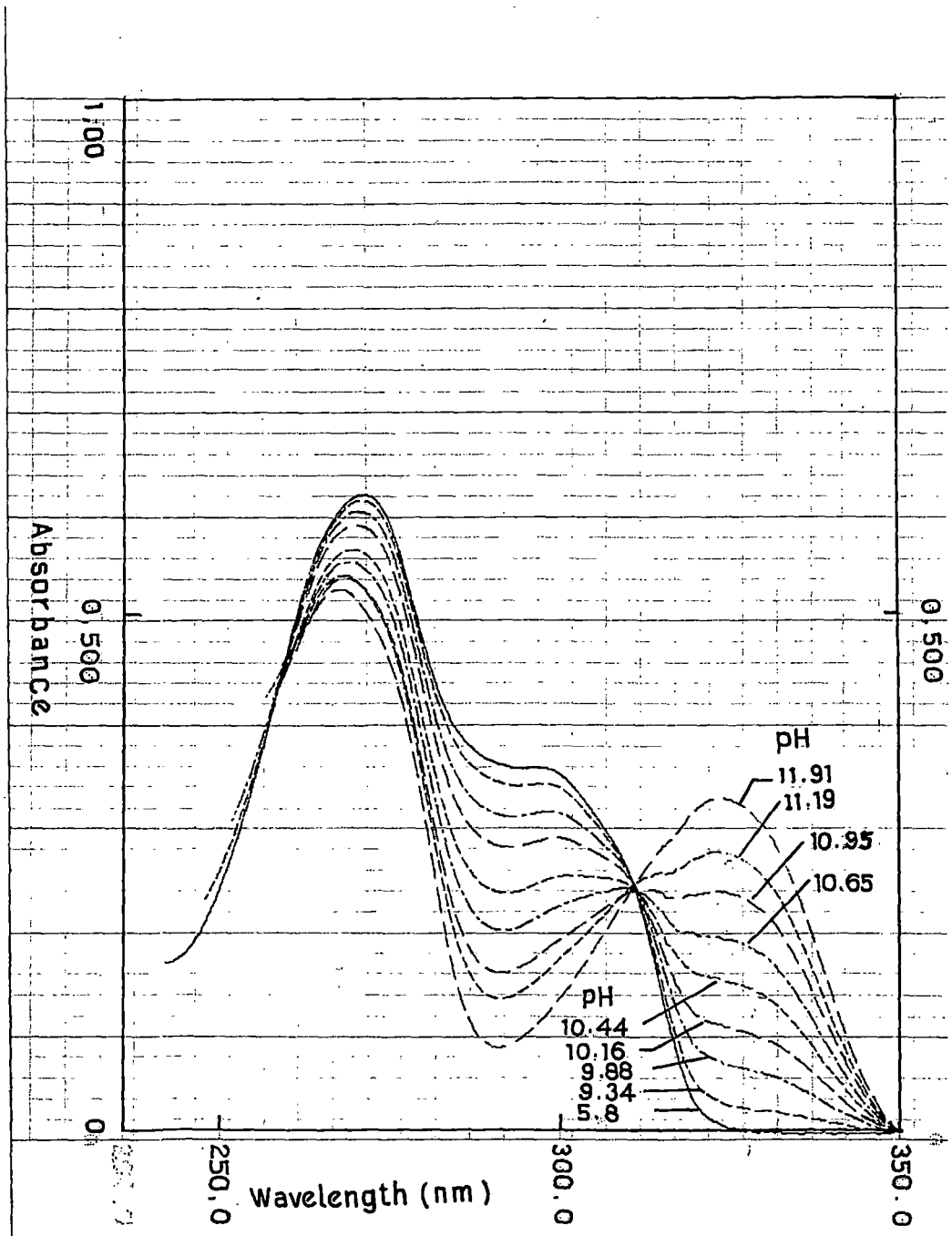

Fig.7. Absorption spectrum of 5-Hydroxy indole ($1x10^{-4}$M) in 0.02M CTAB solution.

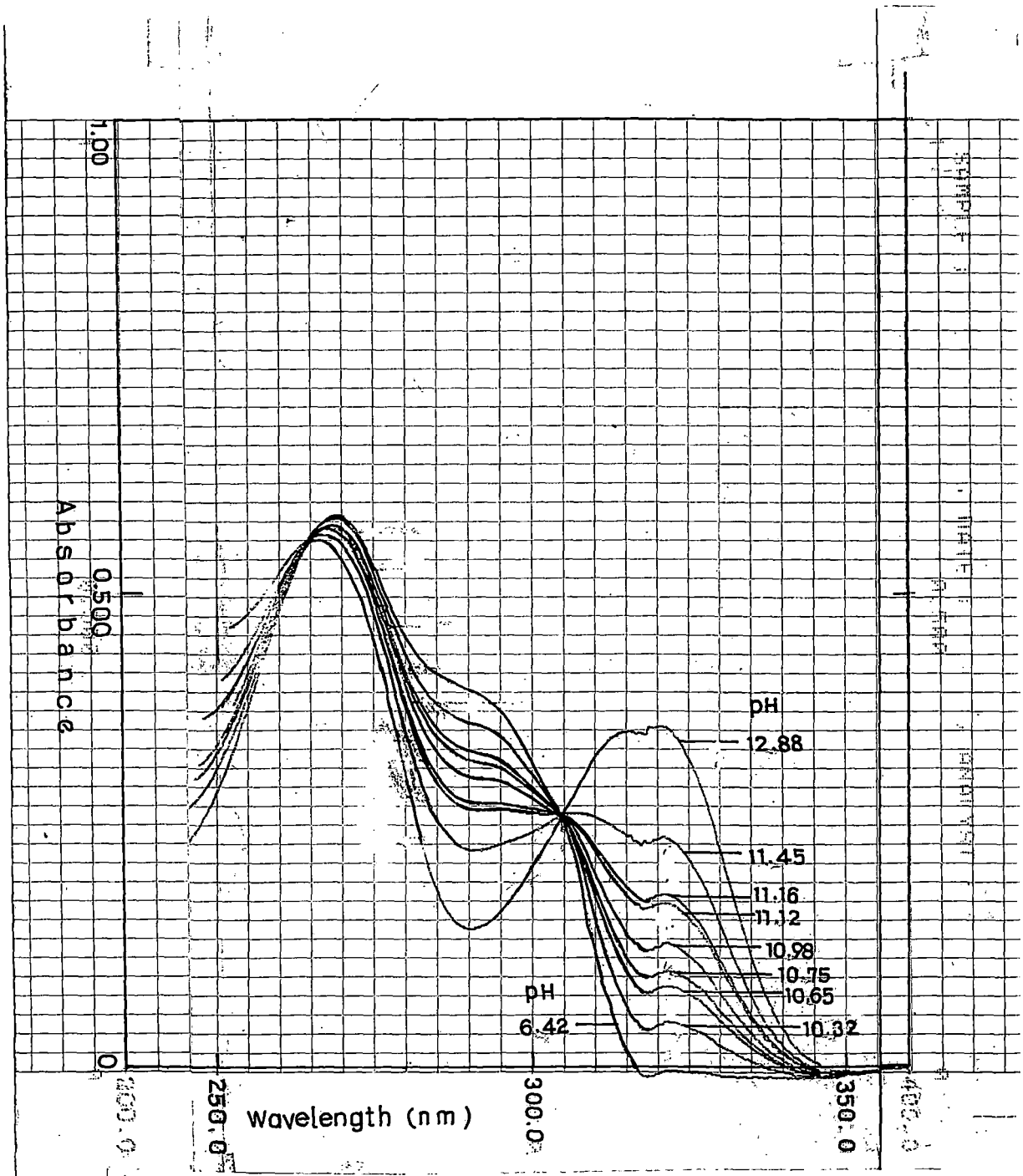

Fig. 8. Absorption spectrum of 5-Hydroxy indole ($1x10^{-4}$M) in 0.05M SDS solution.

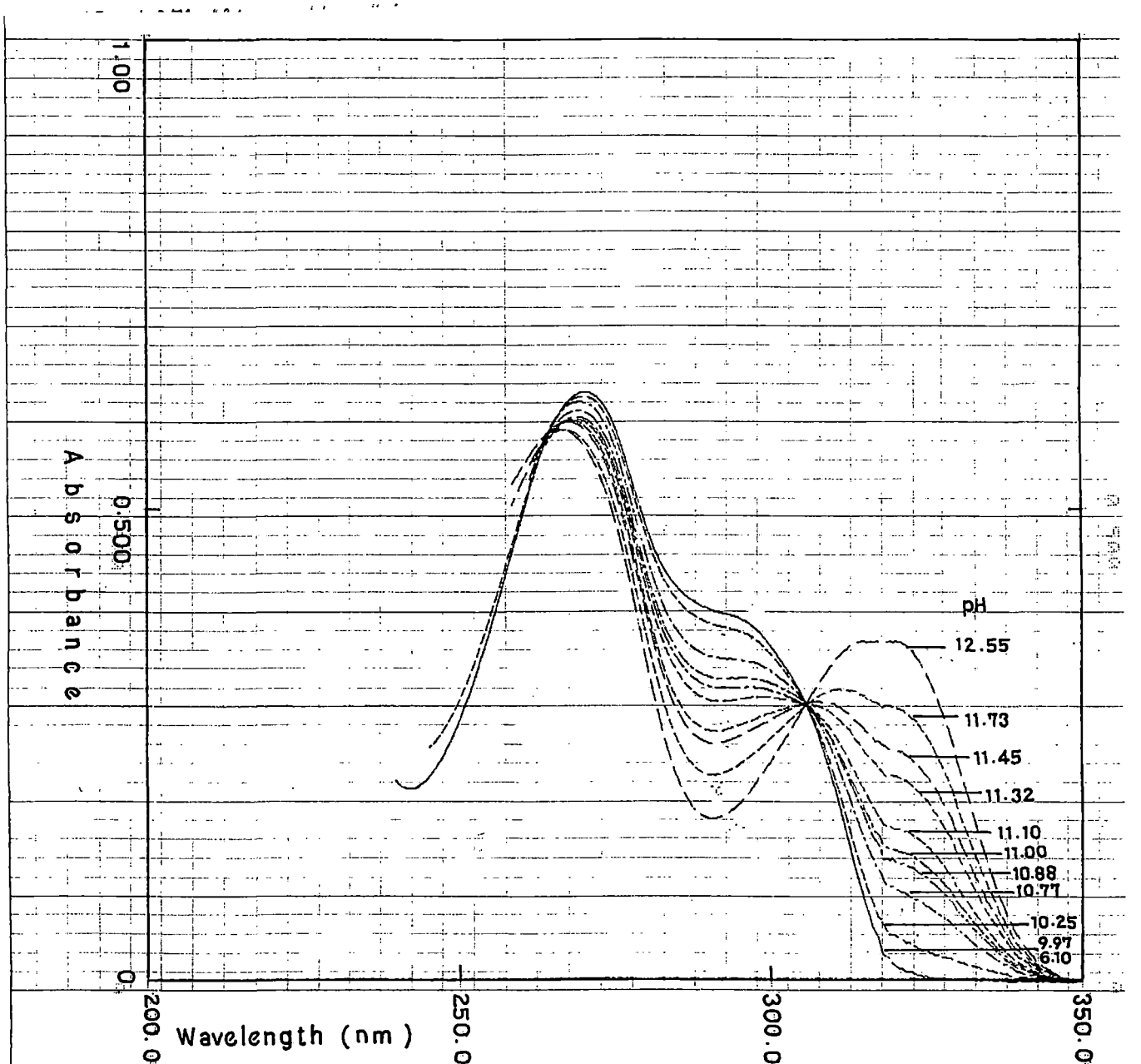

Fig. 9. Absorption spectrum of 5-Hydroxy indole ($1x10^{-4}$M) in 0.01M Brij-35 solution.

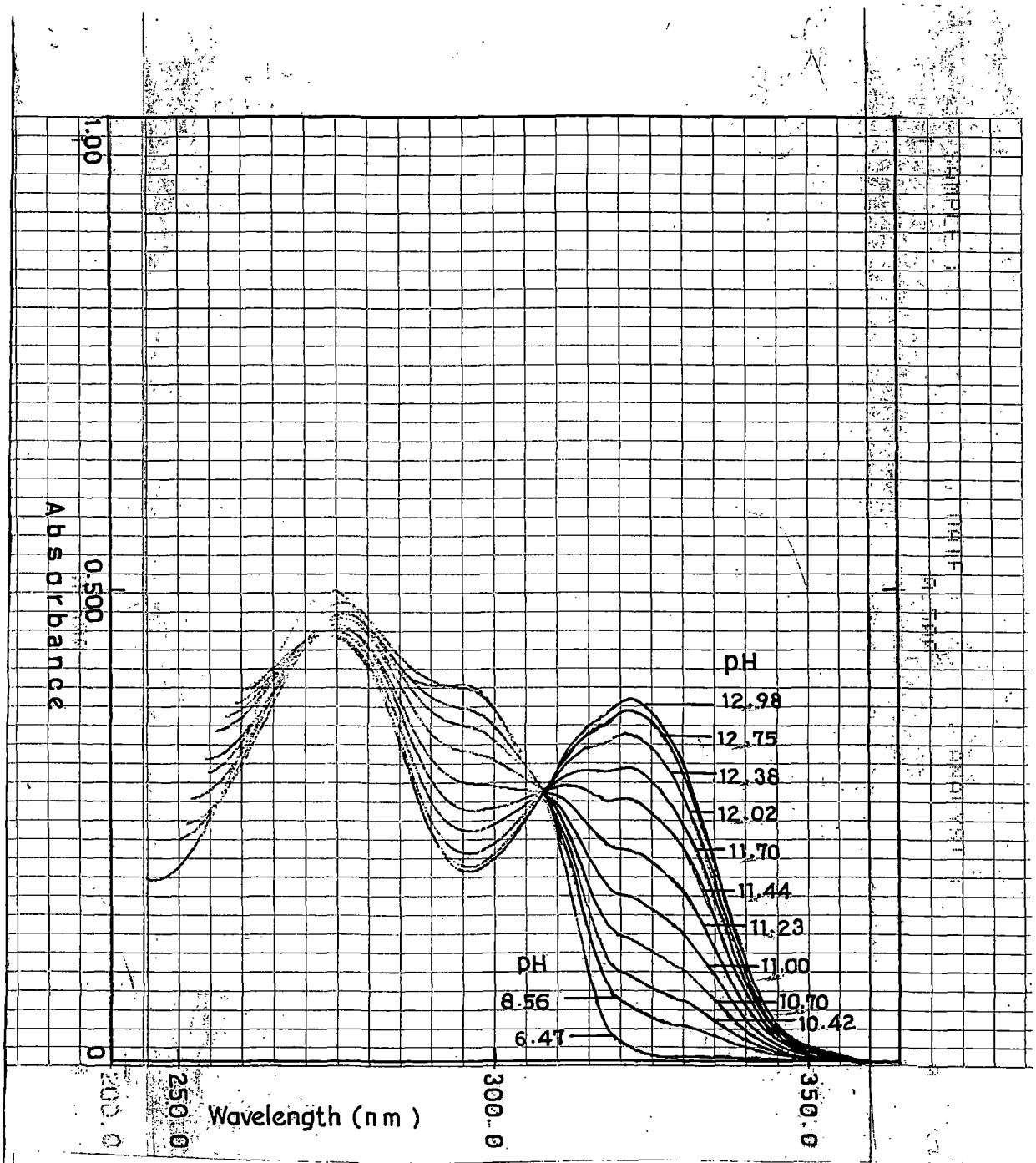

Fig.10. Absorption spectrum of 5-Hydroxy-L-tryptophan ($1x10^{-4}$M) in 0.1M SDS solution.

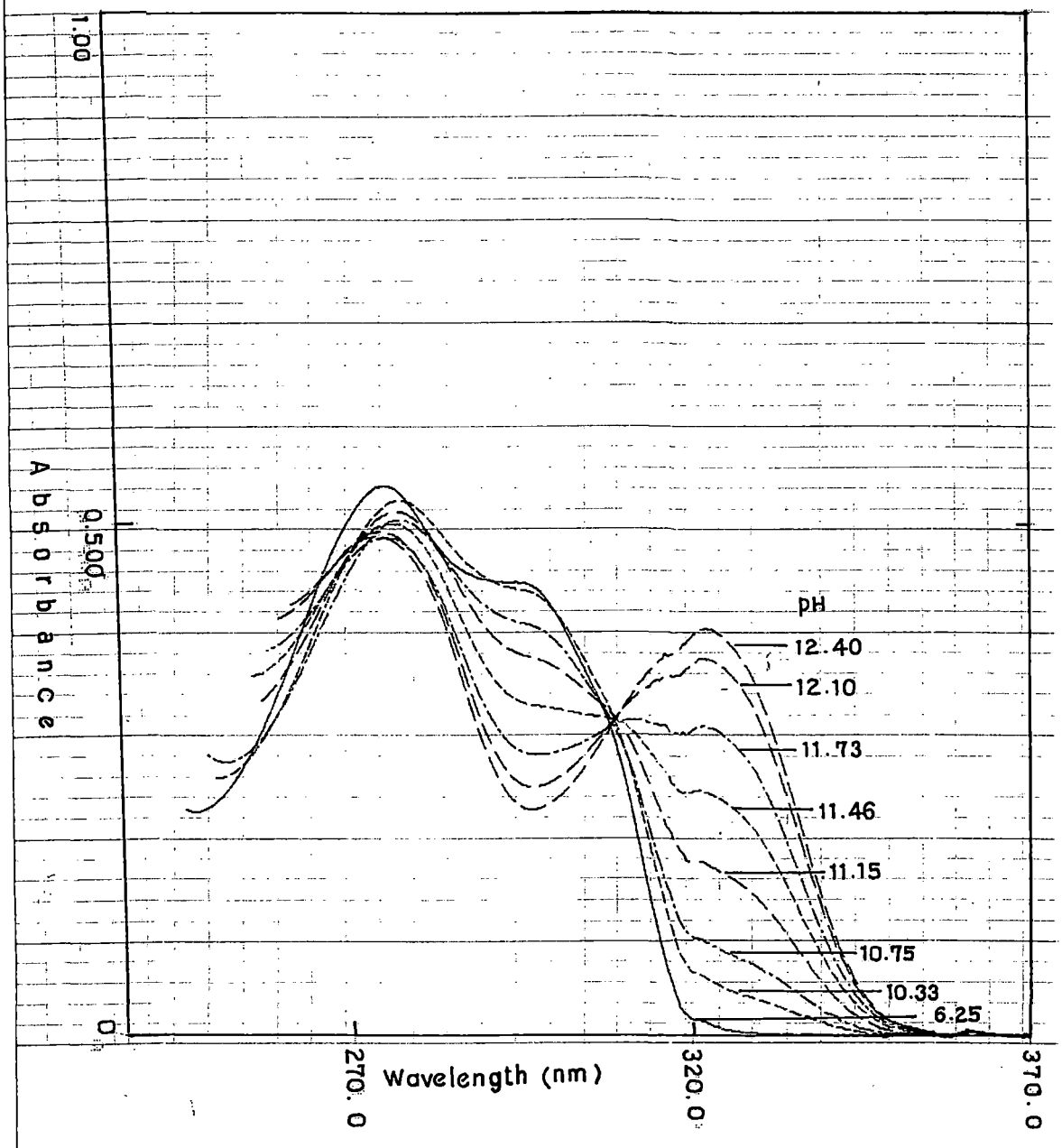

Fig. 11. Absorption spectrum of 5-Hydroxy-L-tryptophan ($1x10^{-4}$M) in 0.001M Brij-35 solution.

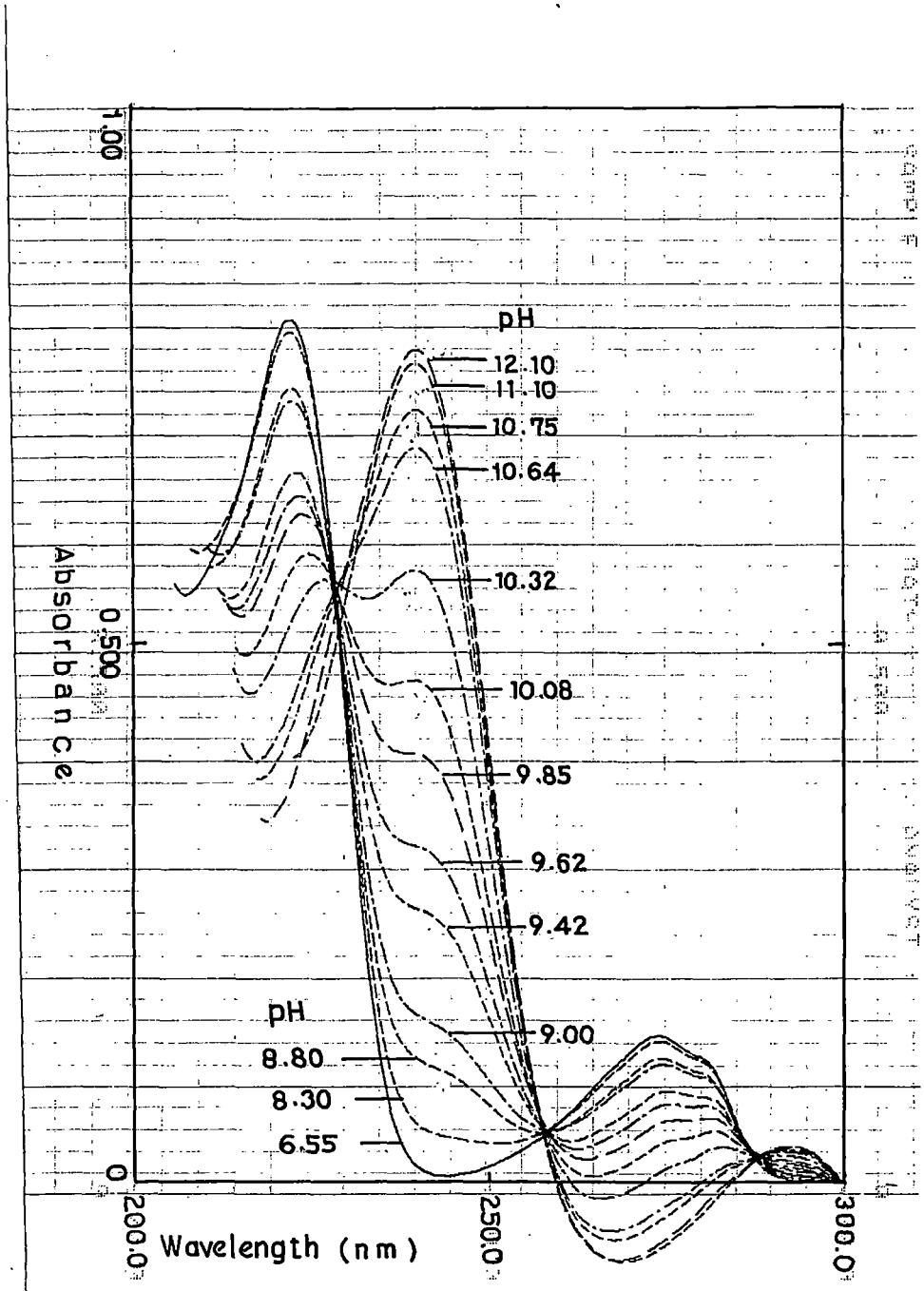

Fig.12. Absorption spectrum of L-Tyrosine ($1x10^{-4}$M) in 0.02M SDS solution.

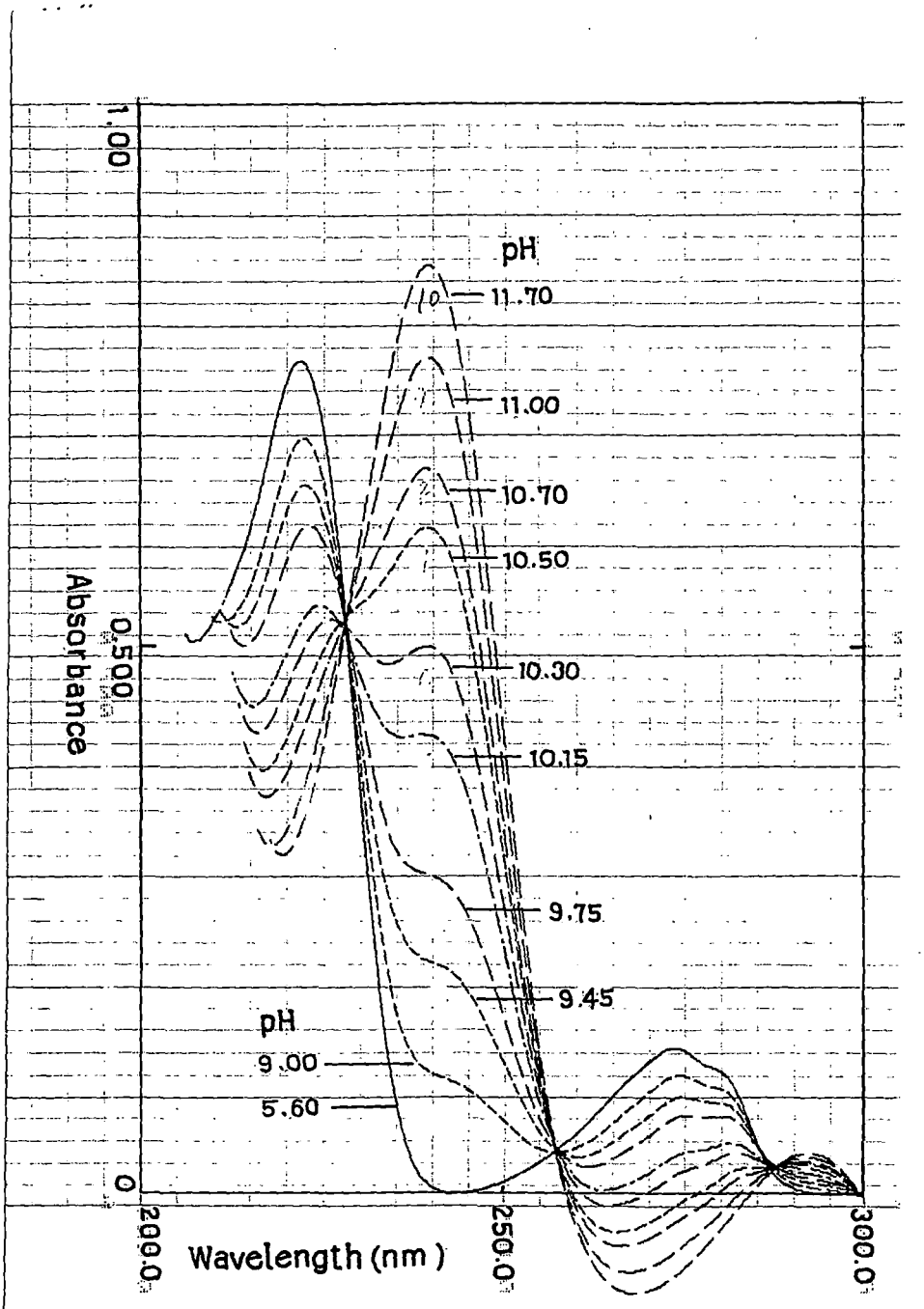

Fig. 13. Absorption spectrum of L-Tyrosine ($1x10^{-4}$M) in 0.001M Tween-40 solution.

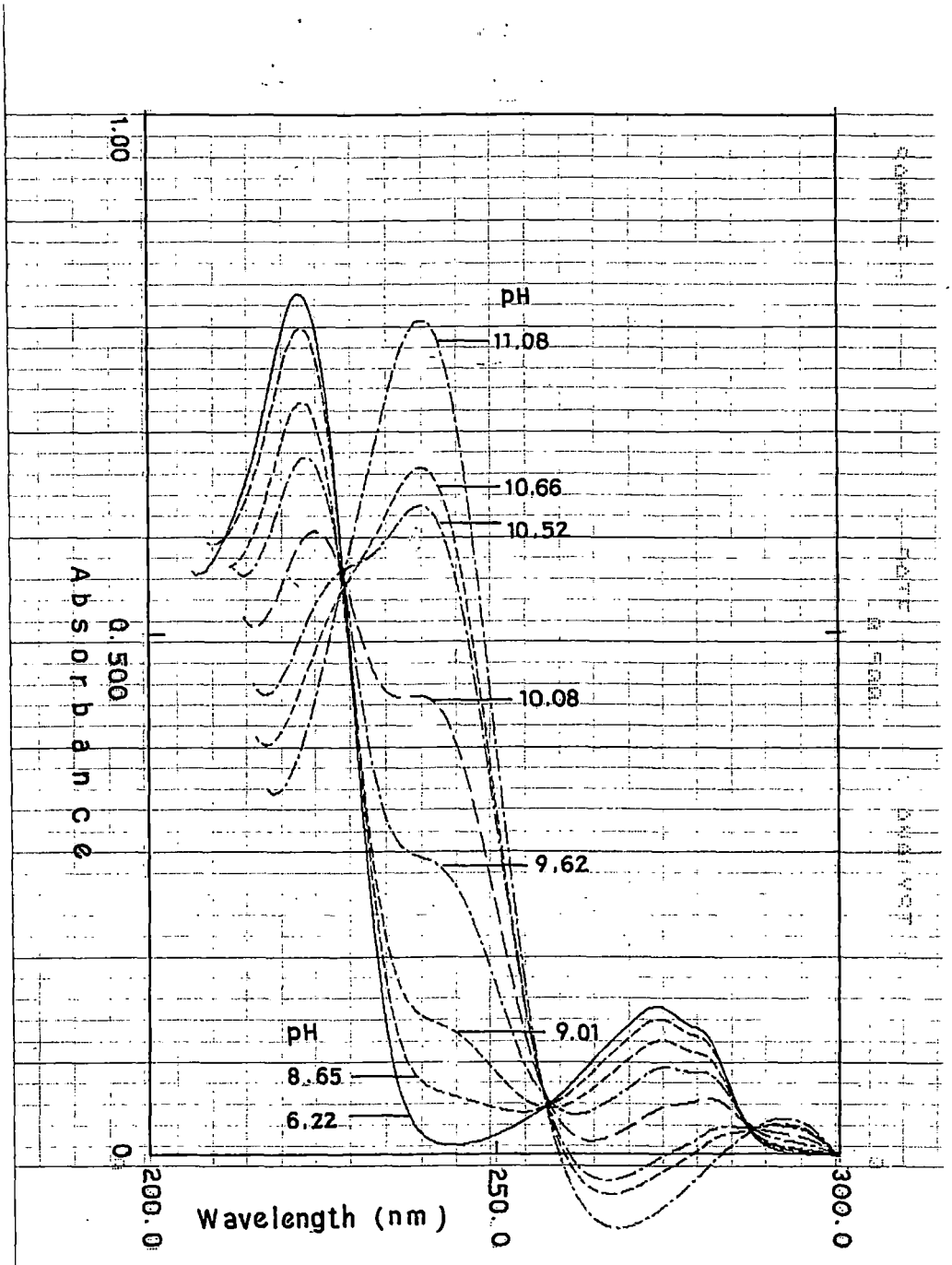

Fig. 14. Absorption spectrum of L-Tyrosine ($1x10^{-4}$M) in 0.001M Brij-35 solution.

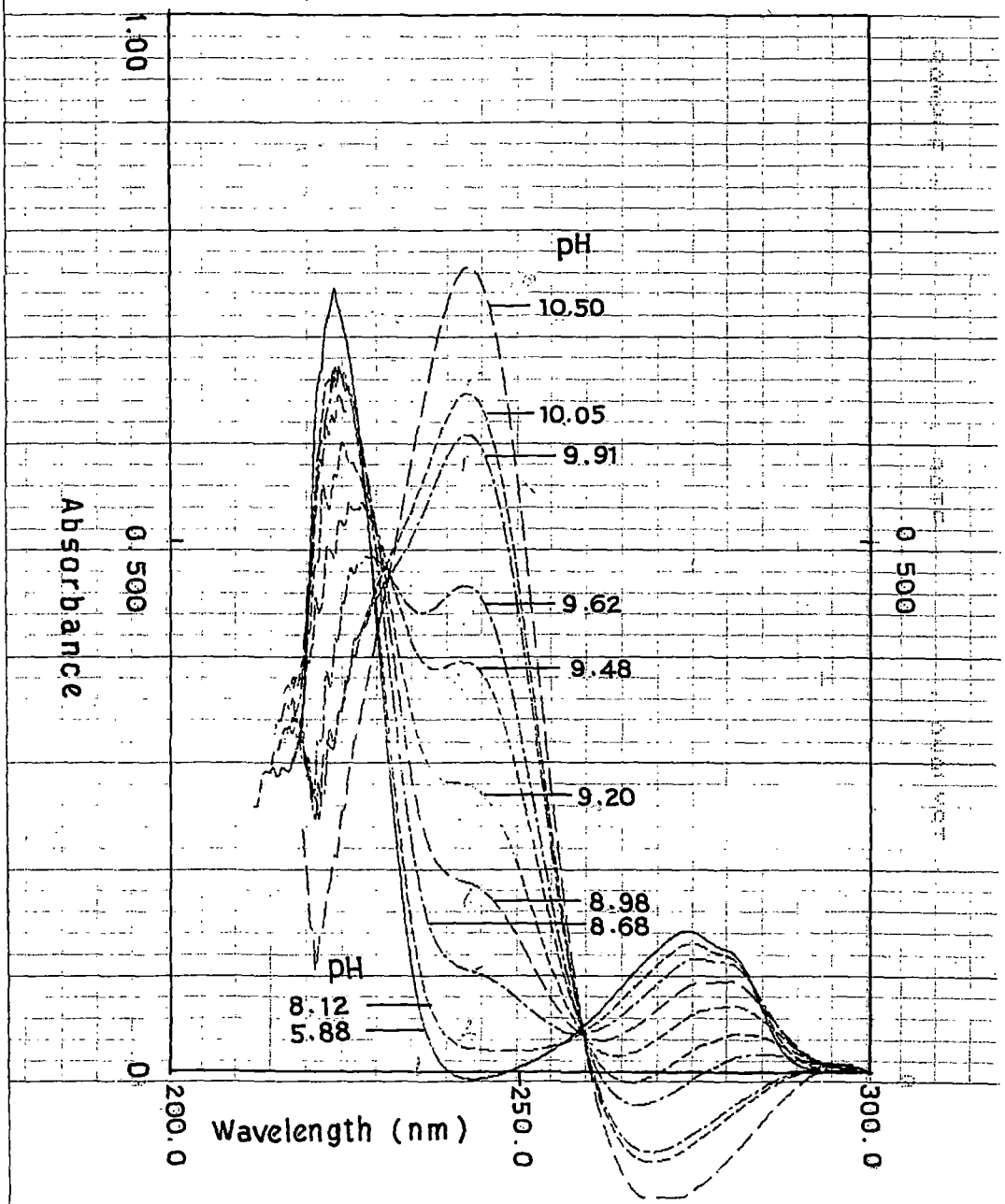

Fig. 15. Absorption spectrum of L-Tyrosine ($1x10^{-4}$M) in 0.02M CTAB solution.

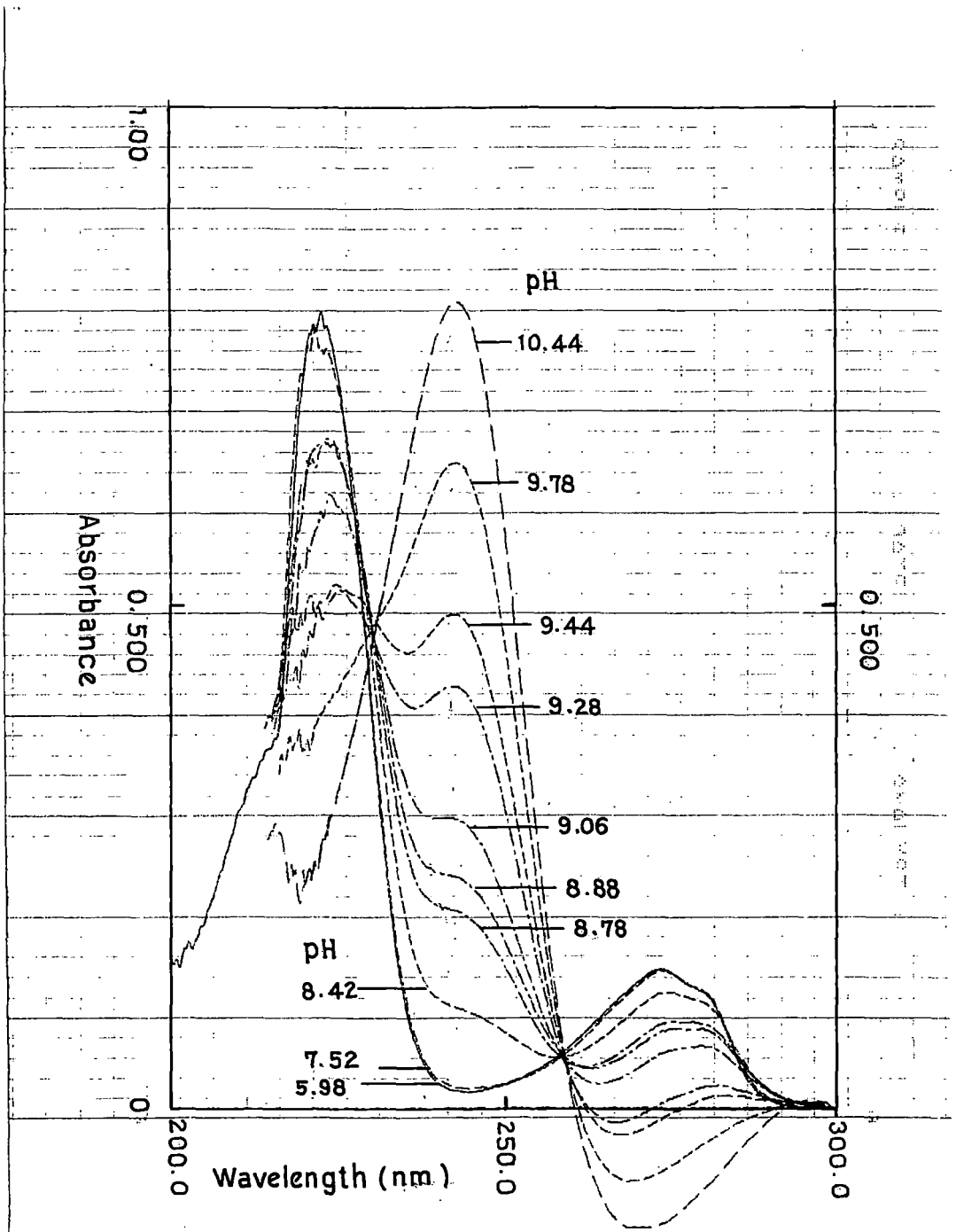

Fig. 16. Absorption spectrum of L-Tyrosine methyl ester ($1x10^{-4}$M) in 0.01M CTAB solution.

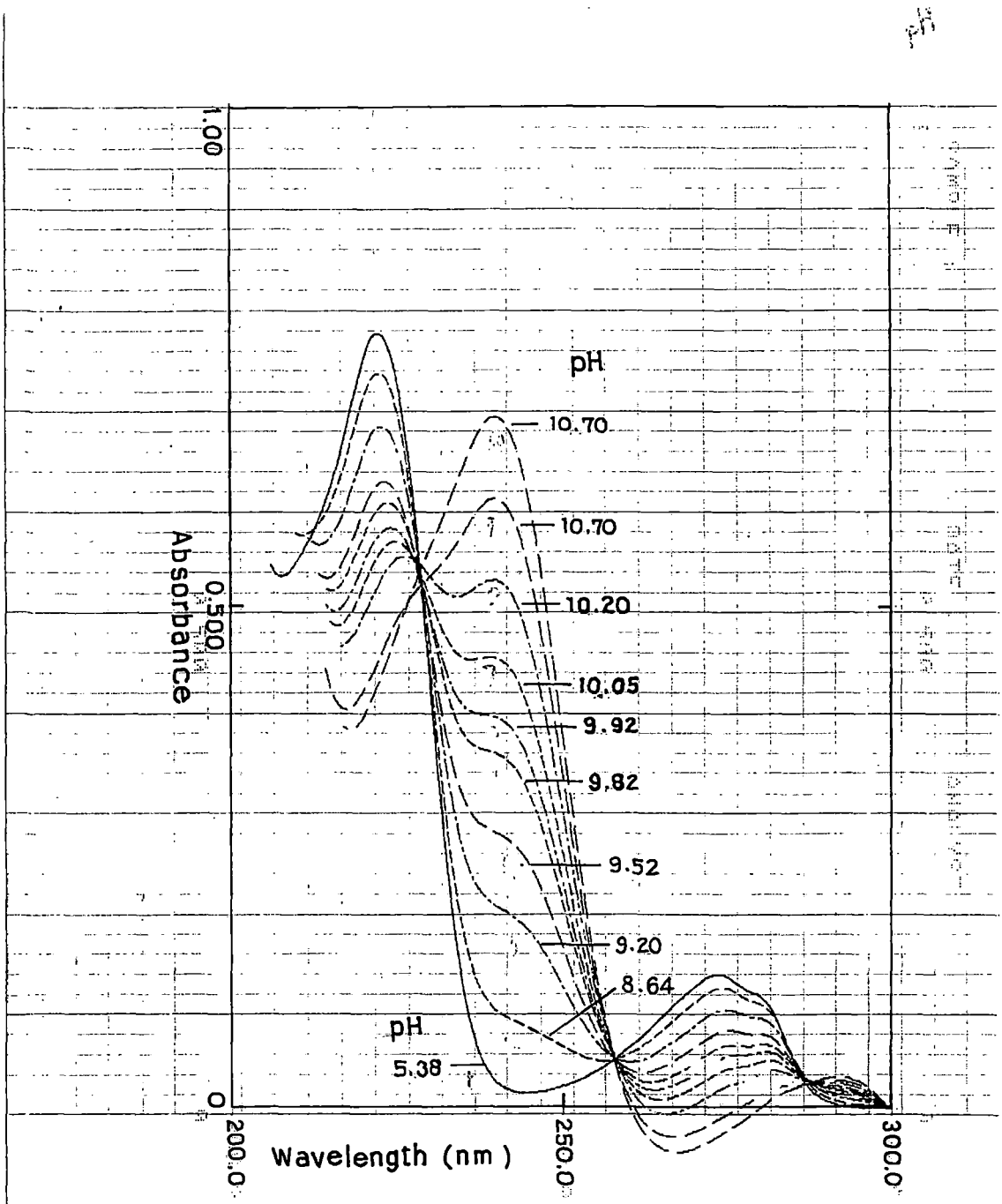

Fig. 17. Absorption spectrum of L-Tyrosine methyl ester ($1x10^{-4}$M) in 0.001M Tween-40 solution.

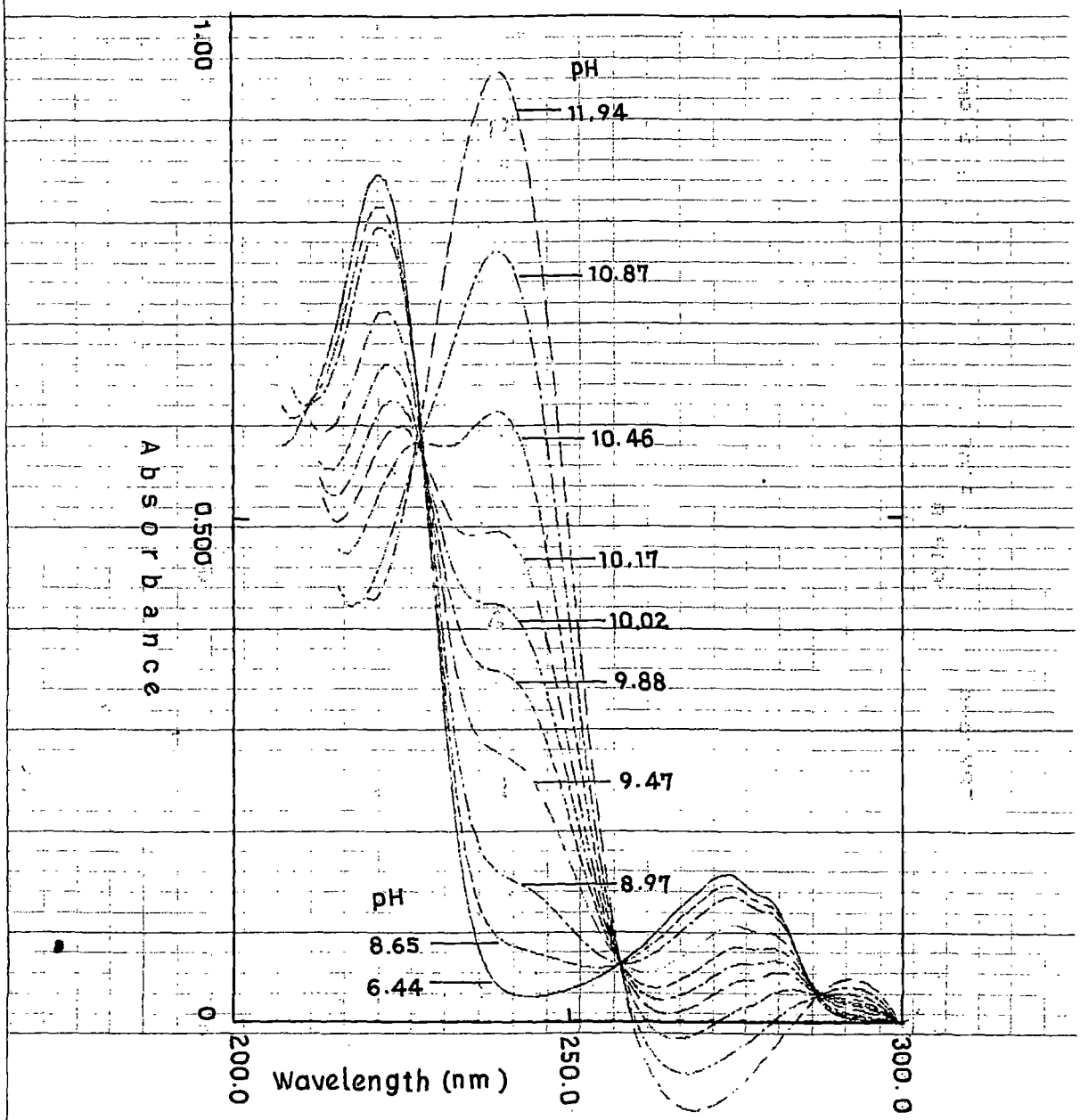

Fig.18. Absorption spectrum of L-Tyrosine methyl ester ($1x10^{-4}$M) in 0.01M Brij-35 solution.

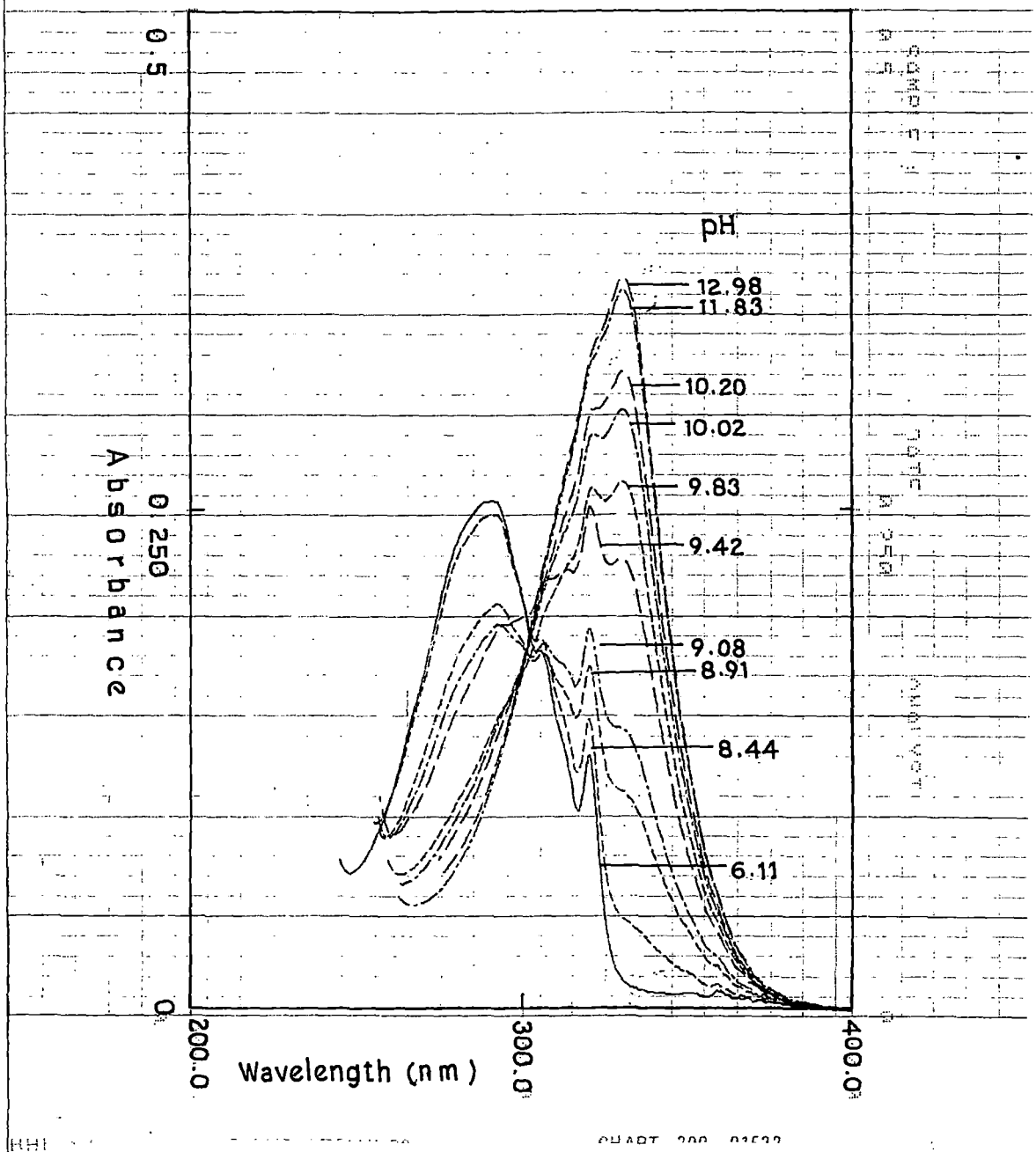

Fig.19. Absorption spectrum of 1-Naphthol ($0.5x10^{-4}$M) in water.

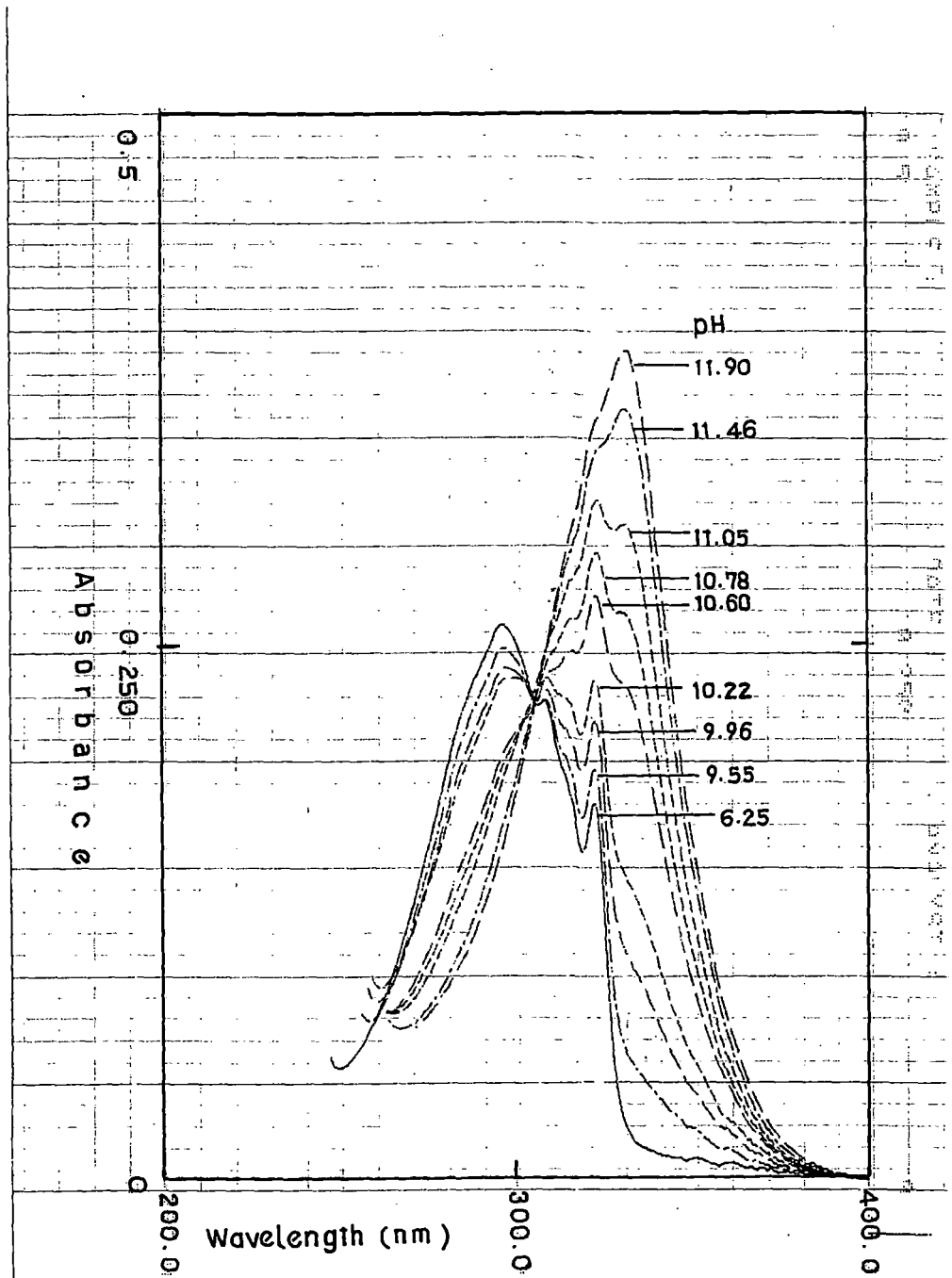

Fig.20. Absorption spectrum of 1-Naphthol ($0.5x10^{-4}$M) in 0.01M Brij-35 solution.

TABLE: 3

The position of the absorption band maximum of the conjugate acid-base forms of 5-Hydroxyindole

Medium	Dielectric Constant (D)	λ_{max} / nm	
		HIN	IN
Water	78.4	293	320
10% Dioxane	69.2	292	322
20% Dioxane	61.9	292	323
30% Dioxane	53.2	292	323
50% Dioxane	40.7	291	324
60% Dioxane	27.2	290	325
80% Dioxane	11.9	290	326
Tween-40	...	288	316
Brij-35	...	290	315
CTAB	...	290	324
SDS	...	290	316
AOT	...	292	315

TABLE: 4

The position of the absorption band maximum of the conjugate acid-base forms of 5-Hydroxy-L-tryptophan

Medium	Dielectric Constant (D)	λ_{max} / nm	
		HIN	IN
Water	78.4	296	322
10% Dioxane	69.2	295	322
20% Dioxane	61.9	295	323
30% Dioxane	53.2	294	323
50% Dioxane	40.7	294	324
60% Dioxane	27.2	294	325
80% Dioxane	11.9	294	326
Tween-40	...	295	322
Brij-35	...	295	322
CTAB	...	296	323
SDS	...	295	321
AOT	...	297	322

TABLE: 5

The position of the absorption band maximum of the conjugate acid-base forms of L-Tyrosine

Medium	Dielectric Constant (D)	λ_{max} / nm	
		HIN	IN
Water	78.4	242	270
10% Dioxane	69.2	240	272
20% Dioxane	61.9	239	273
30% Dioxane	53.2	237	275
50% Dioxane	40.7	236	276
60% Dioxane	27.2	236	277
80% Dioxane	11.9	238	278
Tween-40	...	238	276
Brij-35	...	235	275
CTAB	...	238	274
SDS	...	230	272
AOT	...	240	292

TABLE: 6

The position of the absorption band maximum of the conjugate acid-base forms of L-Tyrosinemethylester

Medium	Dielectric Constant (D)	λ_{max} / nm	
		HIN	IN
Water	78.4	240	274
10% Dioxane	69.2	237	275
20% Dioxane	61.9	236	276
30% Dioxane	53.2	235	276
50% Dioxane	40.7	234	277
60% Dioxane	27.2	233	277
80% Dioxane	11.9	231	278
Tween-40	...	238	276
Brij-35	...	235	275
CTAB	...	238	274
SDS	...	230	272
AOT	...	238	290

TABLE: 7

The position of the absorption band maximum of the conjugate acid-base forms of 1-Naphthol

Medium	Dielectric Constant (D)	λ_{max} / nm	
		HIN	IN
Water	78.4	298	334
10% Dioxane	69.2	295	331
20% Dioxane	61.9	294	335
30% Dioxane	53.2	293	336
50% Dioxane	40.7	292	337
60% Dioxane	27.2	292	339
80% Dioxane	11.9	290	341
Tween-40	...	295	322
Brij-35	...	296	332
CTAB	...	298	325
SDS	...	295	322
AOT	...	290	364

TABLE: 8

pH-Titration results for 5-Hydroxyindole in pure water and aqueous miceller solution with concentrations(M) at 298K

Medium	pK_a^{obs}	ΔpK_a^{obs}	pK_a^0	ΔpK_a^0
Water	11.041	–	–	–
0.001M CTAB	10.874	-0.167	13.258	2.217
0.01M CTAB	10.375	-0.666	12.759	1.718
0.02M CTAB	10.586	-0.455	12.970	1.929
0.05M CTAB	10.783	-0.258	13.167	2.126
0.1M CTAB	10.885	-0.156	13.269	2.228
0.001M SDS	10.802	-0.164	8.435	-2.606
0.01M SDS	11.328	0.287	8.961	-2.080
0.02M SDS	11.276	0.235	8.909	-2.132
0.05M SDS	11.464	0.423	9.097	-1.944
0.1M SDS	11.542	0.501	9.175	-1.866
0.001M Tween-40	11.026	-0.015	11.026	-0.015
0.01M Tween-40	11.135	0.094	11.135	0.094
0.02M Tween-40	11.154	0.113	11.154	0.113
0.05M Tween-40	11.598	0.557	11.598	0.557
0.1M Tween-40	11.677	0.636	11.677	0.636
0.001M Brij-35	11.180	0.139	11.180	0.139
0.01M Brij-35	11.299	0.258	11.299	0.258
0.02M Brij-35	11.532	0.491	11.532	0.491
0.03M Brij-35	11.537	0.496	11.537	0.496
0.001M AOT	10.767	-0.274	8.400	-2.641
0.01M AOT	10.589	-0.452	8.222	-2.819
0.02M AOT	10.586	-0.455	8.219	-2.822
0.03M AOT	10.534	-0.507	8.167	-2.874

TABLE: 9

pH-Titration results for 5-Hydroxy-L-tryptophan in pure water and aqueous miceller solution with concentrations(M) at 298K

Medium	pK_a^{obs}	ΔpK_a^{obs}	pK_a^0	ΔpK_a^0
Water	11.145	–	–	–
0.001M CTAB	10.771	-0.374	13.155	2.010
0.01M CTAB	10.344	-0.811	12.728	1.583
0.02M CTAB	10.598	-0.547	12.982	1.837
0.05M CTAB	10.516	-0.629	12.900	1.755
0.1M CTAB	10.814	-0.331	13.198	2.053
0.001M SDS	10.783	-0.362	8.416	-2.729
0.01M SDS	11.267	0.122	8.900	-2.245
0.02M SDS	11.321	0.176	8.954	-2.191
0.05M SDS	11.353	0.208	8.986	-2.159
0.1M SDS	11.290	0.145	8.923	-2.222
0.001M Tween-40	11.072	-0.073	11.072	-0.073
0.01M Tween-40	11.093	-0.052	11.093	-0.052
0.02M Tween-40	11.134	-0.011	11.134	-.011
0.05M Tween-40	10.912	-0.233	10.912	-0.233
0.1M Tween-40	11.326	-0.181	11.326	0.181
0.001M Brij-35	11.331	0.186	11.331	0.186
0.01M Brij-35	11.240	0.095	11.240	0.095
0.02M Brij-35	11.280	0.135	11.280	0.135
0.03M Brij-35	11.323	0.178	11.323	0.178
0.001M AOT	10.750	-0.395	8.383	-2.762
0.01M AOT	10.600	-0.546	8.233	-2.912
0.02M AOT	10.684	-0.462	8.317	-2.828
0.03M AOT	10.666	-0.479	8.299	-2.846

TABLE: 10

pH-Titration results for L-Tyrosine in pure water and aqueous miceller solution with concentrations(M) at 298K

Medium	pK_a^{obs}	ΔpK_a^{obs}	pK_a^0	ΔpK_a^0
Water	10.052	–	–	–
0.001M CTAB	9.755	-0.297	12.139	2.087
0.01M CTAB	9.514	-0.538	11.898	1.846
0.02M CTAB	9.599	-0.453	11.983	1.931
0.05M CTAB	9.630	-0.422	12.041	1.989
0.1M CTAB	9.756	-0.296	12.140	2.088
0.001M SDS	9.988	-0.064	7.621	-2.437
0.01M SDS	10.023	-0.029	7.656	-2.402
0.02M SDS	9.784	-0.268	7.417	-2.641
0.05M SDS	10.156	0.104	7.789	-2.269
0.1M SDS	9.968	-0.084	7.601	-2.457
0.001M Tween-40	10.241	0.189	10.241	0.189
0.01M Tween-40	10.217	0.165	10.217	0.165
0.02M Tween-40	10.207	0.155	10.207	0.155
0.001M Brij-35	10.081	0.029	10.081	0.029
0.01M Brij-35	10.089	0.037	10.089	0.037
0.02M Brij-35	10.112	0.600	10.112	0.060
0.03M Brij-35	10.451	0.399	10.451	0.399
0.001M AOT	10.226	0.174	7.859	-2.153
0.01M AOT	10.084	0.316	7.717	-2.335
0.02M AOT	10.154	0.102	7.787	-2.265
0.03M AOT	9.726	-0.326	7.359	-2.693

TABLE: 11

pH-Titration results for L-Tyrosinemethylester in pure water and aqueous miceller solution with concentrations(M) at 298K

Medium	pK_a^{obs}	ΔpK_a^{obs}	pK_a^0	ΔpK_a^0
Water	10.087	–	–	–
0.001M CTAB	9.883	-0.204	12.267	2.180
0.01M CTAB	9.503	-0.583	11.887	1.800
0.02M CTAB	9.610	-0.477	11.994	1.907
0.05M CTAB	9.711	-0.376	12.095	2.008
0.1M CTAB	9.411	-0.676	11.795	1.708
0.001M SDS	9.938	-0.149	7.571	-2.516
0.01M SDS	10.095	0.008	7.728	-2.359
0.02M SDS	10.028	-0.059	7.661	-2.426
0.05M SDS	10.123	0.036	7.756	-2.331
0.1M SDS	9.981	-0.106	7.614	-2.473
0.001M Tween-40	10.008	-0.079	10.008	-0.079
0.01M Tween-40	10.232	-0.145	10.232	0.145
0.02M Tween-40	10.052	-0.035	10.052	-0.035
0.001M Brij-35	10.132	0.045	10.132	0.045
0.01M Brij-35	10.177	0.090.	10.177	0.090
0.02M Brij-35	10.270	0.183	10.270	0.183
0.03M Brij-35	10.393	0.306	10.393	0.306
0.001M AOT	9.978	-0.109	7.611	-2.476
0.01M AOT	9.940	-0.147	7.573	-2.514
0.02M AOT	9.789	-0.298	7.422	-2.665
0.03M AOT	9.789	-0.298	7.422	-2.665

TABLE: 12

pH-Titration results for 1-Naphthol in pure water and aqueous miceller solution with concentrations(M) at 298K

Medium	pK_a^{obs}	ΔpK_a^{obs}	pK_a^0	ΔpK_a^0
Water	9.388	–	–	–
0.001M CTAB	8.387	-1.001	10.771	1.383
0.01M CTAB	8.023	-1.365	10.407	1.019
0.02M CTAB	8.623	-1.765	11.007	1.619
0.05M CTAB	8.679	0.709	11.063	1.675
0.1M CTAB	8.914	0.474	11.298	1.910
0.001M SDS	9.666	0.278	7.299	-2.089
0.01M SDS	9.459	0.071	7.092	-2.296
0.02M SDS	10.132	0.744	7.765	-1.623
0.05M SDS	10.415	1.027	8.048	-1.340
0.1M SDS	9.925	0.537	7.558	-1.830
0.001M Tween-40	9.644	0.256	9.644	0.256
0.01M Tween-40	9.601	0.308	9.601	0.213
0.02M Tween-40	10.868	1.480	10.868	1.480
0.05M Tween-40	10.798	1.401	10.798	1.410
0.001M Brij-35	9.971	0.583	9.971	0.583
0.01M Brij-35	10.563	1.175	10.563	1.175
0.02M Brij-35	10.829	1.441	10.829	1.441
0.03M Brij-35	11.025	1.637	11.025	1.637
0.001M AOT	9.369	-0.019	7.002	-2.386
0.01M AOT	9.499	0.111	7.132	-2.256
0.02M AOT	9.805	0.417	7.438	-1.950
0.03M AOT	9.447	0.059	7.080	-2.308

TABLE: 13

5-Hydroxyindole in 1,4-Dioxane-water Mixtures

Dioxane %	D_{eff}	pK_a^m	ΔpK_a^m	pK_a^i	ΔpK_a^i
10%	69.2	11.395	0.354	12.395	1.354
20%	61.9	11.767	0.726	12.587	1.546
30%	53.2	12.302	1.261	12.902	1.861
50%	40.7	13.233	2.192	13.423	2.382
60%	27.2	13.972	2.931	13.992	2.951
80%	11.9	16.213	5.172	15.833	4.792

TABLE: 14

5-Hydroxy-L-tryptophan in 1,4-Dioxane-water Mixtures

Dioxane %	D_{eff}	pK_a^m	ΔpK_a^m	pK_a^i	ΔpK_a^i
10%	69.2	11.608	0.463	12.395	1.463
20%	61.9	12.017	0.872	12.837	1.692
30%	53.2	12.442	1.297	13.042	1.897
50%	40.7	13.435	2.290	13.625	2.480
60%	27.2	13.968	2.823	13.988	2.843
80%	11.9	15.630	4.485	15.250	4.105

TABLE: 15

L-Tyrosine in 1,4-Dioxane-water Mixtures

Dioxane %	D_{eff}	pK_a^m	ΔpK_a^m	pK_a^i	ΔpK_a^i
10%	69.2	10.503	0.451	11.503	1.451
20%	61.9	10.898	0.846	11.718	1.666
30%	53.2	11.274	1.222	11.847	1.822
50%	40.7	12.519	2.467	12.709	2.657
60%	27.2	13.234	3.182	13.254	3.202
80%	11.9	15.066	5.014	14.686	4.634

TABLE: 16

L-Tyrosinemethylester in 1,4-Dioxane-water Mixtures

Dioxane %	D_{eff}	pK_a^m	ΔpK_a^m	pK_a^i	ΔpK_a^i
10%	69.2	10.600	0.513	11.600	1.513
20%	61.9	10.686	0.599	11.506	1.419
30%	53.2	11.350	1.263	11.950	1.863
50%	40.7	12.413	2.326	12.603	2.516
60%	27.2	13.093	3.006	13.113	3.026
80%	11.9	15.599	5.512	15.219	5.132

TABLE: 17

1-Naphthol in 1,4-Dioxane-water Mixtures

Dioxane %	D_{eff}	pK_a^m	ΔpK_a^m	pK_a^i	ΔpK_a^i
10%	69.2	9.712	0.324	10.712	1.324
20%	61.9	10.126	0.738	10.946	1.558
30%	53.2	10.574	1.186	11.174	1.786
50%	40.7	11.459	2.071	11.649	2.261
60%	27.2	11.783	2.395	11.803	2.415
80%	11.9	13.978	4.590	13.598	4.210

TABLE: 18

Values of effective dielectric constant (D_{eff}) for 5-Hydroxyindole in CTAB

Medium	D_{eff}
0.001M CTAB	38.8
0.01M CTAB	52.2
0.02M CTAB	46.3
0.05M CTAB	40.5
0.1M CTAB	37.8

TABLE: 19

Values of effective dielectric constant (D_{eff}) for 5-Hydroxy-L-tryptophan in CTAB

Medium	D_{eff}
0.001M CTAB	47.5
0.01M CTAB	68.1
0.02M CTAB	53.4
0.05M CTAB	59.8
0.1M CTAB	47.1

TABLE: 20

Values of effective dielectric constant (D_{eff}) for L-Tyrosine in CTAB

Medium	D_{eff}
0.001M CTAB	44.6
0.01M CTAB	53.1
0.02M CTAB	52.1
0.05M CTAB	51.7
0.1M CTAB	44.5

TABLE: 21

Values of effective dielectric constant (D_{eff}) for L-Tyrosinemethylester in CTAB

Medium	D_{eff}
0.001M CTAB	43.5
0.01M CTAB	52.5
0.02M CTAB	51.5
0.05M CTAB	44.7
0.1M CTAB	56.9

TABLE: 22

Values of effective dielectric constant (D_{eff}) for 1-Naphthol in CTAB

Medium	D_{eff}
0.001M CTAB	60.0
0.01M CTAB	50.0
0.02M CTAB	50.0
0.05M CTAB	45.0
0.1M CTAB	45.0

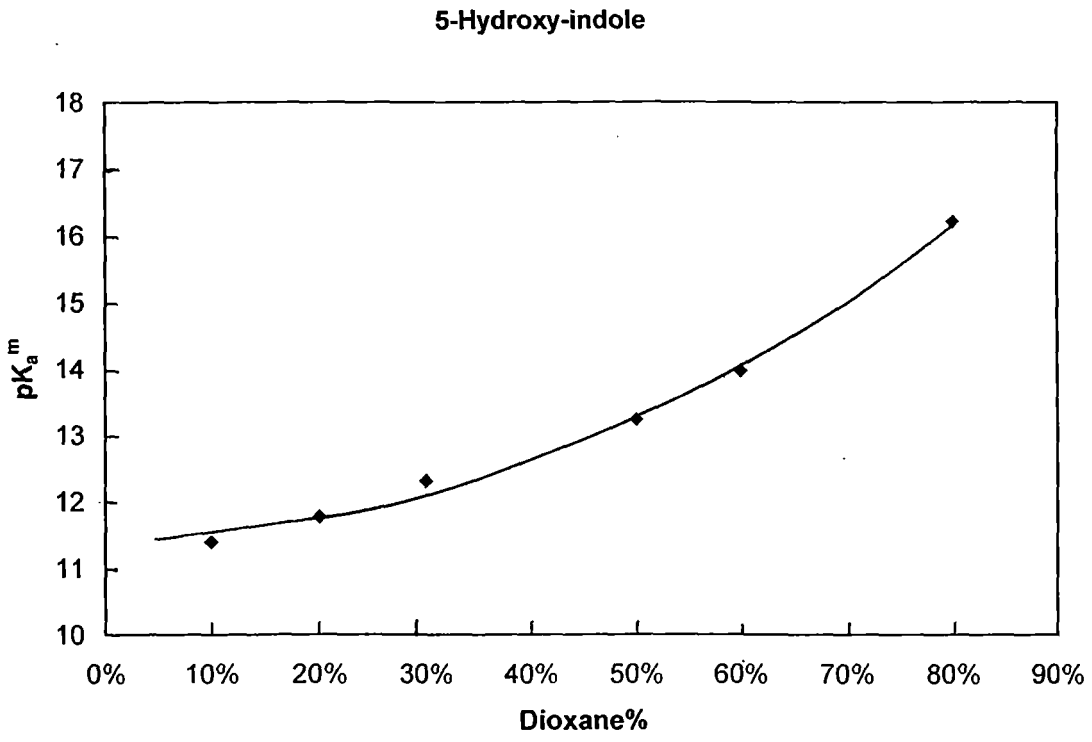

Fig.21.Plot of pK_a^m versus dioxane% of dioxane-water mixtures

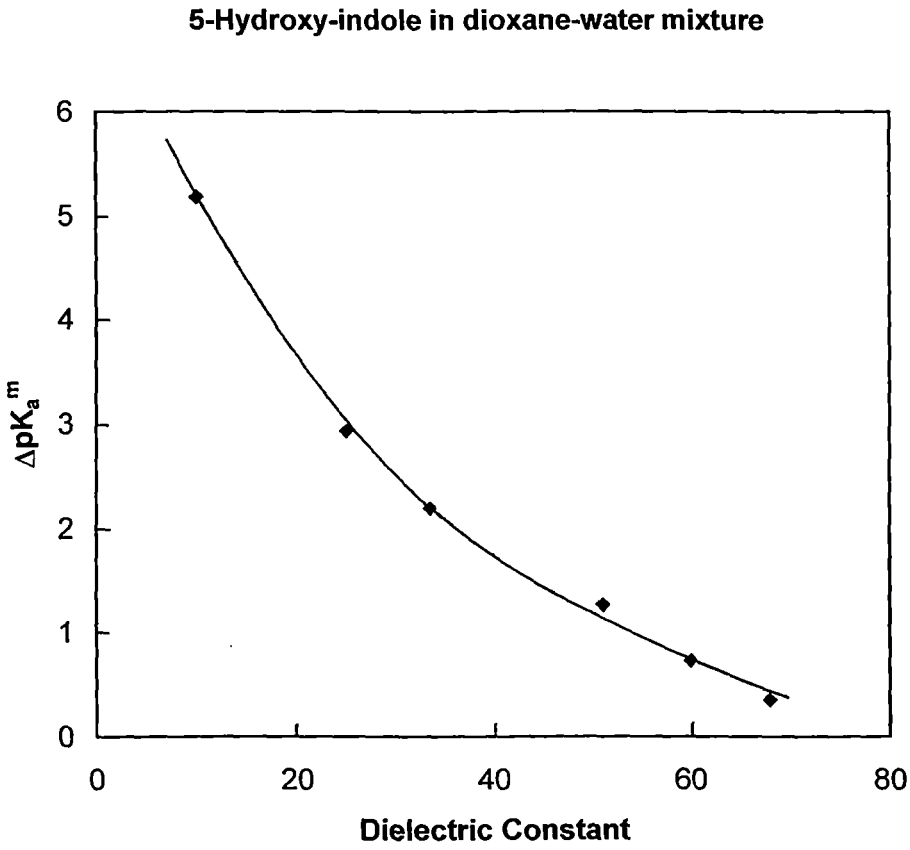

Fig.22.Plot of ΔpK_a^m versus dielectric constant of dioxane-water mixtures.

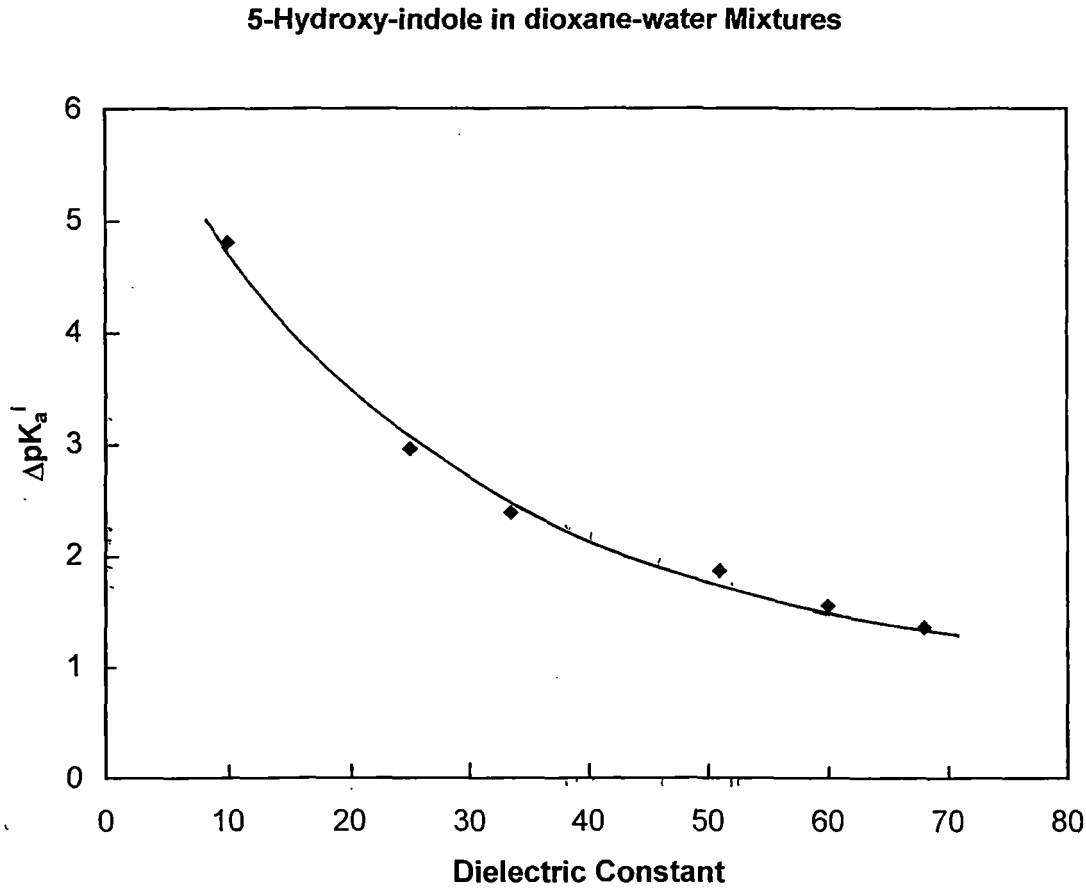

Fig.23.Plot of ΔpK_a^i versus dielectric constant of dioxane-water mixtures.

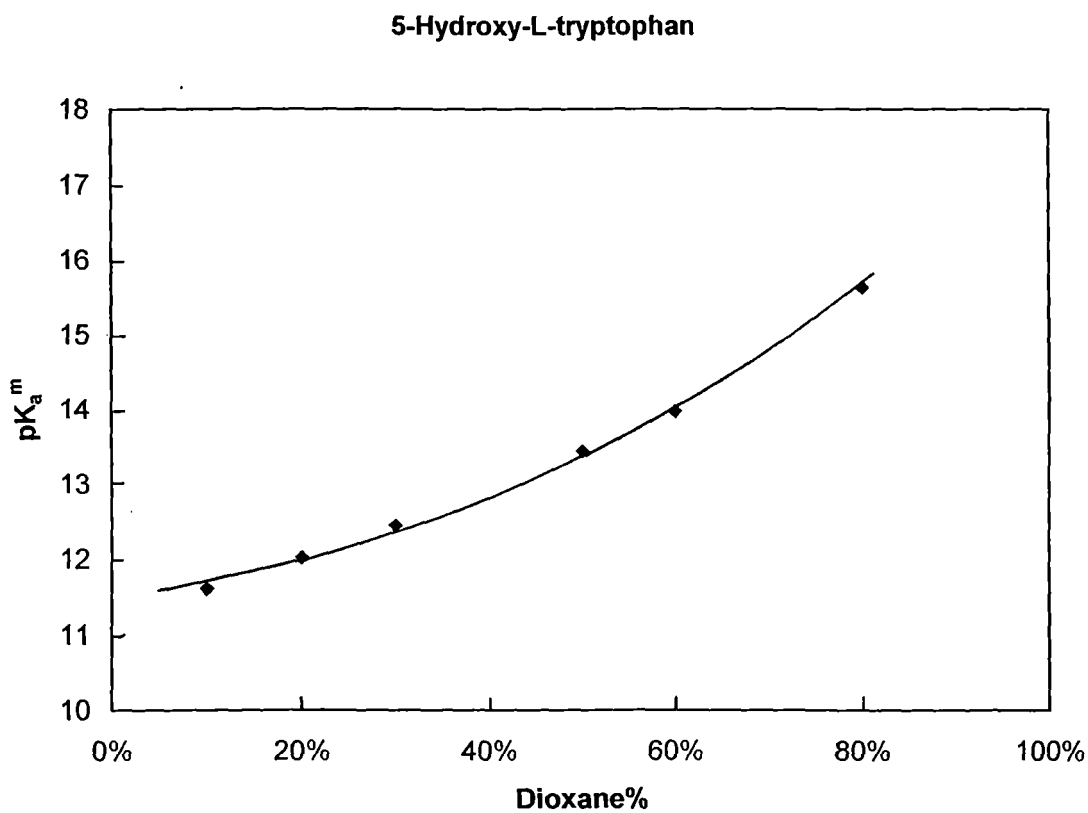

Fig.24.Plot of pK_a^m versus dioxane% of dioxane-water mixtures

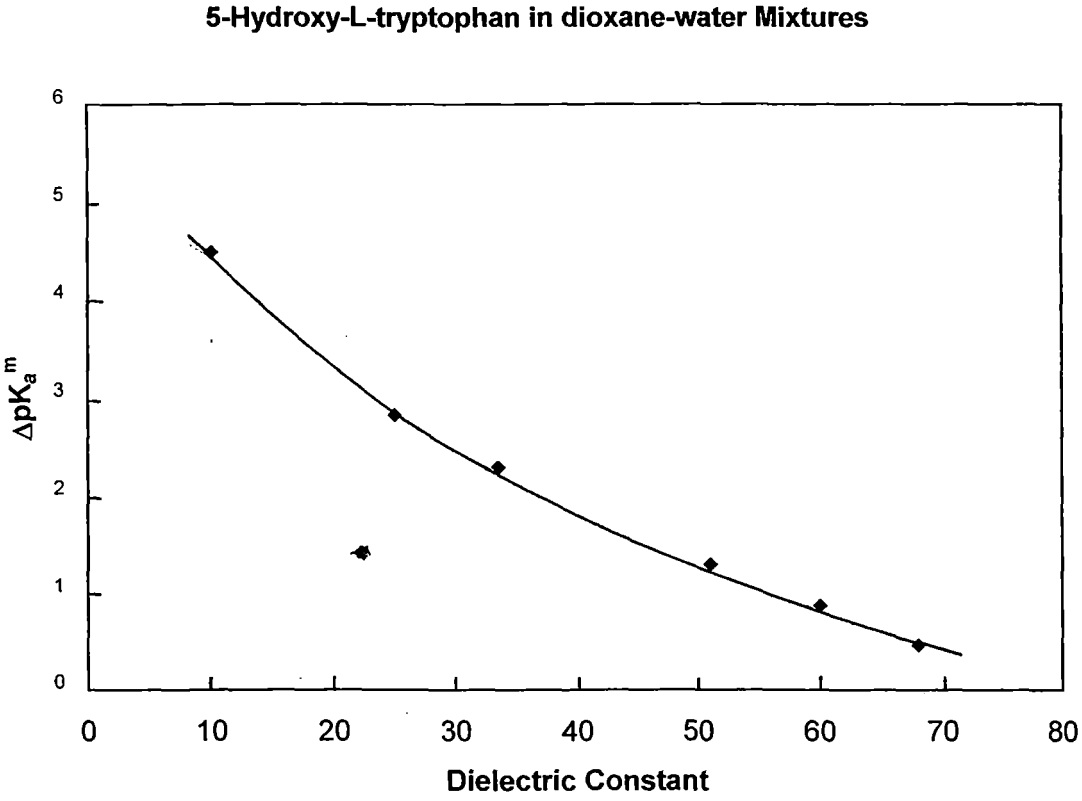

Fig.25.Plot of ΔpK_a^m versus dielectric constant of dioxane-water mixtures.

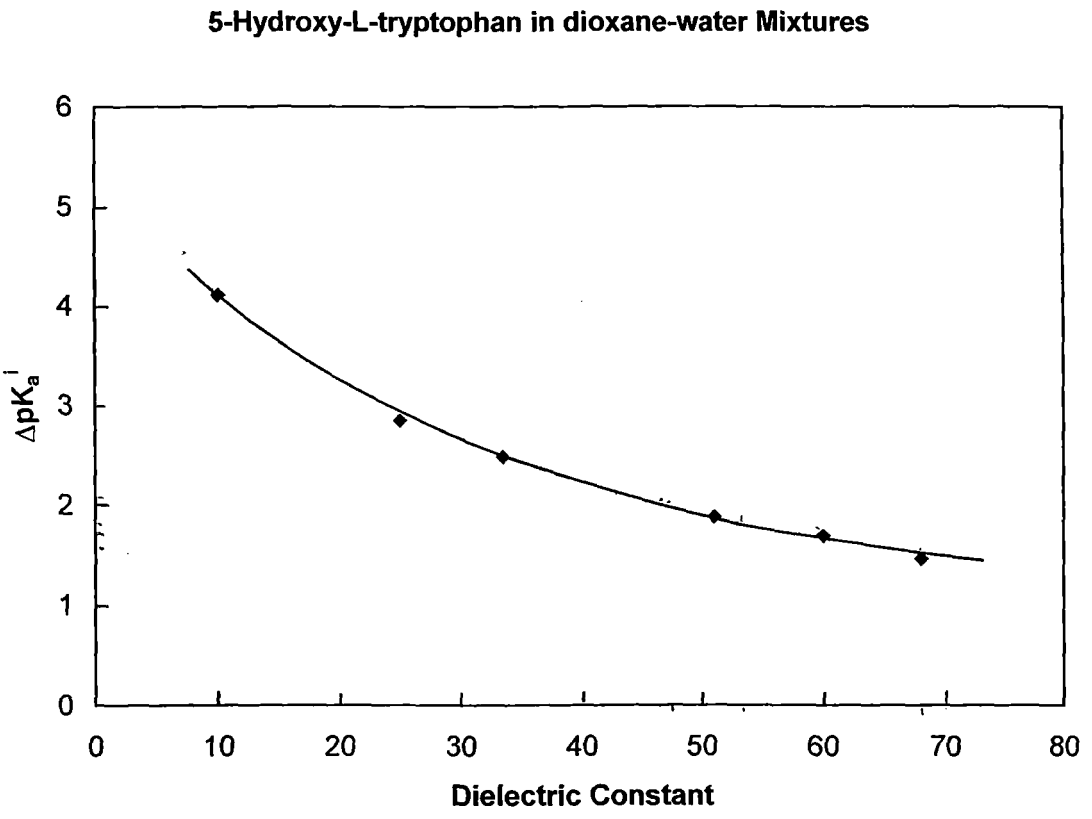

Fig.26.Plot of ΔpK_a^i versus dielectric constant of dioxane-water mixtures.

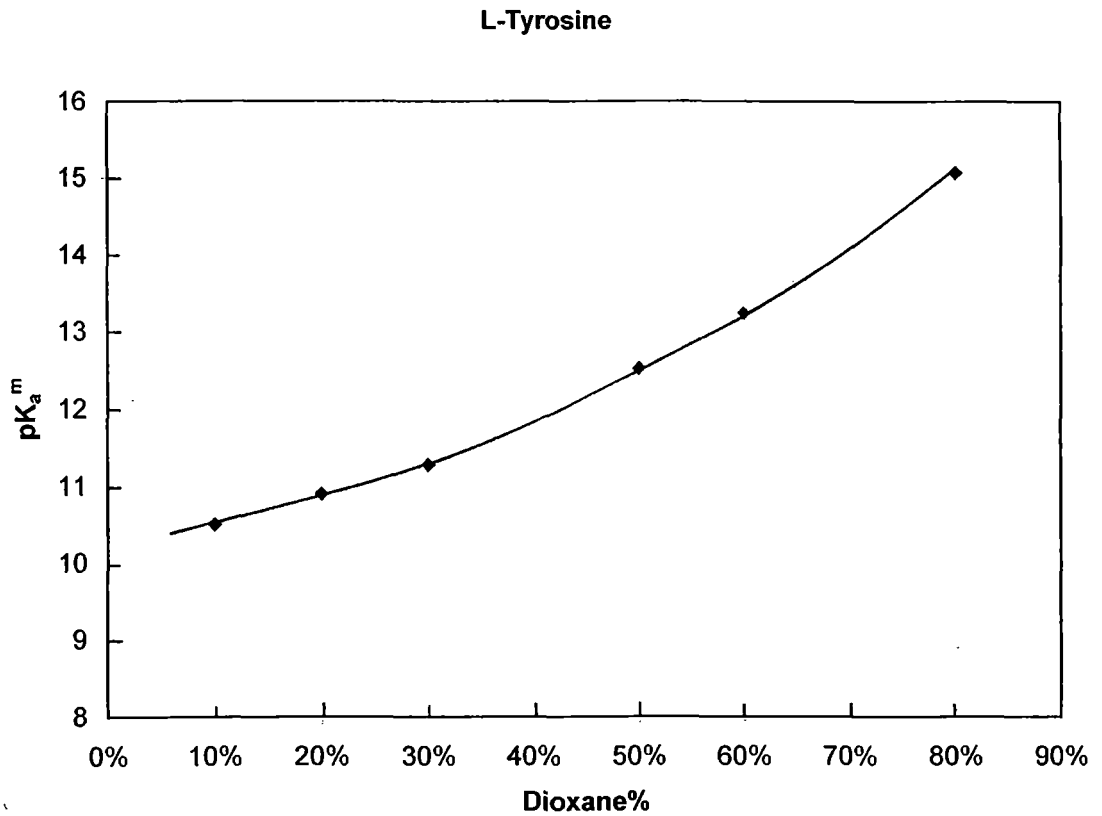

Fig.27 Plot of pK_a^m versus dioxane% of dioxane-water mixtures

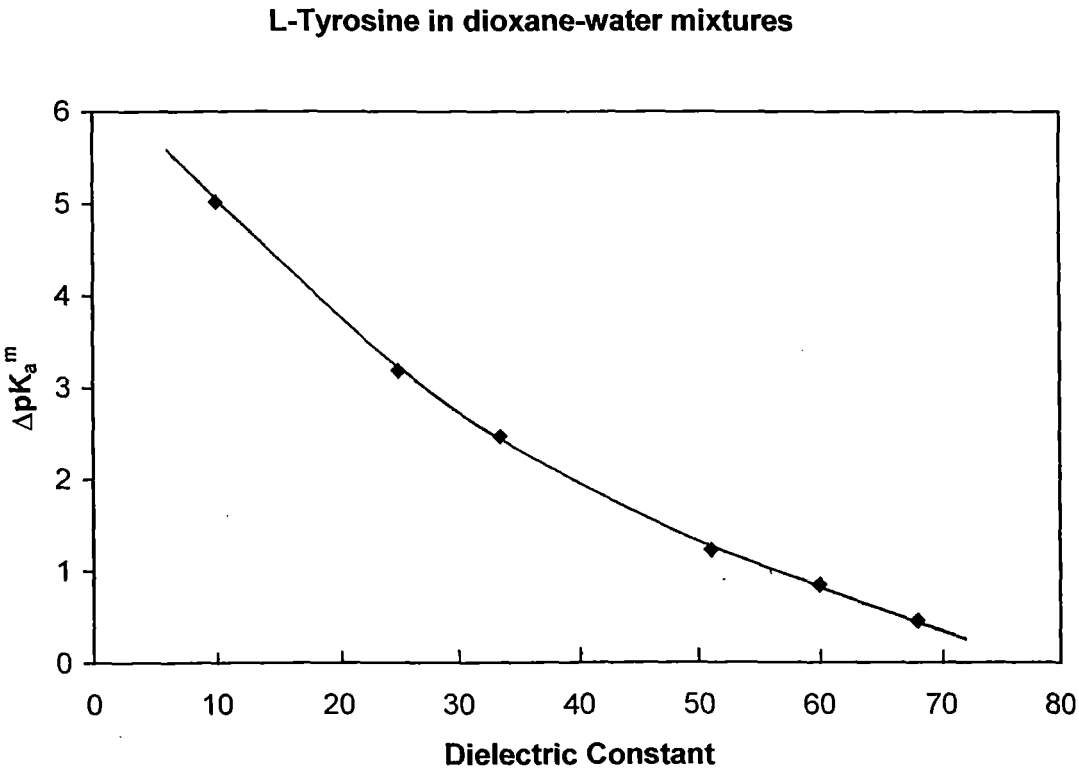

Fig.28.Plot of ΔpK_a^m versus dielectric constant of dioxane-water mixtures.

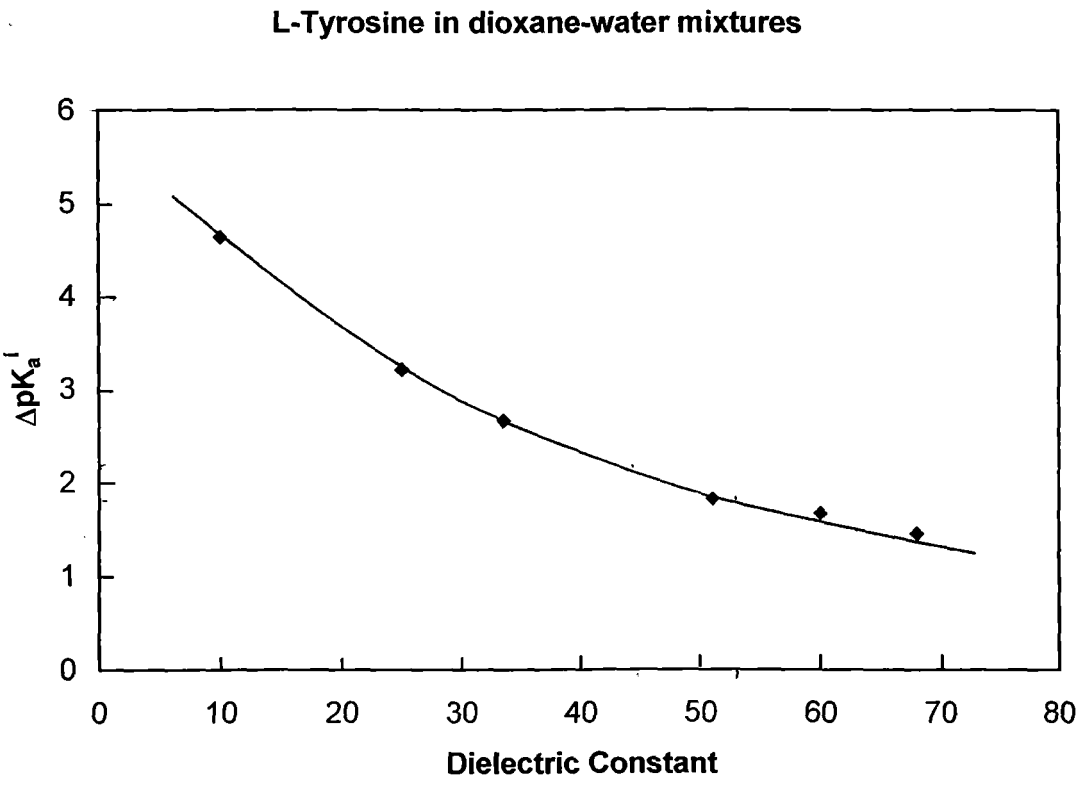

Fig. 29. Plot of ΔpK_a^i versus dielectric constant of dioxane-water mixtures.

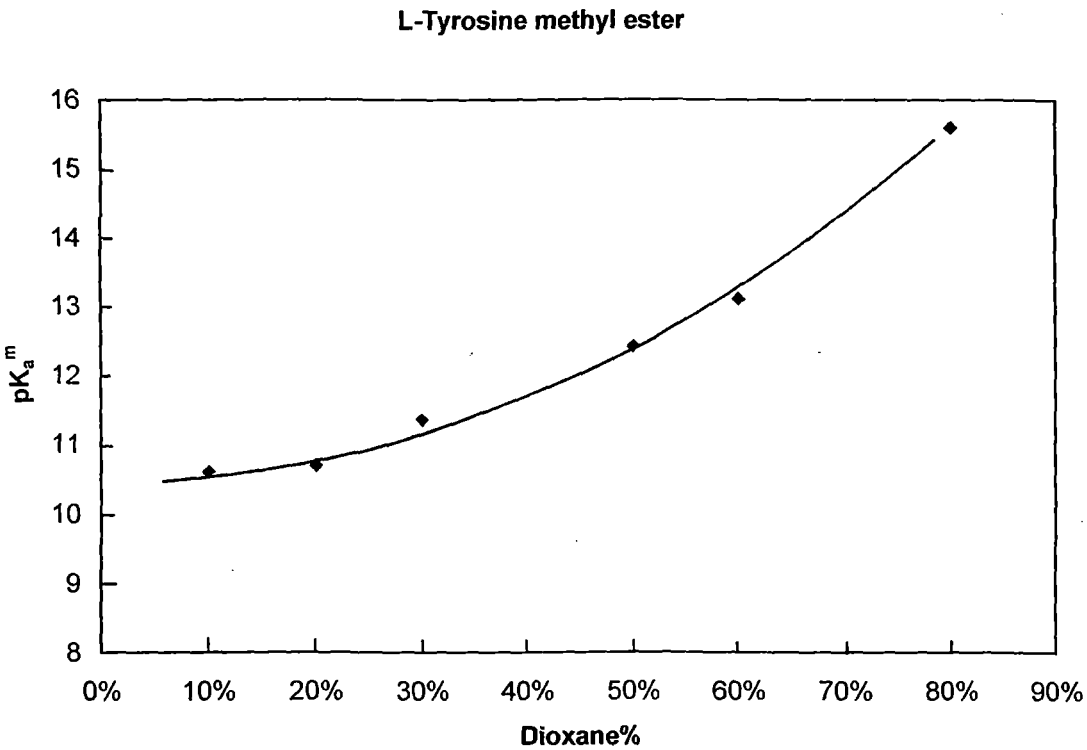

Fig.30.Plot of pK_a^m versus dioxane% of dioxane-water mixtures

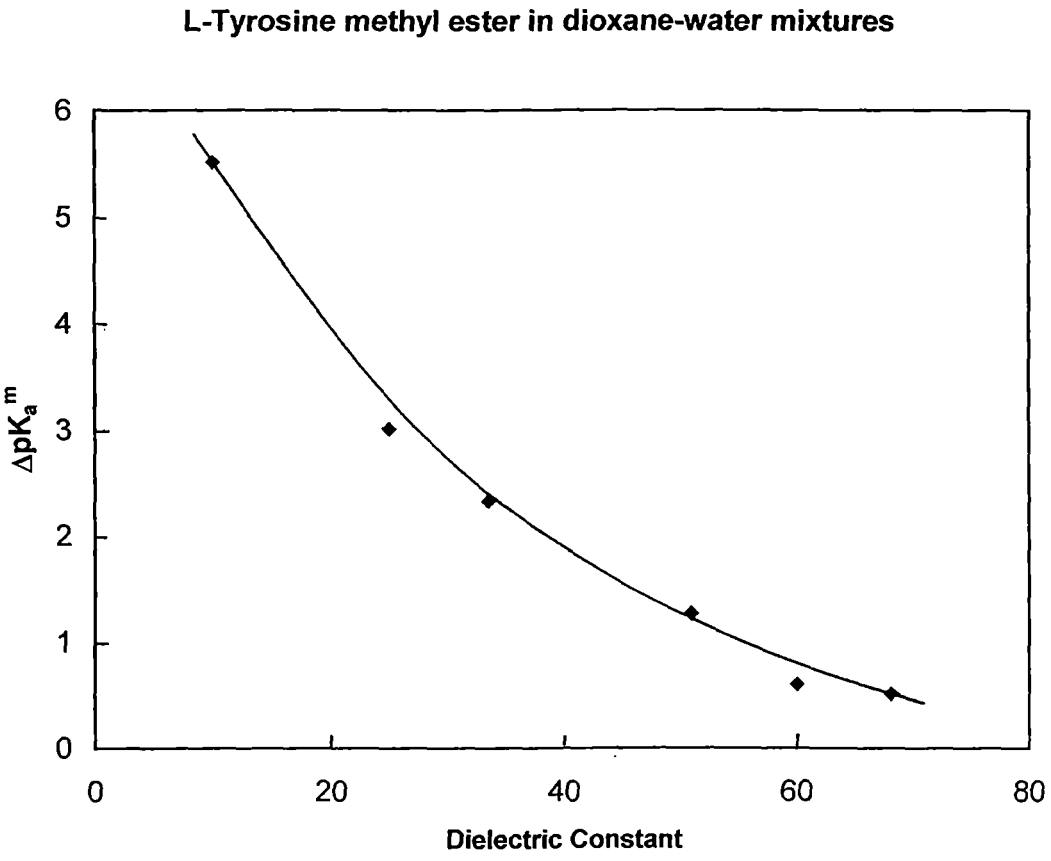

Fig.31.Plot of ΔpK_a^m versus dielectric constant of dioxane-water mixtures.

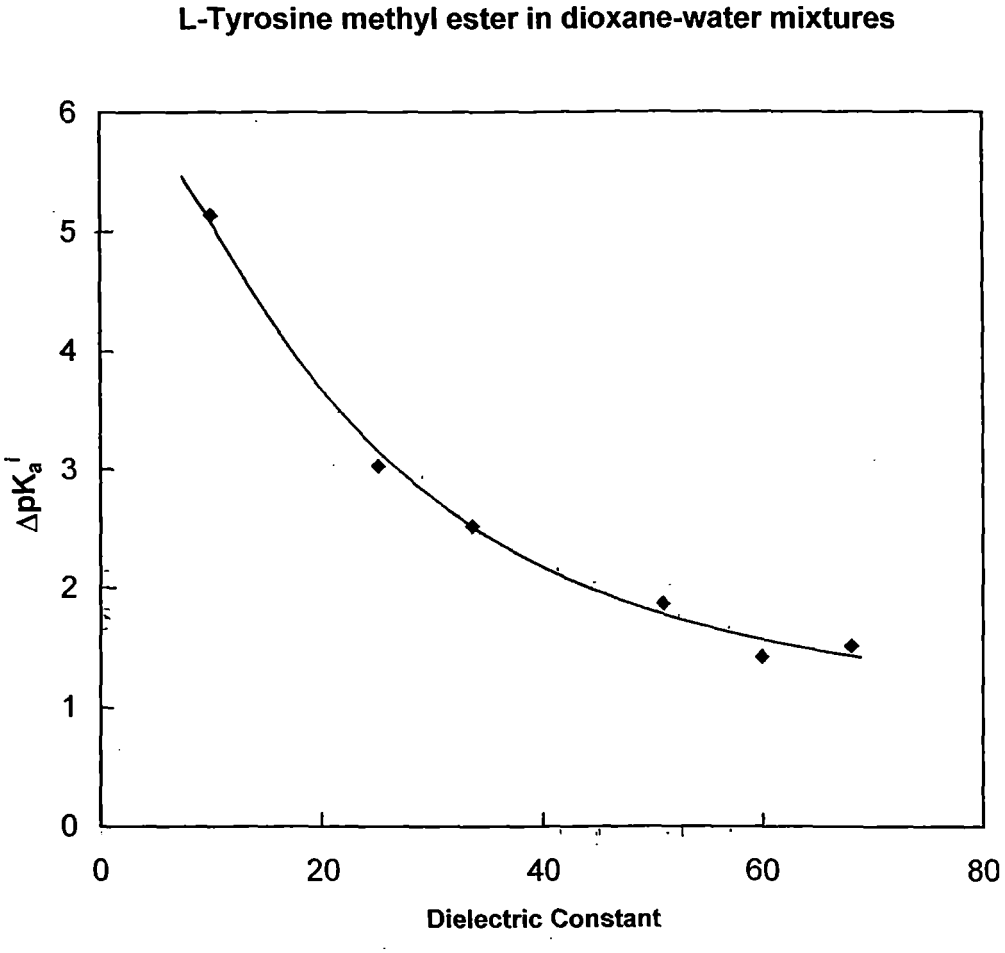

Fig.32.Plot of ΔpK_a^i versus dielectric constant of dioxane-water mixtures.

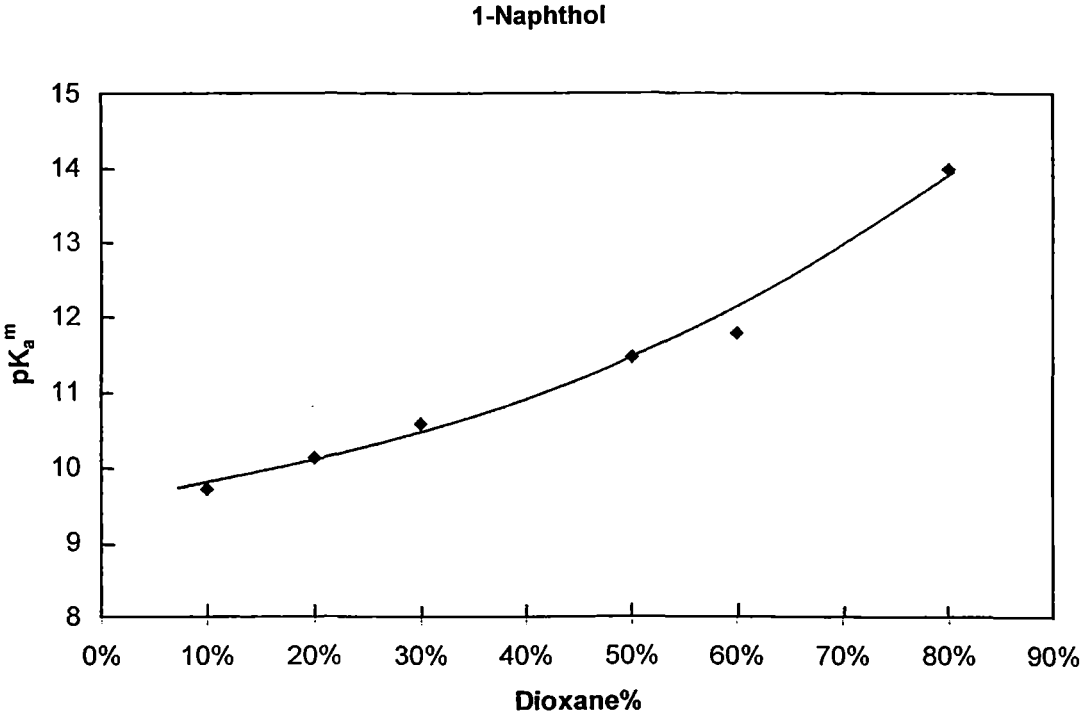

Fig.33.Plot of pK_a^m versus dioxane% of dioxane-water mixtures.

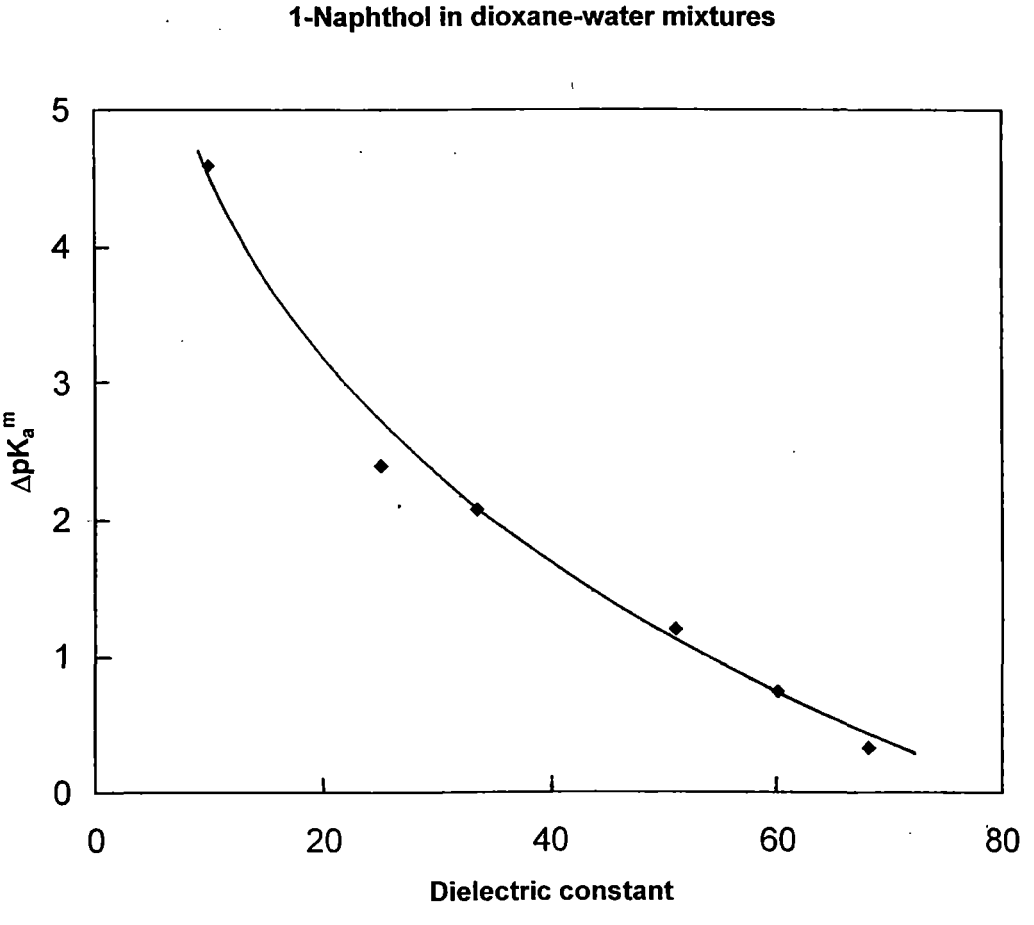

Fig.34.Plot of ΔpK_a^m versus dielectric constant of dioxane-water mixtures.

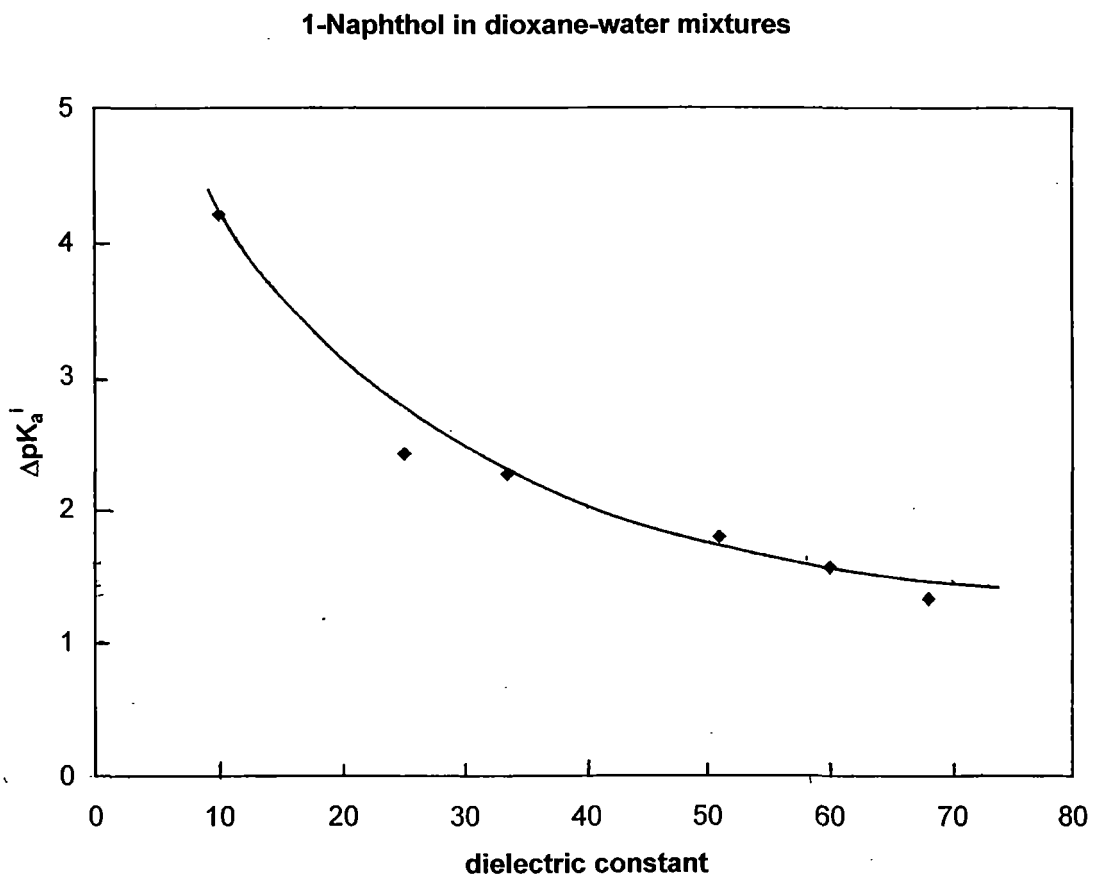

Fig.35.Plot of ΔpK_a^i versus dielectric constant of dioxane-water mixtures.

References

1. Hartley, G. S., *Quart. Rev.*, **2**, 152 (1948).
2. Hartley, G. S., *Micellization, Solubilisation and Microemulsions*, Ed. Mittal, K. L., Plenum New York, 23 (1977).
3. Fendler, J. H., Fendler, E. J., *Catalysis in Micellar and Macromolecular Systems*, Academic Press, New York, 48 (1975).
4. Fendler, J. H., *Membrane Mimetic Chemistry*, Wiley Interscience, New York (1982).
5. Lindman, B., Wennerström, H., *Top. Curr. Chem.*, **87**, 1 (1980).
6. Sudhölter, E. J. R., van der Langkruis, G. B., EngBerts, J. B. F. N., *Recl. Trav. Chim. Pay-Bas Belg*, **99**, 73 (1979).
7. Brown, J. M., Colloid Science, A. *Specialist Periodical Report*, Chemical Society, London, **3**, 253 (1979).
8. Kunitake, T., Shinkai, S., *Adv. Phys. Org. Chem.*, **17**, 435 (1980).
9. Ray, A., *Nature*, **231**, 313 (1971).
10. Ray, A., Nemethy, G., *J. Phys. Chem.*, **75**, 809 (1971).
11. Ionescu, L. G., Fung, D. S., *J. Chem., Soc., Faraday Trans. I*, **77**, 2907 (1981).
12. Evans, D. F., Nimham, B. W., *J. Phys. Chem.*, **87**, 5025 (1983).
13. Menger, F. M., Jerkunica, J. M., J. *Am. Chem. Soc.*, **101**, 1896 (1979).
14. Tanford, C., *The Hydrophobic Effect*, 2nd Edn., Wiley Interscience, New York, (1980).
15. Debye. P., *J. Phys. Colloid Chem.*, **53**, 1 (1949).
16. Debye. P., Anacker, E. W., *J. Phys. Colloid Chem.*, **55**, 644 (1951).
17. Mukherjee, P., Mysels, K. J., *Critical Micelle Concentrations of Aqueous Surfactant Systems*, National Bureau of Standerds, Washington D. C., (1970).
18. Menger, F. M., Portnoy, C. E., *J. Am. Chem. Soc.*, **89**, 4698 (1967).

19. Gunnarsson, G., Jonsson, B., Wennerström, H., *J. Phys. Chem.*, **84**, 3114 (1980).
20. Duynstee, E. F. J., Grunwald, E., *J. Am. Chem. Soc.*, **81**, 4540, 4542 (1959).
21. Kurz, J. L., *J. Phys. Chem.*, **66**, 2239 (1962).
22. Motsavage, V. A., Kostenbauder, H. B., *J. Colloid Sci.*, **18**, 603 (1963).
23. Bellocq, A. M., Biais, J., Bothorel, P., Clin, B., Fourche, G., Lalanne, P., Lemaire, B., Lemanceau, B., Roux, D., *Adv. Colloid Interface Sci.*, **20**, 167 (1984).
24. Mackay, R. A., *Adv. Colloid Interface Sci.*, **15**, 131 (1981).
25. Zana, R., Yiv, S., Strazielle, C., Lianos, P., *J. Colloid Interface Sci.*, **80**, 208 (1981).
26. Danielsson, I., Lindmann, B., *Colloids Surf.*, **3**, 391, (1981).
27. O'Connor, C. J., Lomax, T. D., Ramage, R. E., *Adv. Colloid Interface Sci.*, **20**, 21 (1984).
28. Albrizzio, J., Archila, J., Rodulfo, T., Cordex, E. H., *J. Org. Chem.*, **37**, 871 (1972).
29. O'Connor, C. J., Lomax, T. D., Ramage, R. E., in *Solution Behaviour of Surfactants* (Ed. by Mittal, K. L., Fendler, E. J.), Plenum Press, New York, **2**, 803 (1982).
30. Kitahara, A., *Adv. Colloid Interface Sci.*, **12**, 109 (1980).
31. El Seoud, O. A., Martins, A., Barbur, L. P., de Silva, M. J., Aldrigue., W., *J. Chem. Soc.*, Perkin Trans., **2**, 1674 (1977).
32. Robinson, B. H., Steytler, D. C., Tack, R. D., *J. Chem. Soc., Faraday Trans. I*, **75**, 481 (1979).
33. Thomas, J. K., *A. C. S. Monograph*, Washington D. C., 184 (1984).
34. Fernandez, M. S., Formherz, P., *J. Phys. Chem.*, **81**, 1755 (1977).
35. Mittal, K. L., Lindman, B., in *Surfactants in Solution*, Plenum Press, New York, **1, 2** (1984).
36. Daiz-Garcia, M. E., Sanz-Model, A., *Atlanta* **33**, 255 (1986).

37. Otsuka, K., Terabe, S., Chromatogr, J. A., **875**, 163 (2000).
38. Pileni, M. P., Nimham, B. W., Gulik-Krzywicki, T., Tanori, J., Lisiecki, I., Filancambo, A., *Adv. Mater.*, **11**, 1358 (1999).
39. Jana, N. R., Gearheart, L., Murphy, C. J., *Chem. Commun.*, 617 (2001).
40. Pal, T., Dey, S., Jana, N. R., Pradhan, N., Mandal, R., Pal, A., Beezer, A., Mitchell, J. C., *Langmuir*, **14**, 4724 (1998).
41. Dey, S., Pal, T., Pal, A., *Langmuir*, **16**, 6855 (2000).
42. Dey, S., Pal, T., Pal, A., Jana, N. R., *J. Photochem. Photobiol. A.* **131**, 111 (2000).
43. Pal, T., Ghosh, T. K., Pal, A., *Ind. J. Chem.*, **40 B**, 850 (2001).
44. Mallick, K., Jewrajka, S., Pradhn, N., Pal, *T., Curr. Sci.*, **80**, 1408 (2001).
45. Pal, T., Jana, N. R., *Langmuir*, **12**, 3114 (1996).
46. Lianos, P., *J. Chem. Phys.*, **89**, 5237 (1988).
47. Evesque, P., *I. Phys.* (Paris), **44**, 1217 (1987).
48. Blumen, A., Klafter, J., Zumofen, G., *Fractals in Physics*, Pietronero, L., Tosatt, E., Eds., North Holland, Amsterdam, 399 (1986).
49. Jana, N. R., Gearheart, L., Murphy, C. J., *J. Phys. Chem.*, **B 105**, 4065 (2001).
50. Heartley, G. S., Roe, J. W., *Trans. Faraday Soc.*, **36**, 101 (1940).
51. Mukherjee, P., Banerjee, K., *J. Phys. Chem.*, **68**, 3567 (1964).
52. Montal, M., Gitler, C., *Bioenergetics,* **4**, 363 (1973).
53. Cassidy, M. A., Warr, G. G., *J. Phys. Chem.*, **100**, 3237 (1996).
54. Saroja, G., Samanta, A., *Chem. Soc. Faraday Trans.*, **92**, 2697 (1996).
55. Laguitton, Pasquier, H., Pansu, R., Chauvet, J. P., Pernot, P., Collet, A., Faure, J., *Langmuir*, **13**, 1907 (1997).
56. Karukstis, K. K., Frazier, A. A., Loftus, C. T., Tuan, A. S., *J. Phys. Chem.*, **B 102**, 8163 (1998).
57. Novaki, L. P., O. A., El Seoud, *Langmuir*, **16**, 35 (2000).
58. Suratkar, V., Mahapatra, S., *J. Colloid Interface Sci.*, **225**, 32 (2000).
59. Pal, S. K., Mandal, D., Bhattacharya, K., *J. Phys. Chem.*, **B 102**, 11017 (1998).

60. Das, P. K., Chaudhury, A., *Langmuir,* **15**, 8771 (1999).
61. Bunton, C. A., Nome, F., Quina, R. H., Romsted, L. S., *Acc. Chem. Res.*, **24**, 357 (1991).
62. Romsted, L. S, Bunton, C. A., Yao, J. H., *Curr. Opin. Colloid Int. Sci.*, **2**, 622 (1997).
63. Romsted, L. S, *J. Phys. Chem.*, **89**, 5107(1985).
64. Romsted, L. S, *J. Phys. Chem.*, **89**, 5113(1985).
65. De Giorgio, V., Corti, M., *Physics of Amphiphiles, Micelles, Vesicles and Microemulsions*, Eds. North-Holland, Amsterdam, (1985).
66. Zana, R., Ed., *Surfactant Solutions: New Methods of Investigation*, Marcel Dekker, New York, (1986).
67. Cardinal, J. R., Mukerjee, P., *J. Phys. Chem.*, **82**, 1614(1978).
68. Mukerjee, P., Ber. Bunsen-Ges., *J. Phys. Chem.*, **82**, 931 (1978).
69. Mukerjee, P., Cardinal, J. R., *J. Phys. Chem.*, **82**, 1620 (1978).
70. Almgren, M., Grieser, F., Thomas, J. K., *J. Am. Chem. Soc.*, **101**, 279 (1979).
71. Lianos, P., Viriot, M. L., Zana, R., *J. Phys. Chem.*, **88**, 1098 (1984).
72. Viaene, K., Verbeek, A., Gelade, E., De Schryver, F. C., *Langmuir*, **2**, 456 (1986).
73. Healy, T. W., White, L. R., *Adv. Colloid Interface Sci.*, **9**, 303 (1978).
74. Formherz, P., Kotulla, R., Ber. Bunsen-Ges., *J. Phys. Chem.*, **88,** 1106 (1984).
75. Drummond, C. J., Grieser, F., Healy, T. W., *J. Phys. Chem.*, **92,** 2604 (1988).
76. Drummond, C. J., Grieser, F., Healy, T. W., *Faraday Discuss. Chem. Soc.*, **81**, 95 (1986).
77. Drummond, C. J., Warr, G. G., Grieser, F., Ninham, B. W., Evans, D. F., *J. Phys. Chem.*, **89,** 2103 (1985).
78. Drummond, C. J., Grieser, F., *Langmuir*, **3**, 855 (1987).
79. Drummond, C. J., Grieser, F., White, L. R., Murray, B. S., *J. Phys. Chem.*, **92,** 5586 (1988).

80. Riddick, J. A., Bunger, W. B., *Techniques of Organic Chemistry, Organic Solvents*, Wiley Interscience, New York, **2**, 592 (1970).

81. Van Uitert, L. G., Haas, C. G., *J. Am. Chem. Soc.*, **75**, 541 (1953).

82. Harned, H. S., Owen, B. B., *The Physical Chemistry of Electrolyte Solutions*, Reinhold, New York, 3rd Edn., (1958).

83. Drummond, C. J., Grieser, F., Healy, T. W., *J. Chem. Soc. Faraday Trans. 1*, **85**, 37 (1989).

84. Sanchez-Ruiz, J. M., Llor, J., Cortijo, M., *J. Chem. Soc. Perkin Trans. 2*, 2047 (1984).

85. Critchfield, F. W., Gibson, J. A., Hall, J. L., *J. Am. Chem. Soc.*, **75**, 1991 (1953).

86. Lamm, G., Pack, G. R., *J. Phys. Chem.*, B, **101,** 9589 (1997).

CHAPTER – 4

PHOTOPHYSICAL PROPERTIES OF INDICATOR MOLECULES IN DIFFERENT DIELECTRIC MEDIA

4.1. Introduction and review of previous works

Solvents possesses polar or apolar characteristics. These properties control the reactivity as well as physicochemical characteristics of a process at the molecular level. As a result, solvents play a significant role in chemical and biological processes. One common use of solvent effect is to determine the polarity of the probe-binding site on the macromolecule. This is accomplished by comparison of the emission spectra of the fluorophore when it is bound to the macromolecule and dissolved in solvents of different polarities. However, there are many additional instances where solvent effects are important. When a fluorescent ligand binds to a protein or a fluorophore binds to membranes, the binding is usually accompanied by a spectral shift due to the different environment for the bound ligand or the fluorophore. Compartmentalized water in cells and reverse micelles, microemulsions, liposomes and gels as well as the aqueous environment at the interfaces of normal micelles are known to be physicochemically different from the bulk water[1-8] with regard to polarity, structure and pH. Reactions performed therein may significantly deviate from the normal courses and are often catalyzed in compartmentalized environments.[9-13] It is thus necessary to ascertain the polarity /apolarity of the solvents which are often estimated from the knowledge of their dielectric constant, Kosower-Z value, the charge transfer transition energy, the kinetically derived parameters of Y-man, the Y-value, etc.[14]

Overview of solvent effect

When the fluorophores get excited, emission from the fluorophores generally occurs at longer wavelengths as compared to the absorption. This loss of energy is due to a variety of dynamic processes that occur following light absorption (fig.1). The fluorophore is typically excited to the first singlet state (S_1).

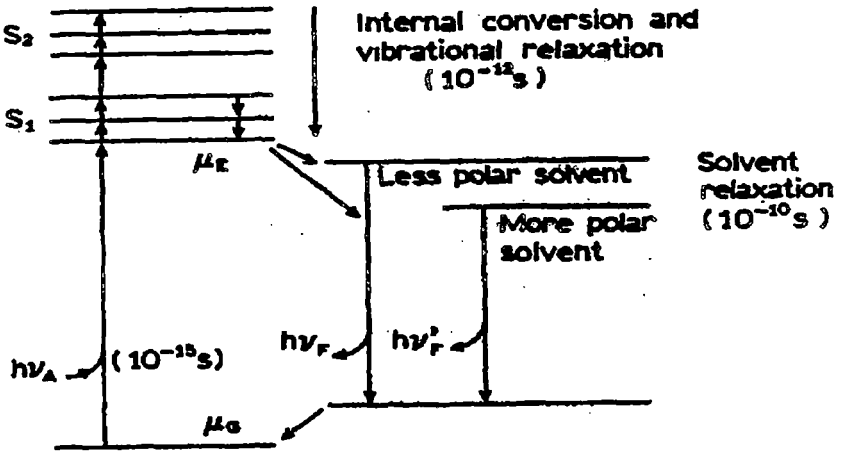

Fig.1. Jabloński diagram for fluorescence with solvent relaxation

The excess vibrational energy is rapidly lost to the solvent. If the fluorophore is excited to the second state (S_2), it rapidly lost to the S_1 state in 10^{-12} s due to the internal conversion. Solvent effect shifts the emission to still lower energy owing to the stabilization of the excited state by the polar solvent molecules. Typically, a fluorophore has a larger dipole moment in the excited state (μ_E) than the ground state (μ_G). Following excitation, the solvent dipoles can reorient or relax to around μ_E, which lowers the energy of the excited state. As the polarity of the solvent is increased, the effect becomes larger, resulting in the emission at lower energies or longer wavelengths. In general, nonpolar molecules are much less sensitive than polar molecules towards the solvent polarity.

Fluorescence life time (1-10 ns) is generally longer than the time required for solvent relaxation (10-100 ns). So, observing the emission spectra, one can understand the solvent relaxation state. Fig 1 shows why the absorption spectra are less sensitive to the solvent polarity than the emission spectra.

Mechanism of the spectral shifts:

It is well known that due to the general solvent effects, fluorescence spectral shifts occur. But this theory is often insufficient because there are some other reasons, one of which is that there is a variety of environment, which changes the nature of the fluorophores. Fluorophores often undergoes specific interactions with the local environment causing a spectral shift by amounts comparable to the general solvent effects. As for instance, when small amount of ethanol is added to indole[15] in a nonpolar solvent cyclohexane, causes a spectral shift more than that caused due to general solvent effects. This is specific because the amount of ethanol added is too small to change the polarity of the solvent. Here, the specificity is due to the hydrogen bonding to the imino group of indole ring.

Besides this specific interaction, another type of interaction has been reported which occurs due to the internal charge-transfer state or a twisted charge-transfer state.[16] This happens in case of fluorophores containing both an electron donating and electron-accepting group. When this type of fluorophores gets excited, there is an increase in charge-separation within it. In polar solvents, the charge-transferred state becomes the lowest energy state, following Kashes' rule[17] which states that emission occurs from the lowest energy excited state. In nonpolar solvents, no charge-transfer takes place, and the species got locally excited which becomes the lowest energy excited state. In some cases, the internal charge transfer state requires rotation of groups on fluorophore to form twisted charge transfer state. Thus, polarity of the solvent sometimes determines which will be the lowest energy excited state due to the charge transfer.

Therefore, there are mainly two types of solvent effects. One is the general solvent effect that is caused due to the interaction of the dipole of the fluorophore with its environment and the other is the specific solvent effect that again may be of two types. One is caused due to fluorophore-solvent

interaction and the other due to the charge transfer or twisted charge transfer state formation depending on the probe structure and the solvent.

General solvent effect – Lippert equation[19]

Though there are various types of solvent effects, the general solvent effect is most important. This effect provides many information for solvent dependent spectral shifts. While considering this theory, other effects can be detected as deviation from this theory. According to this general solvent effect theory, the fluorophore is assumed to be a dipole in a continuous medium of uniform dielectric constant (fig.2).

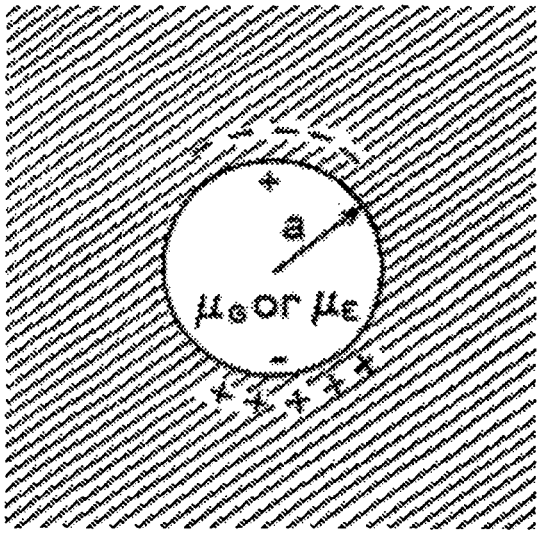

Fig. 2. Dipole in a dielectric medium

The dielectric constant (D) and the refractive index (n) of a solvent affect the emission and absorption.[18,19] The interactions between the solvent and fluorophore affects the energy difference between the ground state and the excited state. Lippert[19] related this energy difference (in cm^{-1}) to the solvent properties like dipole moment (μ), dielectric constant (D) and refractive index (n) by the equation:

$$\tilde{\nu}_A - \tilde{\nu}_F = \frac{2}{hc}\left(\frac{D-1}{2D+1} - \frac{n^2-1}{2n^2+1}\right)\frac{(\mu_E - \mu_G)^2}{a^3} + \text{const.} \qquad (1)$$

In the above equation $\tilde{\nu}_A$ and $\tilde{\nu}_F$ are the wave numbers of absorption and emission respectively, *h* is the Plank's constant, *c* is the speed of light, μ_G and μ_E are the dipole moments of the solvent in the ground state and excited state respectively and *a* is the radius of the cavity in which the fluorophore resides. The eqn. (1) is useful to correlate the observed and calculated energy losses in non-protic solvents. The protic and non-protic solvents are those having hydroxyl groups or other groups that are capable of hydrogen bonding or not.

The refractive index and the dielectric constants have opposite effects on the Stokes' shift. The dielectric constant (D) is a static property, which depends on both electronic and molecular motions. By molecular motions, solvent reorientation around the excited state occurs whereas the refractive index (n) depends on motion of electrons within the solvent molecules. An increase in refractive index decreases the energy losses in the absorption band whereas an increase in dielectric constant results in an increase in Stokes' shift.

The term in the above equation, i.e., $[(D-1)/(2D+1) - (n^2 - 1)/(2n^2 + 1)]$ is called the solvent polarity function or the orientation polarizability (Δf). The first term i.e., $(D - 1)/(2D + 1)$ accounts for the spectral shifts due to the reorientation of the solvent dipoles as well as the redistribution of the electrons in the solvent molecules. The second term, $(n^2 - 1)/(2n^2 + 1)$ accounts only for the re-distribution of electrons. The difference between the two terms is called the orientation polarizability or the solvent polarity function (Δf) as it accounts for the spectral shifts due to the reorientation of the solvent molecules. According to this theory, only the solvent reorientation is expected to result in substantial Stokes' shifts.

Hexane, being a nonpolar solvent, does not possess dipole moment. So, there is no question of dipole reorientation around the excited state of the

fluorophore. From the Lippert equation one can calculate the value of Δf, i.e., the orientation polarizability whereas ($\tilde{\nu}_A$ - $\tilde{\nu}_F$) is expected to be very small or zero. But in case of non-polar solvents both of their bands do not coincide. Most of the excitation occurs usually at higher vibrational energy level and this energy rapidly (10^{-12}s) got dissipated in the solvents. As the emission occurs to an excited vibrational energy level of the ground state, the absorption and emission bands are shifted by an amount that is at equal to the vibrational energy. These energy losses are accounted for by the constant term of Lippert equation.

When the above experiment is performed in a polar solvent like methanol, substantially larger Stokes' losses are expected. This is due to the large orientation polarizability of methanol for its high dipole moment. This sensitivity of Stokes' shift to the solvent polarity is used to measure the polarity of the environment surrounding the fluorophore by means of fluorescence measurements.

Application of the Lippert equation – the general solvent effect

As the polarity of the solvent affects the emission spectral band, so the emission spectra of the fluorophores are often used to label the macromolecules that are sensitive towards the solvent polarity. Various types of macromolecules of this type are known which show very low fluorescence in water but become highly fluorescent in nonpolar solvents or when bound to proteins and membranes. These probes are highly sensitive towards the solvent polarity and can potentially reveal the polarity of their immediate environments.[20]

In order to estimate the solvent sensitivity of a fluorophore, Lippert plot is useful. This is a plot of ($\tilde{\nu}_A$ - $\tilde{\nu}_F$) versus Δf, i.e., the orientation polarizability. The sensitive fluorophores are chosen from those that undergo largest changes

in dipole moments when excited. It is reported that N-phenyl-N-methyl derivative of 6-amino-naphthalene-2-sulphonic acid is more sensitive than unsubstituted amino derivative of naphthalene sulphonic acid.[21] In the case when general solvent effect is operative; a linear Lippert plot is obtained. On the other hand, in the case of specific solvent effect, a non-linear Lippert plot is obtained. Thus the solvent effect on fluorescence emission not only depends on dielectric constant and refractive index of the solvents (the general solvent effect) but also on the specific interaction between the solvent molecules and the fluorophores.

Specific solvent effect:

In contrast to the general solvent interactions with the fluorophores, specific interactions are produced by one or more neighboring molecules of the solvent and are determined by the specific chemical properties of both of solvent and the fluorophore.[22,23] Specific solvent interactions may refer to some factors as mentioned earlier, viz., hydrogen bonding, acid-base reaction or charge transfer interactions. Specific interactions between the solvent and the fluorophore are identified by observing the fluorescence emission spectra of a fluorophore in a variety of solvents. One important example reported is for 2-anilinonaphthalene in hexane[24] where addition of low concentration of ethanol (i.e., 2-3%) can change the solvent molecular properties and the change in the spectral shifts which is about 50% as compared to the change when 100% alcohol is added and a full spectral shift is observed. Above change in spectral feature is an important example of specific solvent interaction. The specific solvent effect occurs due to the addition of trace amount of ethanol via hydrogen bond formation between ethanol and the fluorophore.

The specific solvent-fluorophore interaction may occur either in ground state or in the excited state. In the case of interaction occurred in the excited state, the polar additive does not affect the absorption spectra, but if it is

occurred in the ground state, there is some change in the absorption spectra as expected.

Specific solvent effects and Lippert plot:

Like general solvent effect, evidence for the specific solvent-fluorophore interaction can also be seen in the Lippert Plot. In the Lippert Plot of the system, specific solvent-fluorophore interaction occur, the Stokes' shift is generally larger in the event of hydrogen bonding solvents (like water, methanol, ethanol etc.) than in solvents which less readily forms hydrogen bonds.[25,26] Such behaviour is typical for specific solvent-fluorophore interactions. The excess spectral shifts were explained by hydrogen bonding between the polar solvent and the polar group of the fluorophore.[27] The emission spectra of the fluorophores depend on orientation polarizability (the solvent polarity function) of the solvent as well as on the detailed chemical structures of the fluorophores and the solvents.[28] In these cases, the Stokes' shifts are approximately proportional to the orientation polarizability of the solvents but larger shifts are found in case of those solvents where hydrogen bond formation is possible. The excess spectral shift is also reported for the ester fluorophores.[29] This is due to the localization of a negative charge on the oxygen atom of the ester group and strong hydrogen bond forming ability of this group to the protic solvent.

In the present chapter, studies have been undertaken to understand the behaviour of some organic molecules in water and in a number of selected alkanols (solvent) with varying dielectric constant, refractive index, Kosower-Z values etc. The solutes are, 5-Hydroxyindole, 5-Hydroxy-L-Tryptophan, L-Tyrosine, L-Tyrosinemethylester, 1-Naphthol, 2-Naphthol. The solvents used, are water, Methanol, Ethanol, *iso*-Propyl alcohol, *tert*-Butyl alcohol, Pentanol, Hexanol, Heptanol and Octanol. 1,4 Dioxane-water mixture with varying compositions was used as solvent-water mixture. We have measured the

emission and absorption spectra for the different solutes in water, alkanols and dioxane-water mixtures. The Stokes' shifts calculated from the absorption and emission spectra for all the above solvents have been analyzed in a convincing way to correlate all the studied solvent systems. In this correlation attempt, the roles of Kosower-Z values and the dielectric constant (D) values have also been considered.

4.2. Experimental

The solute molecules, viz., 5-Hydroxyindole, 5-Hydroxy-L-tryptophan, L-Tyrosinemethylester were all Fluka graded and were used as received from Sigma-Aldrich Chemical Co., U.S.A. As mentioned in chapter-3, L-Tyrosine was obtained from Himedia, India and was used without any further purification. 1-Naphthol, 2-Naphthol were supplied by E. Merck, India. These were used after purification twice by vacuum sublimation. The alkanols used were received from Lancaster, England. 1,4- Dioxane was obtained from E. Merck, Germany and was used after purification following procedure mentioned in experimental section of chapter 3. Water used in the present study to prepare stock solutions was double distilled in an all-glass set-up.

The absorption and fluorescence spectra were recorded in double beam uv-visible spectrophotometer (Shimadzu, model UV-240, Japan) and Spectrofluorometer (model: SL- 174, ELICO, India) respectively. Silica cells of 1 cm path length were used in the measurements.

4.3. Results and discussion

The Absorption and Fluorescence spectra were recorded for all the solutes viz., 5-Hydroxyindole, 5-Hydroxy-L-tryptophan, L-Tyrosine, L-Tyrosine-methylester, 1-Naphthol, 2-Naphthol, at a fixed concentration of $1x10^{-4}M$ separately in different solvents such as water, methanol, ethanol, *iso*-propyl

alcohol, *tert*-butyl alcohol, pentanol, hexanol, heptanol, octanol and 1,4 Dioxane-water mixtures of different compositions viz., 10%, 20%, 30%, 50%, 60% and 80% (w/v) respectively at 298K. Representative spectra are shown in the figures 3 to 54. The spectra are significantly sensitive to the change in the polarity of the medium. Different solutes (indicator molecules) show maximum absorption band at different wavelengths for water and different solvents and also in 1,4-dioxane-water mixtures. As for example, the maximum absorption band of 1-Naphthol in water appears at 318 nm, while the maximum absorption bands in different alkanols with increasing alkyl chain length appear in the range of 320-331 nm and upon excitation, the fluorescence maximum of 1-Naphthol in water appears at 440 nm, but in alkanols, with increasing alkyl chain length, the fluorescence maxima appears in the range of 350-352 nm. The intensities of both of absorption and fluorescence bands also increase with increase in alkyl chain length of the alkanols. The wavelengths at which the other additives show maximum absorption bands and fluorescence maxima in different solvents are also observed.

Spectral features in relation to Solvent parameters:

The transition energies (both absorption and fluorescence) of all the additives with Stokes' shift in different media (in cm^{-1}) are presented in Tables 1 and 11. The solvent parameters like dielectric constant (D), refractive index (n), Kosower-Z value etc. can be correlated with the Stokes' shifts ($\Delta\tilde{\nu}$) of all the additives in water and in different alkanols. The plot of Stokes' shift ($\Delta\tilde{\nu}$) against the refractive index function, $(n^2 - 1)/(2n^2 + 1)$ and the dielectric constant function, $(D - 1)/(2D + 1)$ of the different solvents (e.g., water and alkanols) are shown in figures 55-59 and of 1,4-Dioxane-water mixtures (Figs. 60-65). Figs. 66-70 show the linear variation of the Stokes' shift with the Kosower-Z value of the same solvent. Similar plots of Stokes' shift against the solvent polarity parameters viz., $(n^2 - 1)/(2n^2 + 1)$ and $(D - 1)/(2D + 1)$ of

mixed solvents of dioxane-water mixtures of various compositions are depicted in figs. 71-75 for different additives. The linearity of these plots is often regarded as the evidence for the dominant importance of general solvent effect in spectral shifts. The plot of Stokes' shift ($\Delta\tilde{\nu}$) versus solvent polarity function $[(D - 1)/(2D + 1) - (n^2 - 1)/(2n^2 + 1)]$ is also found to be linear where the general solvent effect occurred. The non-linearity of the Lippert plot (plot of Stokes' shift versus solvent polarity function) is due to the specific solvent effects. This is because there is a possibility of hydrogen bonding between the polar solvent molecule and polar group on the fluorophore. In the case of L-Tyrosinemethylester, the specific solvent effect is attributed to the fact that there is a localization of the negative charge on the oxygen atom of the ester group.[29] In water, Stokes shifts are higher as compared to other solvents, which can be interpreted, as due to the higher value of dielectric constant of water as compared to those solvents. While comparing all the plots of Stokes' shift against orientation polarizability, it is assumed that the Stokes' shifts are approximately proportional to the orientation polarizability i.e., solvent polarity function.

In the case of interactions between the fluorophores and dioxane-water mixtures, excess Stokes' shifts are observed in the order 10% > 20% > 30% > 50% > 60% > 80%. This may also be due to the hydrogen bonding between the protic group of the fluorophore and the solvent mixtures. Here 1-Naphthol, 2-Naphthol, 5-Hydroxyindole, 5-Hydroxy-L-tryptophan contain OH group and L-Tyrosine and L-Tyrosinemethylester and 5-Hydroxy-L-tryptophan contain both OH and NH_2 groups both of which are capable of forming hydrogen bond. In all these cases, the Stokes' shifts increases with increase in the solvent polarity function. The immediate spectral shifts occurs which is attributed to the polar nature of both of the solvent and the fluorophore both are polar and both are associated in the ground state.[30] If they were associated in the excited state only these properties would have been dependent on the rates of diffusion of the polar solvent and the fluorophore. In these cases, the dependence on the

concentration of the polar solvent would be similar to that for quenching reactions. From the plot of Stokes' shift and dielectric constant function (D – 1)/(2D + 1) in different solvents in the presence of all the indicators, the Stokes' shift become larger as the dielectric constant function increases (Figs. 55-65). Maximum shift is found in water with maximum dielectric constant function due to its large dielectric constants. Here the spectral shifts are due to both of the orientation of the solvent dipoles and redistribution of electrons in the solvent molecules. While moving towards the other solvents, viz., pentanol, hexanol, heptanol, octanol the shift is less as also the dielectric constant function due to their lower dielectric constant.

In the plots of Stokes' shift verses refractive index function $(n^2 - 1) / (2n^2 + 1)$, the opposite effects are found, i.e., Stokes' shift decreases with the increase in the refractive index function as well as the refractive index of the solvents itself (Figs. 55-65). The term refractive index function accounts only for the redistribution of electrons. In the case of polar solvent water, where the largest shift found has the minimum refractive index function due to minimum refractive index value of water. Actually, the refractive index function affects the Stokes' shift less than the dielectric constant function because according to Lippert theory, only the solvent reorientation is expected to result in the substantial Stokes' shift.

Considering the similar plots of all the additives in dioxane-water mixtures, the maximum shift is observed in 10% dioxane-water mixture due to its maximum dielectric constant value. In all the cases, the variation of Stokes' shift with the dielectric constant function is linear.

Since the solvent properties near the interface of the micelles and reverse micelles of surfactants compare the solvent properties of dioxane-water mixture, these plots are useful to determine the dielectric constant and refractive index of the micelles.

It is also found that the variation of Stokes' shift with the solvent polarity function, i.e., orientation polarizability $[(D - 1)/(2D + 1) - (n^2 - 1)/(2n^2 + 1)]$ of different solvents is an useful way to determine the dipole moment of the solute (fluorophore) both in the ground states as well as in the excited states.[18,19] The variation often can also be used to estimate the polarity of a new solvent.

On the basis of solvent effect on ultra-violet spectra, Kosower[31,32] had established the scale of solvent polarity, which he called the Z-values. The scale is based on particularly solvent dependent absorption band, the charge transfer band of the 1-alkyl pyridinium iodides. The high solvent dependence of this band is understandable in terms of the foregoing arguments since the transition, as charge transfer transition, involves a large change in polarity. The scale of Z-value obtained by Kosower is parallel as far as comparable data available to Grunwald and Winstein's Y values, a kinetic scale of solvent polarity.[33]

In the present investigation, the plot of Stokes' shift verses Kosower-Z values of our solutes, viz., 1-Naphthol, 2-Naphthol, 5-Hydroxyindole, 5-Hydroxy-L-Tryptophan, L-Tyrosinemethylester, L-Tyrosine and in water and different alkanols are found in good agreement with the Kosower-Z value scale. The absorption maxima are transformed to Kosower-Z values (kcal/mol) using the following relation:

$$Z = 2.859 \times 10^5/\lambda$$

Where λ is the wavelength of the absorption maxima in angstroms.

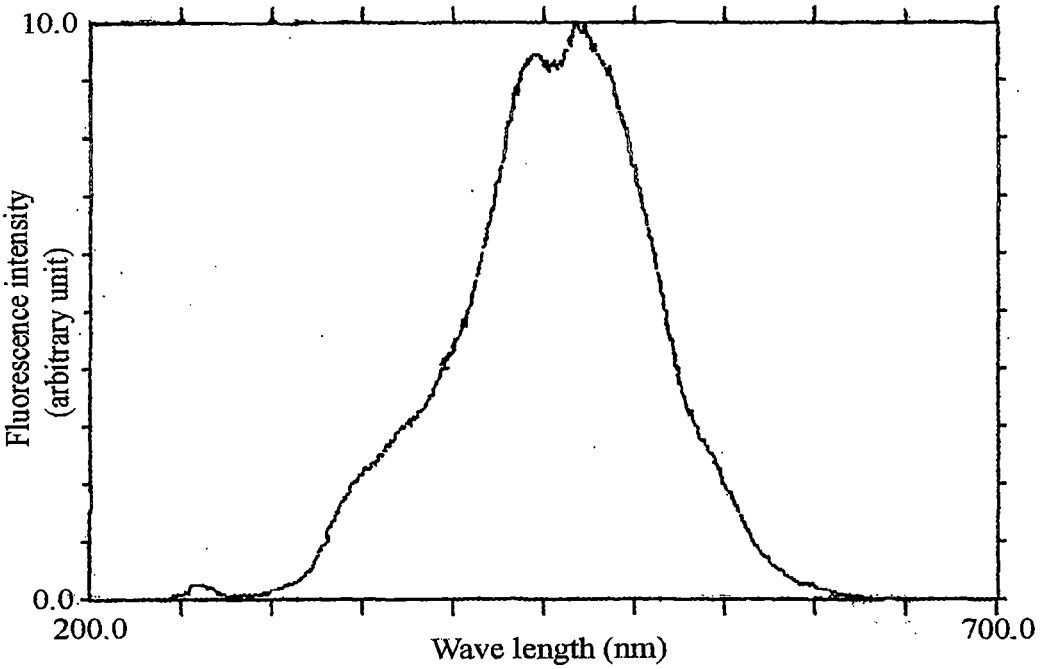

Fig. 3. Emission Spectrum of 1-Naphthol ($1x10^{-4}M$) in water

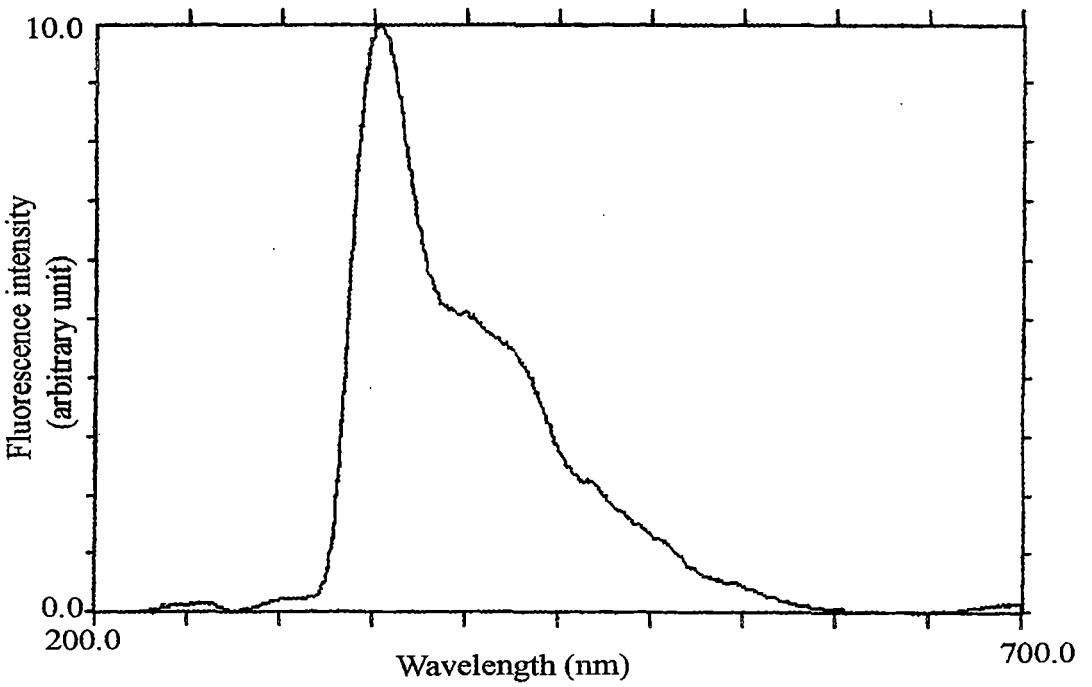

Fig. 4. Emission Spectrum of 2-Naphthol ($1x10^{-4}M$) in water

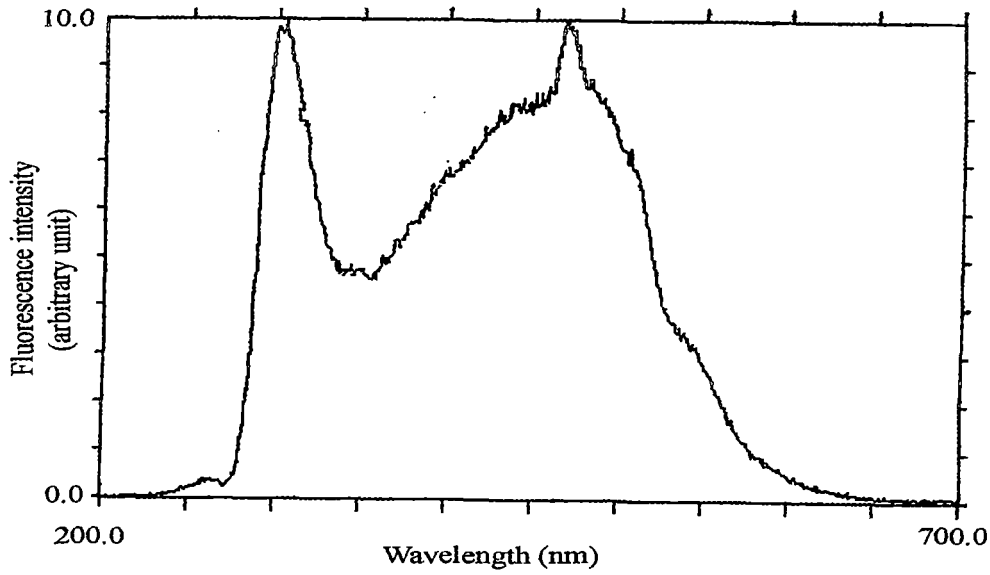

Fig. 5. Emission Spectrum of L-Tyrosine ($1x10^{-4}M$) in water

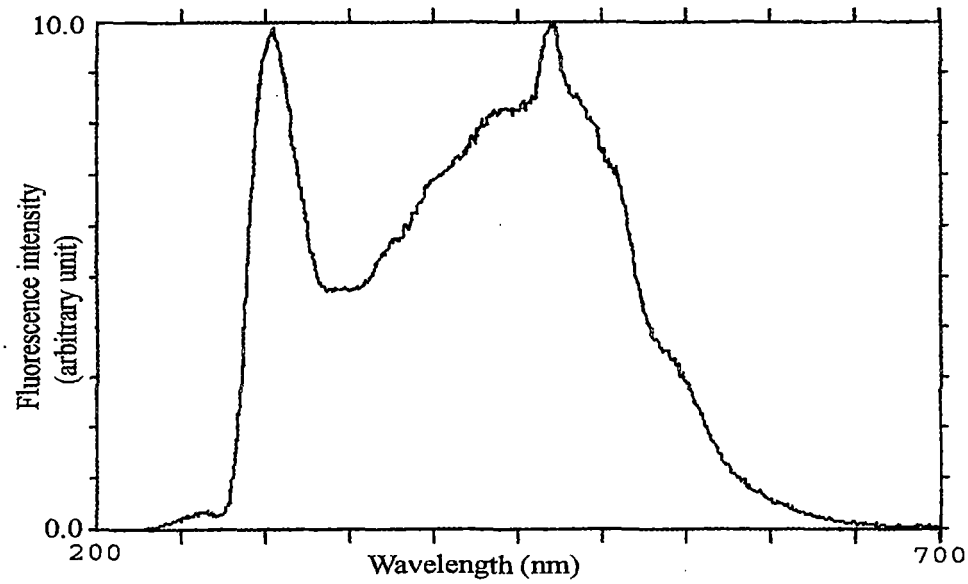

Fig. 6. Emission Spectrum of L-Tyrosinemethylester ($1x10^{-4}M$) in water

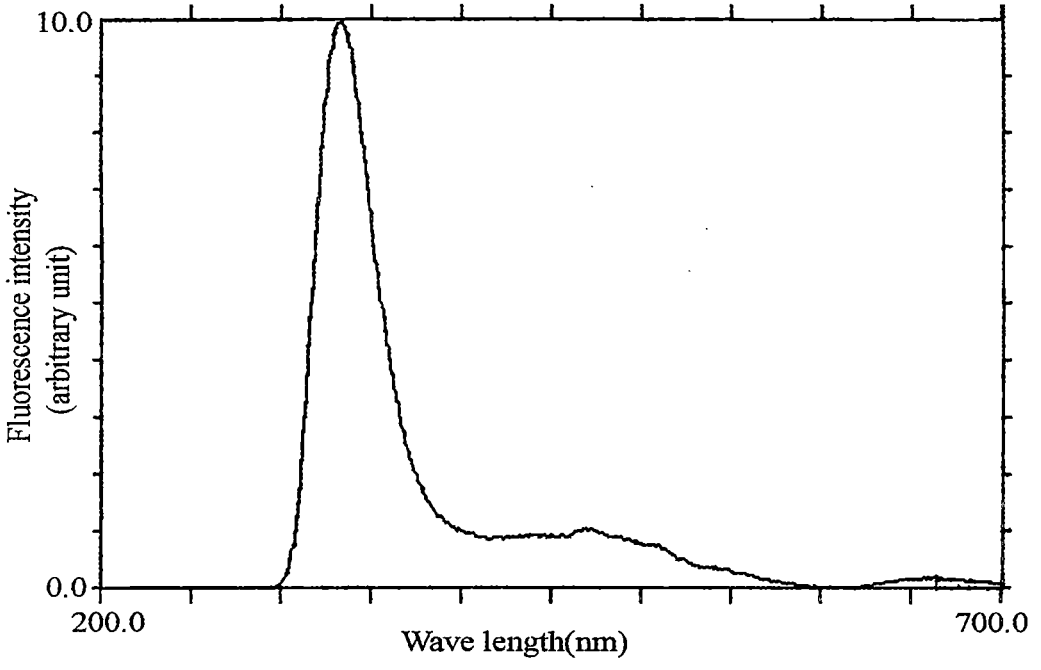

Fig. 7. Emission Spectrum of 5-Hydroxyindole ($1x10^{-4}M$) in water

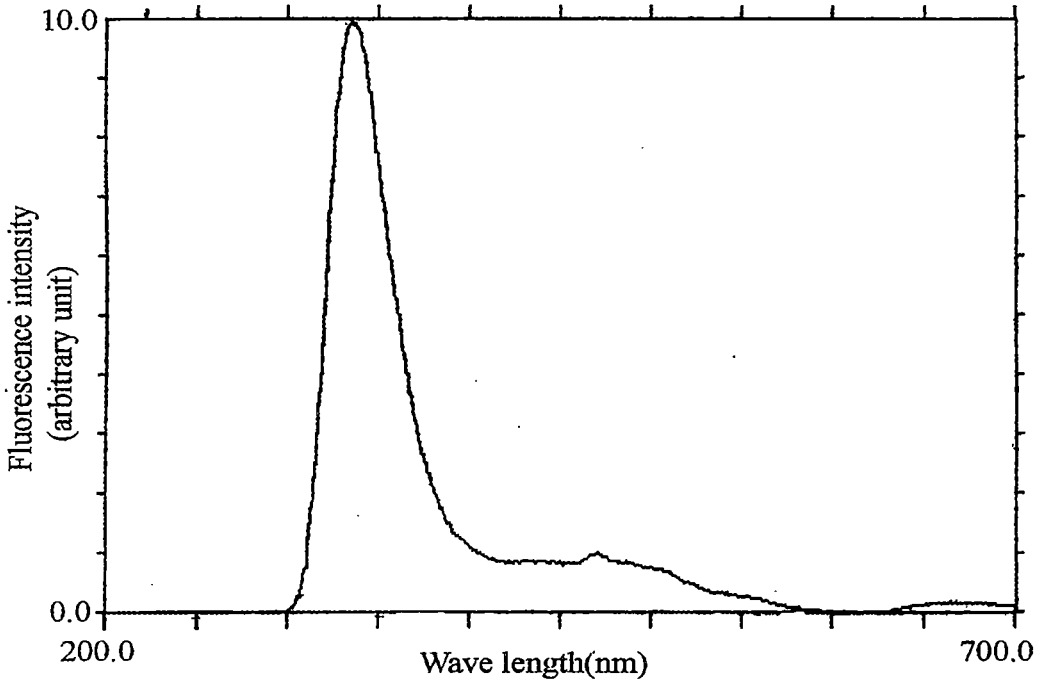

Fig. 8. Emission Spectrum of 5-Hydroxy-L-tryptophan ($1x10^{-4}M$) in water

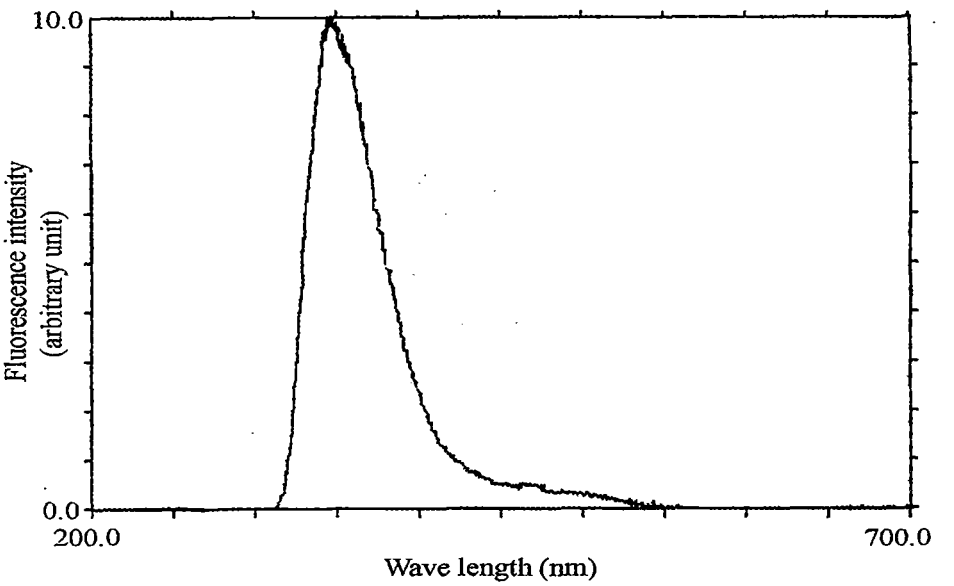

Fig. 9. Emission Spectrum of 1-Naphthol ($1x10^{-4}M$) in Methanol

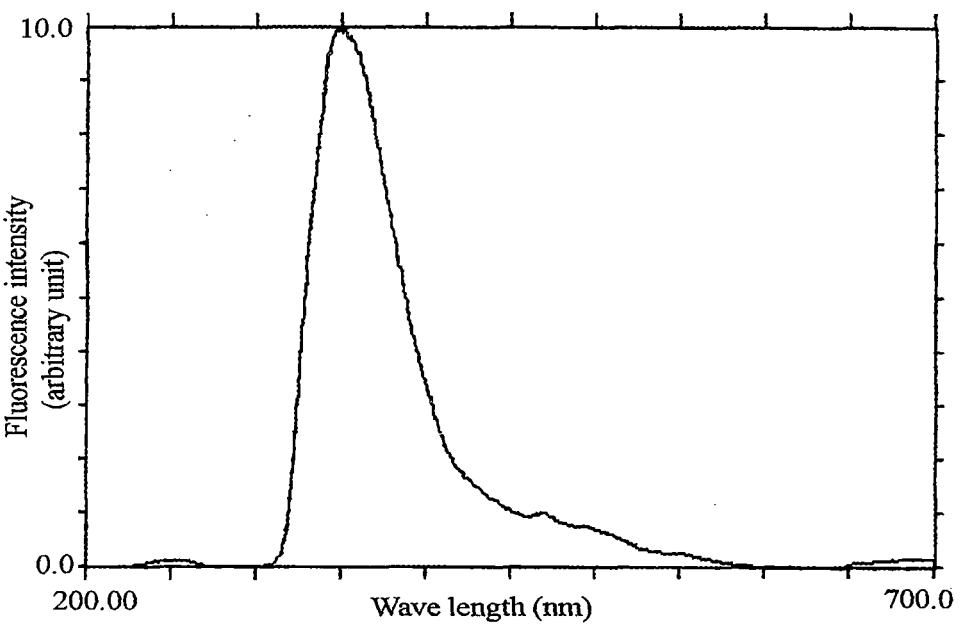

Fig. 10. Emission Spectrum of 1-Naphthol ($1x10^{-4}M$) in Ethanol

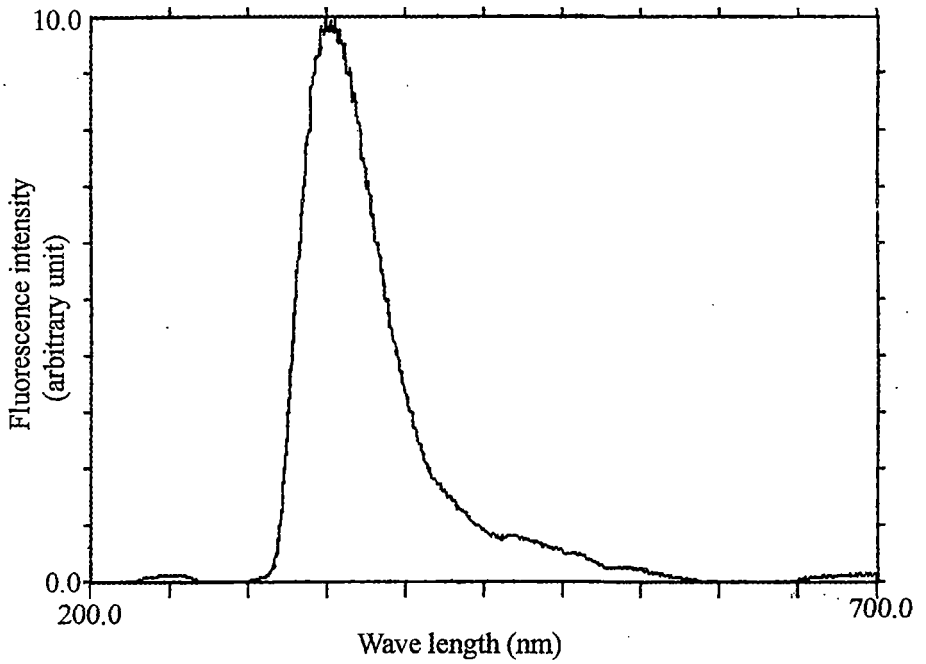

Fig. 11. Emission Spectrum of 1-Naphthol ($1x10^{-4}$M) in *iso*-propyl alcohol

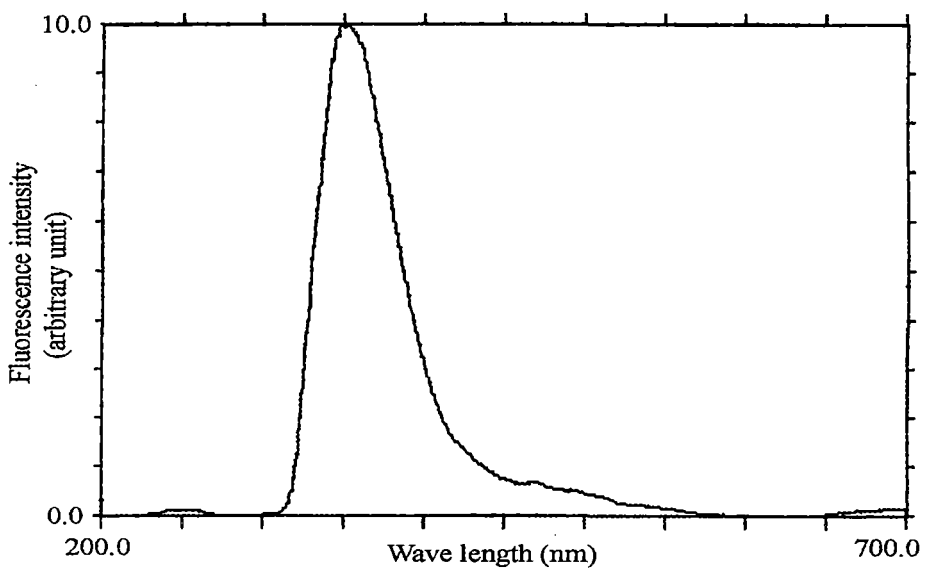

Fig. 12. Emission Spectrum of 1-Naphthol ($1x10^{-4}$M) in *tert*-butyl alcohol

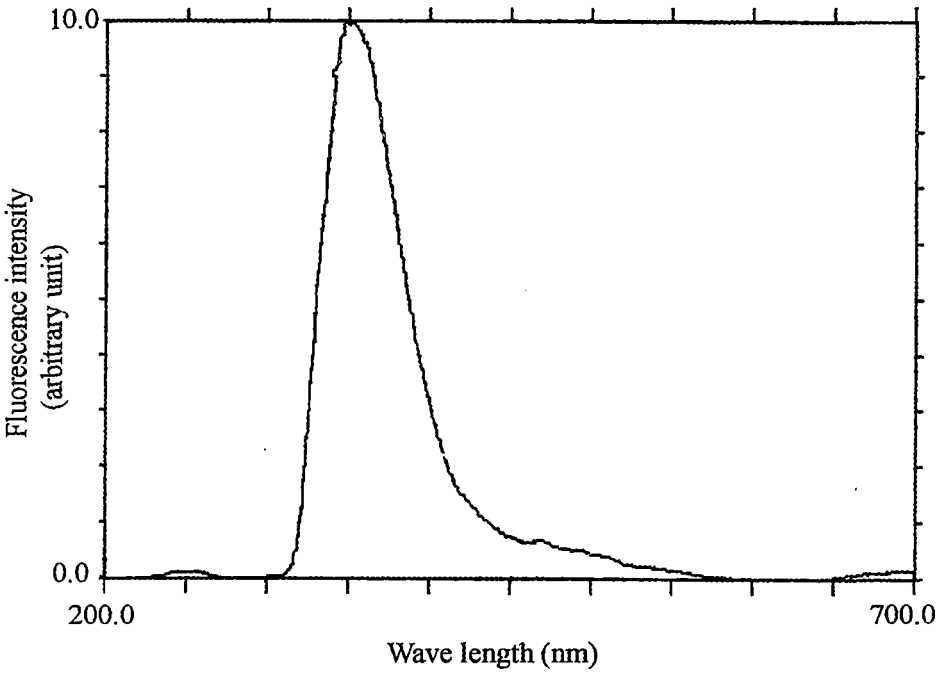

Fig. 13. Emission Spectrum of 1-Naphthol ($1x10^{-4}M$) in Pentanol

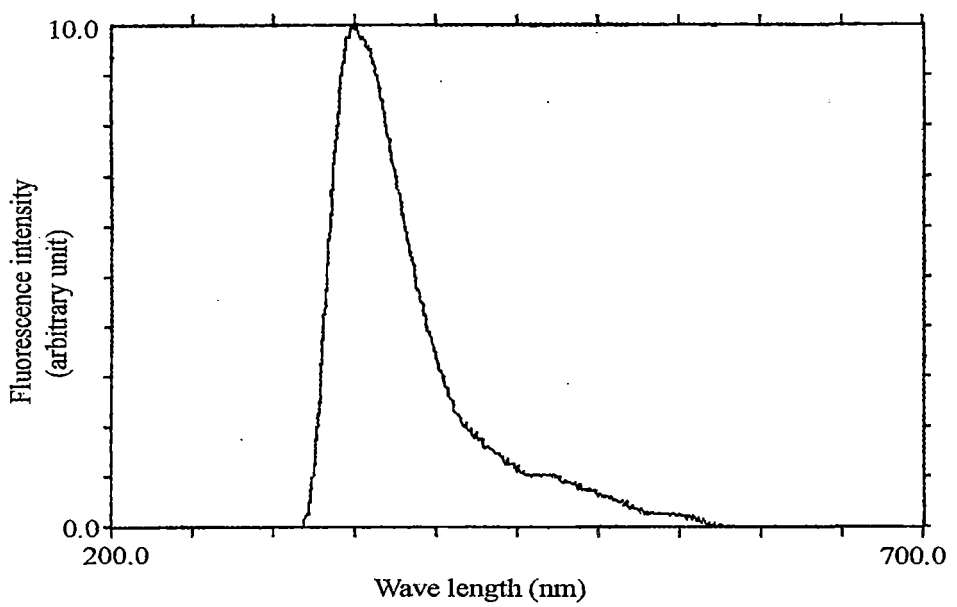

Fig. 14. Emission Spectrum of 1-Naphthol ($1x10^{-4}M$) in Hexanol

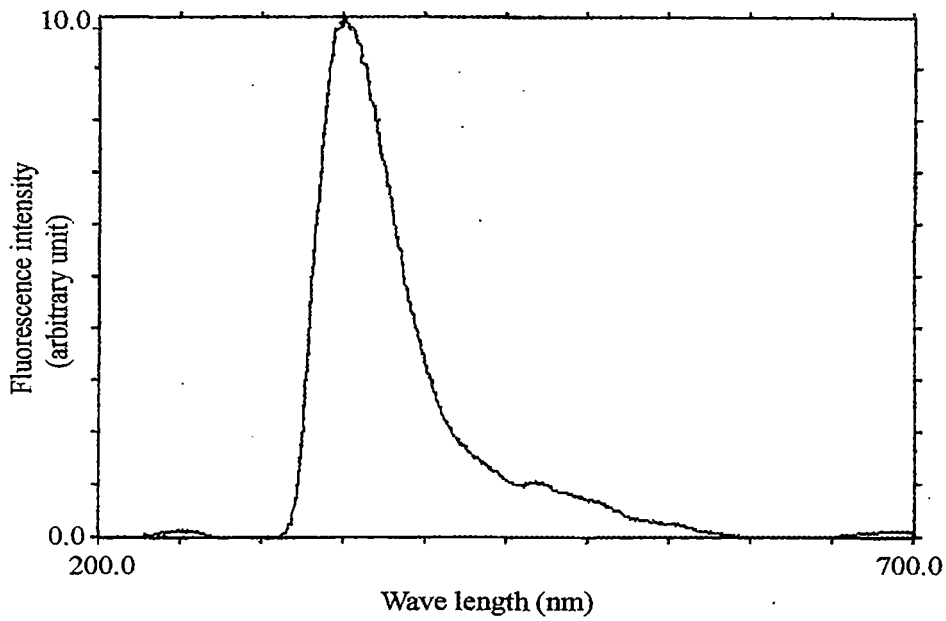

Fig. 15. Emission Spectrum of 1-Naphthol ($1x10^{-4}$M) in Heptanol

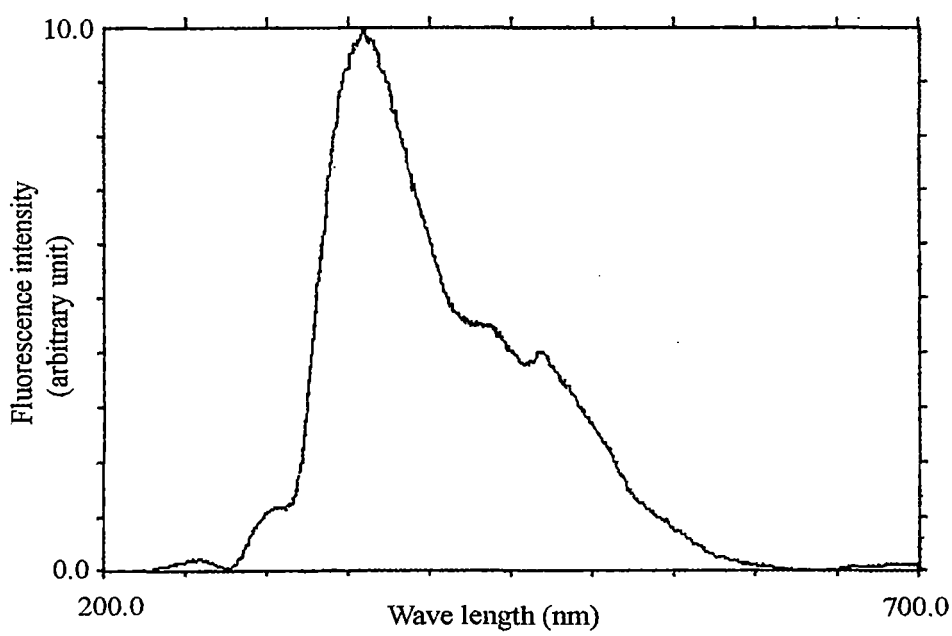

Fig. 16. Emission Spectrum of 1-Naphthol ($1x10^{-4}$M) in Octanol

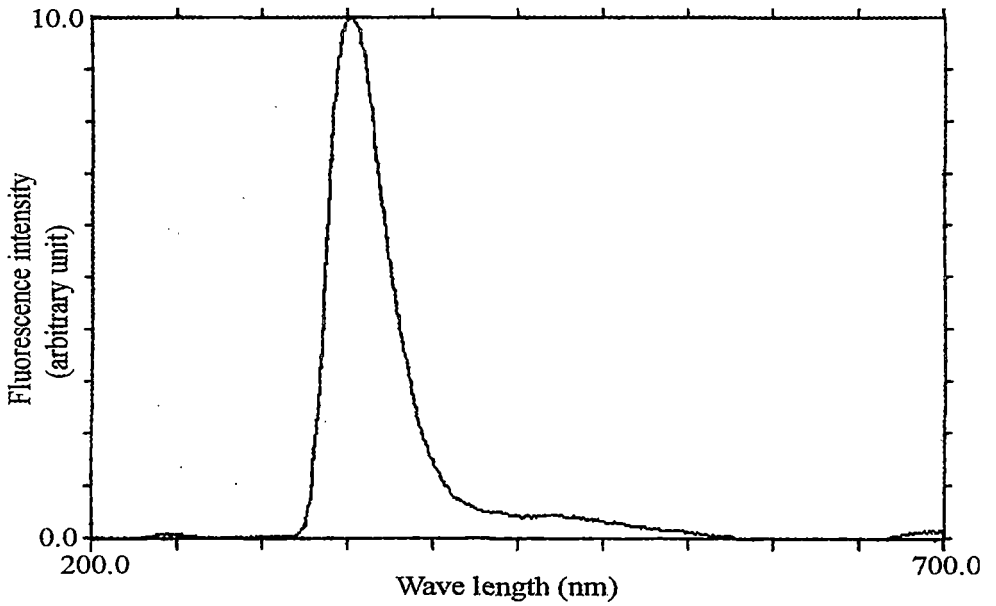

Fig. 17. Emission Spectrum of 2-Naphthol ($1x10^{-4}$M) in Methanol

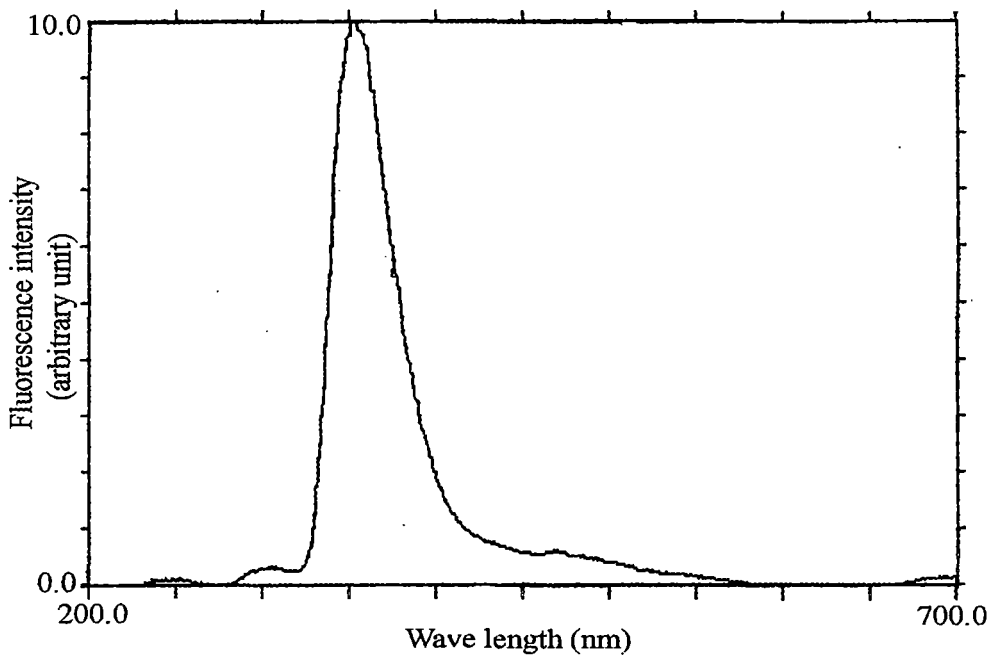

Fig. 18. Emission Spectrum of 2-Naphthol ($1x10^{-4}$M) in Ethanol

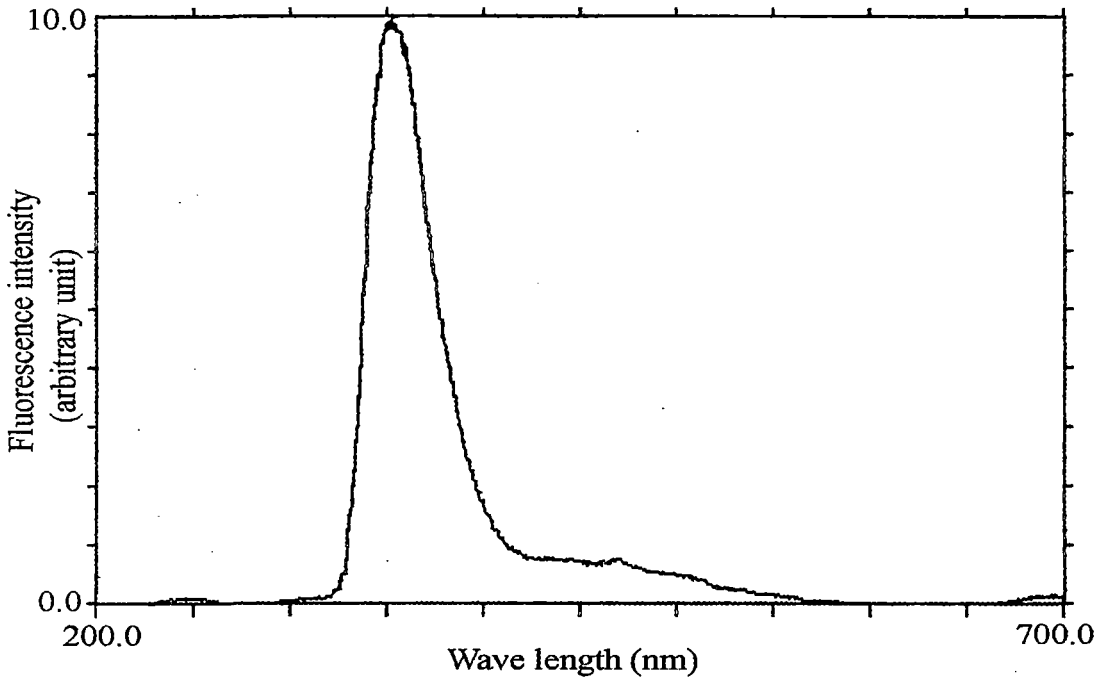

Fig. 19. Emission Spectrum of 2-Naphthol ($1x10^{-4}$M) in *iso*-Propyl alcohol.

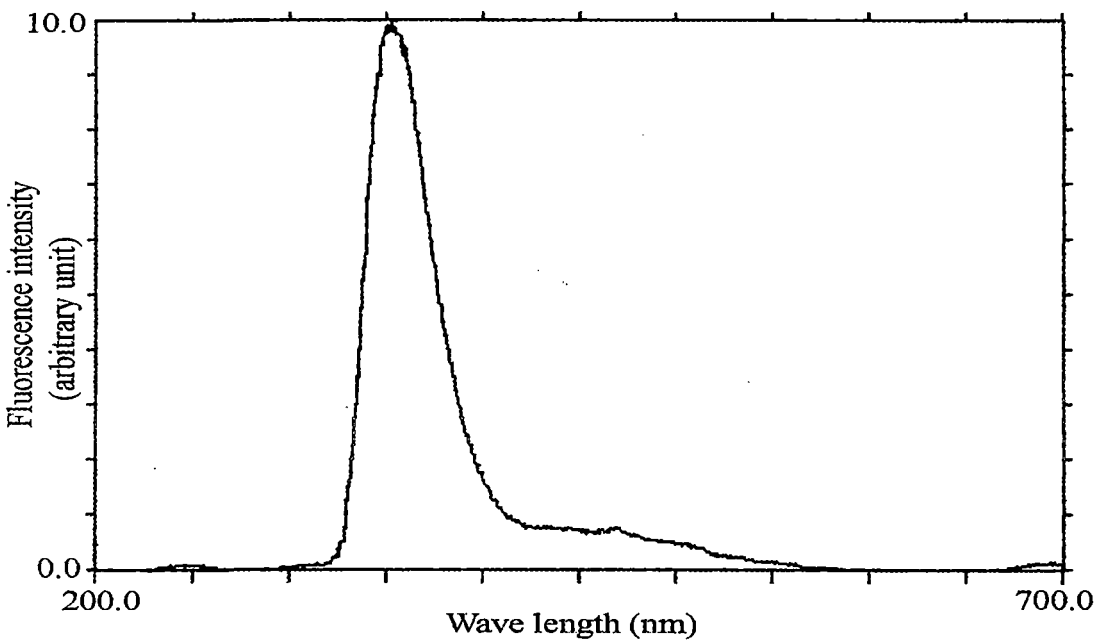

Fig. 20. Emission Spectrum of 2-Naphthol ($1x10^{-4}$M) in *tert*-Butyl alcohol

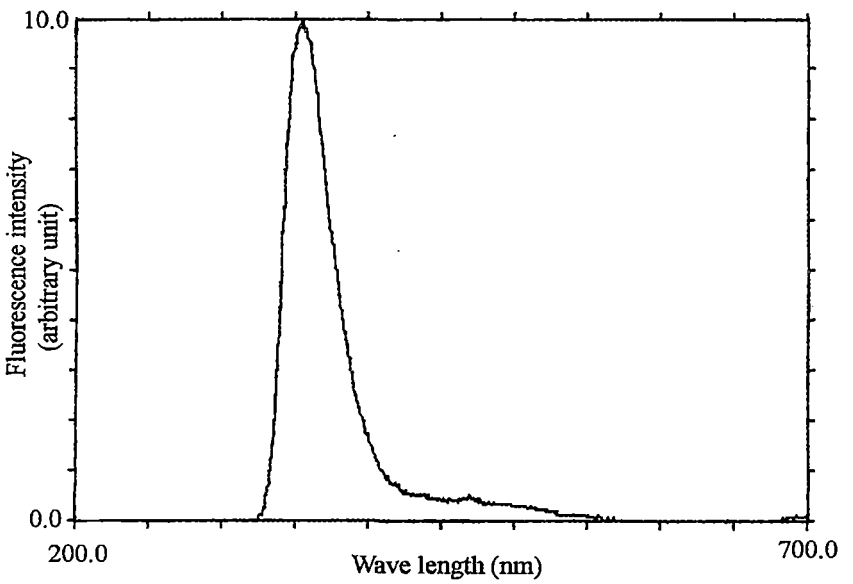

Fig. 21. Emission Spectrum of 2-Naphthol ($1x10^{-4}M$) in Pentanol

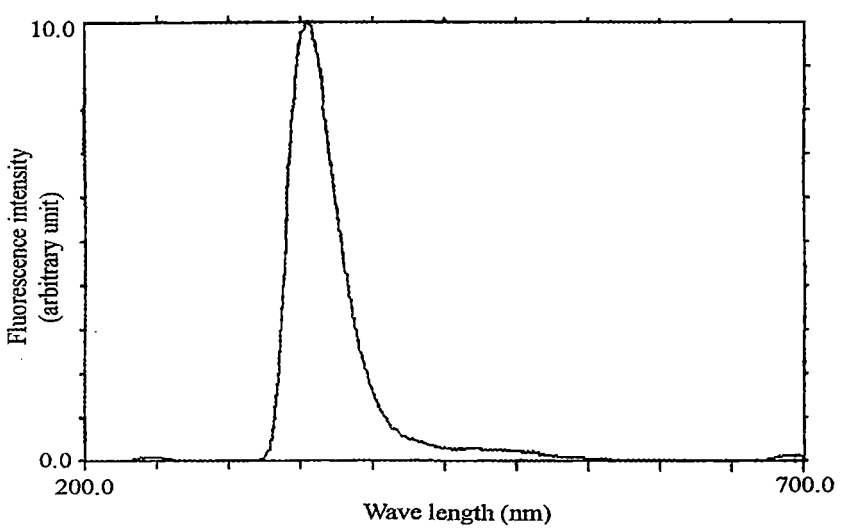

Fig. 22. Emission Spectrum of 2-Naphthol ($1x10^{-4}M$) in Hexanol

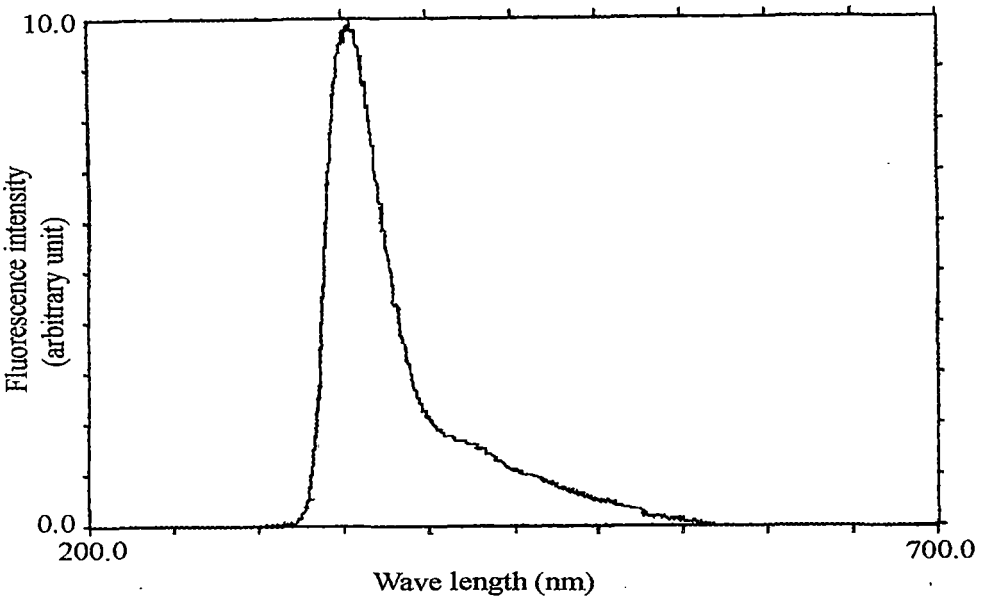

Fig. 23. Emission Spectrum of 2-Naphthol ($1x10^{-4}M$) in Heptanol

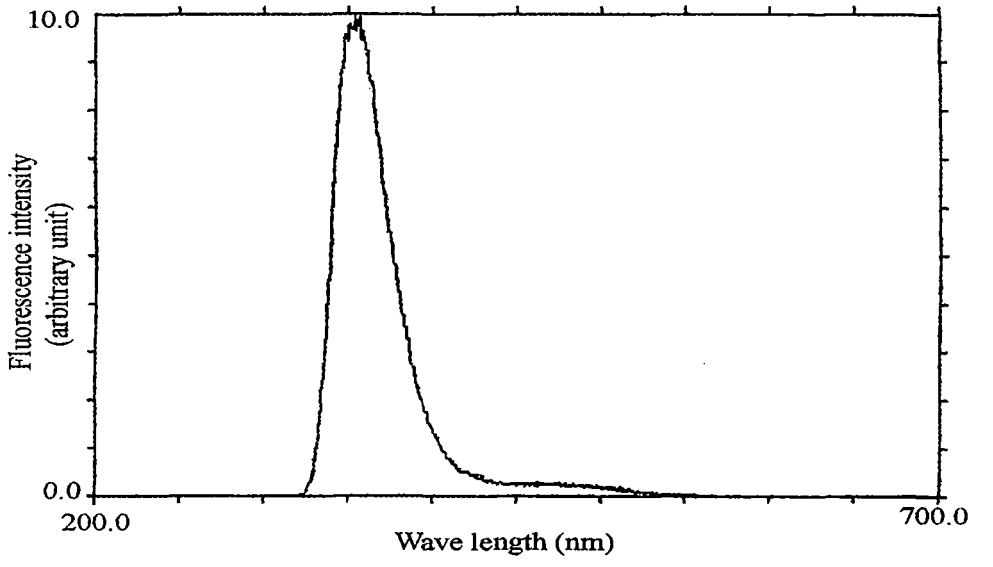

Fig. 24. Emission Spectrum of 2-Naphthol ($1x10^{-4}M$) in Octanol

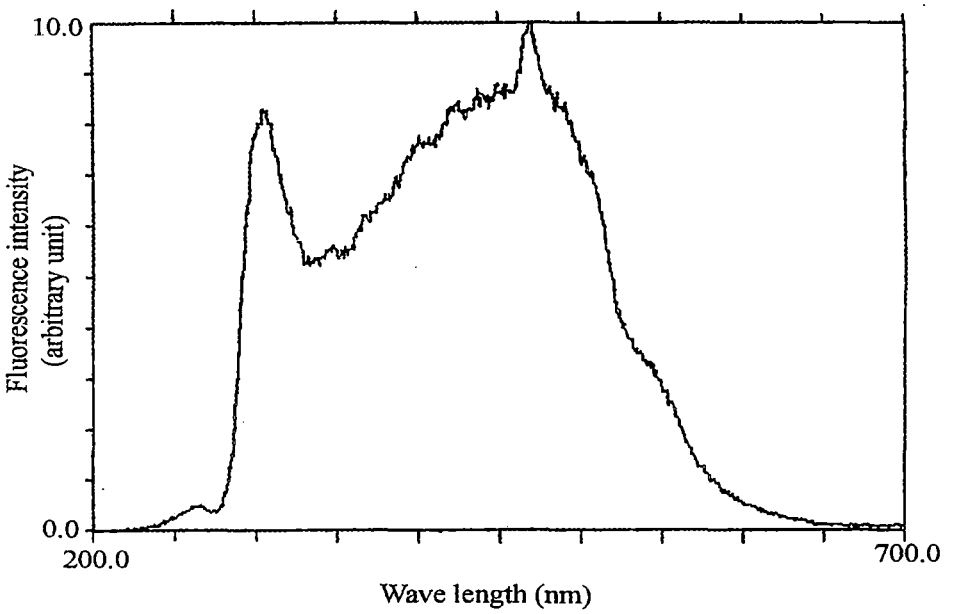

Fig. 25. Emission Spectrum of L-Tyrosinemethylester ($1x10^{-4}M$) in Methanol

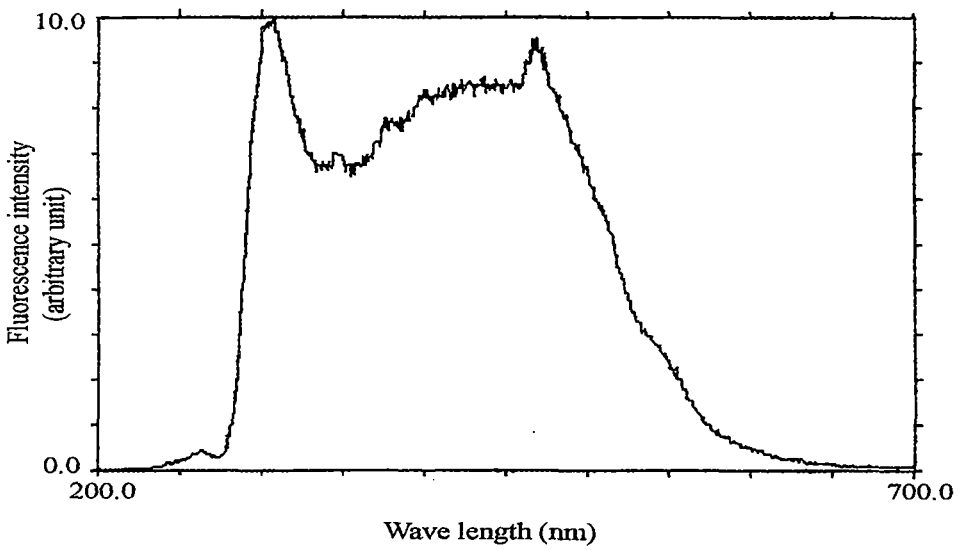

Fig. 26. Emission Spectrum of L-Tyrosinemethylester ($1x10^{-4}M$) in Ethanol

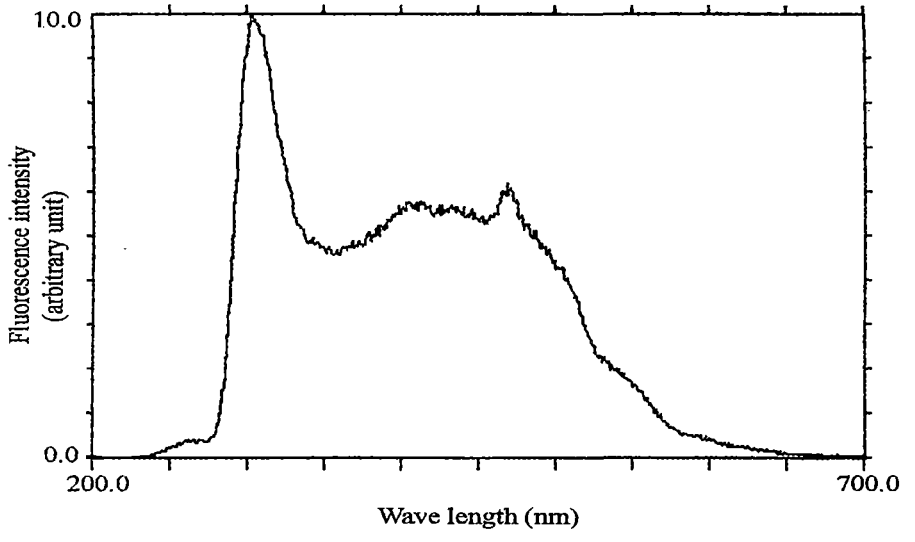

Fig. 27. Emission Spectrum of L-Tyrosinemethylester ($1x10^{-4}M$) in *iso*-Propyl alcohol

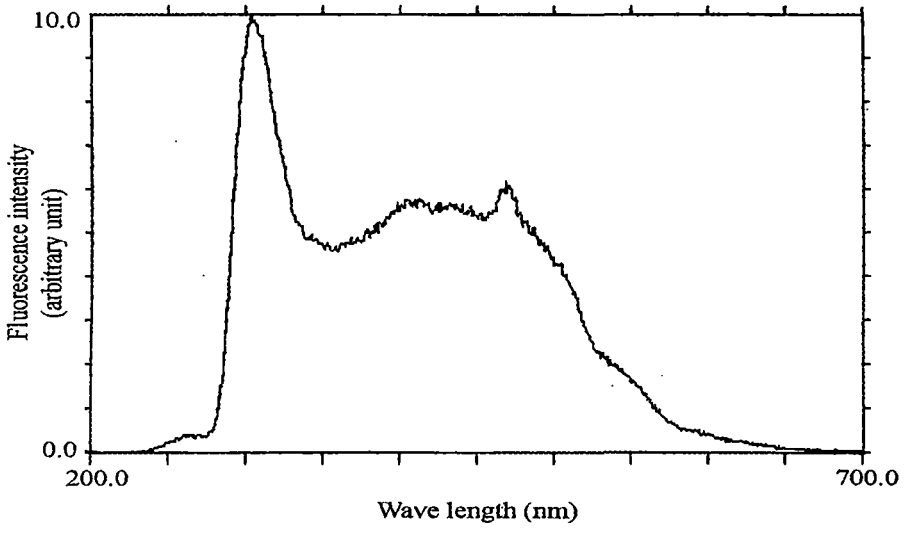

Fig. 28. Emission Spectrum of L-Tyrosinemethylester ($1x10^{-4}M$) in *tert*-Butyl alcohol

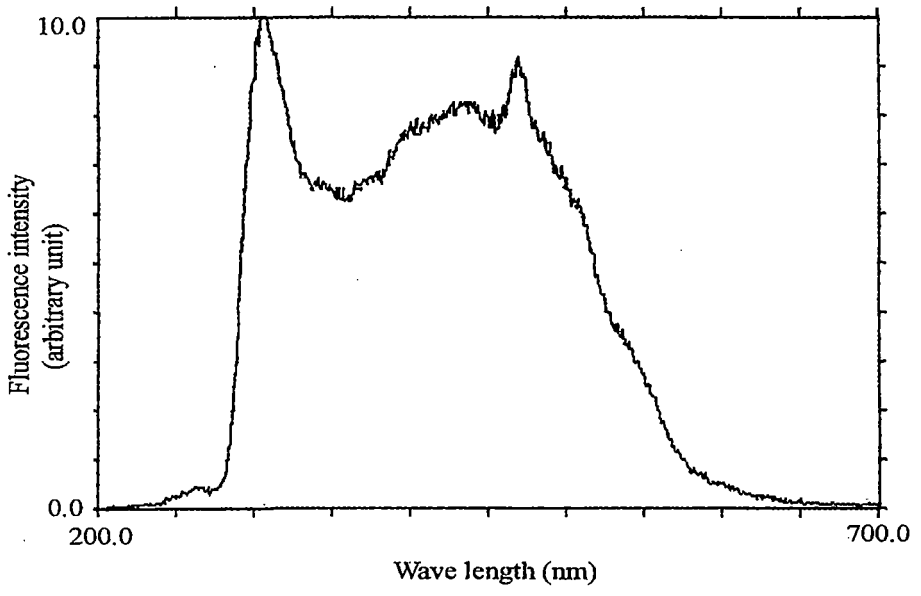

Fig. 29. Emission Spectrum of L-Tyrosinemethylester ($1x10^{-4}M$) in Pentanol

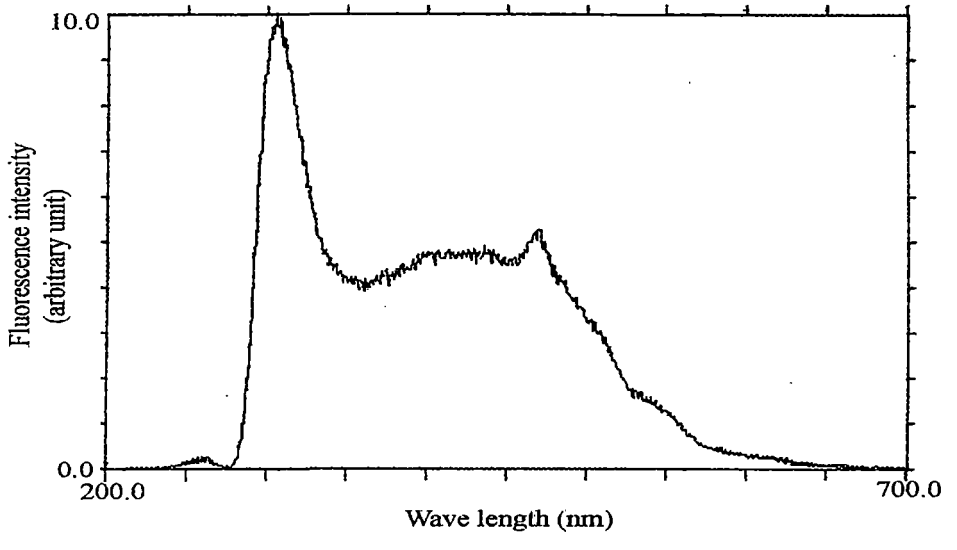

Fig. 30. Emission Spectrum of L-Tyrosinemethylester ($1x10^{-4}M$) in Hexanol

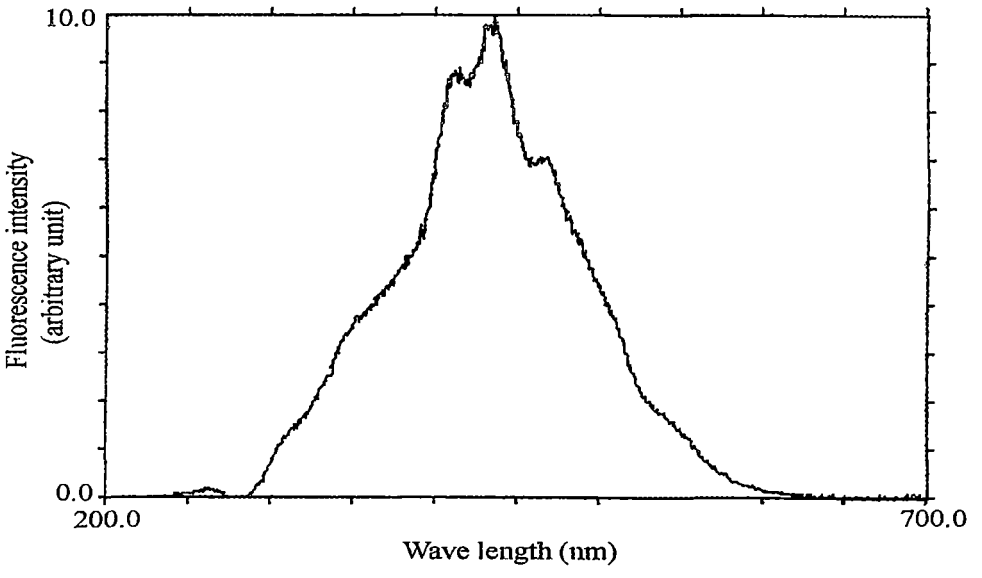

Fig. 31. Emission Spectrum of L-Tyrosinemethylester ($1x10^{-4}M$) in Heptanol

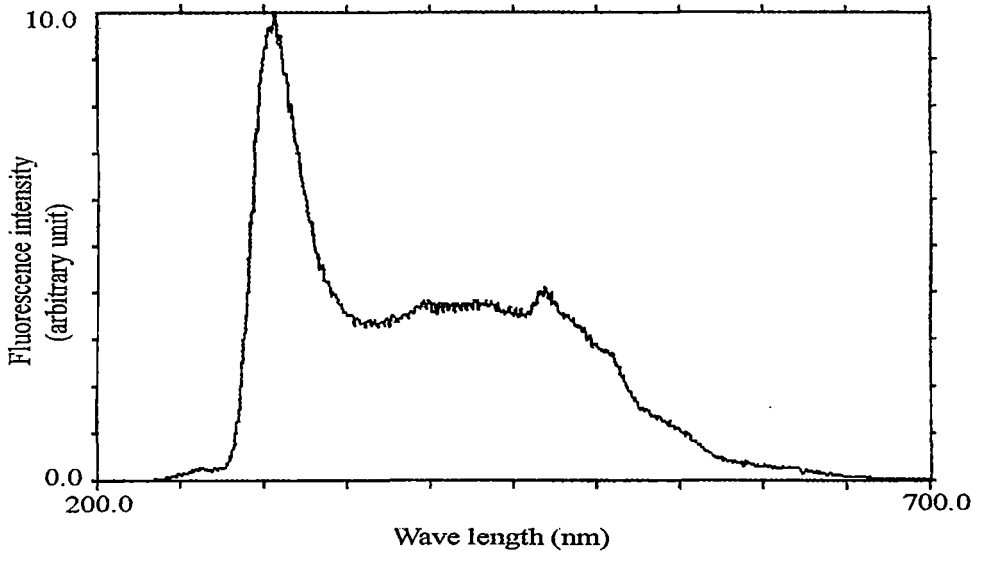

Fig. 32. Emission Spectrum of L-Tyrosinemethylester ($1x10^{-4}M$) in Octanol

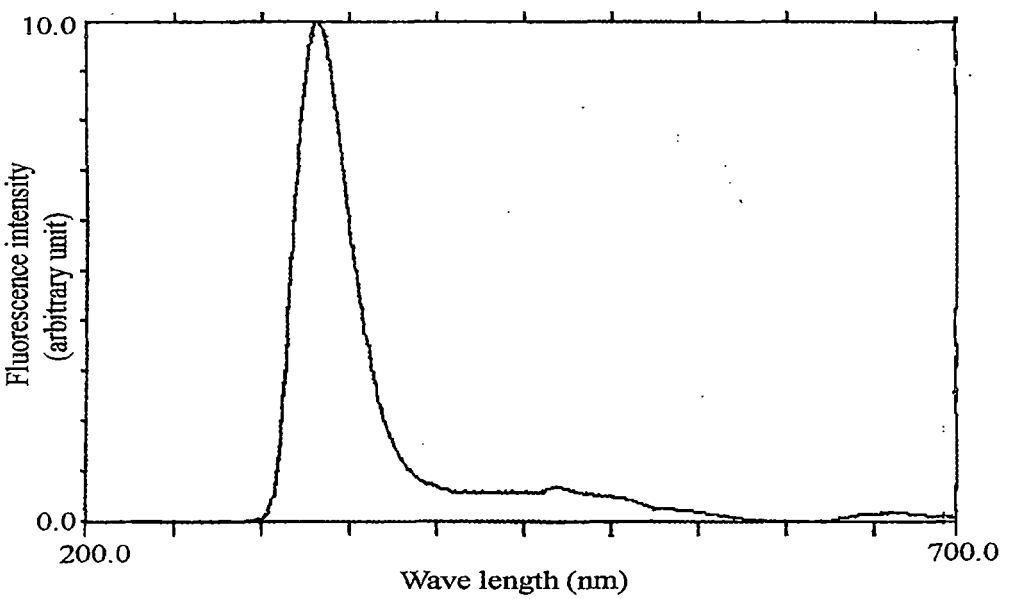

Fig. 33. Emission Spectrum of 5-Hydroxyindole ($1x10^{-4}M$) in Methanol.

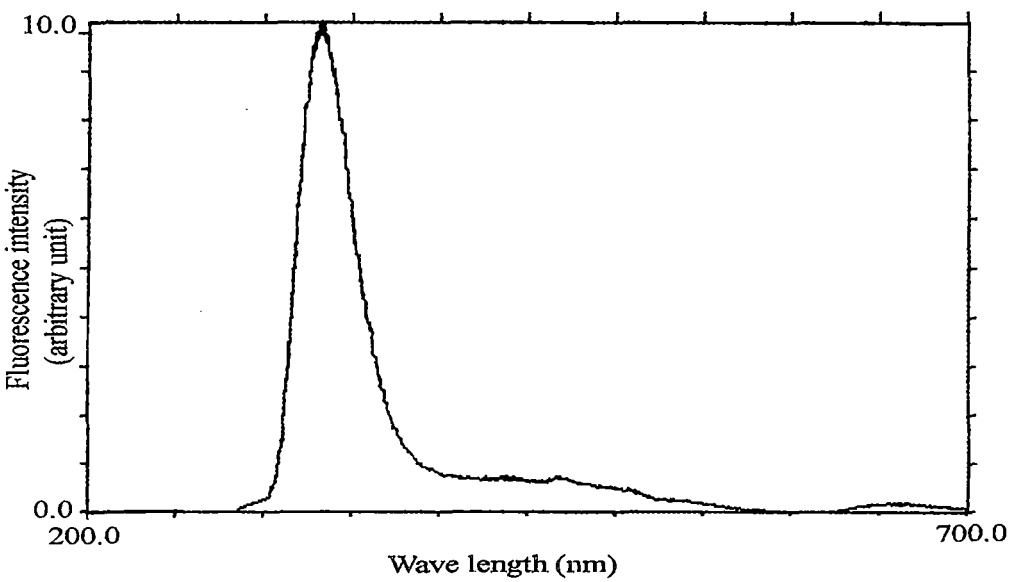

Fig. 34. Emission Spectrum of 5-Hydroxyindole ($1x10^{-4}M$) in Ethanol.

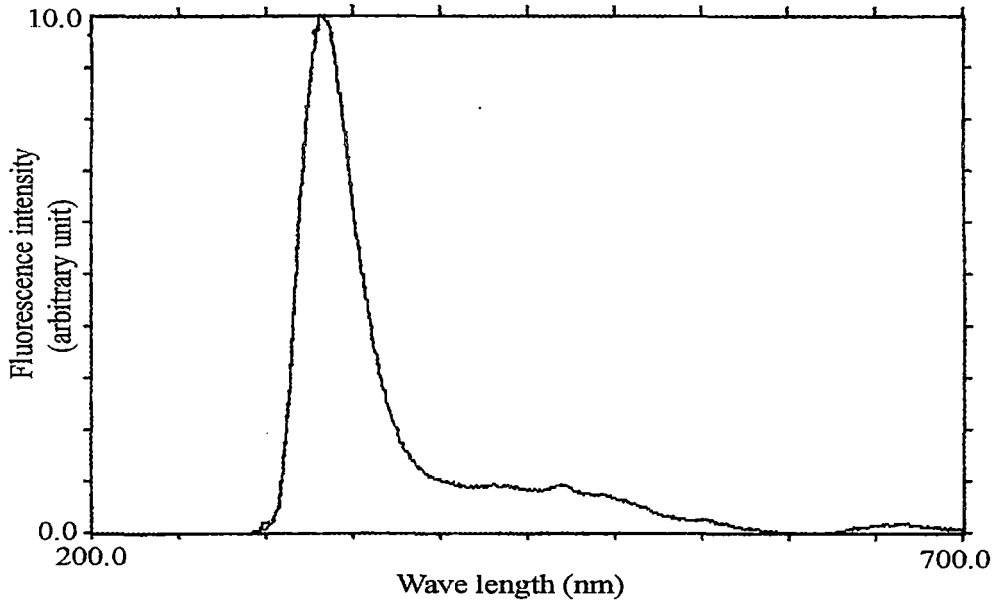

Fig. 35. Emission Spectrum of 5-Hydroxyindole ($1x10^{-4}M$) in *iso*-Propyl alcohol.

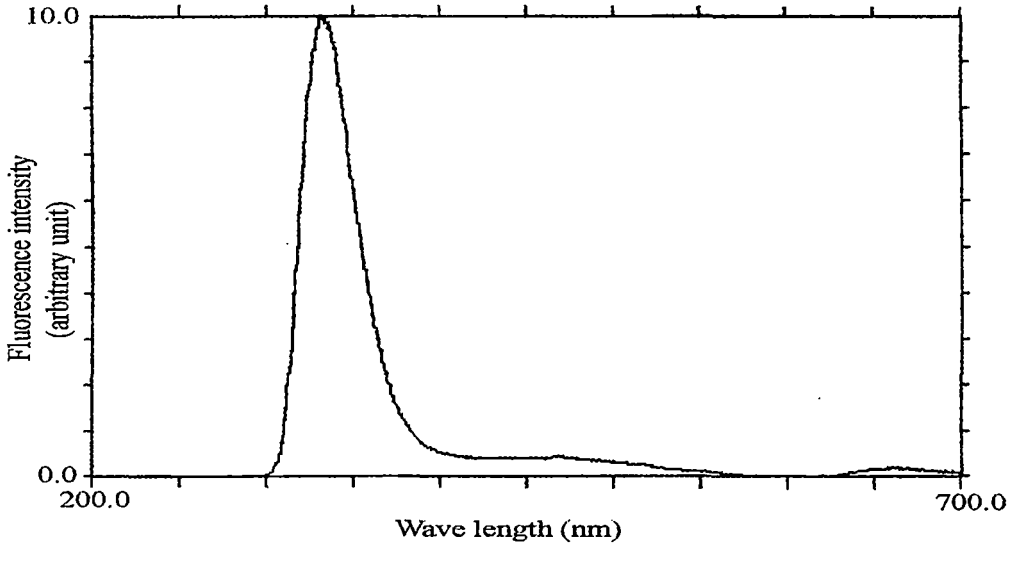

Fig. 36. Emission Spectrum of 5-Hydroxyindole ($1x10^{-4}M$) in *tert*-Butyl alcohol.

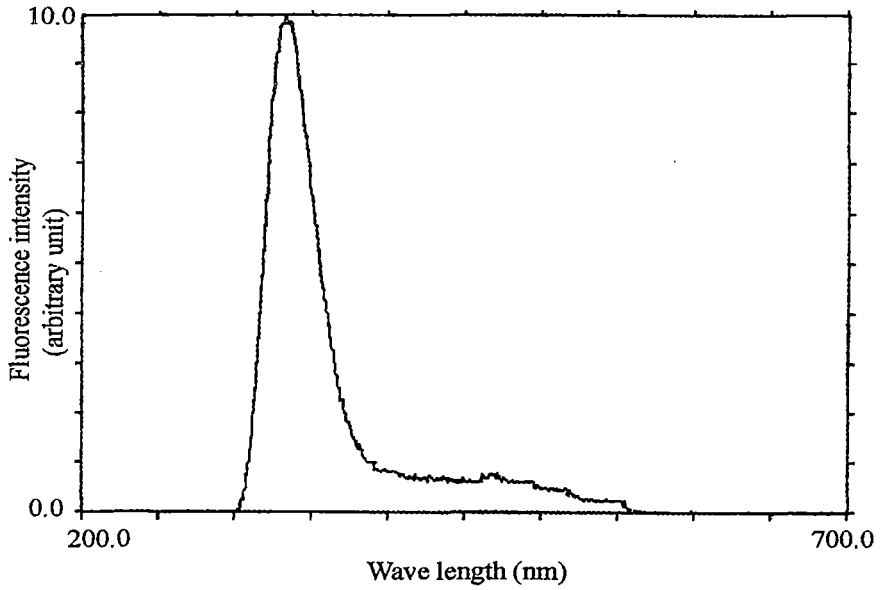

Fig. 37. Emission Spectrum of 5-Hydroxyindole ($1x10^{-4}$M) in Pentanol.

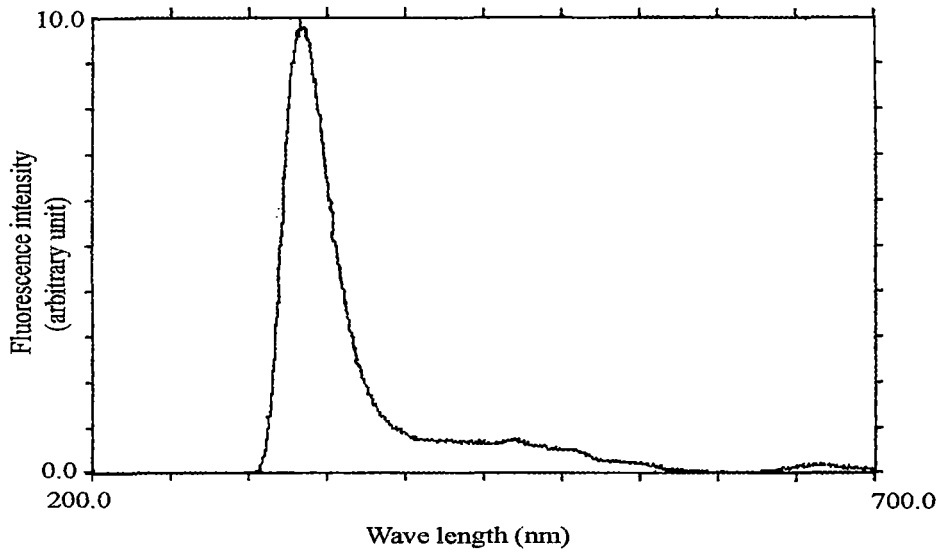

Fig. 38. Emission Spectrum of 5-Hydroxyindole ($1x10^{-4}$M) in Hexanol.

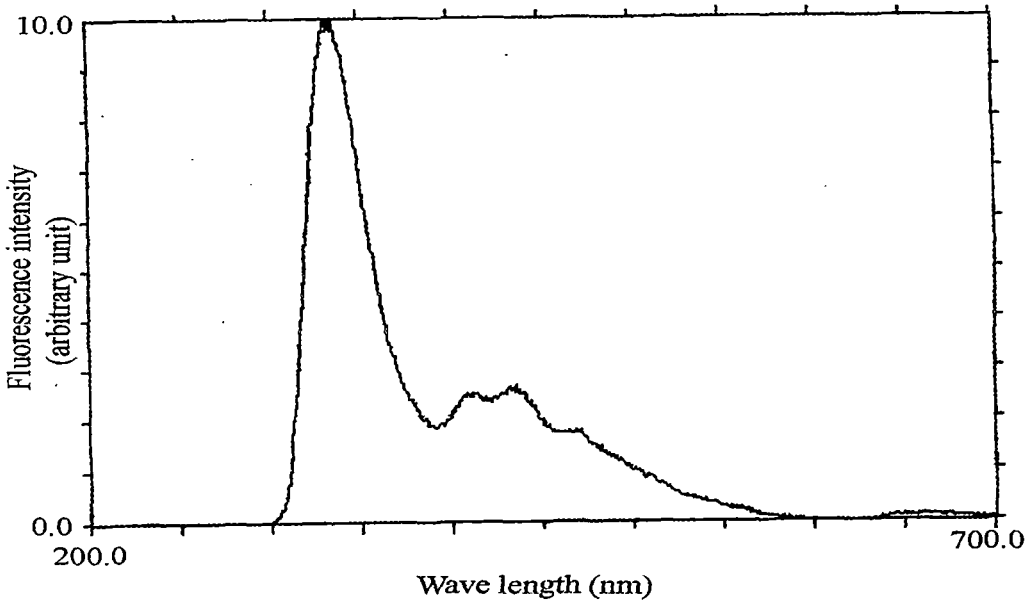

Fig. 39. Emission Spectrum of 5-Hydroxyindole ($1x10^{-4}M$) in Heptanol.

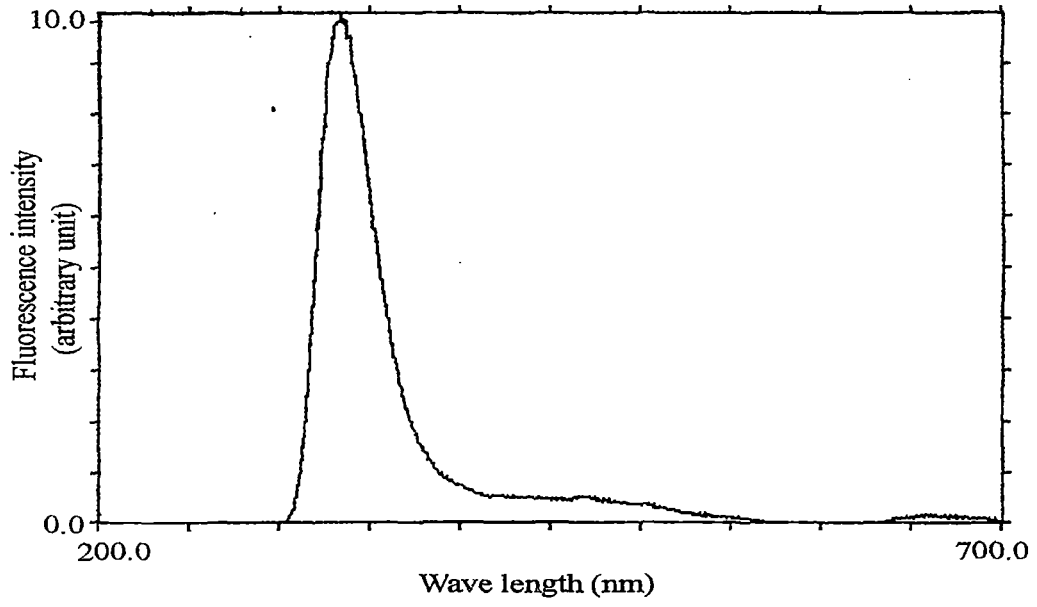

Fig. 40. Emission Spectrum of 5-Hydroxyindole ($1x10^{-4}M$) in Octanol.

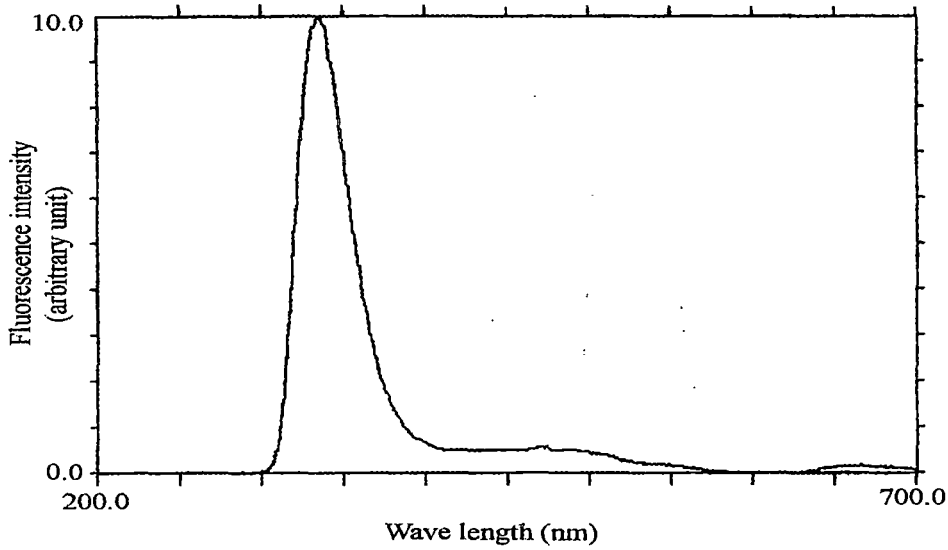

Fig. 41. Emission Spectrum of 5-Hydroxy-L-tryptophan ($1x10^{-4}M$) in Methanol.

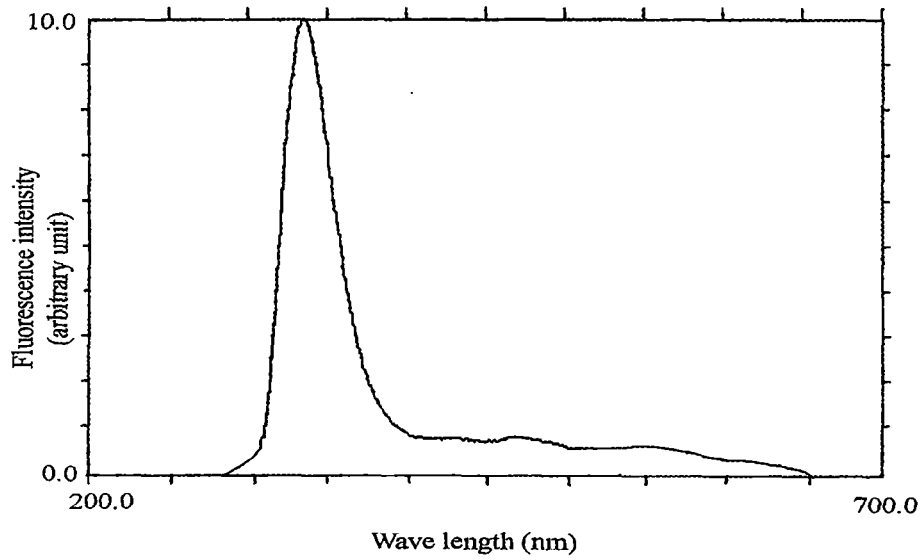

Fig. 42. Emission Spectrum of 5-Hydroxy-L-tryptophan ($1x10^{-4}M$) in Ethanol.

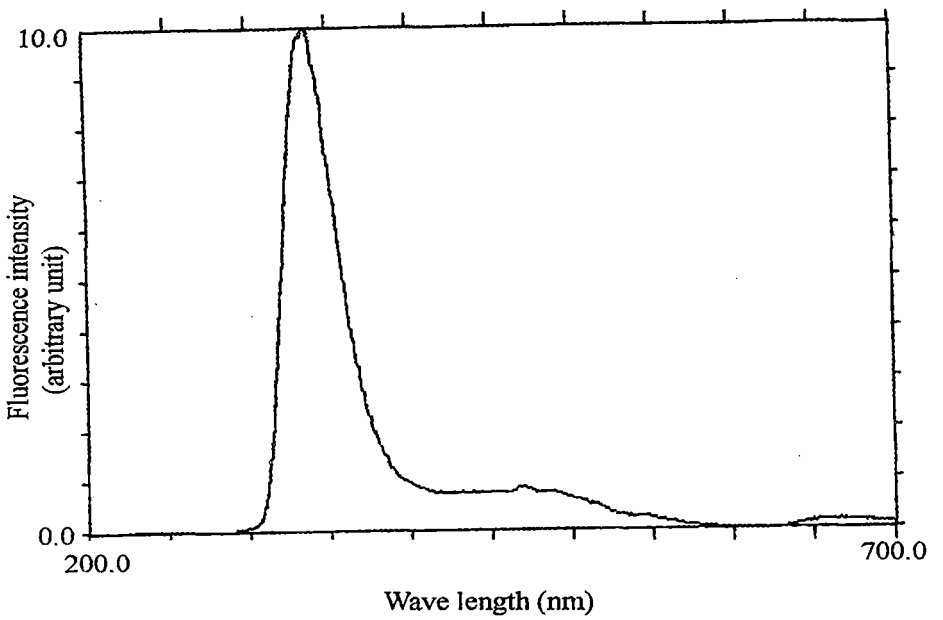

Fig. 43. Emission Spectrum of 5-Hydroxy-L-tryptophan ($1x10^{-4}$M) in *iso*-Propyl alcohol.

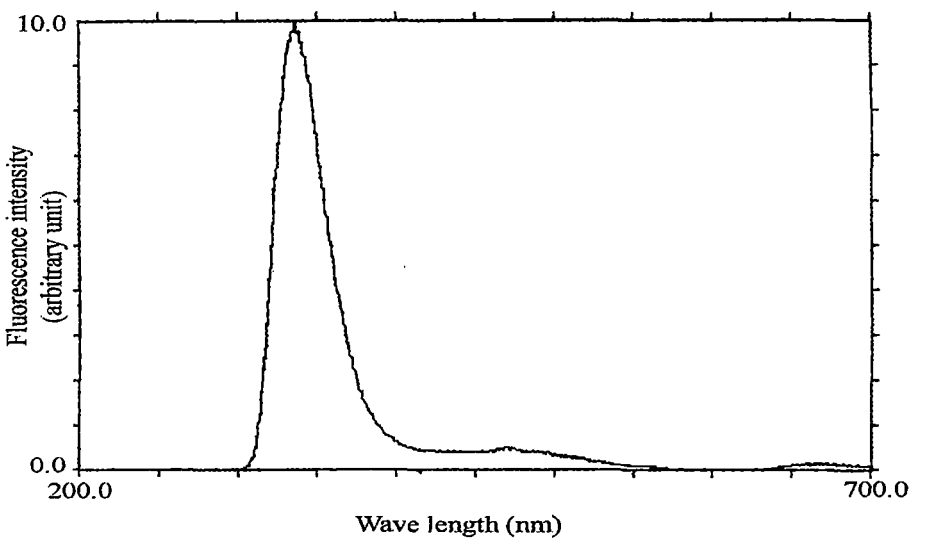

Fig. 44. Emission Spectrum of 5-Hydroxy-L-tryptophan ($1x10^{-4}$M) in *tert*-Butyl alcohol.

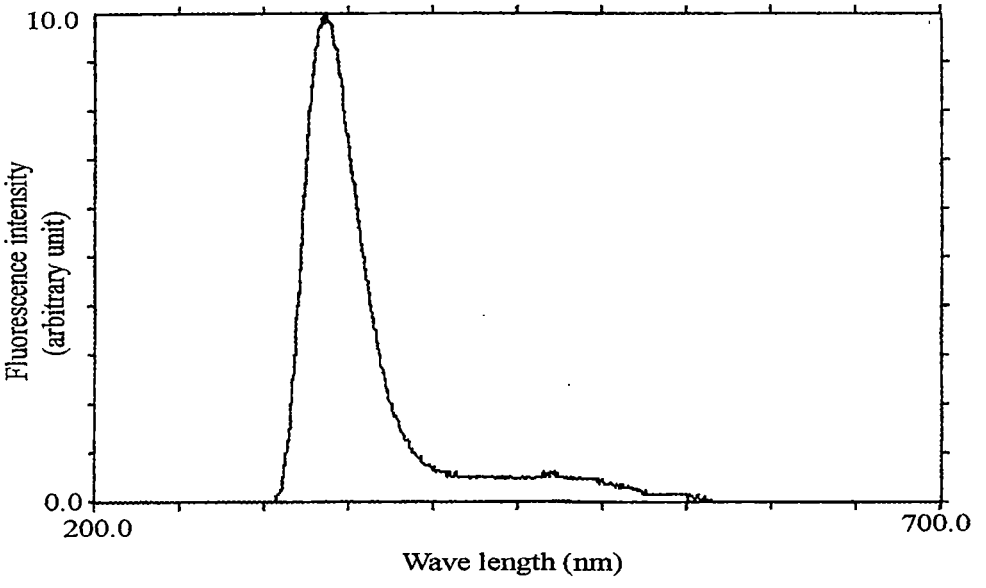

Fig. 45. Emission Spectrum of 5-Hydroxy-L-tryptophan ($1x10^{-4}M$) in Pentanol.

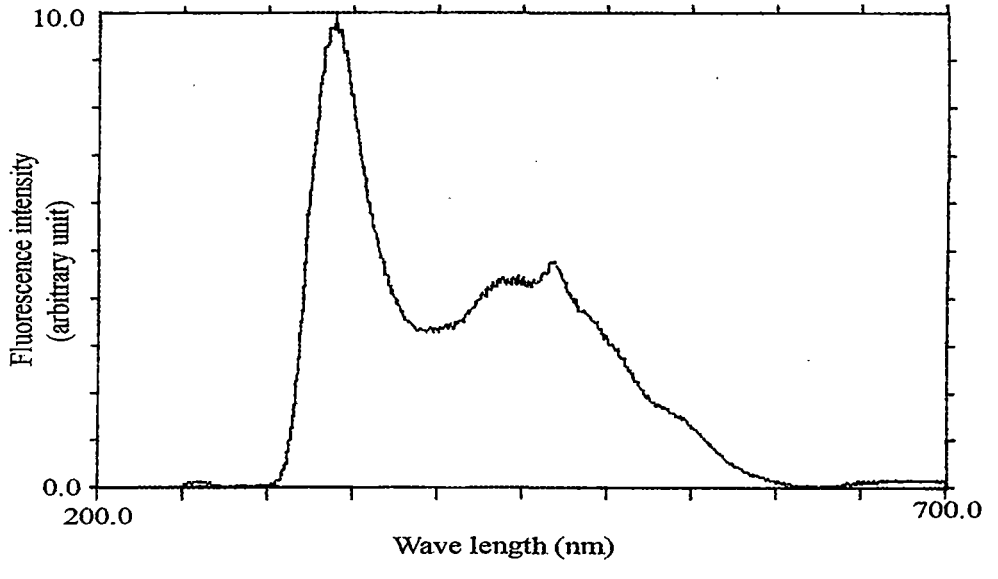

Fig. 46. Emission Spectrum of 5-Hydroxy-L-tryptophan ($1x10^{-4}M$) in Hexanol.

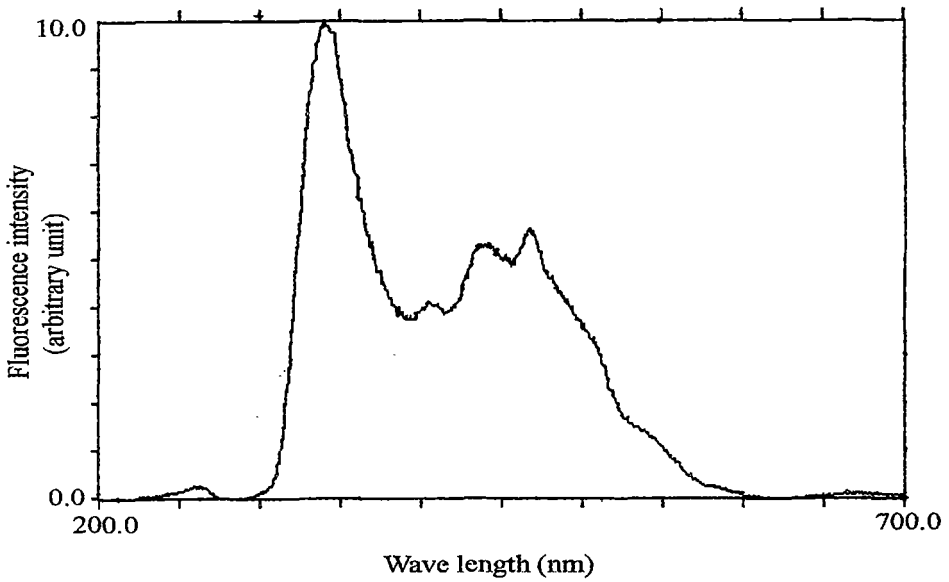

Fig. 47. Emission Spectrum of 5-Hydroxy-L-tryptophan ($1x10^{-4}$M) in Heptanol.

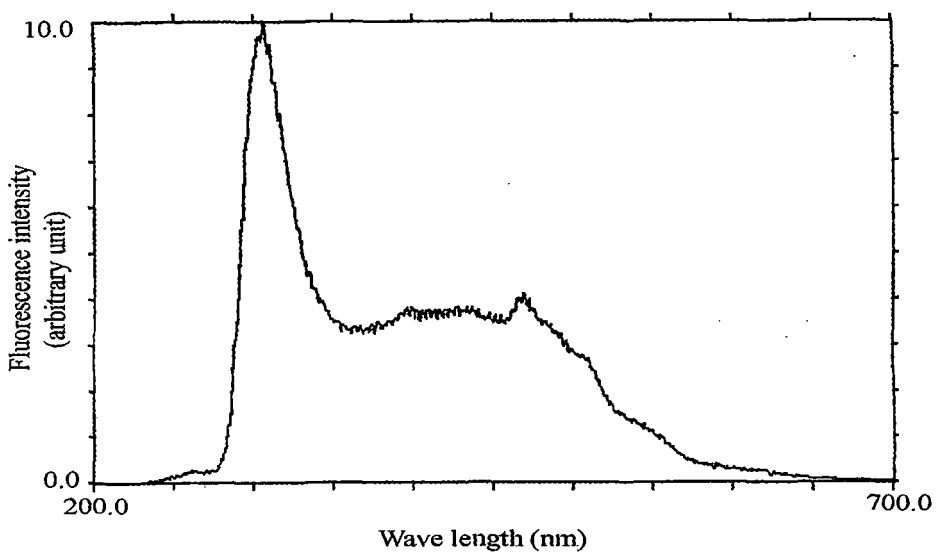

Fig. 48. Emission Spectrum of 5-Hydroxy-L-tryptophan ($1x10^{-4}$M) in Octanol.

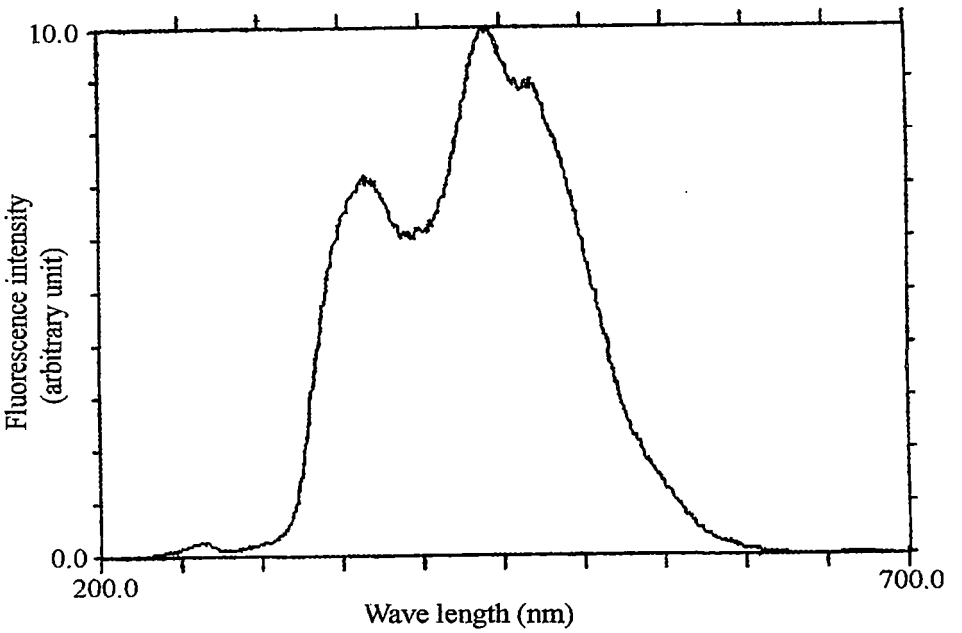

Fig. 49. Emission Spectrum of 1-Naphthol ($1x10^{-4}M$) in 50% 1,4-Dioxane.

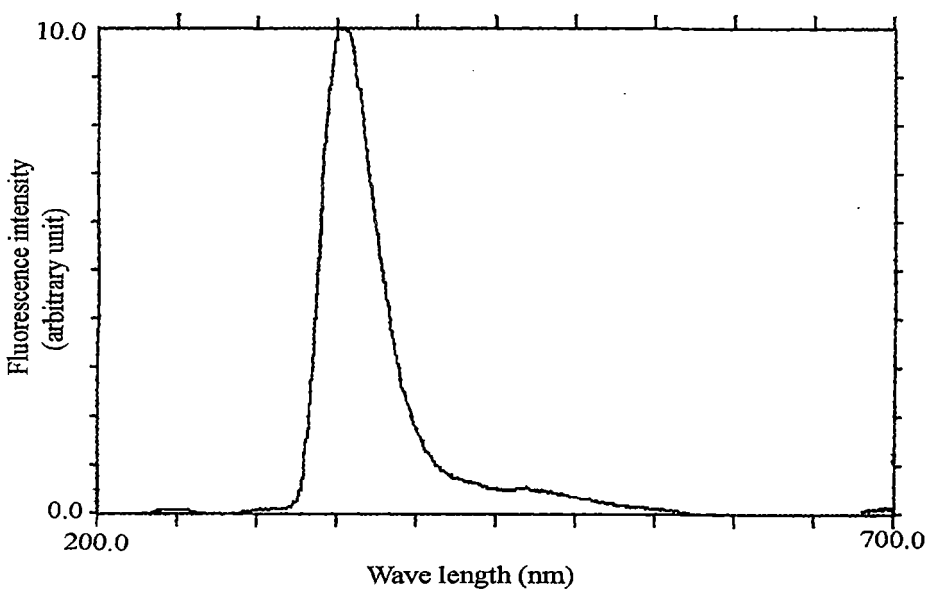

Fig. 50. Emission Spectrum of 2-Naphthol ($1x10^{-4}M$) in 60% 1,4-Dioxane.

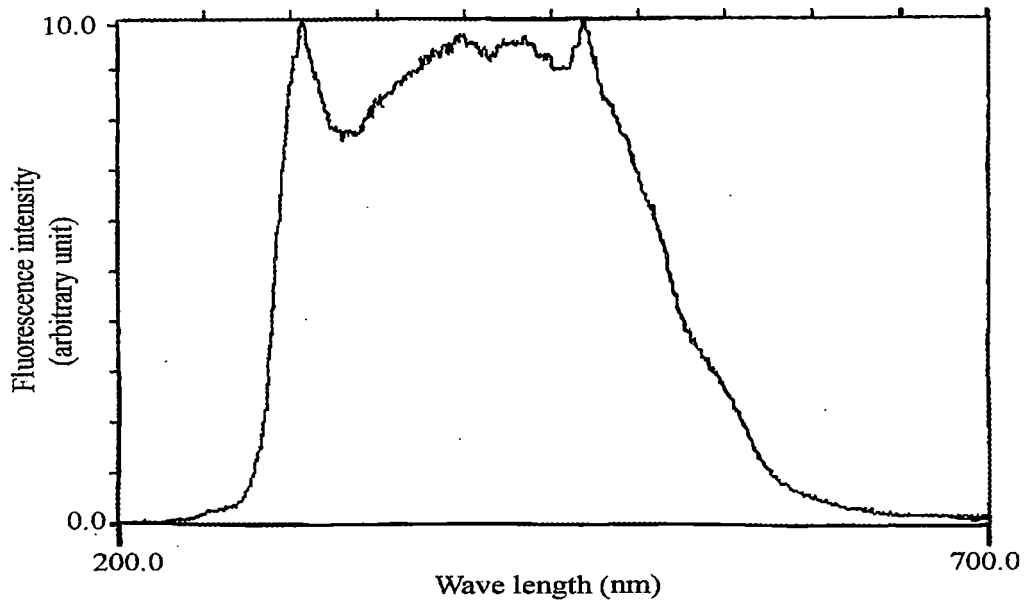

Fig. 51. Emission Spectrum of L-Tyrosine ($1x10^{-4}M$) in 80% 1,4-Dioxane.

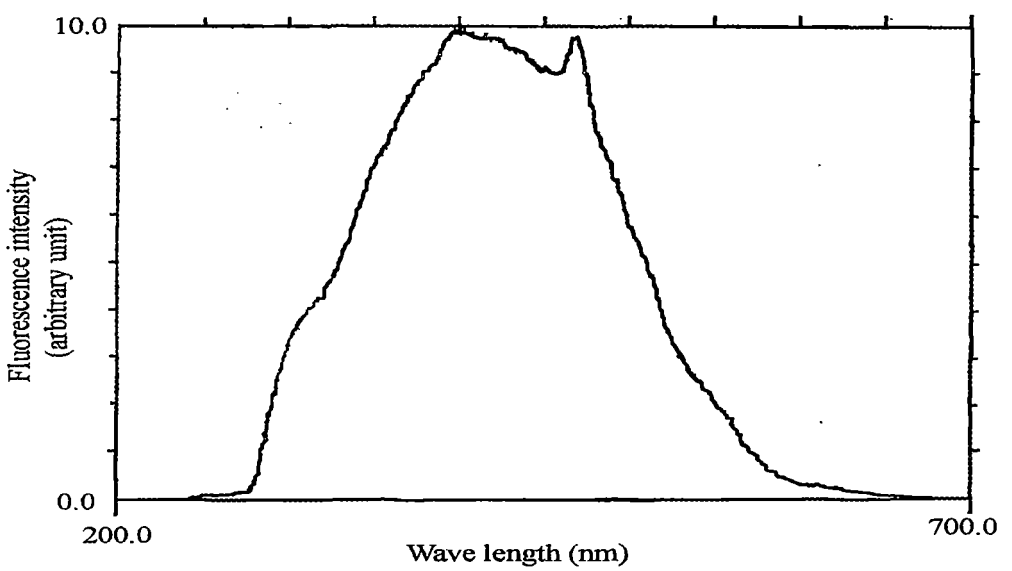

Fig. 52. Emission Spectrum of L-Tyrosinemethylester ($1x10^{-4}M$) in 50% 1,4-Dioxane.

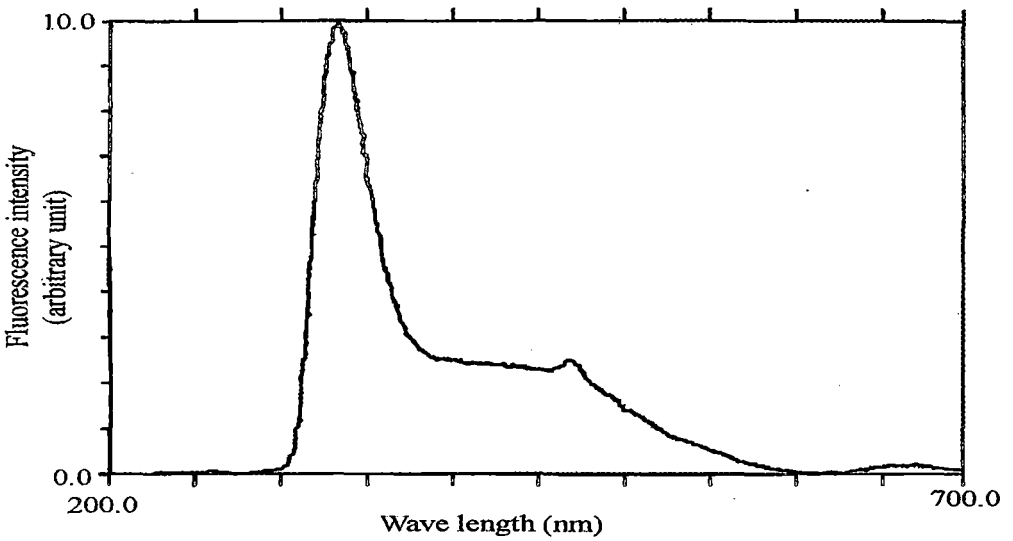

Fig. 53. Emission Spectrum of 5-Hydroxyindole ($1x10^{-4}$M) in 60% 1,4-Dioxane.

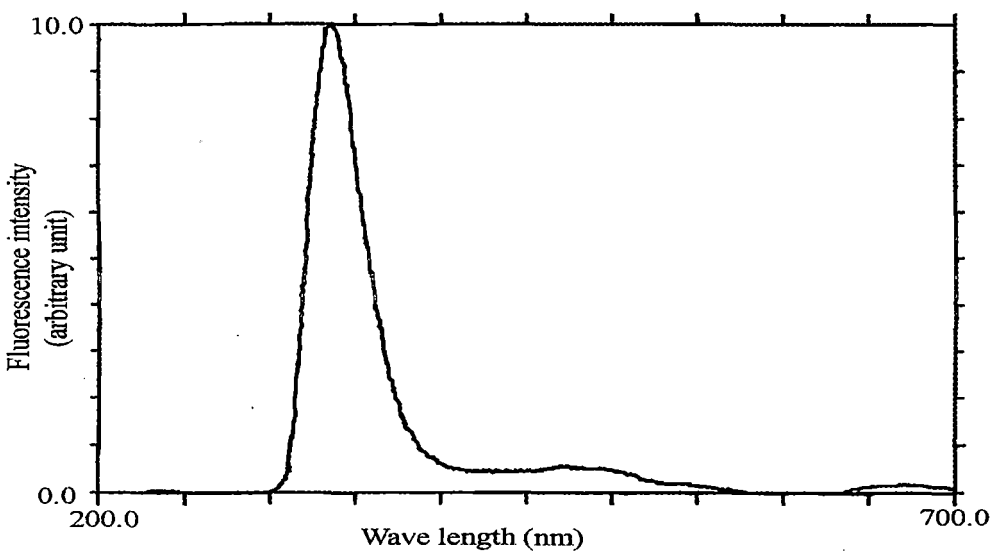

Fig. 54. Emission Spectrum of 5-Hydroxy-L-tryptophan ($1x10^{-4}$M) in 80% 1,4-Dioxane.

TABLE: 1

Transition energies of absorption and emission of 1-Naphthol in water and different alkanols along with the solvent parameters at 298K

Solvent	Transition Energy ($\bar{\nu}$)/cm^{-1}		Stokes Shift ($\bar{\nu}$)/cm^{-1}	Dielectric Constant(D)	Refractive Index(n)	Kosower-Z /kjmol^{-1}
	Absorption	Emission				
Water	31447	22727	8720	78.4	1.3333	395.8
Methanol	31250	28571	2679	32.6	1.3288	349.8
Ethanol	31056	28490	2566	24.3	1.3576	333.1
iso-Propyl alcohol	30864	28490	2374	20.1	1.3859	327.6
tert-Butyl Alcohol	30769	28490	2279	17.1	1.3993	325.1
Pentanol	30675	28409	2266	15.2	1.4101	315.5
Hexanol	30488	28409	2079	13.4	1.4198	311.3
Heptanol	30303	28409	1894	11.2	1.4249	304.2
Octanol	30211	28409	1802	10.0	1.4509	303.3

TABLE: 2

Transition energies of absorption and emission of 2-Naphthol in water and different alkanols along with the solvent parameters at 298K

Solvent	Transition Energy ($\bar{\nu}$)/cm^{-1}		Stokes Shift ($\bar{\nu}$)/cm^{-1}	Dielectric Constant(D)	Refractive Index(n)	Kosower-Z /kjmol^{-1}
	Absorption	Emission				
Water	30303	28169	2134	78.4	1.3333	395.8
Methanol	30120	28090	2030	32.6	1.3288	349.8
Ethanol	30030	28090	1940	24.3	1.3576	333.1
iso-Propyl alcohol	29940	28090	1850	20.1	1.3859	327.6
tert-Butyl Alcohol	29674	28011	1663	17.1	1.3993	325.1
Pentanol	29586	27933	1653	15.2	1.4101	315.5
Hexanol	29499	27933	1566	13.4	1.4198	311.3
Heptanol	29412	27778	1634	11.2	1.4249	304.2
Octanol	29326	27778	1548	10.0	1.4509	303.3

TABLE: 3

Transition energies of absorption and emission of 5-Hydroxyindole in water and different alkanols along with the solvent parameters at 298K

Solvent	Transition Energy ($\bar{\nu}$)/cm^{-1}		Stokes Shift ($\bar{\nu}$)/cm^{-1}	Dielectric Constant(D)	Refractive Index(n)	Kosower-Z /kjmol^{-1}
	Absorption	Emission				
Water	32258	29851	2407	78.4	1.3333	395.8
Methanol	32051	29762	2289	32.6	1.3288	349.8
Ethanol	31874	29674	2173	24.3	1.3576	333.1
iso-Propyl alcohol	31746	29586	2160	20.1	1.3859	327.6
tert-Butyl Alcohol	31646	29586	2060	17.1	1.3993	325.1
Pentanol	31546	29499	2047	15.2	1.4101	315.5
Hexanol	31348	29412	1936	13.4	1.4198	311.3
Heptanol	31259	29412	1838	11.2	1.4249	304.2
Octanol	31056	29412	1644	10.0	1.4509	303.3

TABLE: 4

Transition energies of absorption and emission of 5-Hydroxy-L-Tryptophan in water and different alkanols along with the solvent parameters at 298K

Solvent	Transition Energy (ν)/cm^{-1}		Stokes Shift (ν)/cm^{-1}	Dielectric Constant(D)	Refractive Index(n)	Kosower-Z /kjmol^{-1}
	Absorption	Emission				
Water	31948	29499	2449	78.4	1.3333	395.8
Methanol	31646	29412	2234	32.6	1.3288	349.8
Ethanol	31546	29412	2134	24.3	1.3576	333.1
iso-Propyl alcohol	31447	29240	2207	20.1	1.3859	327.6
tert-Butyl Alcohol	31250	29155	2095	17.1	1.3993	325.1
Pentanol	31152	29155	1997	15.2	1.4101	315.5
Hexanol	31056	29070	1986	13.4	1.4198	311.3
Heptanol	30960	29070	1890	11.2	1.4249	304.2
Octanol	30864	29070	1974	10.0	1.4509	303.3

TABLE: 5

Transition energies of absorption and emission of L-Tyrosinemethylester in water and different alkanols along with the solvent parameters at 298K

Solvent	Transition Energy ($\bar{\nu}$)/cm^{-1}		Stokes Shift ($\bar{\nu}$)/cm^{-1}	Dielectric Constant(D)	Refractive Index(n)	Kosower-Z /kjmol^{-1}
	Absorption	Emission				
Water	35714	32258	3456	78.4	1.3333	395.8
Methanol	35416	32258	3203	32.6	1.3288	349.8
Ethanol	35336	32258	3078	24.3	1.3576	333.1
iso-Propyl alcohol	35088	32154	2934	20.1	1.3859	327.6
tert-Butyl Alcohol	34965	32051	2914	17.1	1.3993	325.1
Pentanol	34843	32051	2792	15.2	1.4101	315.5
Hexanol	34722	31949	2773	13.4	1.4198	311.3
Heptanol	34602	31949	2653	11.2	1.4249	304.2
Octanol	34364	31847	2517	10.0	1.4509	303.3

TABLE: 6

Transition energies of absorption and emission of 1-Naphthol in 1,4-Dioxane-water mixtures along with the medium parameters at 298K

Dioxane % (v/v)	Transition Energy ($\bar{\nu}$)/cm^{-1}		Stokes Shift ($\bar{\nu}$)/cm^{-1}	Dielectric Constant(D)	Refractive Index(n)	Kosower-Z /kjmol^{-1}
	Absorption	Emission				
10%	31746	22321	9425	69.2	1.3444	392.8
20%	31646	22321	9325	61.9	1.3515	379.1
30%	31546	22371	9175	53.2	1.3675	363.2
50%	31348	22422	8926	40.7	1.3810	347.8
60%	31250	22422	8828	27.2	1.3910	335.6
80%	31056	22472	8584	11.9	1.4070	319.7

TABLE: 7

Transition energies of absorption and emission of 2-Naphthol in 1,4-Dioxane-water mixtures along with the medium parameters at 298K

Dioxane % (v/v)	Transition Energy ($\bar{\nu}$)/cm^{-1}		Stokes Shift ($\bar{\nu}$)/cm^{-1}	Dielectric Constant(D)	Refractive Index(n)	Kosower-Z /kjmol^{-1}
	Absorption	Emission				
10%	32789	30120	2669	69.2	1.3444	392.8
20%	32680	30211	2469	61.9	1.3515	379.1
30%	32573	30303	2270	53.2	1.3675	363.2
50%	32362	30488	1874	40.7	1.3810	347.8
60%	32258	30581	1677	27.2	1.3910	335.6
80%	32258	30675	1583	11.9	1.4070	319.7

TABLE: 8

Transition energies of absorption and emission of 5-Hydroxyindole in 1,4-Dioxane-water mixtures along with the medium parameters at 298K

Dioxane % (v/v)	Transition Energy ($\bar{\nu}$)/cm^{-1}		Stokes Shift ($\bar{\nu}$)/cm^{-1}	Dielectric Constant(D)	Refractive Index(n)	Kosower-Z /kjmol^{-1}
	Absorption	Emission				
10%	32258	30120	2138	69.2	1.3444	392.8
20%	32154	30120	2034	61.9	1.3515	379.1
30%	32051	30211	1840	53.2	1.3675	363.2
50%	31847	30303	1544	40.7	1.3810	347.8
60%	31746	30488	1258	27.2	1.3910	335.6
80%	31546	30488	1058	11.9	1.4070	319.7

TABLE: 9

Transition energies of absorption and emission of 5-Hydroxy-L-tryptophan in 1,4-Dioxane-water mixtures along with the medium parameters at 298K

Dioxane % (v/v)	Transition Energy ($\bar{\nu}$)/cm^{-1}		Stokes Shift ($\bar{\nu}$)/cm^{-1}	Dielectric Constant(D)	Refractive Index(n)	Kosower-Z /kjmol^{-1}
	Absorption	Emission				
10%	32051	29851	2200	69.2	1.3444	392.8
20%	31949	30030	1919	61.9	1.3515	379.1
30%	31746	30120	1626	53.2	1.3675	363.2
50%	31646	30120	1526	40.7	1.3810	347.8
60%	31447	30211	1236	27.2	1.3910	335.6
80%	31250	30303	0947	11.9	1.4070	319.7

TABLE: 10

Transition energies of absorption and emission of L-Tyrosinemethylester in 1,4-Dioxane-water mixtures along with the medium parameters at 298K

Dioxane % (v/v)	Transition Energy ($\bar{\nu}$)/cm^{-1}		Stokes Shift ($\bar{\nu}$)/cm^{-1}	Dielectric Constant(D)	Refractive Index(n)	Kosower-Z /kjmol^{-1}
	Absorption	Emission				
10%	36496	21231	15265	69.2	1.3444	392.8
20%	36366	21231	15135	61.9	1.3515	379.1
30%	36232	21231	15001	53.2	1.3675	363.2
50%	35971	21277	14694	40.7	1.3810	347.8
60%	35842	21277	14565	27.2	1.3910	335.6
80%	35714	21277	14437	11.9	1.4070	319.7

TABLE: 11

Transition energies of absorption and emission of L-Tyrosine in 1,4-Dioxane-water mixtures along with the medium parameters at 298K

Dioxane % (v/v)	Transition Energy ($\bar{\nu}$)/cm^{-1}		Stokes Shift ($\bar{\nu}$)/cm^{-1}	Dielectric Constant(D)	Refractive Index(n)	Kosower-Z /kjmol^{-1}
	Absorption	Emission				
10%	35714	21008	14706	69.2	1.3444	392.8
20%	35461	21008	14453	61.9	1.3515	379.1
30%	35211	21053	14158	53.2	1.3675	363.2
50%	35088	21053	14035	40.7	1.3810	347.8
60%	34965	21097	13868	27.2	1.3910	335.6
80%	34722	21097	13625	11.9	1.4070	319.7

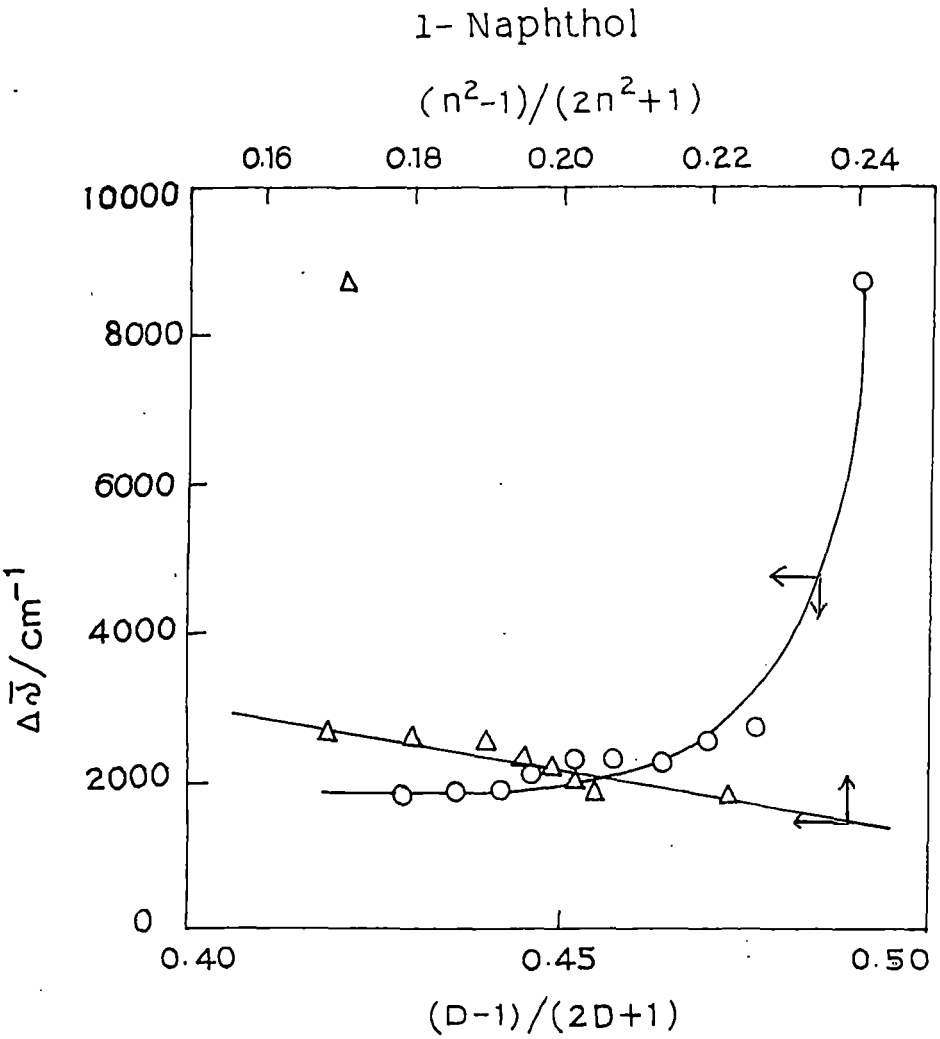

Fig.55. The plot of Stokes' shift, $\Delta\bar{\nu}$ against dielectric constant function and the refractive index function of the solvents (water and alkanols).

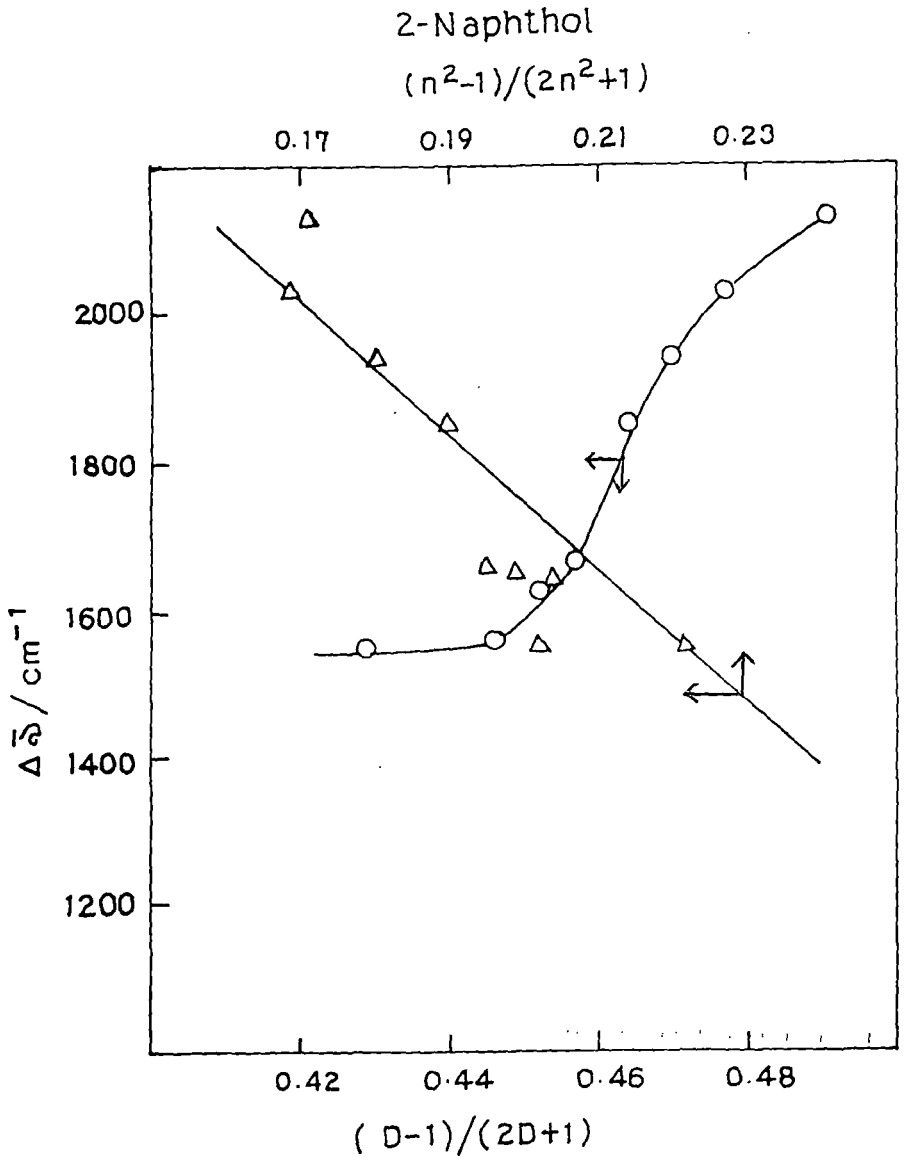

Fig.56. The plot of Stokes' shift, $\Delta\bar{\nu}$ against dielectric constant function and the refractive index function of the solvents (water and alkanols).

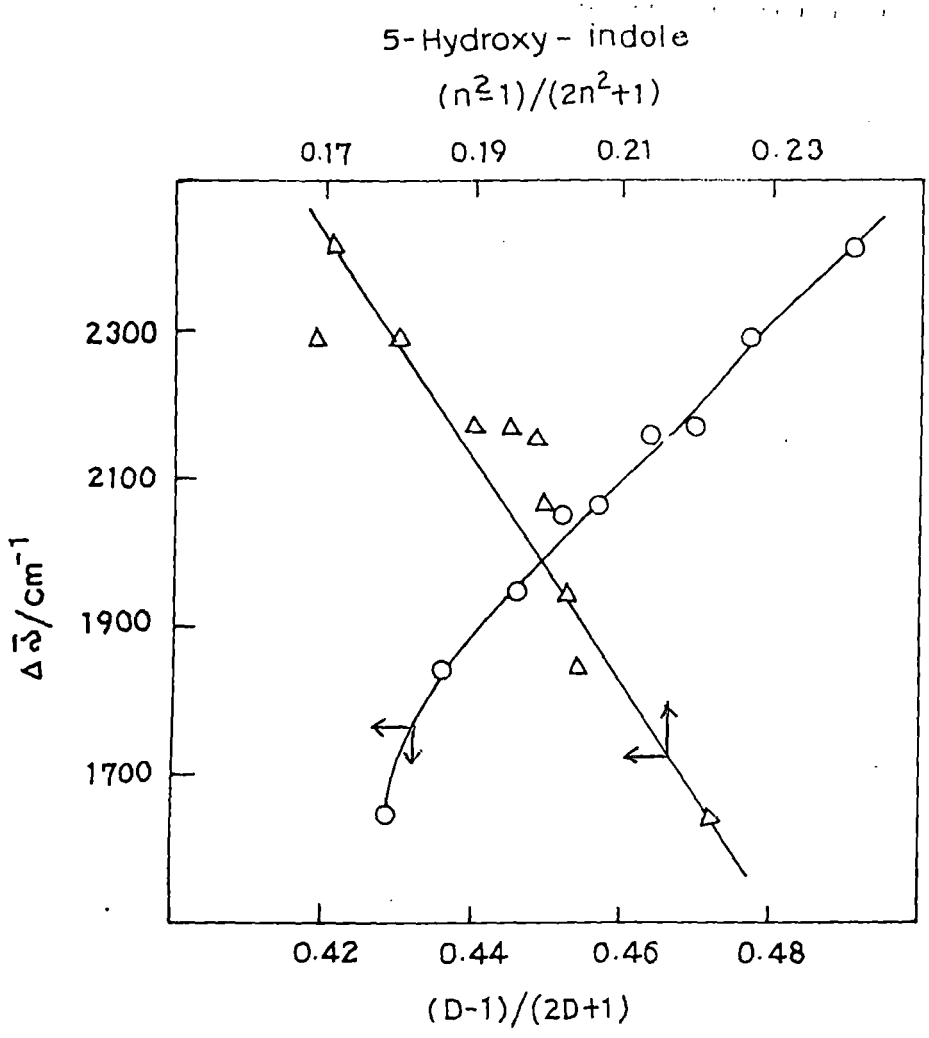

Fig.57. The plot of Stokes' shift, $\Delta\bar{\nu}$ against dielectric constant function and the refractive index function of the solvents (water and alkanols).

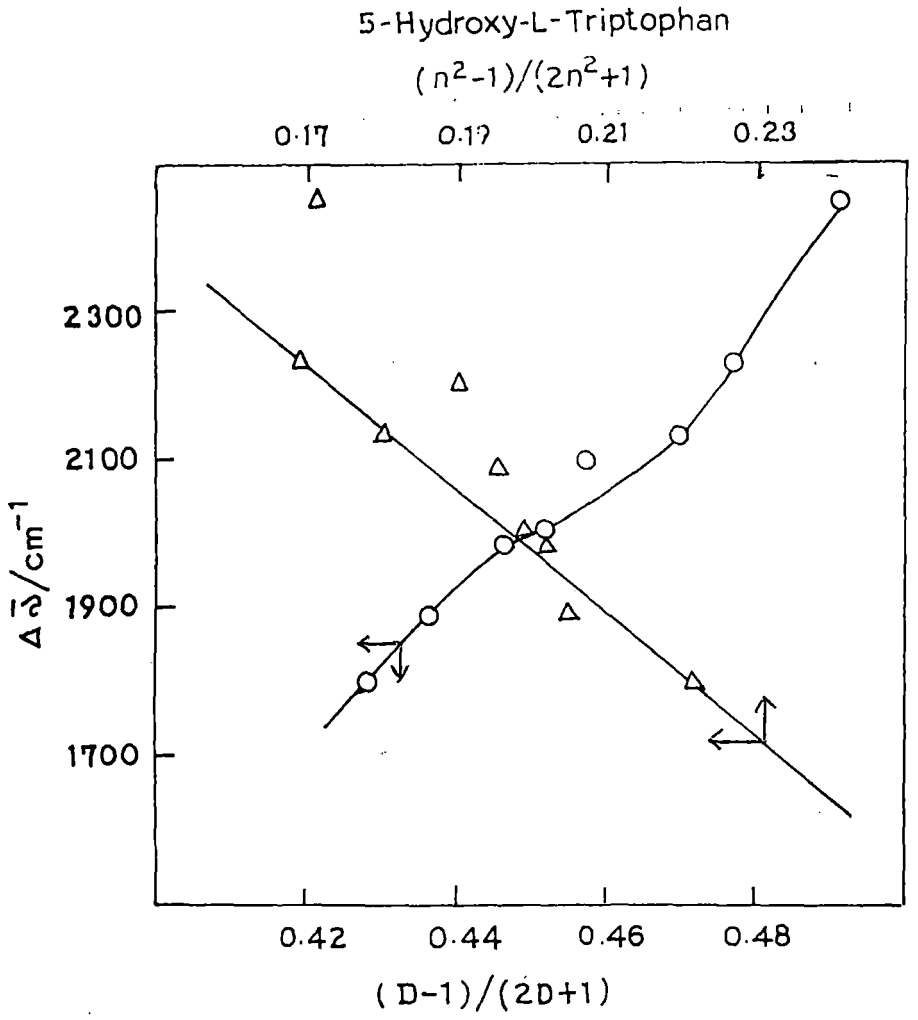

Fig.58. The plot of Stokes' shift, $\Delta\bar{\nu}$ against dielectric constant function and the refractive index function of the solvents (water and alkanols).

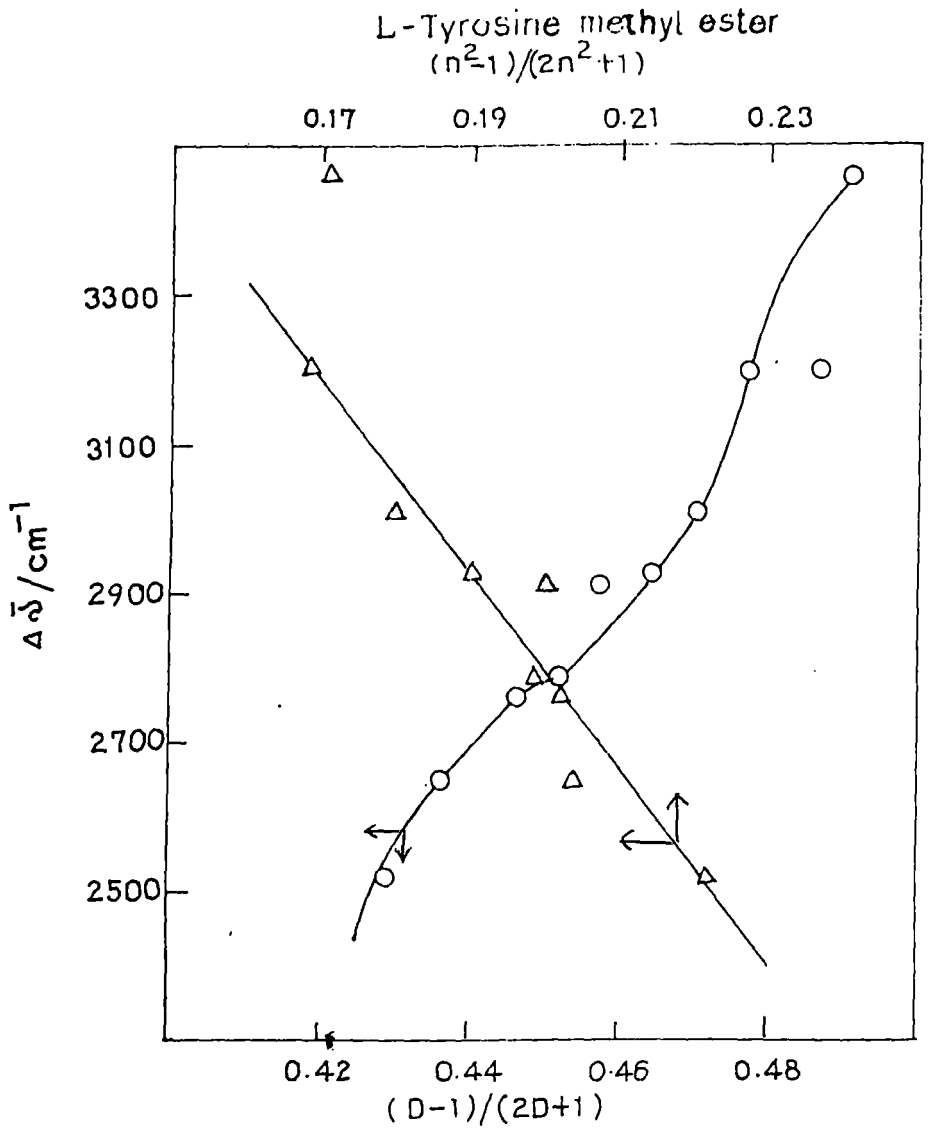

Fig.59. The plot of Stokes' shift, $\Delta\bar{\nu}$ against dielectric constant function and the refractive index function of the solvents (water and alkanols).

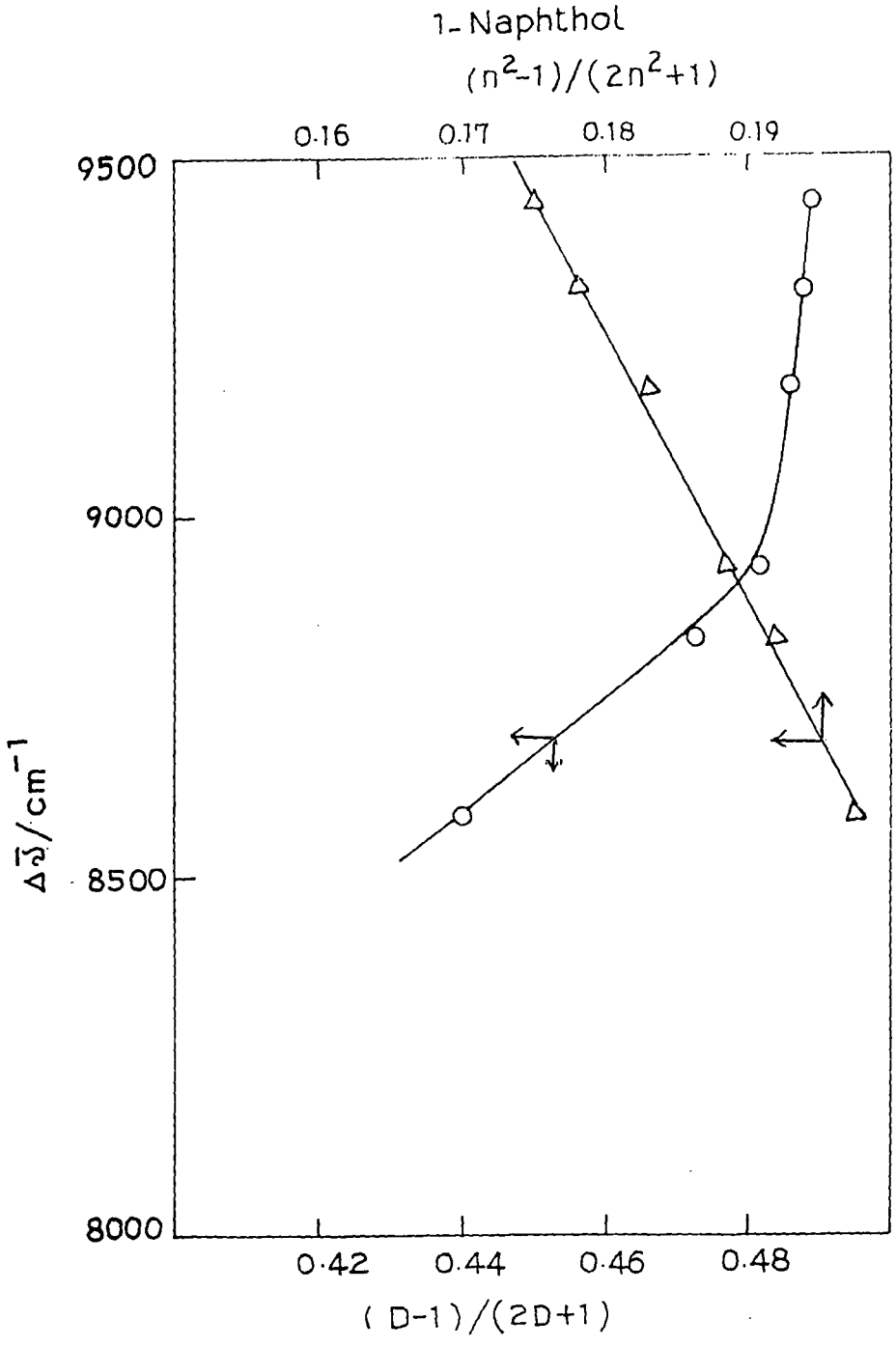

Fig.60.The plot of Stokes' shift, $\Delta\bar{\nu}$ against the dielectric constant function and the refractive index function of dioxane-water mixtures.

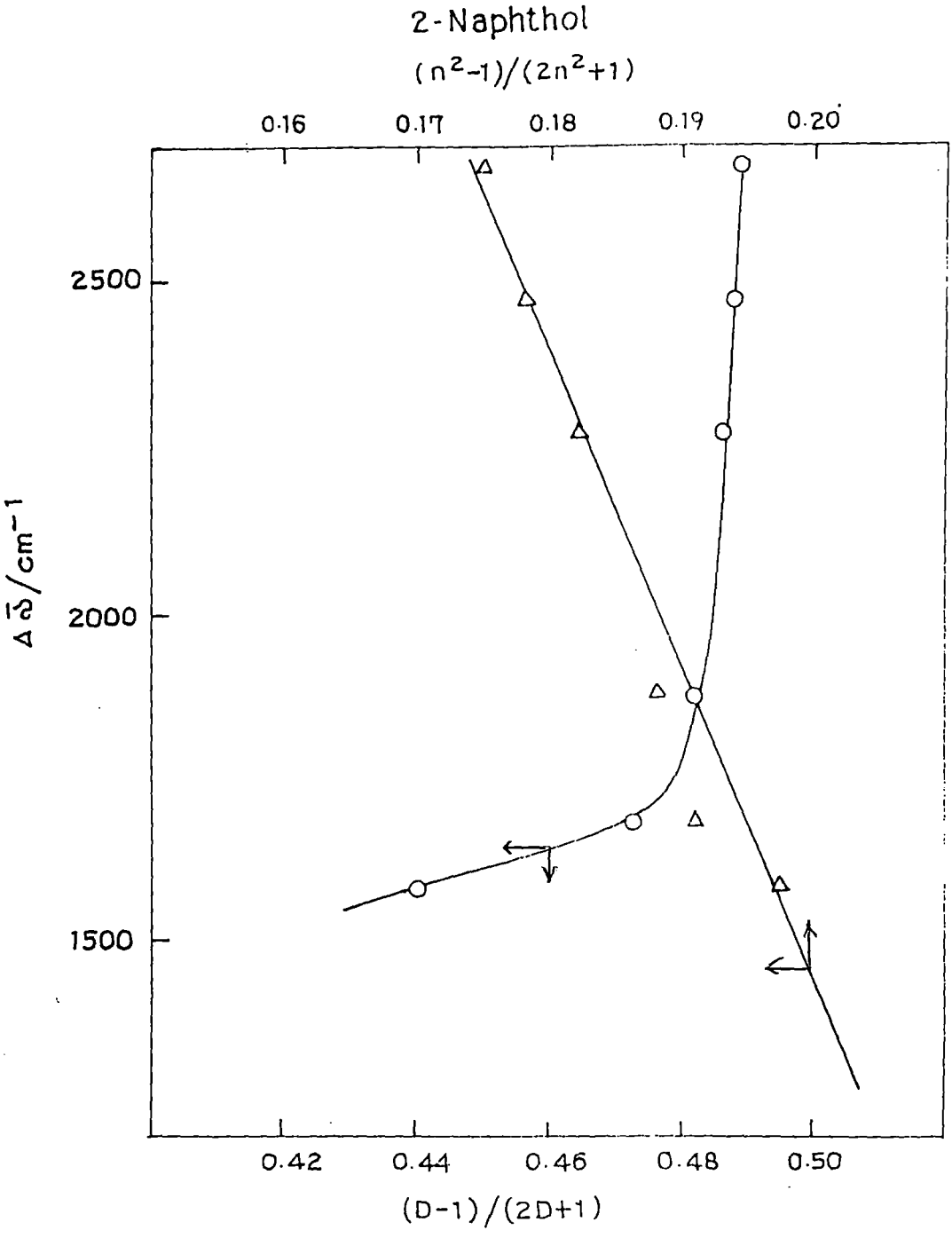

Fig.61. The plot of Stokes' shift, $\Delta\bar{\nu}$ against the dielectric constant function and the refractive index function of dioxane-water mixtures.

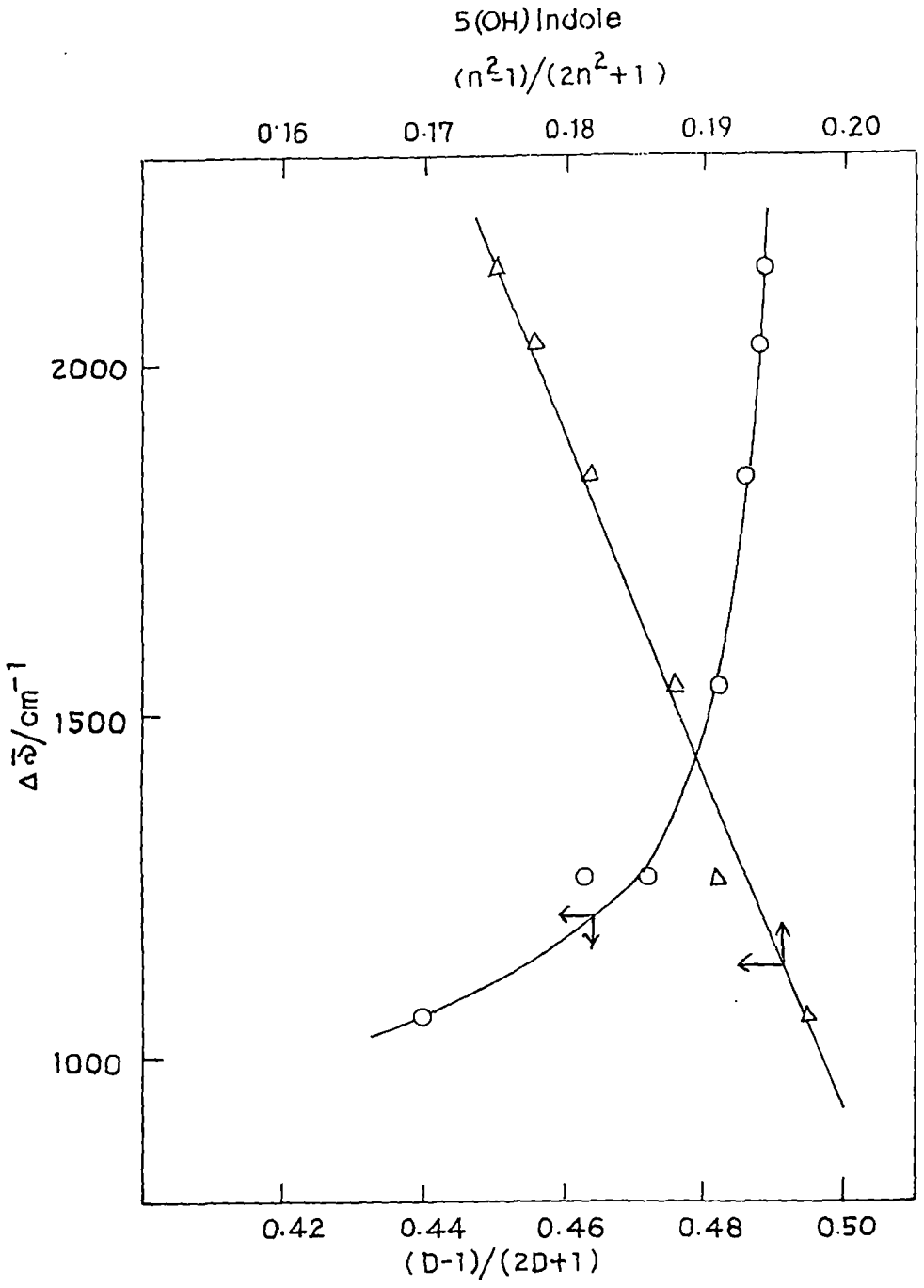

Fig.62. The plot of Stokes' shift, $\Delta\bar{\nu}$ against the dielectric constant function and the refractive index function of dioxane-water mixtures.

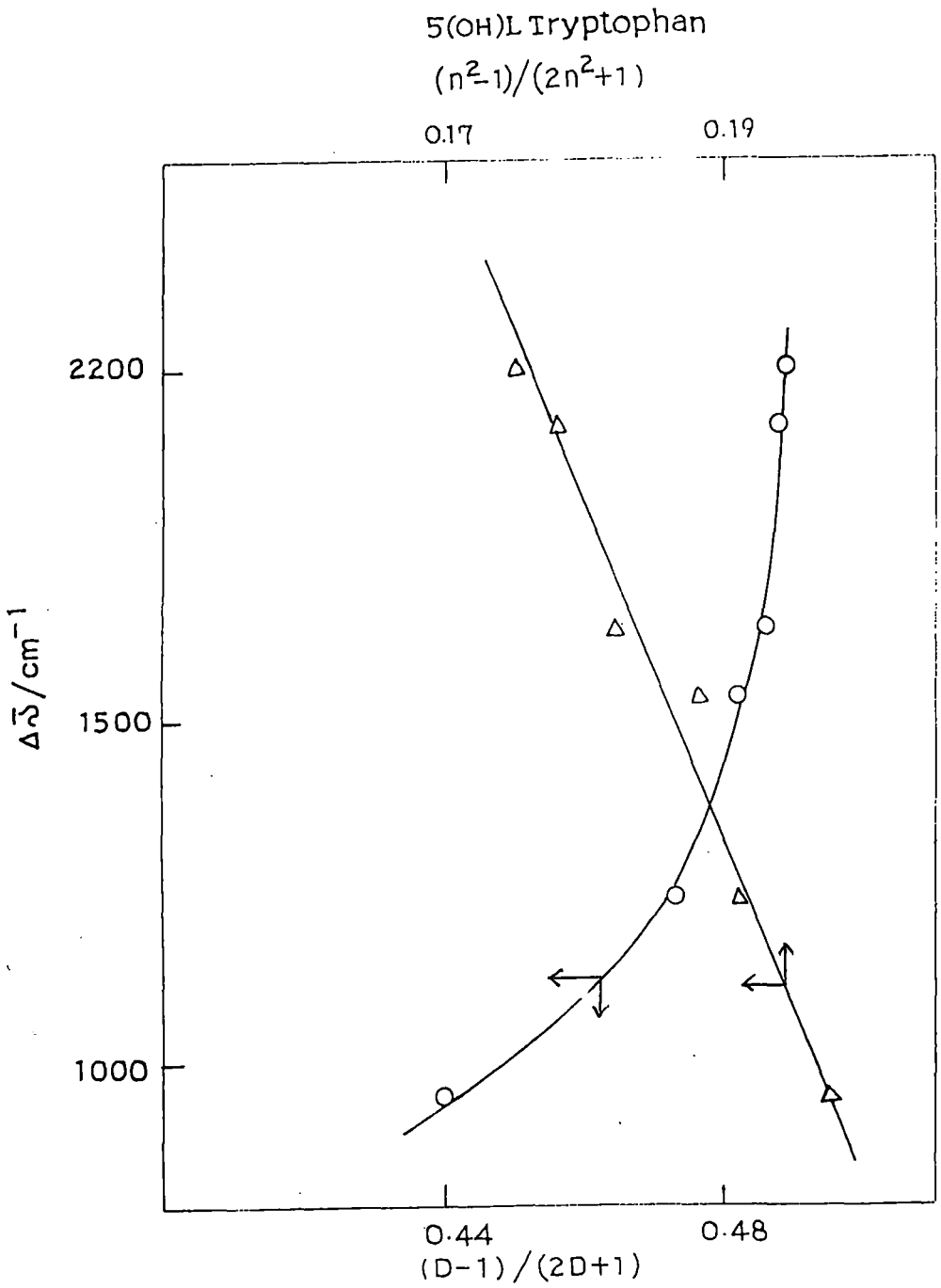

Fig.63. The plot of Stokes' shift, $\Delta\bar{\nu}$ against the dielectric constant function and the refractive index function of dioxane-water mixtures.

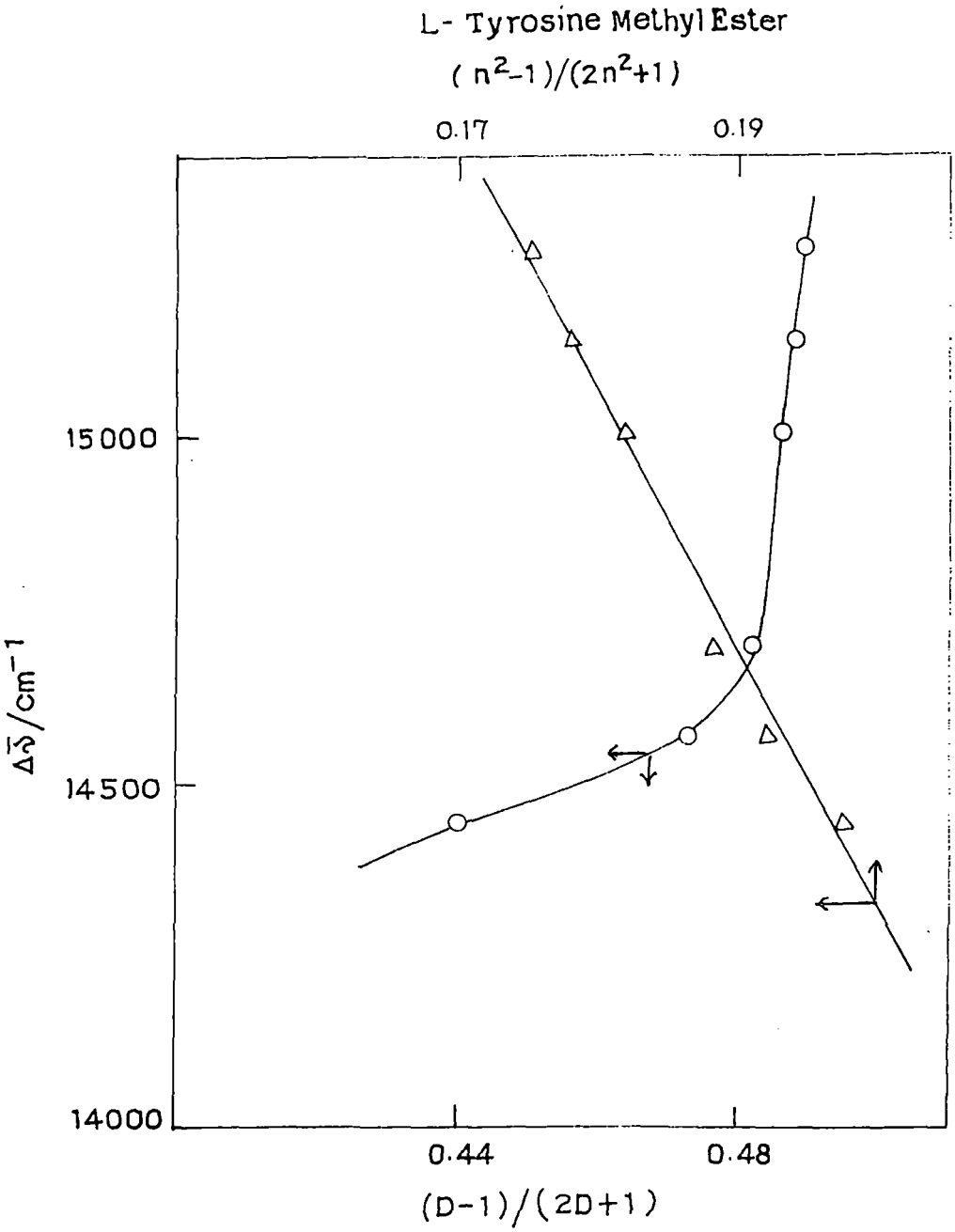

Fig.64.The plot of Stokes' shift, $\Delta\bar{\nu}$ against the dielectric constant function and the refractive index function of dioxane-water mixtures.

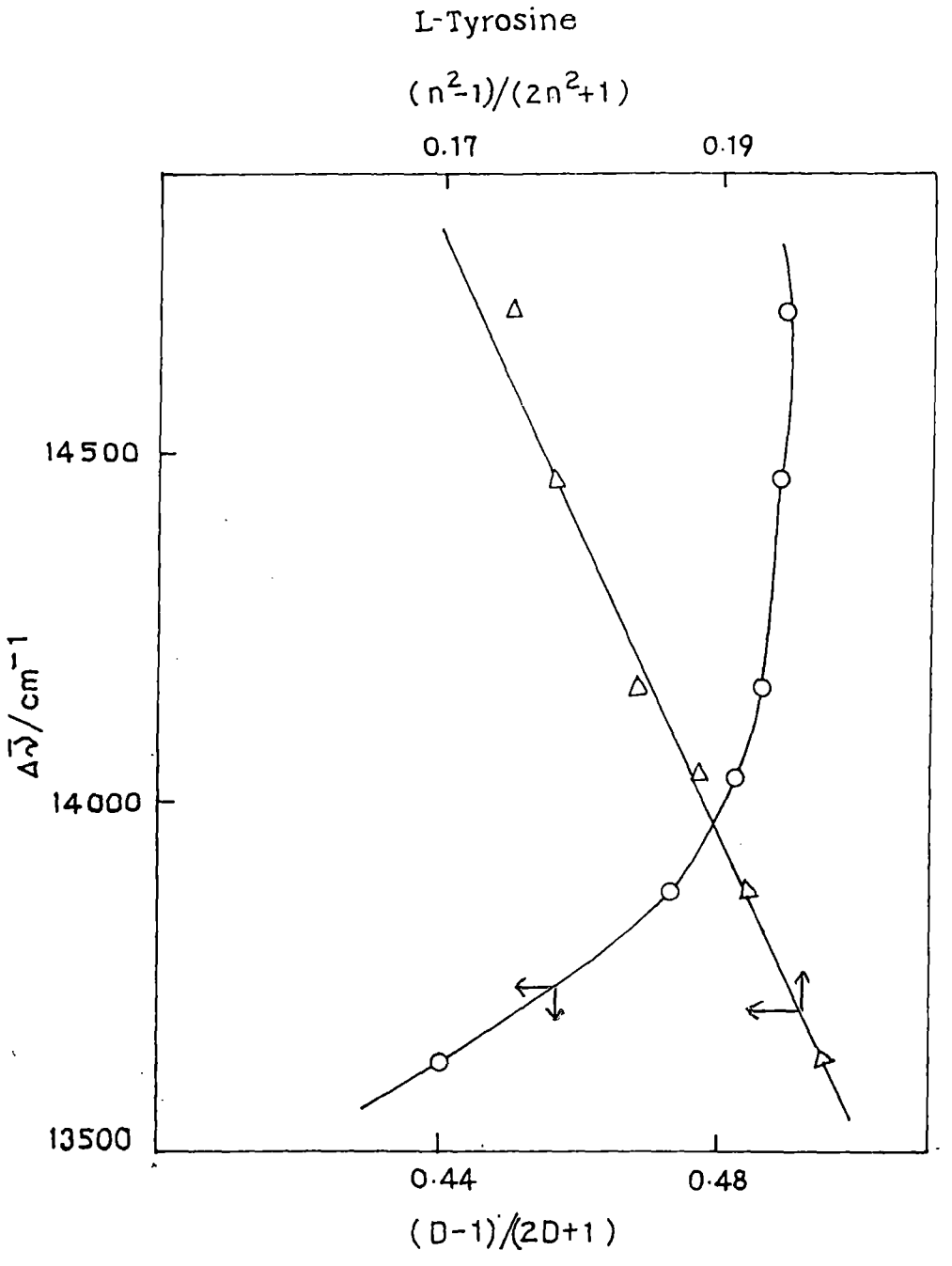

Fig.65. The plot of Stokes' shift, $\Delta\bar{\nu}$ against the dielectric constant function and the refractive index function of dioxane-water mixtures.

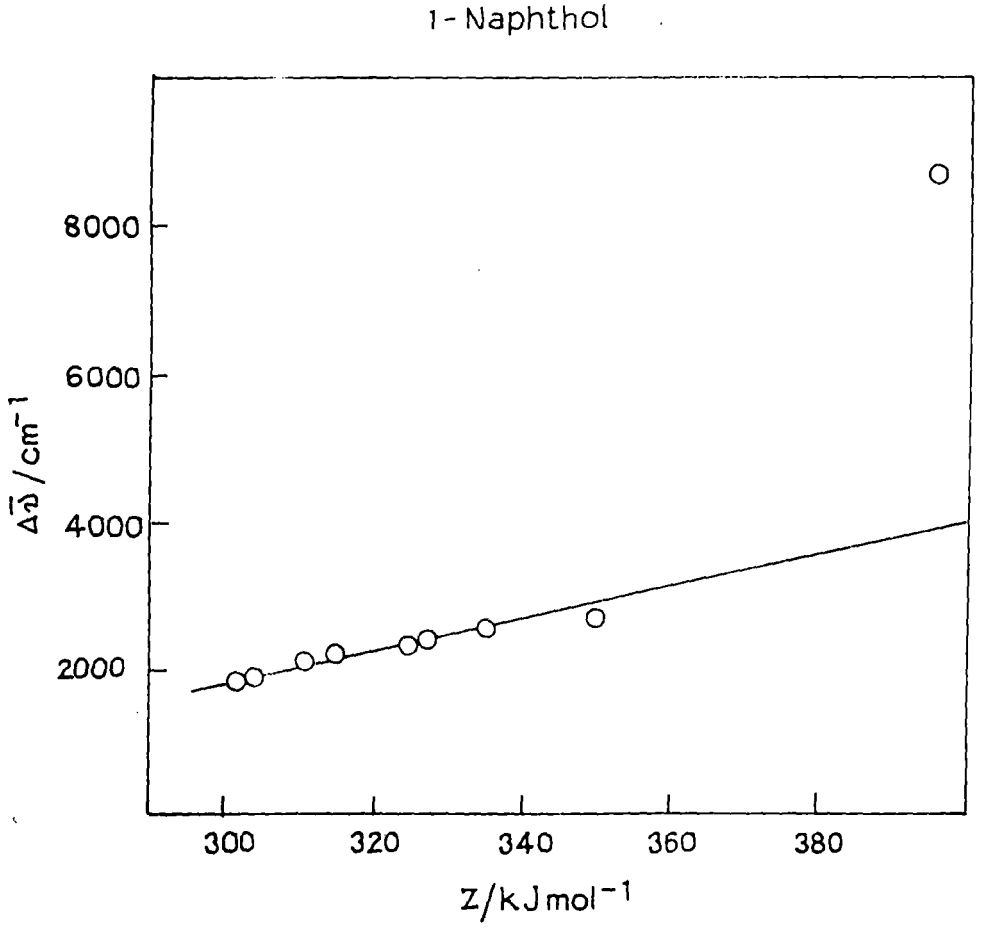

Fig.66. The plot of Stokes' shift, $\Delta\bar{\nu}$ against Kosower-Z values of the solvents (water and alkanols).

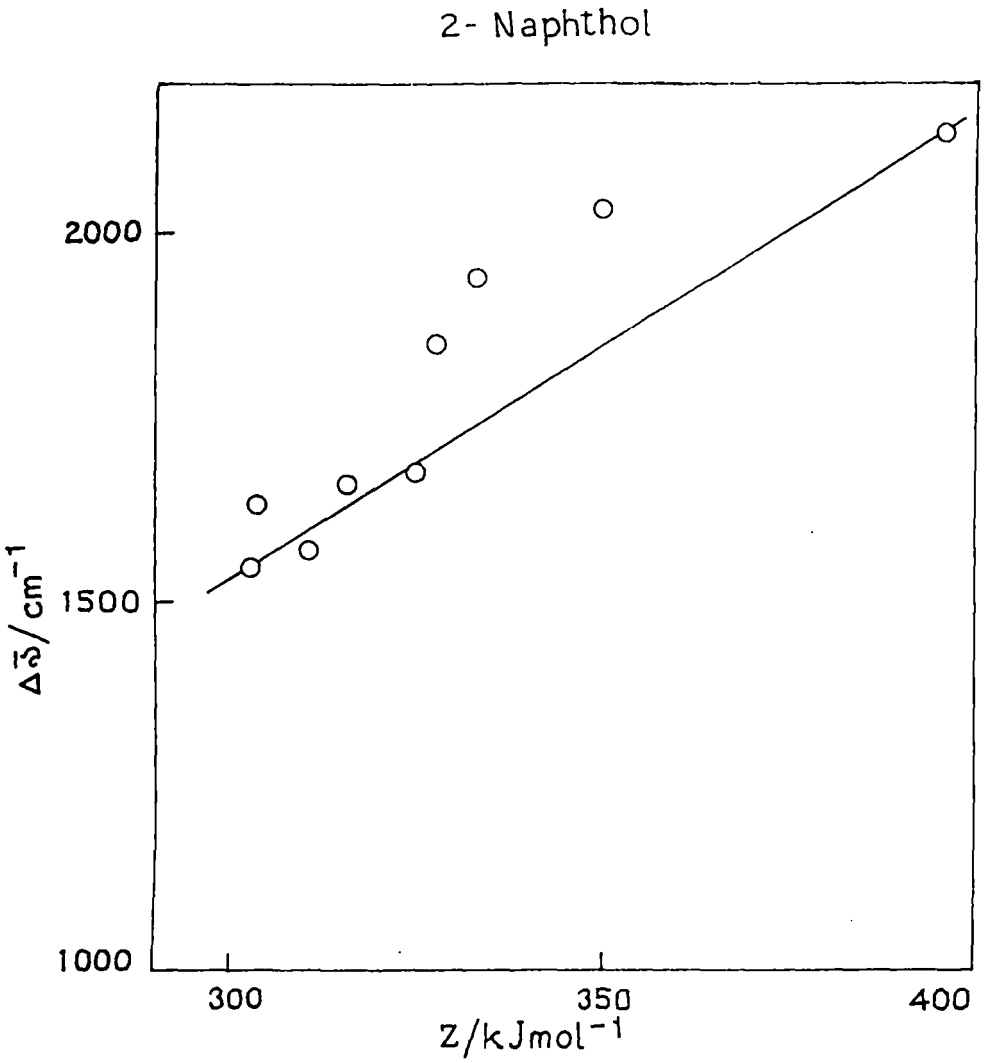

Fig.67. The plot of Stokes' shift, $\Delta\bar{\nu}$ against Kosower-Z values of the solvents (water and alkanols).

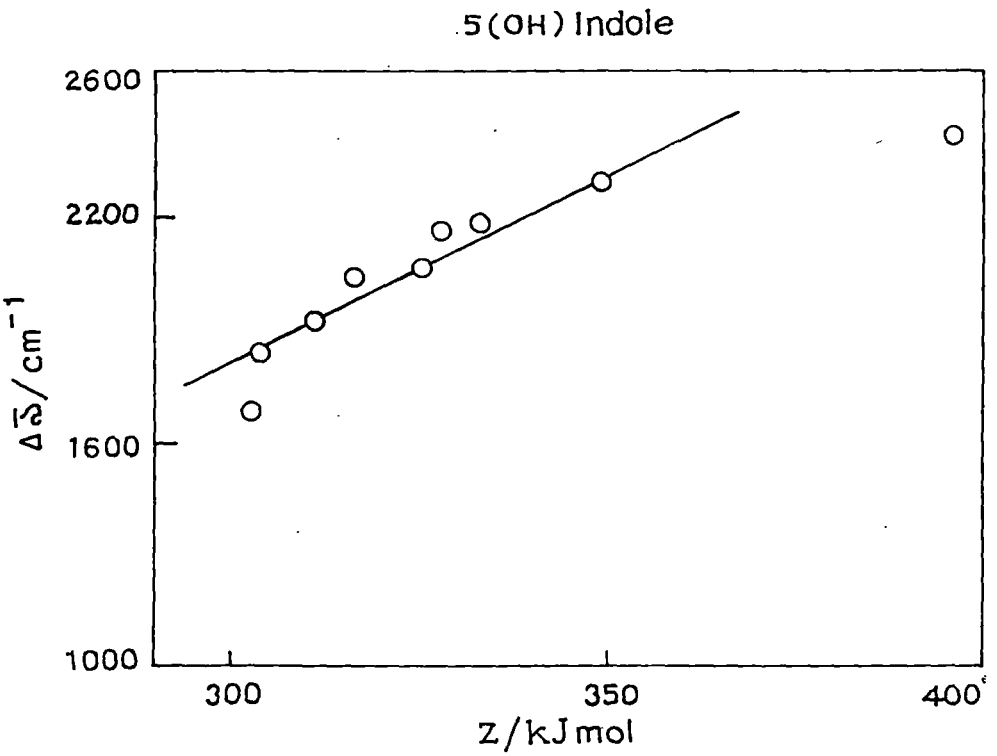

Fig.68. The plot of Stokes' shift, $\Delta\bar{\nu}$ against Kosower-Z values of the solvents (water and alkanols).

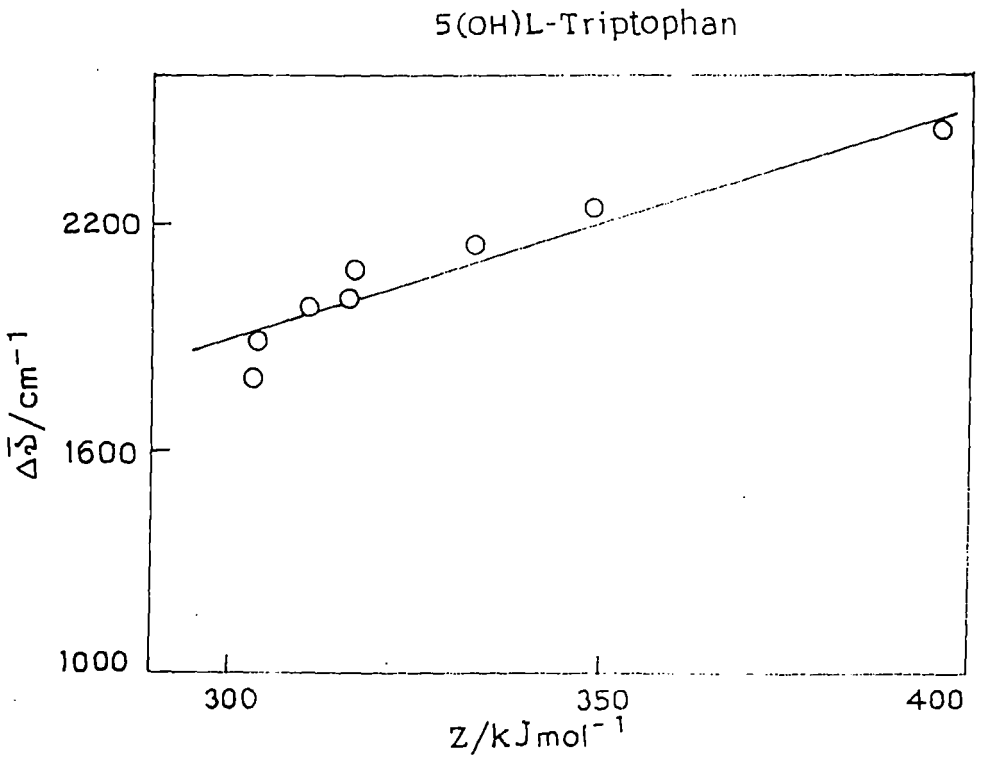

Fig.69. The plot of Stokes' shift, $\Delta\bar{\nu}$ against Kosower-Z values of the solvents (water and alkanols).

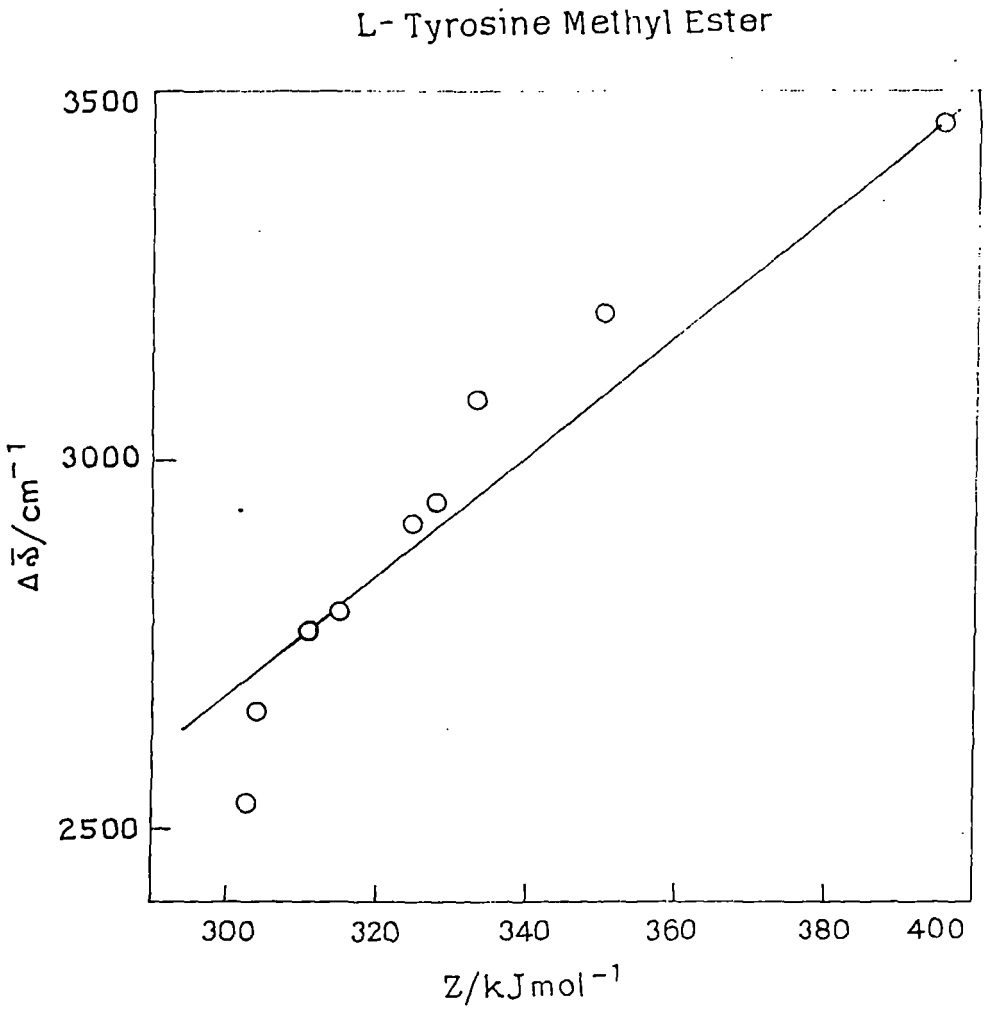

Fig.70. The plot of Stokes' shift, $\Delta\bar{\nu}$ against Kosower-Z values of the solvents (water and alkanols).

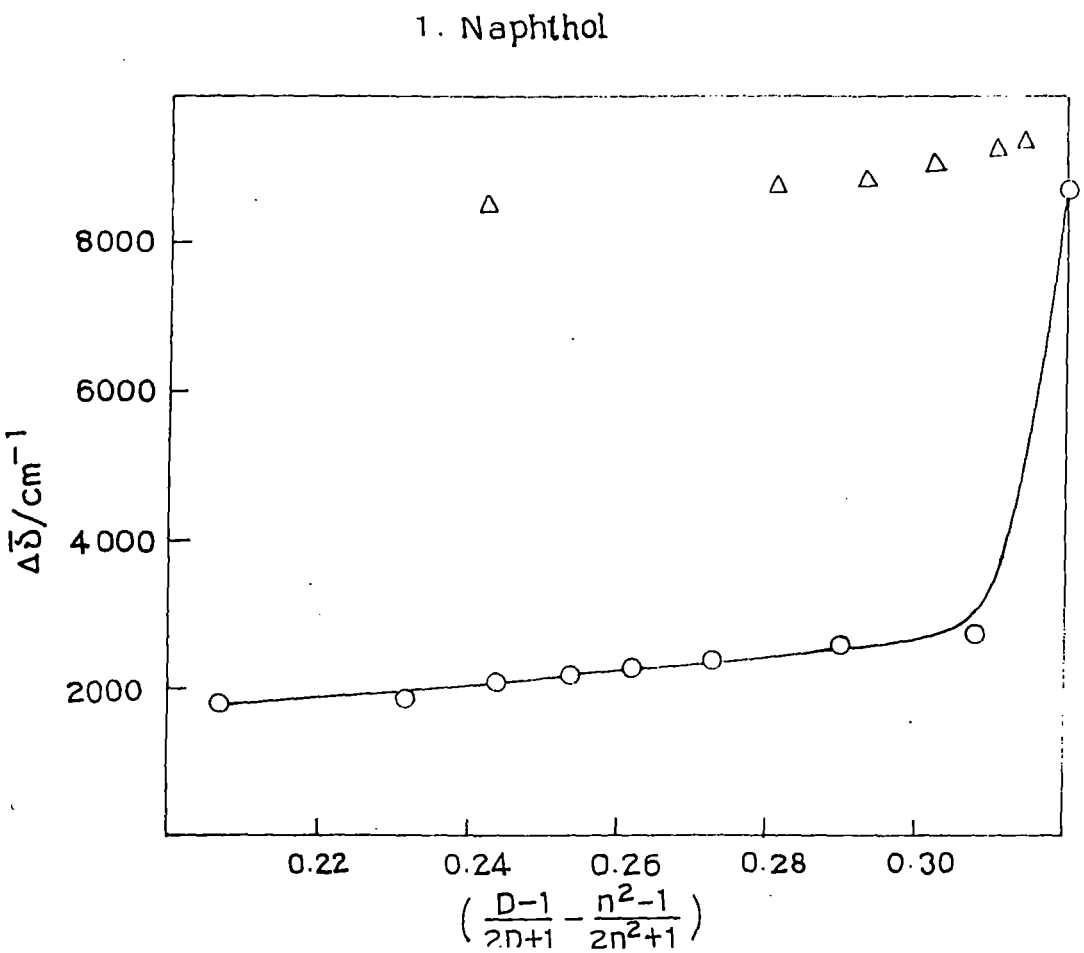

Fig.71. The plot of Stokes' shift, $\Delta\bar{\nu}$ against the solvent polarity function, $[(D-1)/(2D+1)] - [(n^2-1)/(2n^2+1)]$ of different alkanols [O] and dioxane-water mixtures [Δ].

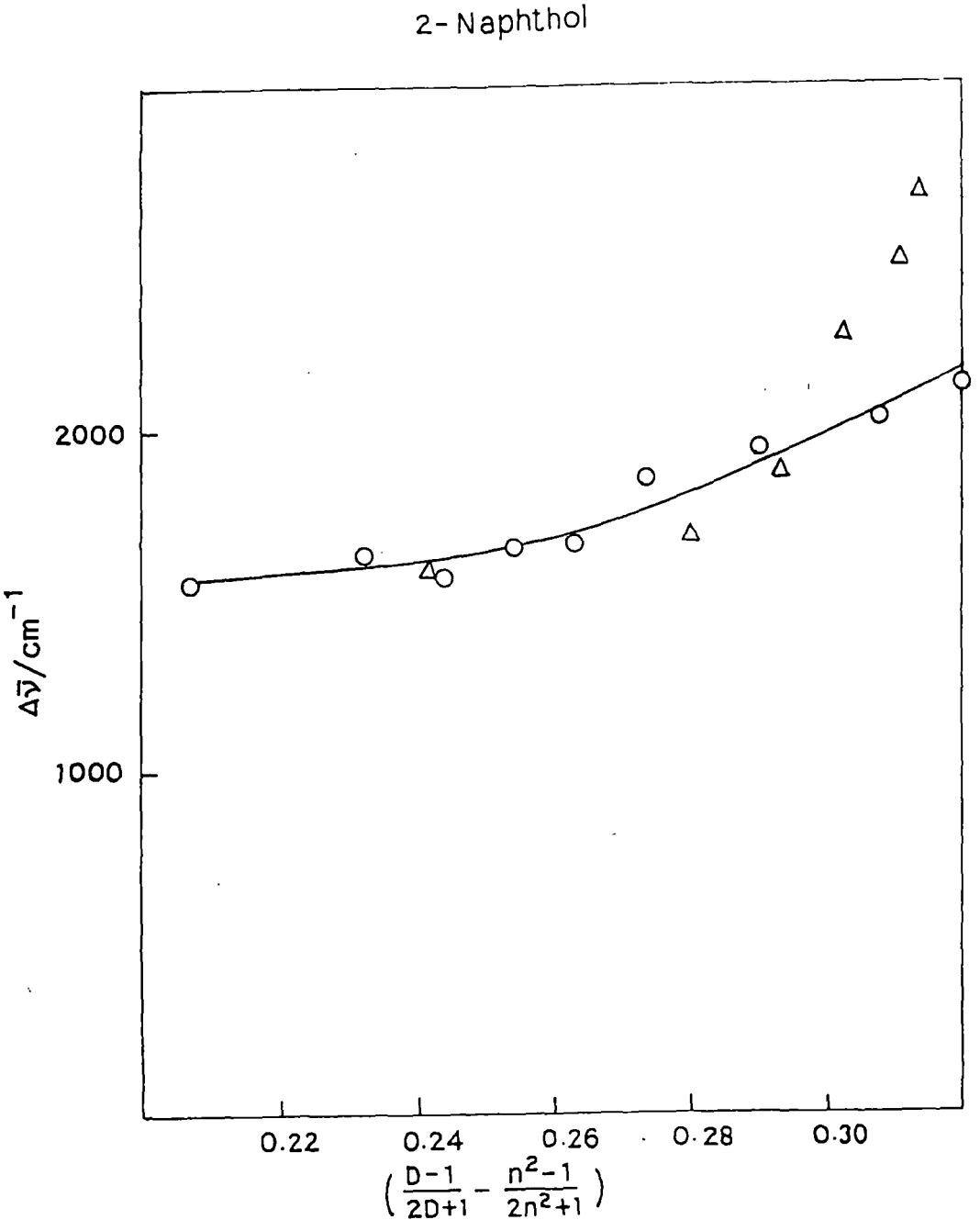

Fig.72. The plot of Stokes' shift, $\Delta\bar{\nu}$ against the solvent polarity function, $[(D-1)/(2D+1)] - [(n^2-1)/(2n^2+1)]$ of different alkanols [O] and dioxane-water mixtures [Δ].

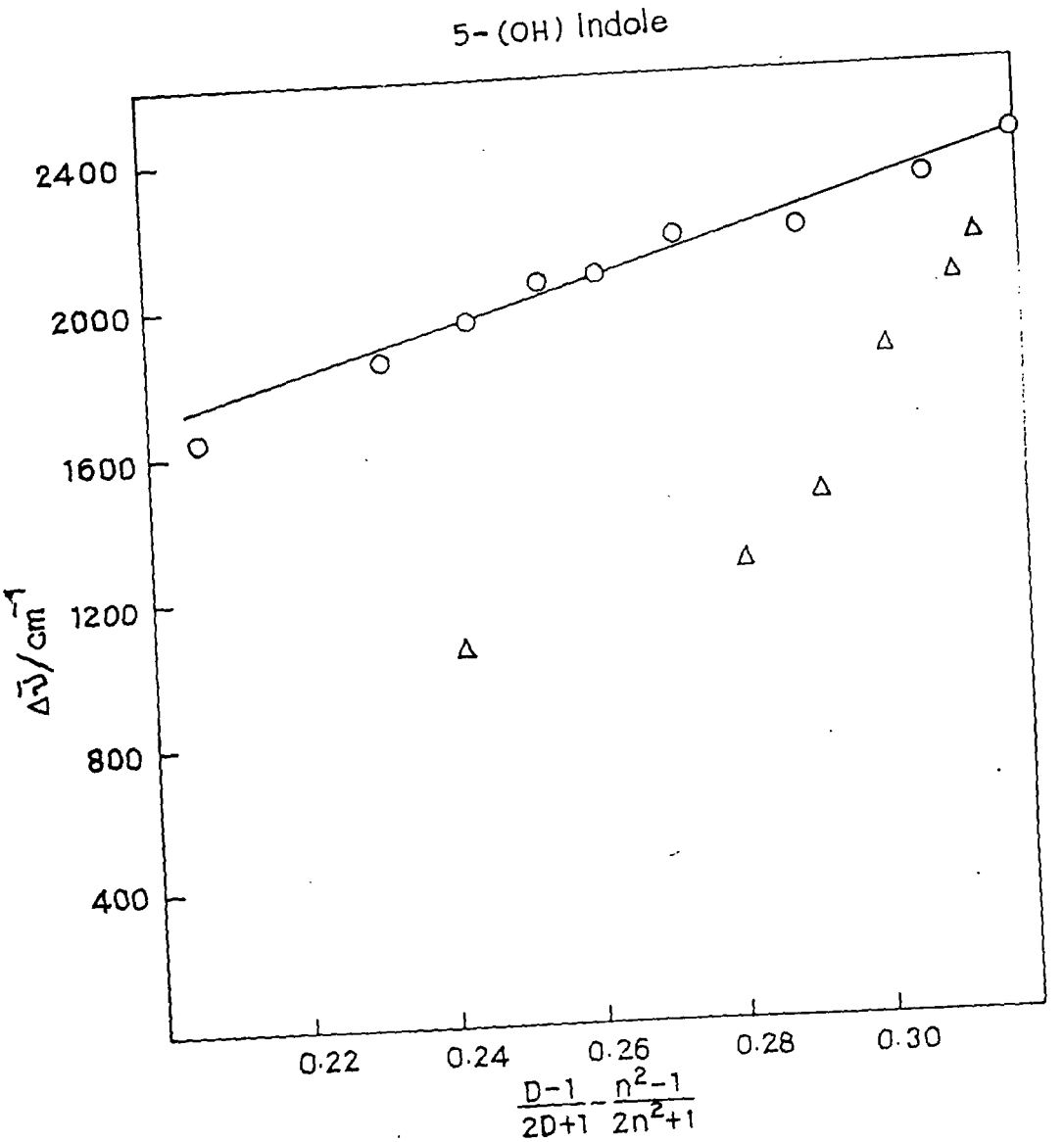

Fig.73. The plot of Stokes' shift, $\Delta\tilde{\nu}$ against the solvent polarity function, $[(D-1)/(2D+1)] - [(n^2-1)/(2n^2+1)]$ of different alkanols [O] and dioxane-water mixtures [Δ].

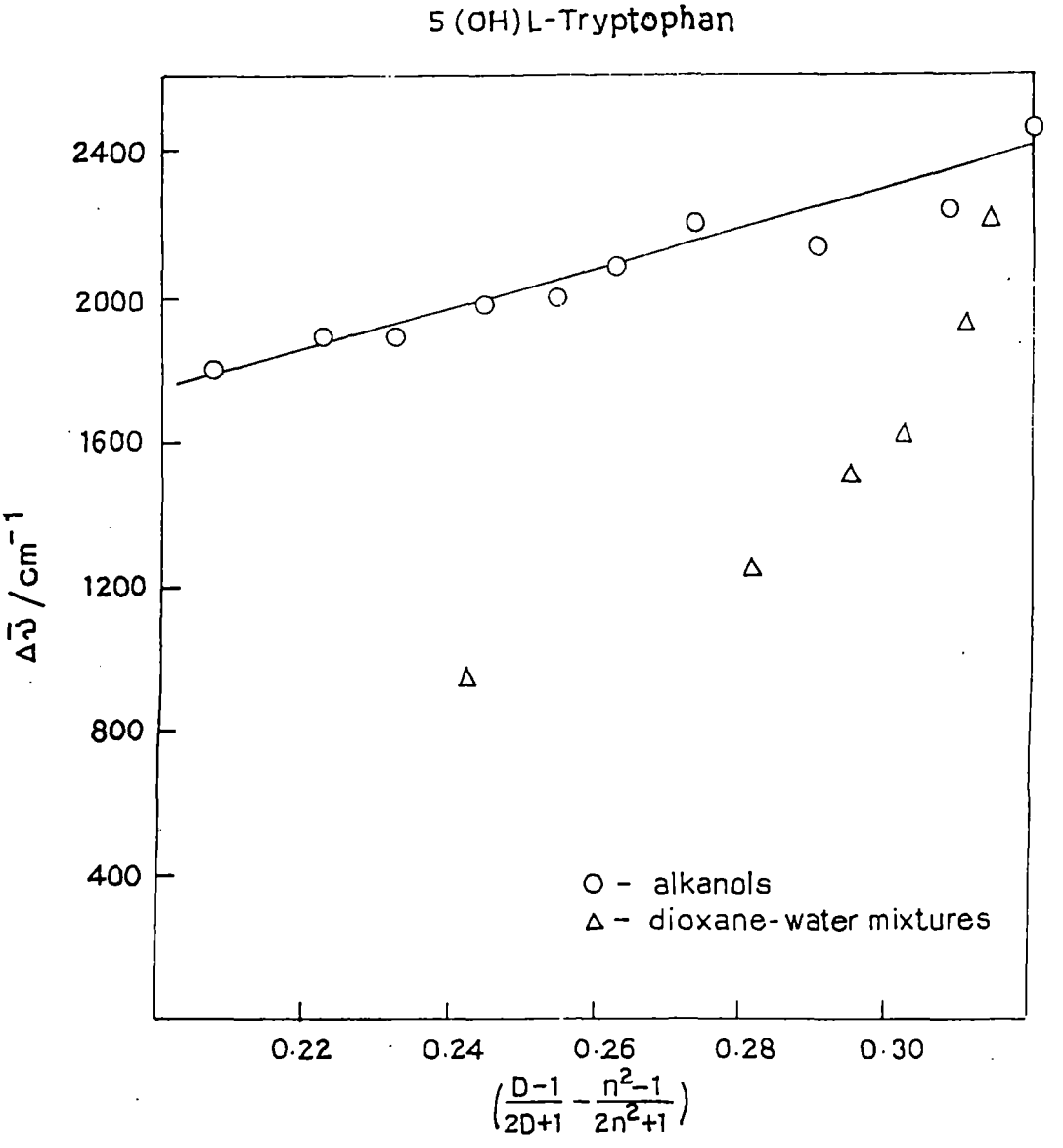

Fig. 74. The plot of Stokes' shift, $\Delta\bar{\nu}$ against the solvent polarity function, $[(D-1)/(2D+1)] - [(n^2-1)/(2n^2+1)]$ of different alkanols [O] and dioxane-water mixtures [Δ].

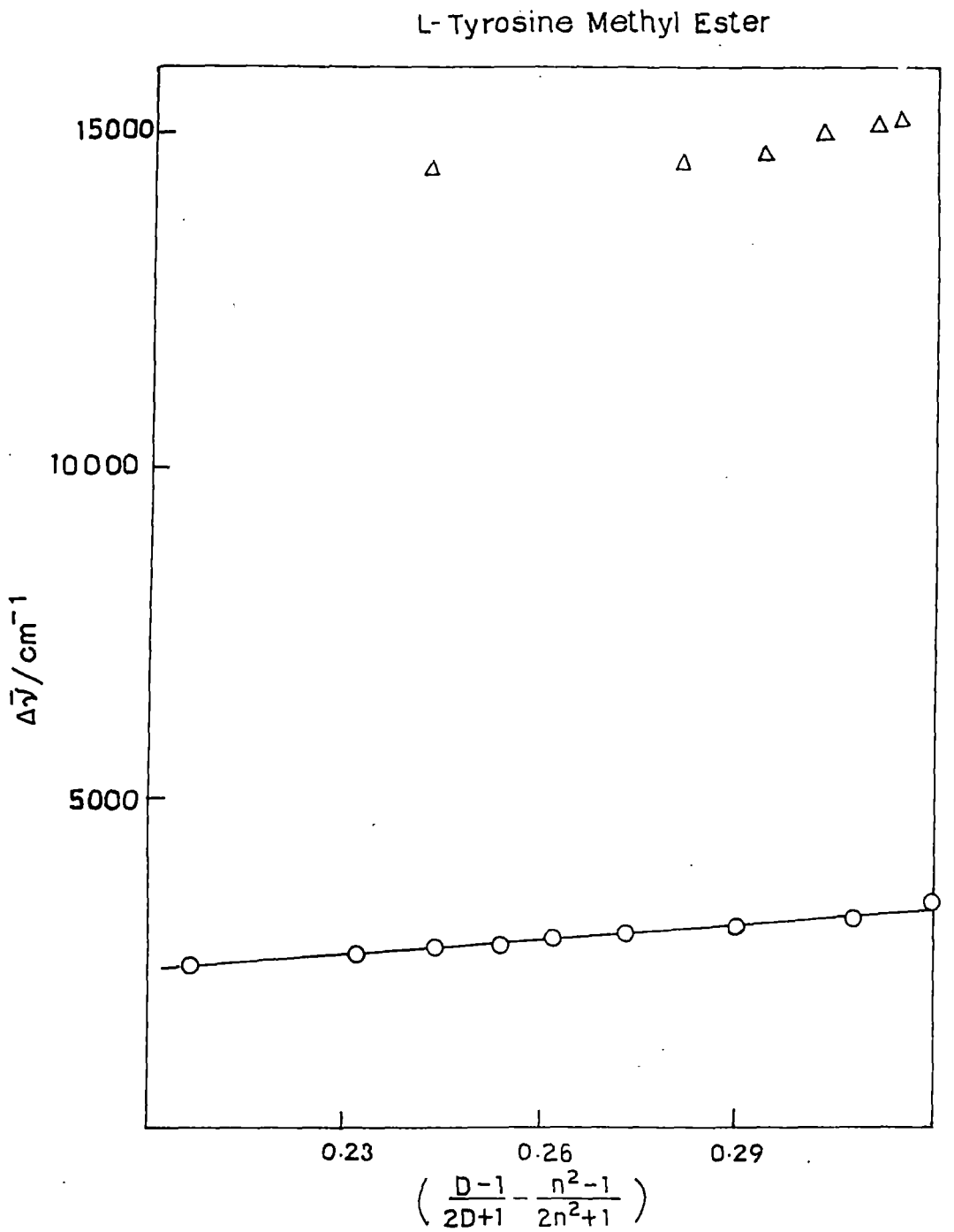

Fig.75. The plot of Stokes' shift, $\Delta\bar{\nu}$ against the solvent polarity function, $[(D-1)/(2D+1)] - [(n^2-1)/(2n^2+1)]$ of different alkanols [O] and dioxane-water mixtures [Δ].

References

1. Klose, G., Stelzmer, F., *Biochim. Biophys. Acta.*, **1**, 363 (1974).
2. Chance, B., *Proc. Natl. Acad. Sci.*, USA, **67**, 560 (1970).
3. Goto, A., Harada, S., Fujita, T., Miwa, Y., Yoshioka, Kishimoto, H., *Langmuir*, **9**, 86 (1993).
4. Maitra, A. N., *J. Phys. Chem.*, **88**, 5122 (1984).
5. Boned, C., Peyrelasse, J., Moha Ouchane, M., *J. Phys. Chem.*, **90**, 634 (1986).
6. Sarkar, N., Das, K., Datta, A., Das, S., Bhattacharya, K., *J. Phys. Chem.*, **100**, 10523 (1996).
7. Dutta, A., Mandal, D., Pal, S. K., Bhattacharya, K., *J. Phys. Chem.*, **101**, 10221 (1996).
8. Mandal, D., Pal, S. K., Dutta, A., Bhattacharya, K., *Anal. Sci.*, **14**, 199 (1998).
9. Moulik, S. P., Pal, B. K., *Adv. Colloid Interface Sc.*, **78**, 99 (1998).
10. Mukherjee, L., Mitra, N., Bhattacharya, P. K., Moulik, S. P., *Langmuir*, **11**, 2866 (1995).
11. Gupta, S., Mukhopadhyay, L., Moulik, S. P., *Colloids Surf. B: Biointerfaces*, **3**, 191 (1994).
12. Mukherjee, K., Mukherjee, D. C., Moulik, S. P., *Bull. Chem. Soc. Jpn.*, **70**, 1245 (1997).
13. Das, M. L., Bhattacharya, P. K., Moulik, S. P., *Langmuir*, **6**, 1591 (1990).
14. Kosower, E. M., *An Introduction to Physical Organic Chemistry*, John Wiley and Sons. Inc., New York (1968).

15. Rayner, D.M., Krajcarski, D.T., and Szabo, A.G., *Can. J. Chem.*, **56**, 1238 (1978).

16. Rettieg, W., *Angew. Chem. Int. Ed. Engl.*, **25** 971(1986).

17. Bell, J. R., Muthyala, R. S., Larsen, R. W., Alam, M., RSHL, *J. Phys. Chem.*, **102**, 5481(1998).

18. Mataga, N., Kaifu, Y., Koizumi, M., *Bull. Chem. Soc., Jpn.*, **29**, 465 (1956).

19. Lippert, E., *Z. Elektrochem,* **61**, 962 (1957).

20. Slavik, J., *Biochim. Biophys. Acta,* **694**, 1(1982).

21. Seliskar, C.J., and Brand, L., *J. Am. Chem. Soc.*, **93**, 5414 (1971).

22. Perov. A. N., *Opt. Spectrose.*, **49**, 371 (1980).

23. Neporent, B.S. and Bakshiev, N. G., *Opt. Spectrose.*, **8**, 408 (1960).

24. Brand, L., S Seliskar, C.J. and Turner, D. C., Academic Press, New York, 17 (1971).

25. Perochon, E. and Tocanne, J. F., *Chem. Phys. Lipids,* **58**, 7 (1991).

26. Perochon, E, Lopez, A., Toccane, J. F., *Chem. Phys. Lipids,* **59**, 17 (1991).

27. Rosenberg, H.N., and Eimutus, E., *Spectrochem. Acta.*, **22**, 1751(1966).

28. Werner, T.C., and Hoffmann, R.M., *J. Phys. Chem.*, **77**, 1611 (1973).

29. Cherkasov, A. S., *Aked Nauk SSSR Bull, Phy. Sci.*, **24**, 597 (1960).

30. Tamaki, T., *Bull. Chem. Soc., Japan,* **55**, 1761(1982).

31. Kosower, E. M., *J. Am. Chem. Soc.*, **80**, 3253, 3261 (1958).

32. Kosower, E. M., and Ramsay, B. G., *ibid*, **81**, 856 (1959).

33. Grunwald, E. and Winstein, S., *J. Am. Chem. Soc.*, **70**, 846 (1948).

CHAPTER – 5

PROMOTION OF MICELLAR SHAPE TRANSITION OF CATIONIC SURFACTANTS BY SELECTED INDICATOR MOLECULES

5.1. Introduction and review of previous works

Surfactant association is mainly driven by relatively weak hydrophobic and electrostatic interactions. Passing the so-called critical micellar concentration, cmc, the first type of structure usually formed is spherical micelle.[1-3] When the concentration of the surfactant increases these micelles can undergo a structural transition from spherical to rod like micelles under appropriate conditions of salinity, temperature, or addition of some organic compounds.[4-14] Depending on the range of surfactant concentrations ordered aggregates like cubic, hexagonal or lamellar phases can form as well as various disordered phases at lower concentrations can be formed. Cylindrical (Rod) micelles obtained from a mixture of surfactant and suitable salt have recently attracted considerable interest because of their unique viscoelastic properties.[15–23]

$$P = \frac{V}{L}.\frac{1}{A_0} \qquad (1)$$

The type of assembly at a certain concentration will depend on the intrinsic surfactant geometry which is well represented by the packing parameter P (Equation 1) where V and L are respectively the volume and length of the hydrophobic tail, and A_0 is the optimal surface area of the polar head group, which corresponds to the surface per molecule at which the surface free energy is minimized. Therefore, the respective requirements of the hydrophilic head group on the side of the water interface and those of the hydrophobic tails on the other side of the interface determine an optimal curvature, also called the spontaneous curvature.[24]

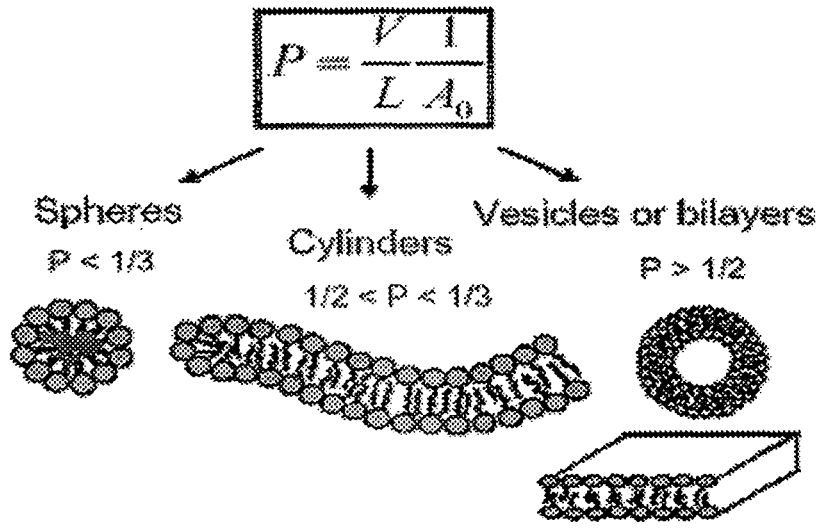

Fig. 1 Different types of micellar aggregates in relation with the geometry of the surfactant molecule

The morphology sequence and phase behaviour of surfactant aggregates is driven by the spontaneous curvature of the hydrophobic/hydrophilic interface, which does not only depend on the space filling dimensions of the surfactant molecule but may be tuned by various external factors, such as the amount and nature of added electrolyte, the presence of other species in solution, the pH or the temperature.[25] For example, if the head groups are charged, they repel each other, which increase the effective head group area and favor the formation of small spherical micelle. The addition of electrolyte tends to screen the electrolytic interactions, even more efficiently in the case of a strongly binding salt, which allow the head groups to approach each other closer and can lead to the formation of cylindrical structures. Surfactant systems show an impressive polymorphism of structures in aqueous solutions, which, in turn, influence a large variety of physical properties, in particular rheological properties.[26] Certain cationic surfactants form polymer like micelles in solutions and thus exhibit very interesting rheological properties. At high

concentrations, these solutions show typical viscoelastic behaviour. At very low concentrations, however, they show more complex and unusual rheological phenomena. Rehage and Hoffmann[27] first reported that the viscosity of a 0.9 mM cetylpyridinium salicylate solution slowly increases with time (rheopexy) when subjected to shear flow with a sufficiently higher shear rate, and that it takes an unexpectedly long time, several minutes, for the system to reach steady state. In a detailed study of the tetradecyltrimethylammonium salicylate system, they also reported that an increase in flow birefringence accompanies the stress growth. Actually both the stress and flow birefringence curves show an induction period before rapid growth commences. In addition to the general features reported before, it has been established that the induction time is inversely proportional to the applied shear rate and is independent of the flow direction. On the basis of this information, a kinetic coagulation mechanism, first proposed by Rehage, Wunderlich and Hoffmann[4] were favoured to account for the rheopectic phenomenon. According to this model, the initial small micelles collide with each other more frequently in shear flow than in quiescene, resulting in formation of large micelles. The same results are also obtained when the influence of sodium salicylate and sodium bromide concentration on the shear thickening behaviour of aqueous micellar solutions of cetyltrimethylammonium bromide (CTAB) and sodium salicylate (NaSal) is studied experimentally. The realization that there could be micelles and aggregates of different types are recent, though manifestations of unusual properties of such systems have been known for sometimes. The classic example of such an 'abnormal' system is a solution containing cationic surfactant cetylpyridinium chloride (CPC) with sodium salicylate (NaSal) as the additive.[28] These systems show strong viscoelastic effects even at extremely low volume fractions – a few millimolar concentrations.

Notable features are the observation of high viscosity even at extremely low concentrations and the existence of two peaks in the viscosity. The electron microscopic pictures of these highly viscoelastic solutions show the existence

of entangled polymeric micelles of length of several microns.[29] Two important developments, which gave clue to at least partial undergoing of these features, are:

i) NaSal is surface active and belong to the class of anionic hydrotropes.

ii) Observation of the formation of two vesicle phases (low viscosity) by Kaler and co-workers in mixed cationic and anionic surfactant systems, one phase containing positively charged vesicles and the other negatively charged.

Through this development, it becomes clear that by mixing surfactants (hydrotropes) of opposite charges, cationic and anionic, but with varying chain lengths one can control the degree of precipitation of the surfactants to produce different supramolecular structures like vesicles and polymeric micelles.[30]

It is known that certain surfactant molecules can, under correct conditions, self assemble reversibly to form large one or two dimensional (2D) structures in solutions. The one-dimensional aggregates are polymer like or rod-like micelles (depending on stiffness) whilst the 2D case represents bilayers.[31-32] In either case the structures formed can be extremely large; in the case of polymeric aggregates linear dimensions of several thousand angstroms can be obtained.[33] Experimental work on these self-assembling systems has shown that the structures have a highly non-linear response in imposed flow fields, which is a consequence of the large size and transient character of the aggregates. Rod-like micelles e.g., TTAS (tetradecyltrimethylammonium salicylate) are known to be extremely stiff in the absence of added salt one can expect the micelles to be semiflexible although it remains a sensible starting point to treat the rods as completely stiff.[34]

Single-tailed surfactants usually form globular micelles in aqueous solution above their cmc's.[35]An increase in surfactant concentration may induce the formation of wormlike micelles.[36]Similarly, addition of organic or

inorganic counterions,[36,37] uncharged compounds such as aromatic hydrocarbons,[38] or an oppositely charged surfactant[39]can transform spherical micelles into wormlike micelles. Alkyl trimethylammonium and alkyl-pyridinium surfactants are the most extensively studied surfactant systems in this respect.[40,41] Halide counterions bind moderately strongly to cationic surfactant aggregates, and therefore, micellar growth is gradual. Upon changing of the counterions to aromatic ones which usually display higher counterion binding, micellar growth already occurs at low surfactant and counterion concentrations.[42] However, not only high counterion binding is a prerequisite for micellar growth, but also the orientation of substituents on the aromatic ring is important. ^{1}H nmr studies reveal that $+N(CH_3)_3$ proton signals are shifted to higher fields and that they are broadened upon addition of salicylate counterions.[43] It was shown that the aromatic ring of salicylate is located between the headgroups and that the OH and COO^- substituents protrude out of the micellar surface.[43]Theoretical studies showed that wormlike micelles are long and flexible and that they undergo transformations on relatively short time scales.[44] This was confirmed by negative staining[45] and cryo electron microscopy,[46] which showed that wormlike micelles can become several hundreds of nanometers in length. Upon increase of the surfactant concentration, an entangled network of worm-like micelles is formed which displays viscoelastic behaviour. [35] As has already been mentioned, the rheological behaviour observed for these surfactant systems is similar to that of solutions of flexible polymers, and therefore, aqueous solutions of entangled wormlike micelles are often called living polymer systems.[40,47] Upon increase of the size of the hydrophobic portion of the counterion, the formation of vesicles has been observed. Lin *et al.*[48] studied the aggregation behavior of mixtures of hexadecyltrimethylammonium bromide (C_{16}TAB) and 5-methyl-salicylic acid. Upon changing the mole ratio of 5-methylsalicylic acid to C_{16}TAB from 0.1 to 1.1, a gradual change from spherical micelles to vesicles via wormlike and entangled wormlike micellar phases was observed. Also

sodium 3-hydroxynaphthalene-2-carboxylate (NaHNC) is able to induce the formation of vesicles in aqueous solutions of C_{16}TAB.[49] This system is compared to cationic surfactants since the phase behavior shows similarities to that of mixtures of cationic and anionic surfactants. The same system without excess of salt (C_{16}TAHNC) has also been studied. The critical aggregation concentration (cac) of C_{16}TAHNC is 0.03 mM,[50] which is significantly smaller than that of C_{16}TAB (1.0 mM). Aqueous solutions of C_{16}TAHNC show interesting temperature-dependent phase behaviour. Upon increase of the temperature, the system undergoes a transition from a turbid vesicular phase to a clear viscoelastic phase containing a network of entangled wormlike micelles. Fluorescence anisotropy and nmr spectroscopy showed an increase in fluidity of the aggregate surface upon increasing the temperature.[51] The phase transition has also been studied by differential scanning calorimetry (DSC) and conductivity experiments.[52] The temperature-induced morphological change has been explained using the theory of phase transitions in a 2D Coulomb gas.[53] It was shown that increasing the temperature results in a decrease of the HNC^- counterion binding; concurrently the head group repulsions between $C_{16}TA^+$ moieties in the bilayer increase which eventually leads to a change in aggregate shape from vesicles to wormlike micelles. A vesicle to micelle transition in aqueous solutions of C_{16}TAHNC can also be induced by shear [54] or by adding C_{16}TAB or NaHNC.[55] Thus, so far, most studies have focused on mixtures of C_{16}TAB and N-methylsalicylic acid [50]or NaHNC.[51,52,56-58]

In aqueous solution, cationic surfactants self assembled into a threadlike or wormlike micelles.[59,60] Typically, when a wormlike micellar solution is heated, the micellar contour length L decays exponentially with temperature.[61,62] The reason for this is that, at higher temperatures, surfactant unimers can hop more rapidly between the cylindrical body and the hemispherical end-cap of the worm (the end-cap is energetically unfavorable over the body by a factor equal to the end-cap energy Ec).Thus, because the end-cap constraint is less severe at higher temperatures, the worms grow to a

lesser extent. The reduction in micellar length, in turn, leads to an exponential decrease in rheological properties such as the zero-shear viscosity η_0 and the relaxation time t_R.[61-62] Accordingly, an Arrhenius plot of ln η_0 versus 1/T (where T is the absolute temperature) falls on a straight line, the slope of which yields the flow activation energy Ea. Values of Ea ranging from 70 to 300 kJ/mol have been reported for various micellar solutions.[62-64]

Through this development it became clear that by mixing surfactants (hydrotropes) of opposite charges, cationic and anionic, but with varying chain lengths one can control the degree of precipitation of the surfactants to produce different supramolecular structures like vesicles and polymeric micelles.[65-80] One can also produce tubules, ribbons, etc. by controlling the solubility of surfactants.[81,82] This facilitates an easy control over the aggregate structure and hence it is possible to induce transformations from vesicles to micelles by a proper choice of additives which are cationic,[83-85] anionic[86-90] or neutral.[91-93] Although a number of early investigations were carried out on surfactant-mediated solubilization of vesicles due to its important implications in biochemistry, there are very few studies describing such vesicle–micelle transition induced by temperature.[94-95]

From the foregoing discussion it is apparent that shear thickening occurs at low surfactant-hydrotropic core, because free worm-like micelles join a transient network under shear, the microstructures have been broadly named as shear induced structure or phase (SIS or SIP). However, a wide variety of worm like micellar solutions display rheological responses virtually identically to those described here but a common element in nearly all the systems is the presence of salt anions which associates strongly with the surfactant cations. For the first time it has been observed in this work that due to unique contribution of strong hydrophobic aromatic moiety and a polar hydroxy group in the molecular structures, 1 and 2-Naphthols are efficient in promoting SIS in CTAB and CPB micelles under salt free condition. In this chapter, viscoelastic behaviour of CTAB and CPB surfactants in presence of 1- and 2- Naphthols

have been investigated. Stimuli responsive properties of these systems are examined and microstructure of SIP is proposed.

5.2. Experimental

Cetylpyridinium bromide (CPB) was purchased from Aldrich Chemical Co., USA and was used as received. Sources and purification of other materials used in the present work have been mentioned in chapter 3.2 (page 21). ^1H nmr spectra were run at room temperature in D_2O on a Brüker spectrometer (Germany) operating at 300 MHz. FTIR spectra were recorded on a Shimazu FTIR spectrophotometer (Japan, Model:08300). Solution pH was measured by a Systronics (India) pH meter (Model: 361).

For the steady state viscosity measurement, solutions with different mole ratios of CTAB/Naphthols were prepared. Since optimum viscoelasticity was shown at 1:1 mole ratio of CTAB/Naphthols, when induced measurement was done at 1:1 mole ratio but at various concentrations (e.g., 1mM, 5mM, 10mM). Both 1- and 2- Naphthols are practically insoluble in water at low pH but soluble in surfactants. Therefore, appropriate amount of 1- and 2-Naphthols were added directly to CTAB or CPB solutions. In some experiments dilute alcoholic solution of naphthols were used and alcohols were dried off before the addition of surfactant in the experimental set. Utmost care was taken to prepare Naphthol-CTAB or Naphthol-CPB solutions with minimum shaking. The samples were equilibrated at desired temperatures in a thermostat for 2 days before study. For rheological experiment, an Anton Paar digital viscometer (Model: DV - 3PR), Austria, with low viscosity adapter was used. This is a rotational viscometer with the facility of applying variable shear. Here, the viscosity measurement is based on measuring the torque of spindle rotating at a given speed in the sample solution kept in a concentric cylinder, which is maintained at a constant temperature. The diameter and length of the inner cylinder are 2.5 cm and 9 cm respectively, whereas, those of outer

cylinder are 2.8 cm and 14 cm respectively shear rate is calculated as rpm × 1.2236 s^{-1} (assuming the characteristics of the spindle).

5.3. Results and discussion

Aqueous CTAB or CPB (1 – 10 mM) and 1- or 2- Naphthol (1 – 10 mM in 5% Methanol) show viscosities similar to that of water. But as soon as the solutions are mixed together, a thick gel with high viscoelasticity is developed. The gel vibrates upon knocking the sample vials, which indicate their elastic behaviour. This well-defined rapid gelation indicates a definite microstructure in the gelation process. Fig. 2 illustrates how the 1- and 2- Naphthols concentrations influence the steady state viscosity of the solution at constant CTAB concentration. It is interesting to note that the viscosity has maximum value when CTAB/Naphthol (or CPB/Naphthol) is present at 1:1 ratio. This result is similar to that observed previously by other workers in CTAB-NaSal or CPB-NaSal systems. It may be argued that in this molar ratio of surfactants and Naphthols, micellar transition from sphere to worm-like micelles is facilitated and most probably the worm elongate most.

Previously, it was emphasized that as the NaSal molecule is incorporated in the micelles more and more thread like micelles grow. When concentration of NaSal is larger than that of CTAB, the excess of NaSal decreases the micellar life time. In other words, the micellar break up rates increases when excess NaSal is present. It should be pointed out that, in the solutions of higher concentrations at equilibrium, a similarly complex dependence of linear viscoelasticity on the NaSal/CTAB ratio has been reported. Shikata[15,16] has suggested that the most stable and rigid micelles are formed by the 1:1 NaSal/CTAB complex. An excess or deficiency of charge on the micelles will tend to shorten the micellar life time and size. It has been proposed that excess salicylate ion catalyses the scission of the micellar network junctions, to account for the decrease of stress relaxation time in semi-

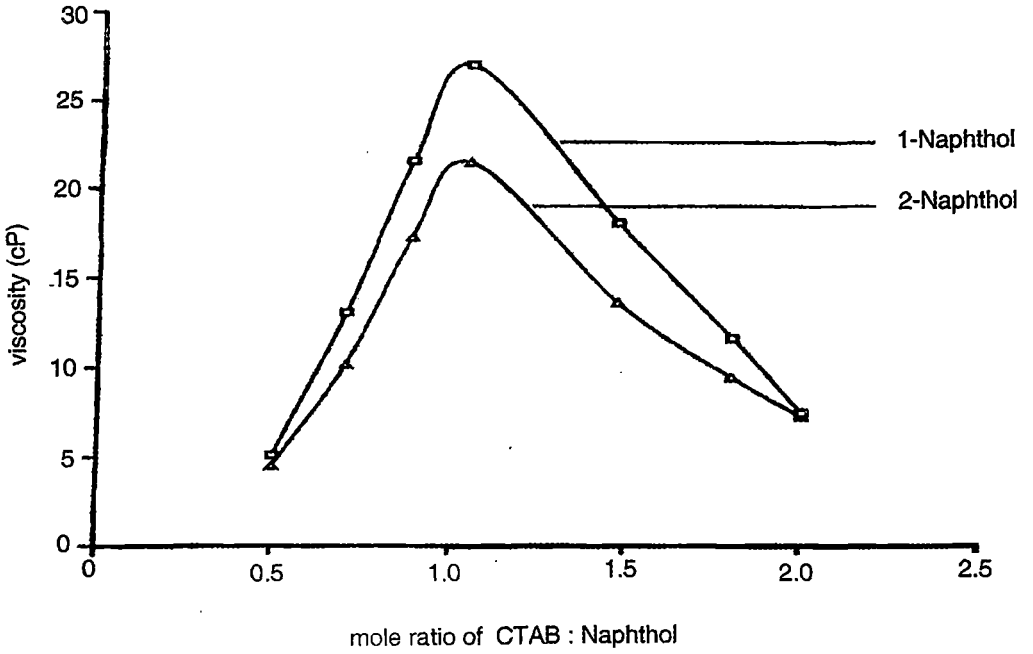

Fig. 2 Variation of viscosity as a function of mole ratio of Naphthols : CTAB.

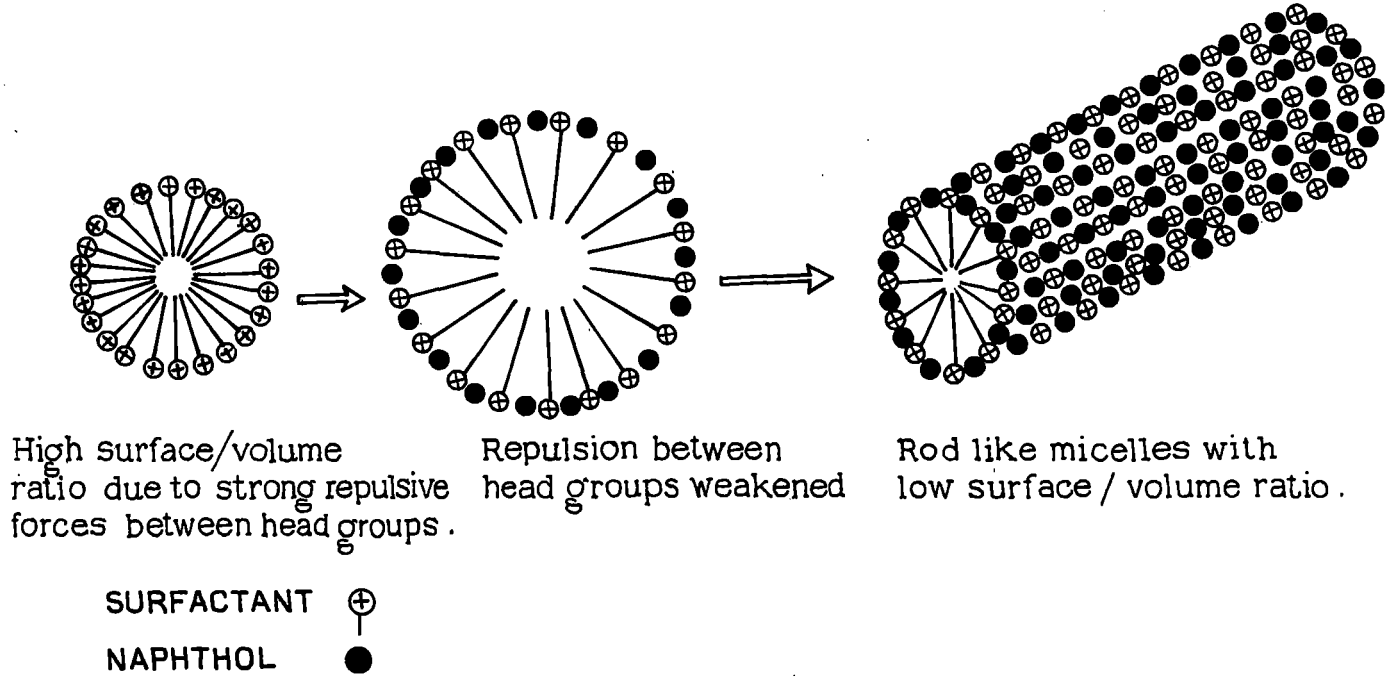

Fig. 3. Sphere to rod transition of cationic micelles in presence of naphthols

dilute solutions at equilibrium, when the NaSal/CTAB ratio becomes larger than unity. However, any explanation emphasizing the involvement of the ionic charges of the promoter molecules (viz., salicylate ion) is not apparently applicable in the present system because naphthols act in the present case as the neutral molecules. Therefore, it seems apparent that symmetrical and homogeneous distribution of surfactant and naphthol molecules (molar ratio 1:1) in the spherical micelles leading to a regular and optimal surface curvature prompted the micellar shape transition to take place (Fig. 3).

Shear induced viscosity (SIV) of aqueous CTAB-Naphthol and CPB-Naphthol systems:

At low concentrations (< 1 mM) of CTAB-Naphthol or CPB-Naphthol solutions, shear thinning features are generally observed like common non-Newtonian liquids (Figs. 4-7) upto applied shear of 200 rpm. Samples were sheared at various shear rates for a specified time with the aid of a rotational viscometer with variable shear (e.g., 10 mins) facility. This is to ensure that the high viscosity regime was reached and shear induced structure is formed.

However, at higher concentrations (1 mM-2 mM) solutions show interesting rheological properties (Figs. 8-11). Upto the applied shear rate 30 rpm, solutions shear thin. Above the shear of 30 rpm, viscosity starts increasing as a function of applied shear upto 200 rpm and SIS is formed. On further increase of applied shear, the solution viscosity decreases steadily (not shown in figure). Finite induction times are also observed before the onset of shear thickening. This is of course associated with the build up of long micellar bundles. The system recoils after the shear is withdrawn (~15 mins. figs. 12-15). Surprisingly, sheared micellar solutions take very long time, some times hours, to recoil completely and to return to an equilibrium unsheared state. Many models have been proposed, including that the microscopic structures are string like, highly aligned rods, small clusters of micelles, pearl strings of

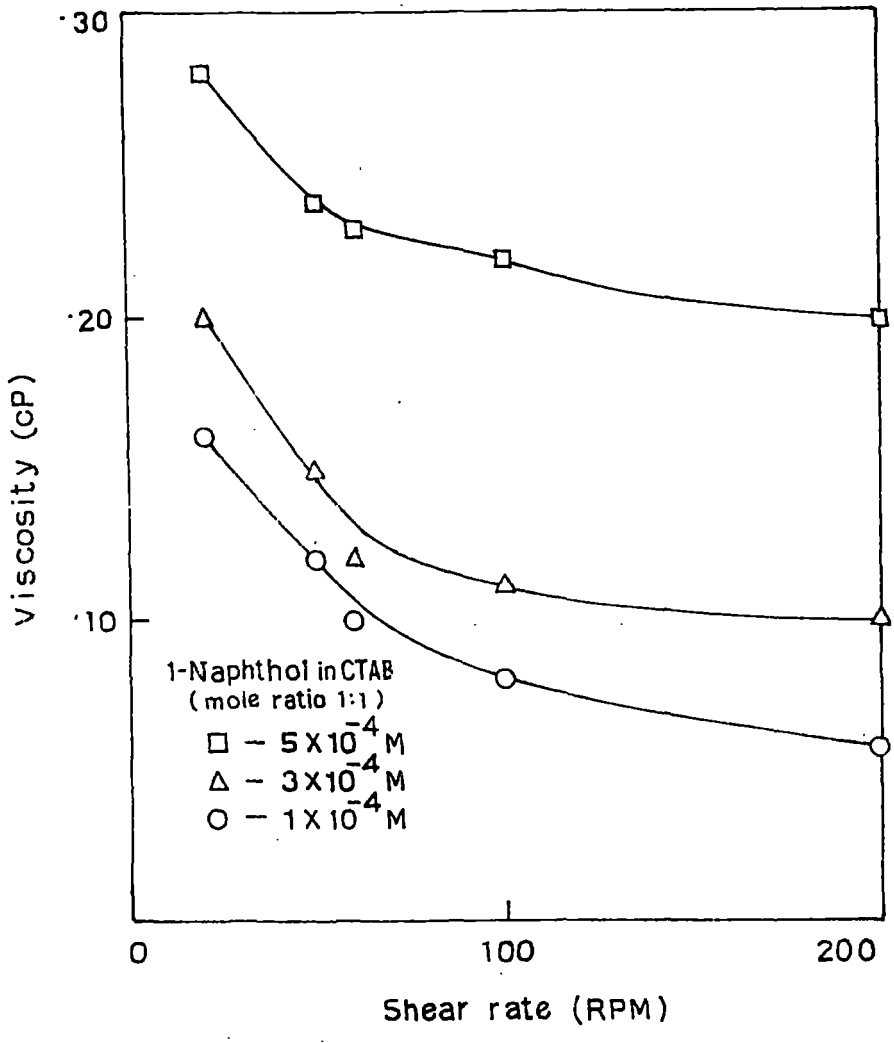

Fig. 4. Shear induced viscosity of 1-Naphthol-CTAB system at low concentration.

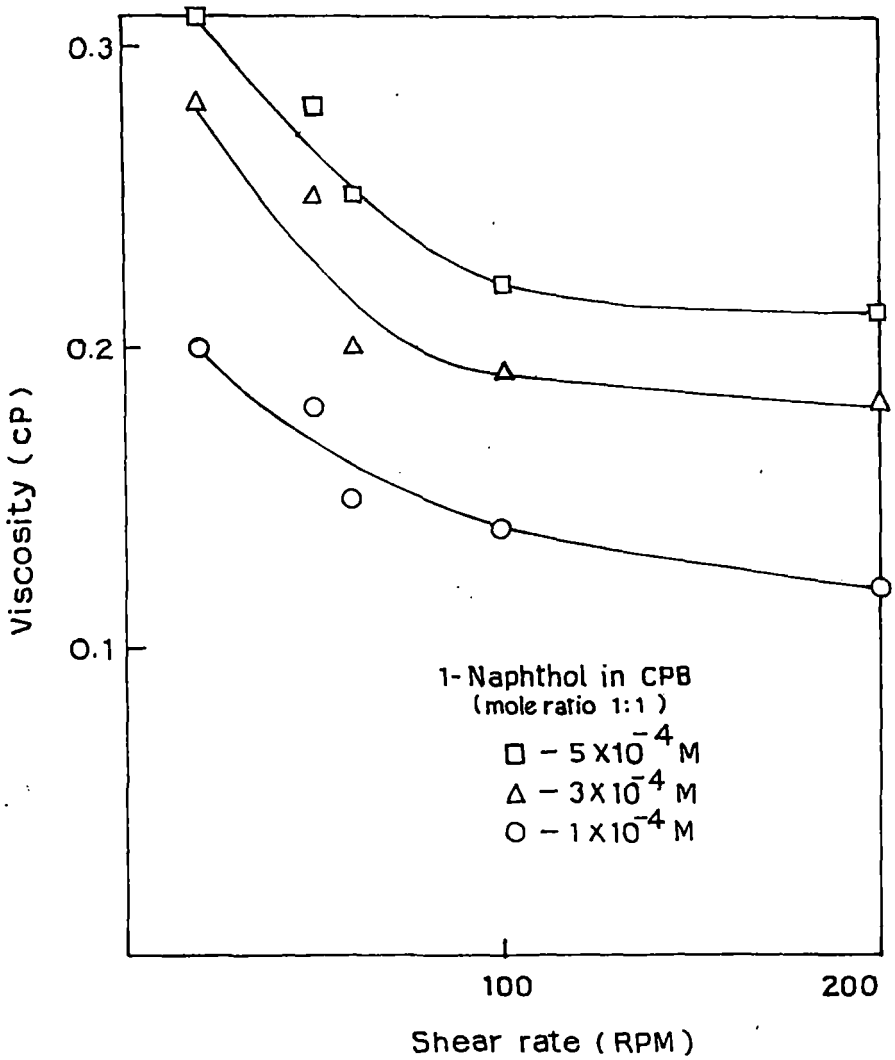

Fig. 5. Shear induced viscosity of 1-Naphthol-CPB system at low concentration.

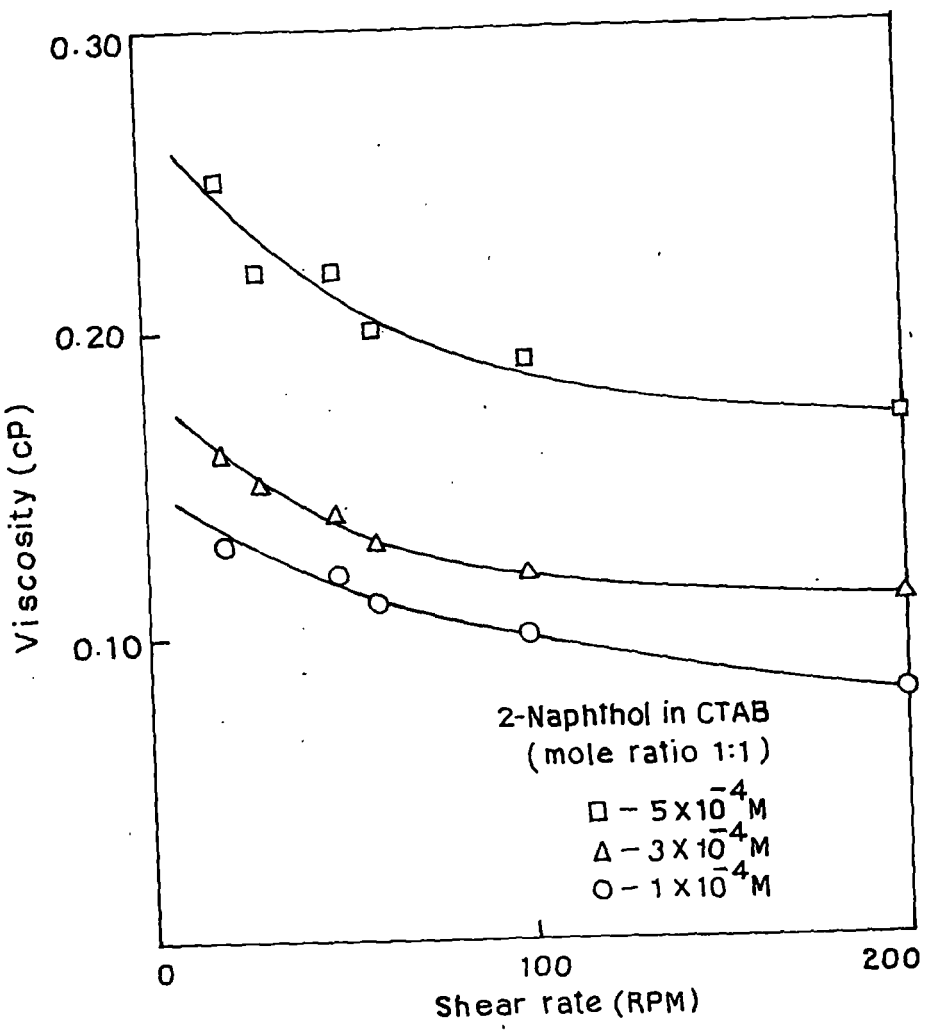

Fig. 6. Shear induced viscosity of 2-Naphthol-CTAB system at low concentration.

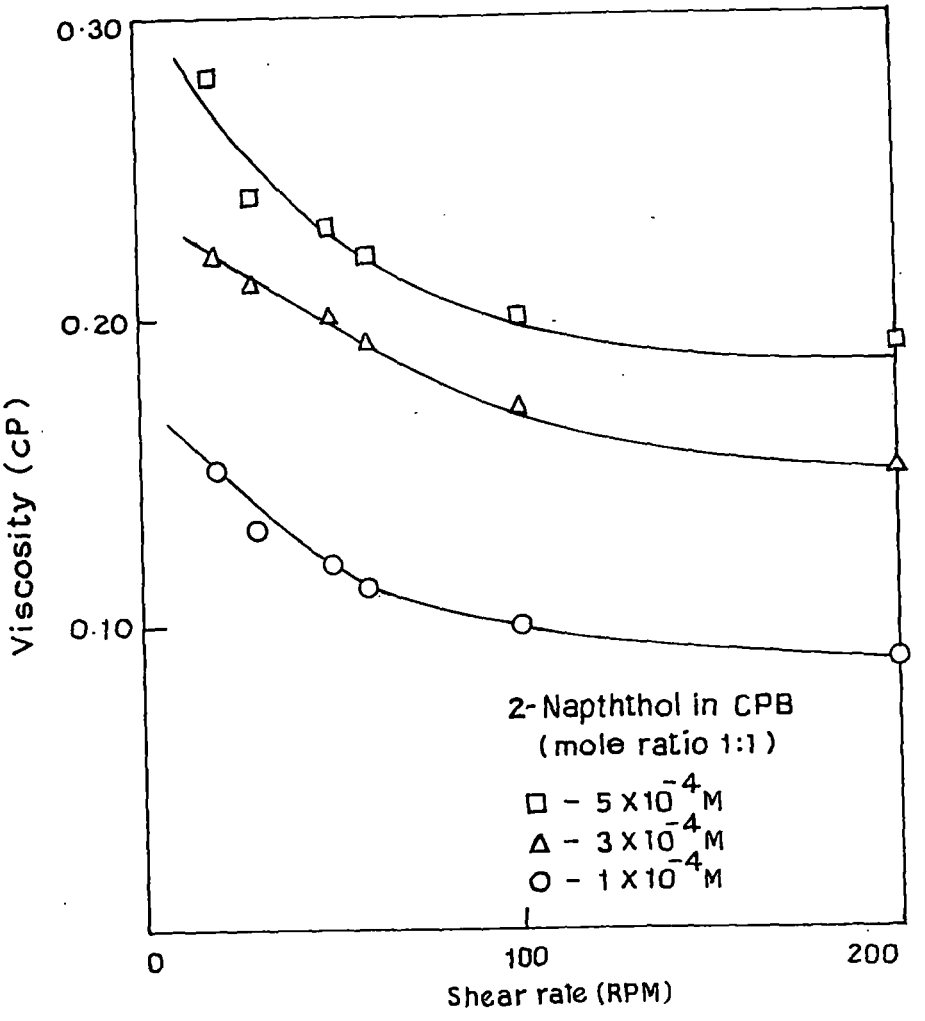

Fig. 7. Shear induced viscosity of 2-Naphthol-CPB system at low concentration.

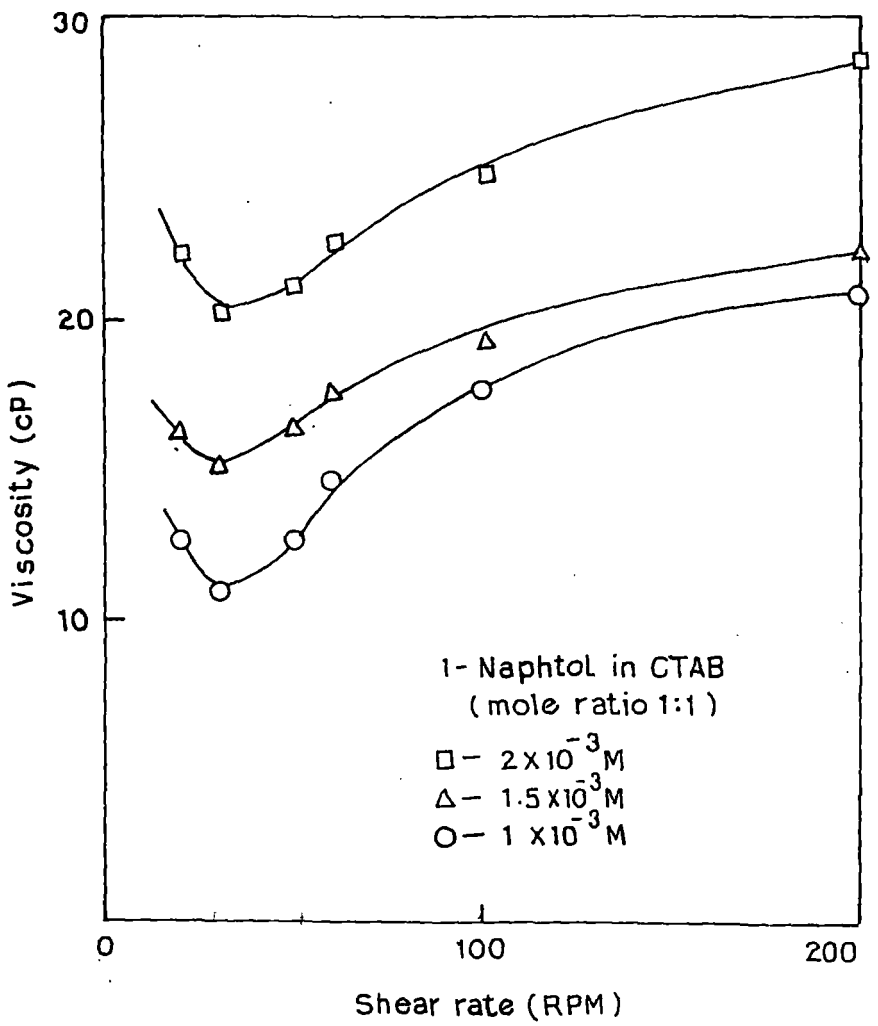

Fig. 8. Shear induced viscosity of 1-Naphthol-CTAB system at high concentration.

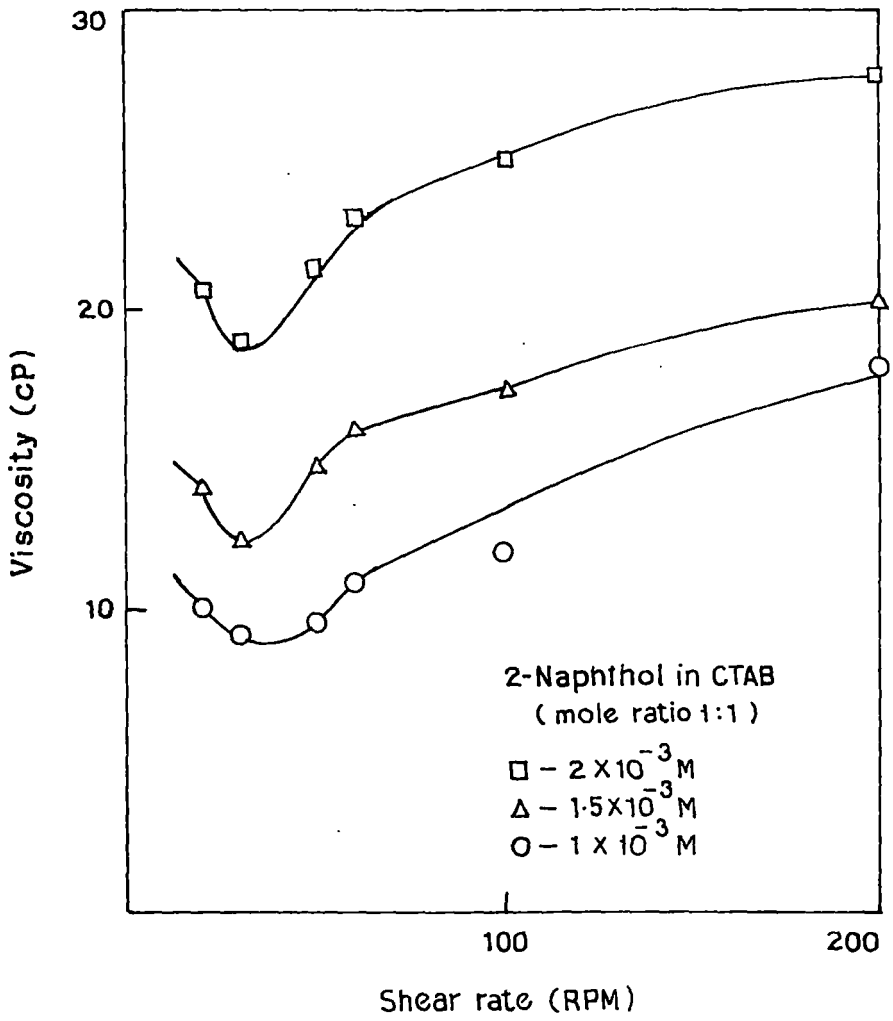

Fig. 9. Shear induced viscosity of 2-Naphthol-CTAB system at high concentration.

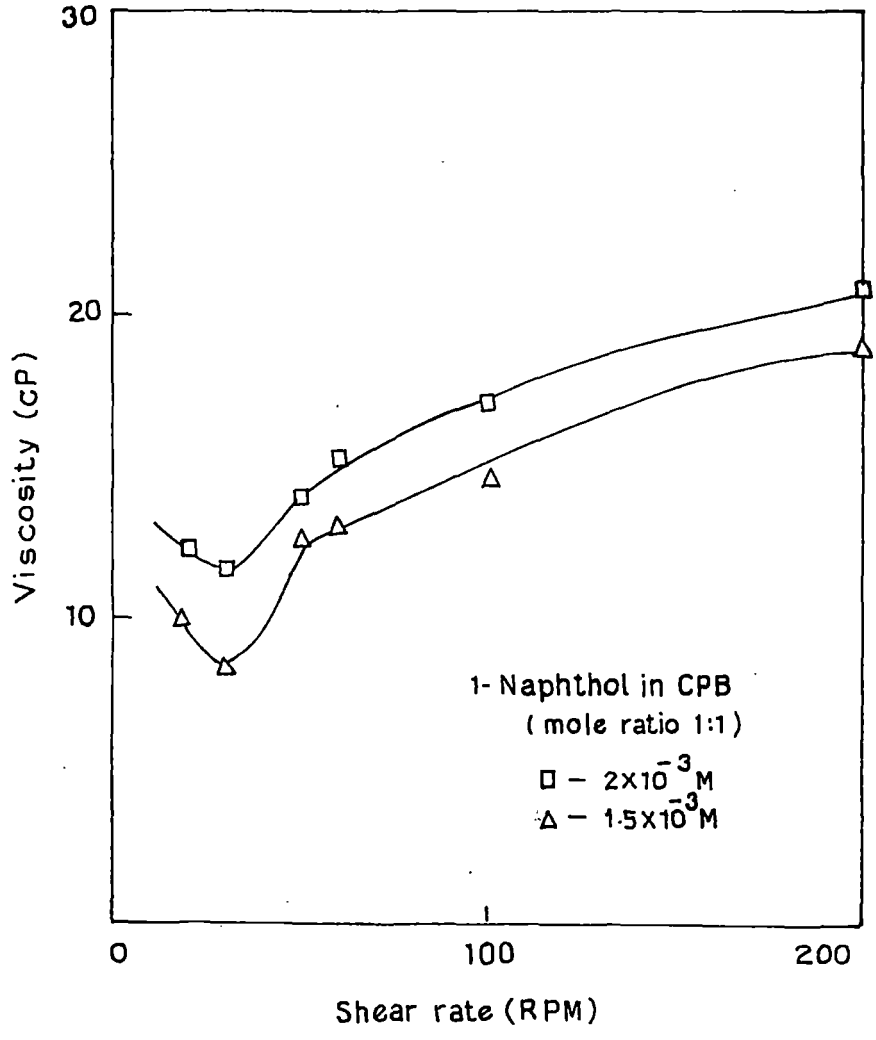

Fig. 10. Shear induced viscosity of 1-Naphthol-CPB system at high concentration.

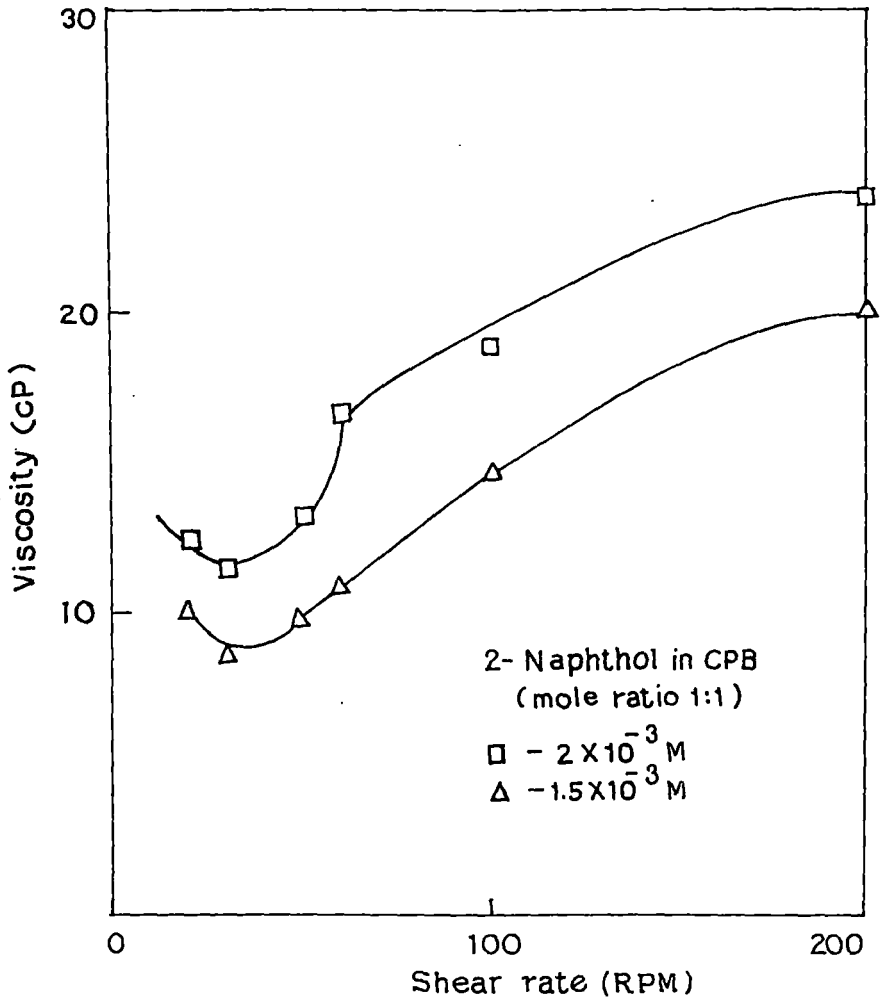

Fig. 11. Shear induced viscosity of 2-Naphthol-CPB system at high concentration.

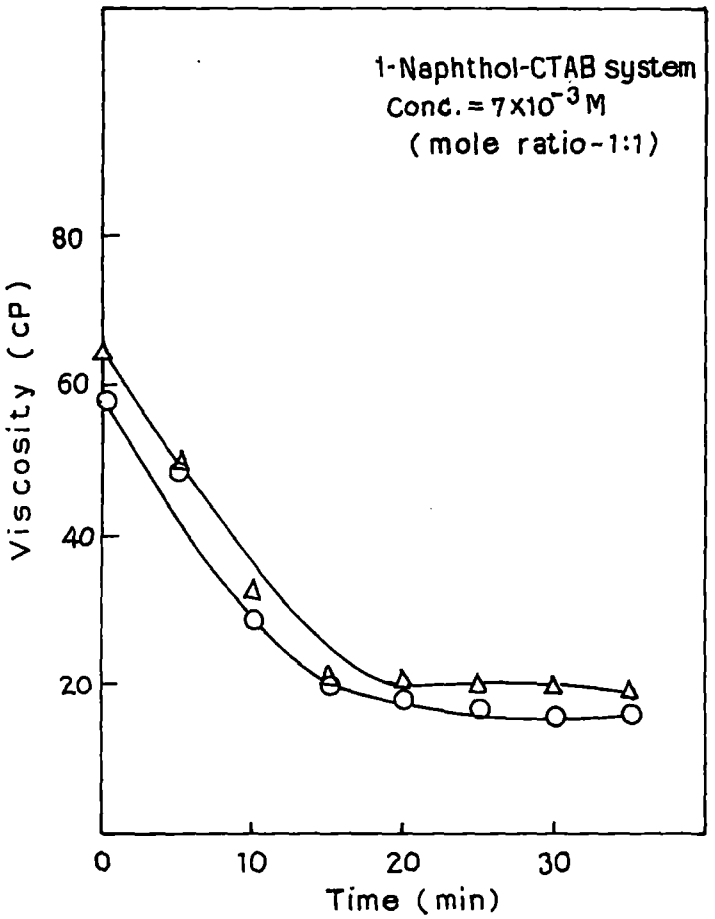

Fig. 12. Decay of shear induced viscosity with time. (applied shear = 244.72 s^{-1} at 298K), 10 mins.(○); 20 mins.(△)

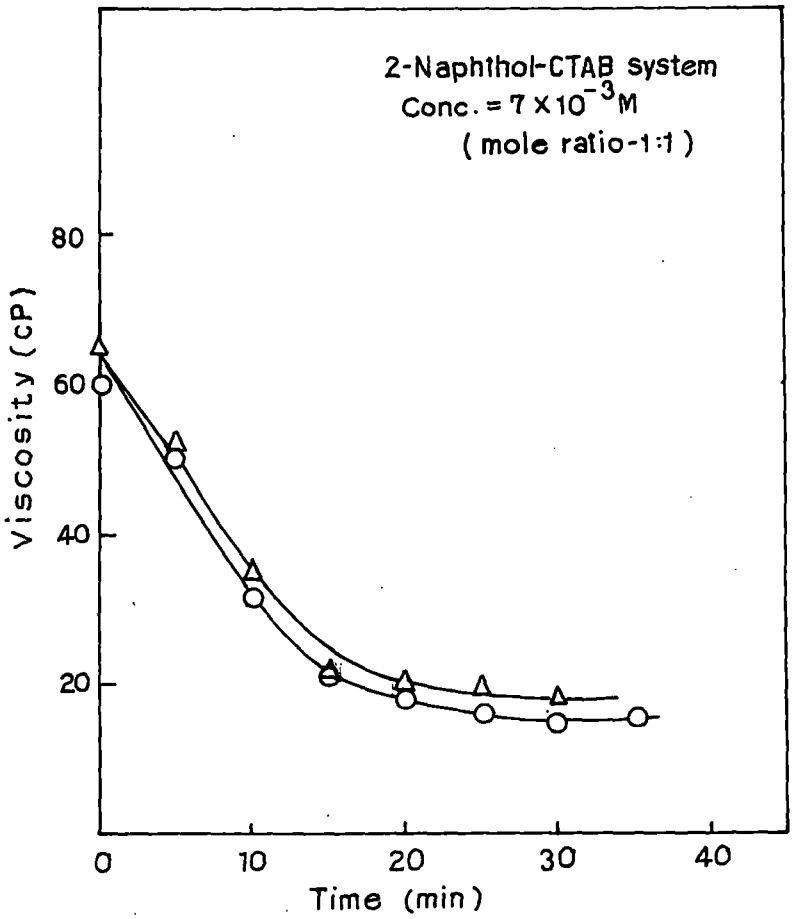

Fig. 13. Decay of shear induced viscosity with time. (applied shear = 244.72 s^{-1} at 298K), 10 mins.(○); 20 mins.(△)

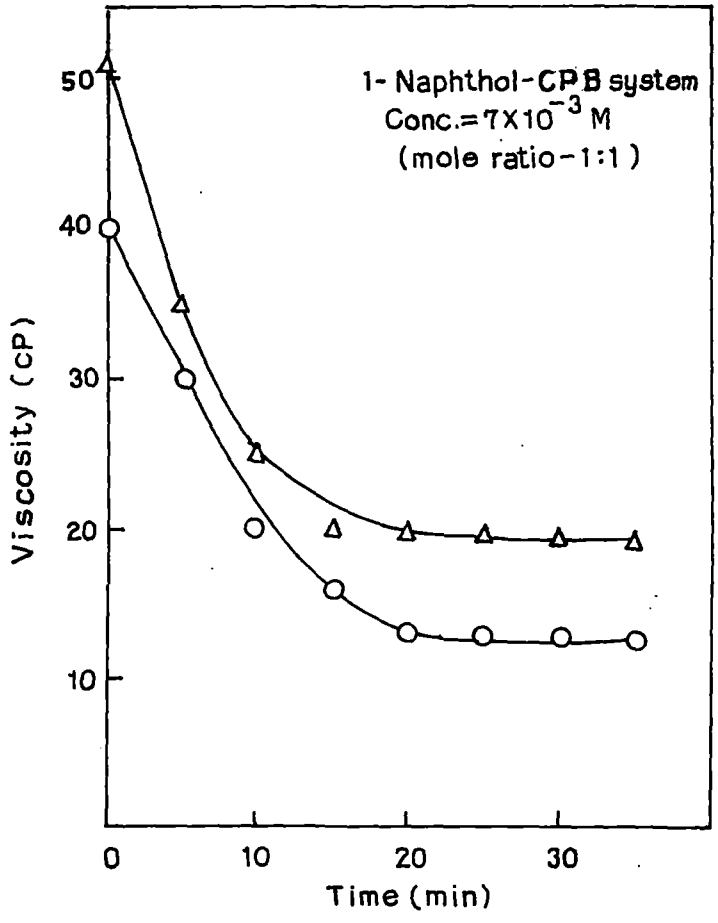

Fig. 14. Decay of shear induced viscosity with time.
(applied shear = 244.72 s^{-1} at 298K),
(O for 10 minutes,Δ for 20 minutes).

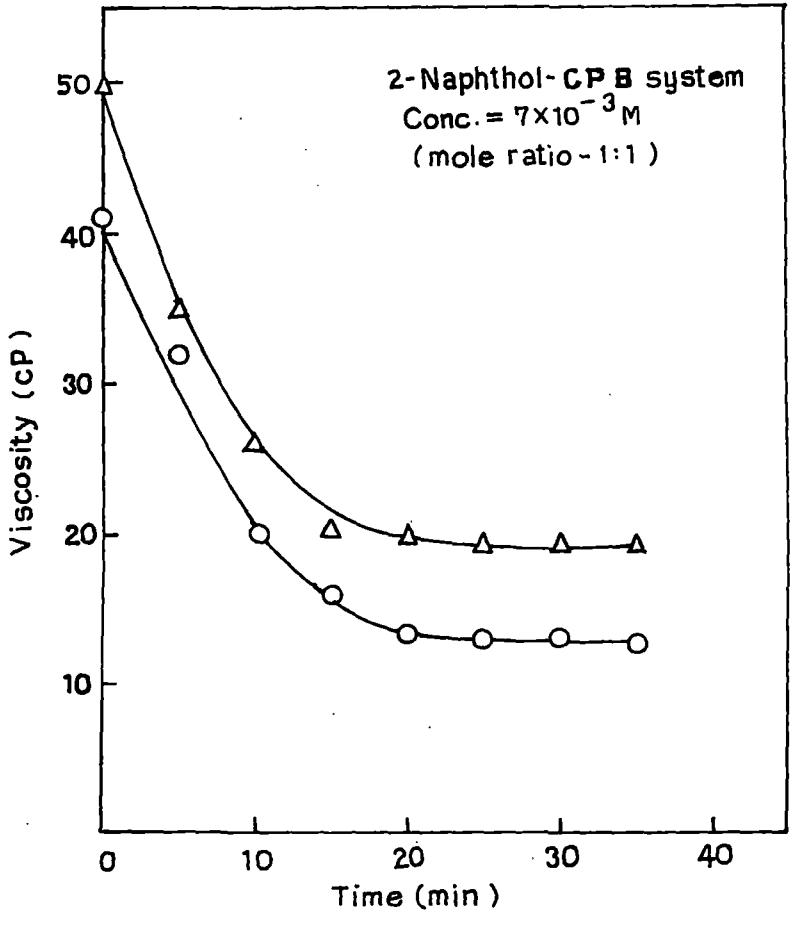

Fig. 15. Decay of shear induced viscosity with time.
(applied shear = 244.72 s^{-1} at 298K),
(O for 10 minutes,Δ for 20 minutes).

micelles, pseudonematic domains or layers of entangled wormlike micelles at high and low shear rates following reptation-reaction model.[96] The lack of direct experimental evidence to discriminate between various models has greatly impeded progress in understanding these phenomena. Previous reports on Freez-Fracture Electron Microscopy (FFEM) technique shows that the shear causes the formation of new micron sized structures that are much larger than the individual micelles and consistent with light scattering results.[96] The new structures are richer in surfactant than the surrounding micellar solution and have a sub-micron stippled or sponge-like textures. Aligned and non-aligned worm like micelles co-exist with the new structures. Also the long persistent length of the wormlike micelles suggests a high bonding rigidity. It is unlikely that electrostatic repulsion prevents worm like micelles from bending because the Debye length is only ~ 30Å in 10 mM monovalent solution. It is interesting to note that the FFEM does not show any evidence that the new structure which is developed in shear induced solution is comprised of micelles, either entangled or branched or in bundles. The bumpy structures, which are formed, resemble sponge phase of bilayers. However, the present study shows that shear induced phase is highly responsive to change in temperature (detail in next section). The gel like property disappears at slightly higher or lower temperature around the optimum one. Therefore, it is important to see that vital information regarding the SIS may not be lost due to the application of extreme temperature during FFEM experiment.

Effect of temperature and pH on viscoelasticity

Temperature dependence of viscoelasticity at different applied shear rate (fixed) are shown in Figs. 16-23 (shear rates in s^{-1} have been calculated from corresponding rpm values). Strong dependence of temperature on the shear induced viscoelasticity is apparent. Viscosity of the solution is measured at different temperatures after applying constant shear for 10 minutes. Maximum

viscoelasticity is shown at ~ 25^{0}C. However, the gel melts completely above 40^{0}C. Below 15^{0}C, also shear induced viscoelasticity disappears completely. Thus, thermoreversible property of gel indicates that shear induced on entanglement leads to SIS which is stable within the temperature of 15- 40^{0}C only in the present concentration conditions.

Effect of temperature on the viscoelastic property of CTAB-naphthol and CPB-naphthol systems is intriguing. Typically, when a wormlike micellar solutions is heated, the micellar contour length decays exponentially with temperature. At higher temperatures, surfactant unimers can hop more rapidly between the cylindrical body and the hemispherical end cap of the worm (the end cap is energetically unfavourable over the body by a factor equal to the end cap energy).Thus, because end cap constraint is less severe at higher temperatures, the worms grow to a lesser extent. The reduction in micellar length, in turn, leads to an exponential decrease in rheological properties such as the viscoelasticity and relaxation time. However, an opposite trend in the rheological behaviour is observed in CTAB-naphthol and CPB-naphthol systems as above. Instead of a decrease in viscoelasticity, it is increased with temperature steadily upto the critical temperature value and then decreases (figs. 16-23). This transition as a function of temperature is reversible, i.e., if the temperature is lowered at the critical temperature, viscosity of the system is found to decrease and approximately follow the same viscosity-temperature profile. This observation is unusual and the only example of this kind is found in a recent reference where wormlike micelle formation was promoted by excess hydroxy-naphthalenecarboxylate salt.[97] It has been argued that due to the presence of strong hydrophobic naphthalene ring in the above promoter molecules, excess salt ions become soluble in the micellar core than that of surfactant molecules causing a residual opposite charge to grow on the micelles. However, at higher temperature the observed micellar growth has been attributed to the desorption of weakly bound excess promoter ions from the micelles reducing the charge density at the micellar surface. This reduction

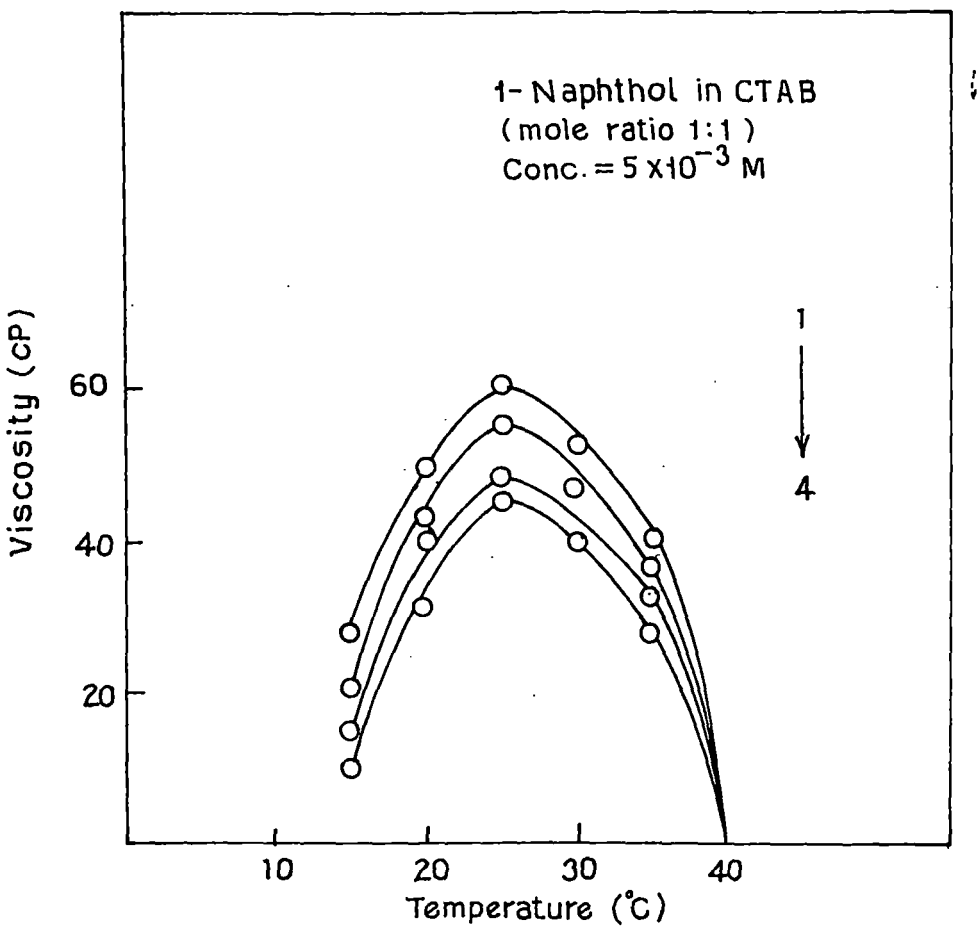

Fig. 16. Shear induced viscosity as a function of temperature. Applied shear (10 minutes): 36.71 s^{-1} (1); 73.42 s^{-1} (2); 122.36 s^{-1} (3); 244.72 s^{-1}(4).

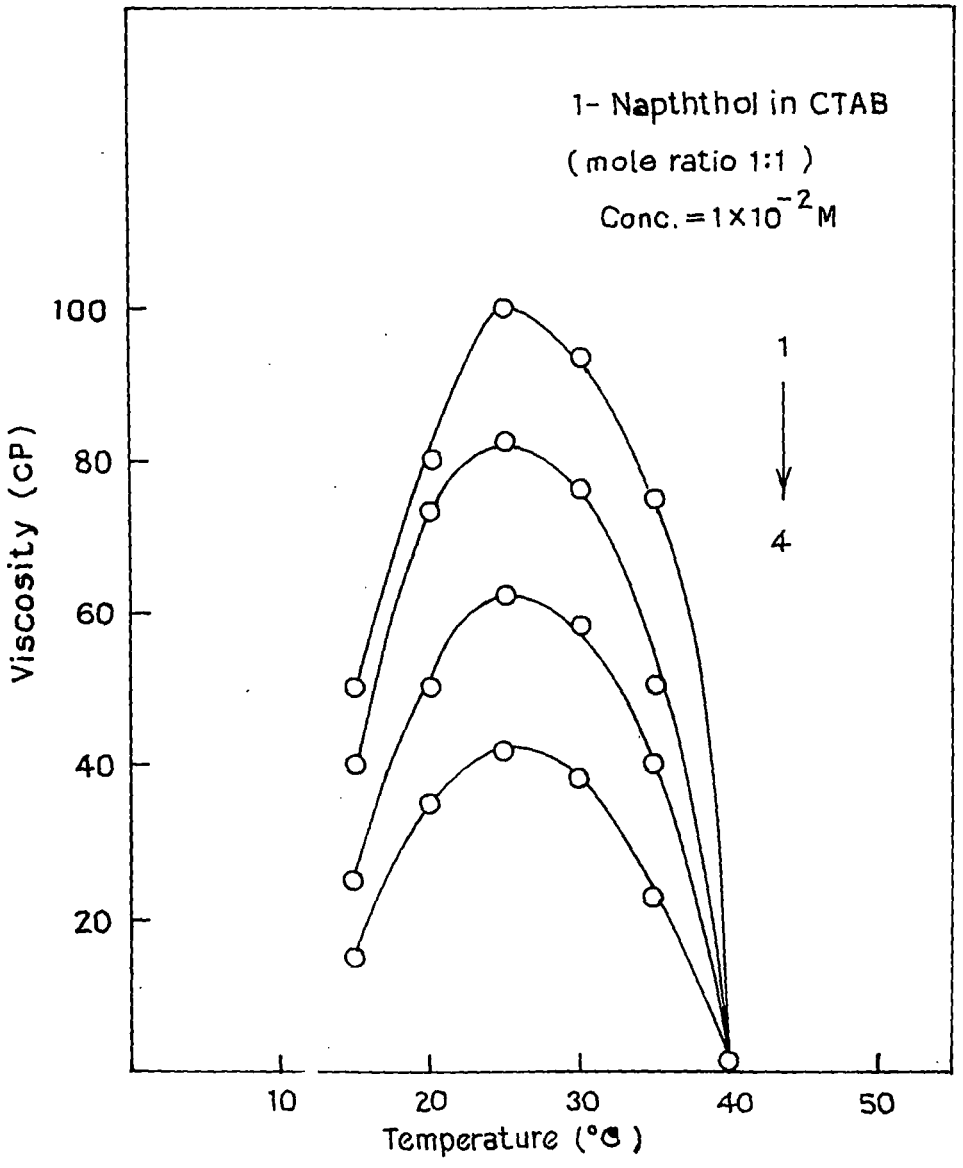

Fig. 17. Shear induced viscosity as a function of temperature. Applied shear (10 minutes): 36.71 s^{-1} (1); 73.42 s^{-1} (2); 122.36 s^{-1} (3); 244.72 s^{-1} (4).

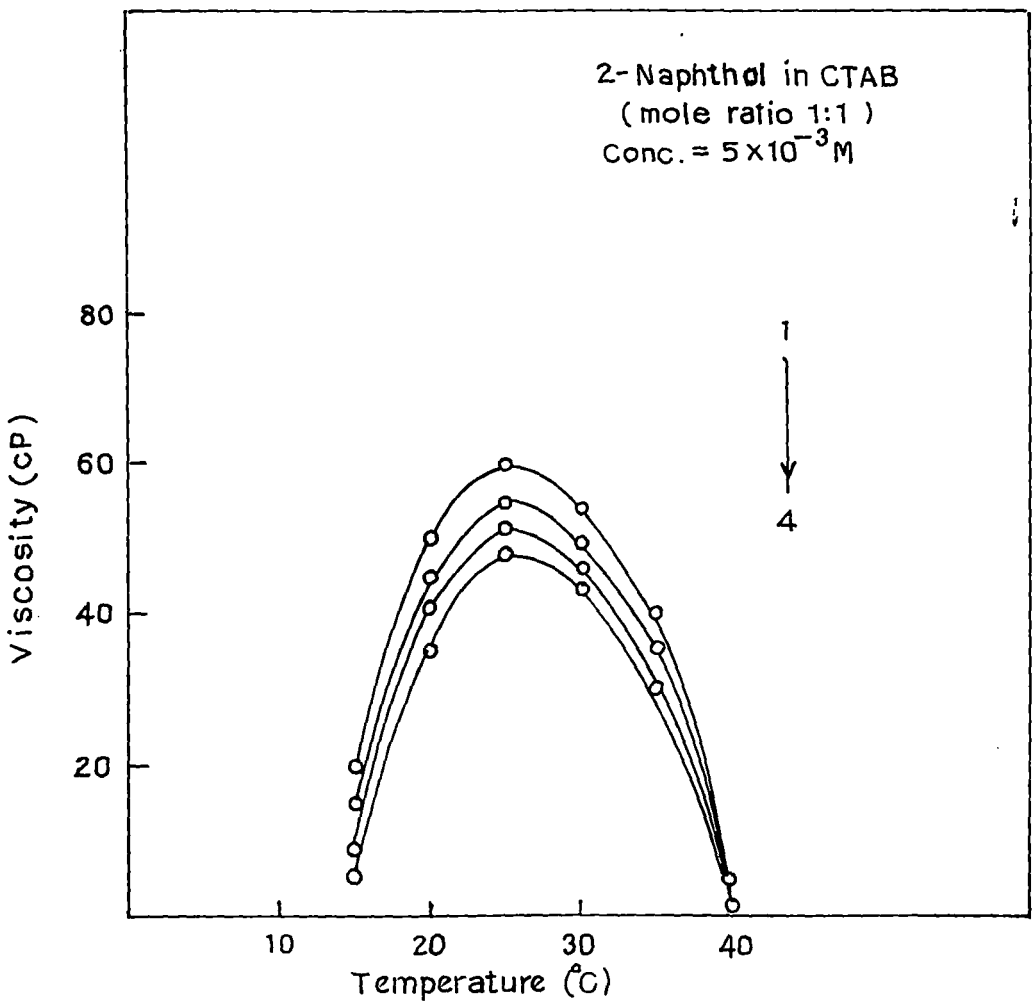

Fig.18. Shear induced viscosity as a function of temperature. Applied shear (10 minutes): 36.71 s^{-1} (1); 73.42 s^{-1} (2); 122.36 s^{-1} (3); 244.72 s^{-1}(4).

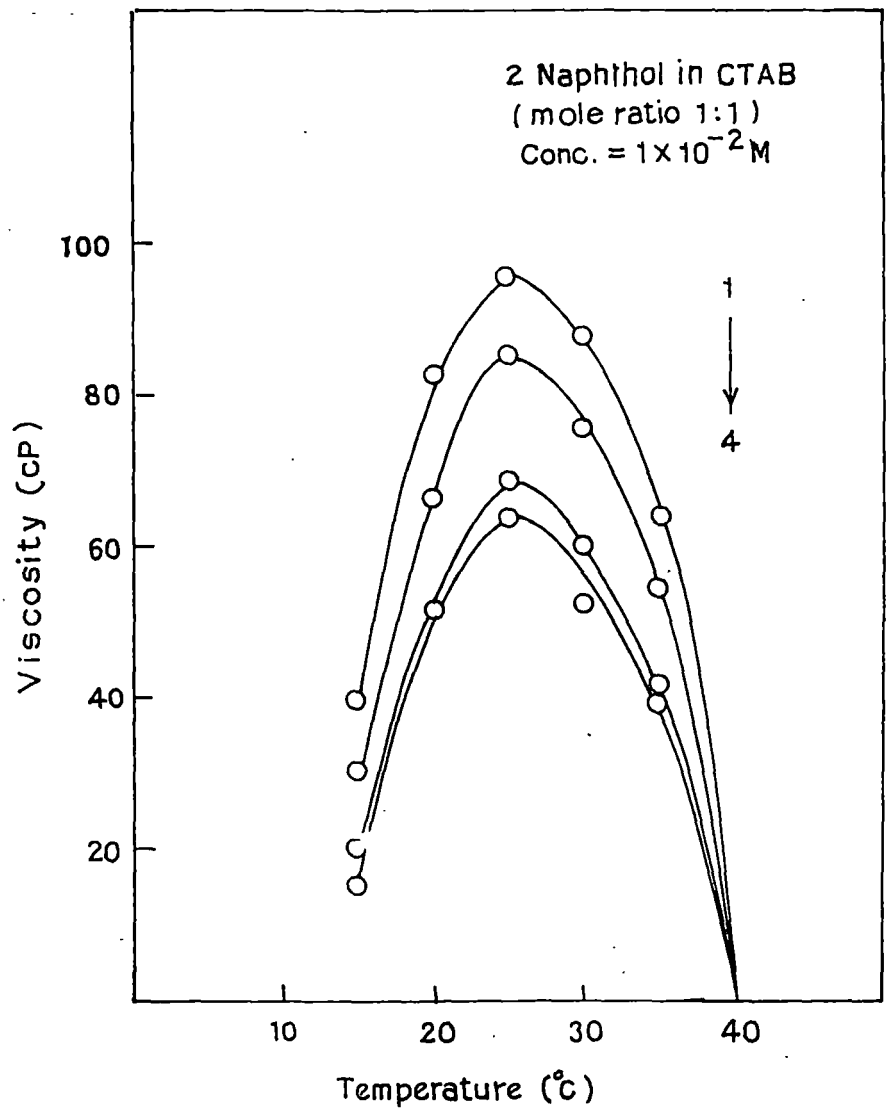

Fig. 19. Shear induced viscosity as a function of temperature. Applied shear (10 minutes): 36.71 s^{-1} (1); 73.42 s^{-1} (2); 122.36 s^{-1} (3); 244.72 s^{-1} (4).

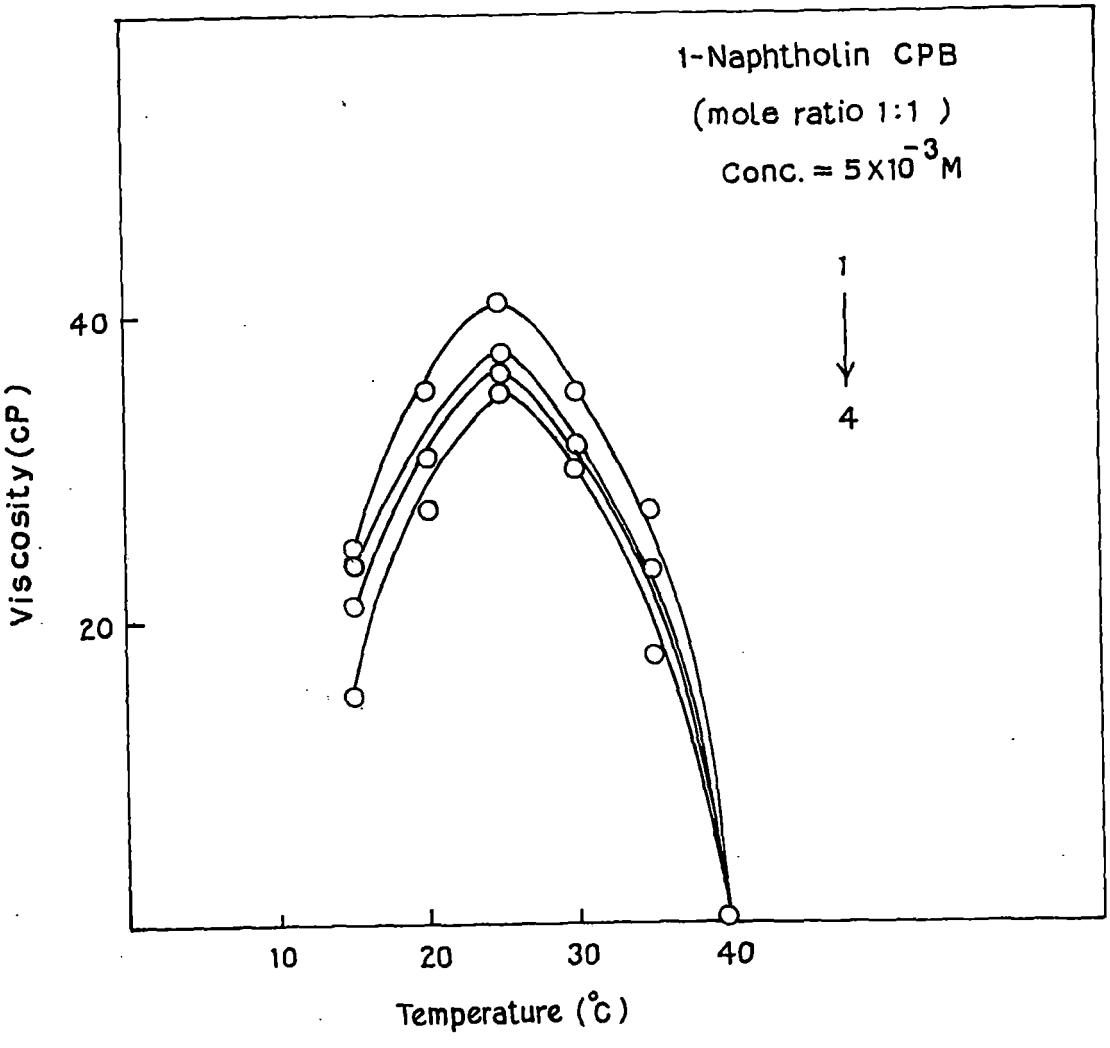

Fig. 20. Shear induced viscosity as a function of temperature. Applied shear (10 minutes): 36.71 s^{-1} (1); 73.42 s^{-1} (2); 122.36 s^{-1} (3); 244.72 s^{-1} (4).

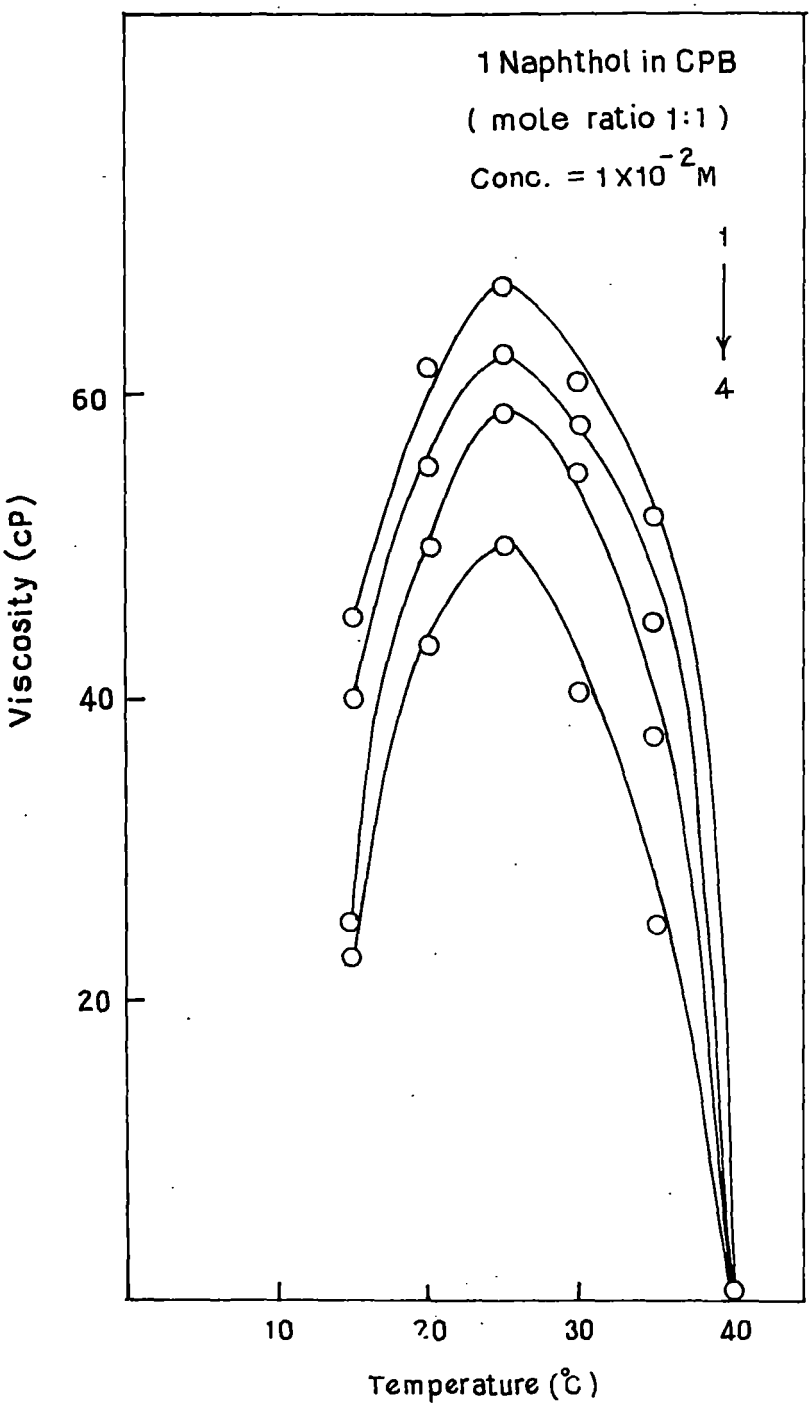

Fig. 21. Shear induced viscosity as a function of temperature. Applied shear (10 minutes): 36.71 s^{-1} (1); 73.42 s^{-1} (2); 122.36 s^{-1} (3); 244.72 s^{-1}(4).

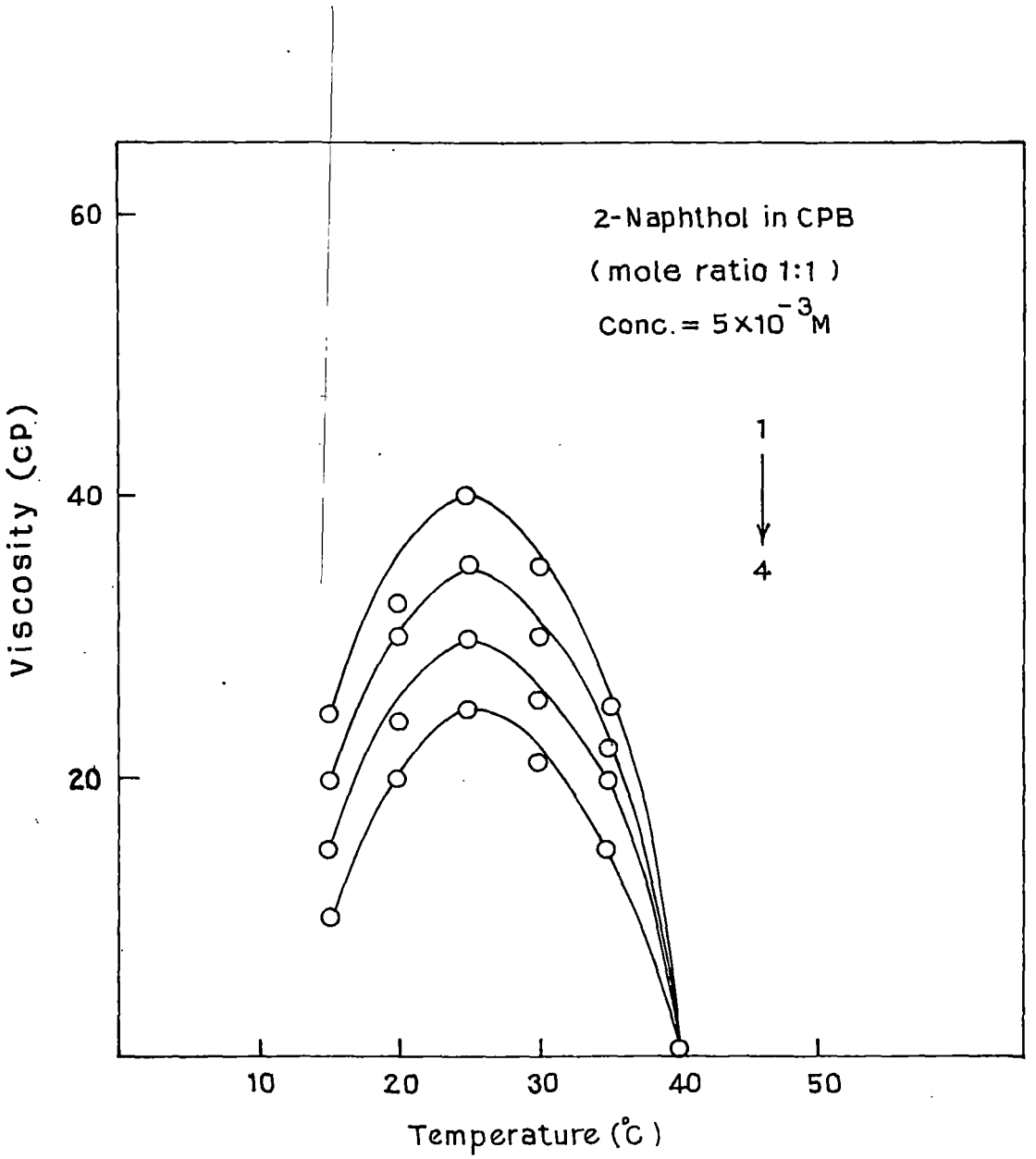

Fig.22. Shear induced viscosity as a function of temperature. Applied shear (10 minutes): 36.71 s^{-1} (1); 73.42 s^{-1} (2); 122.36 s^{-1} (3); 244.72 s^{-1}(4).

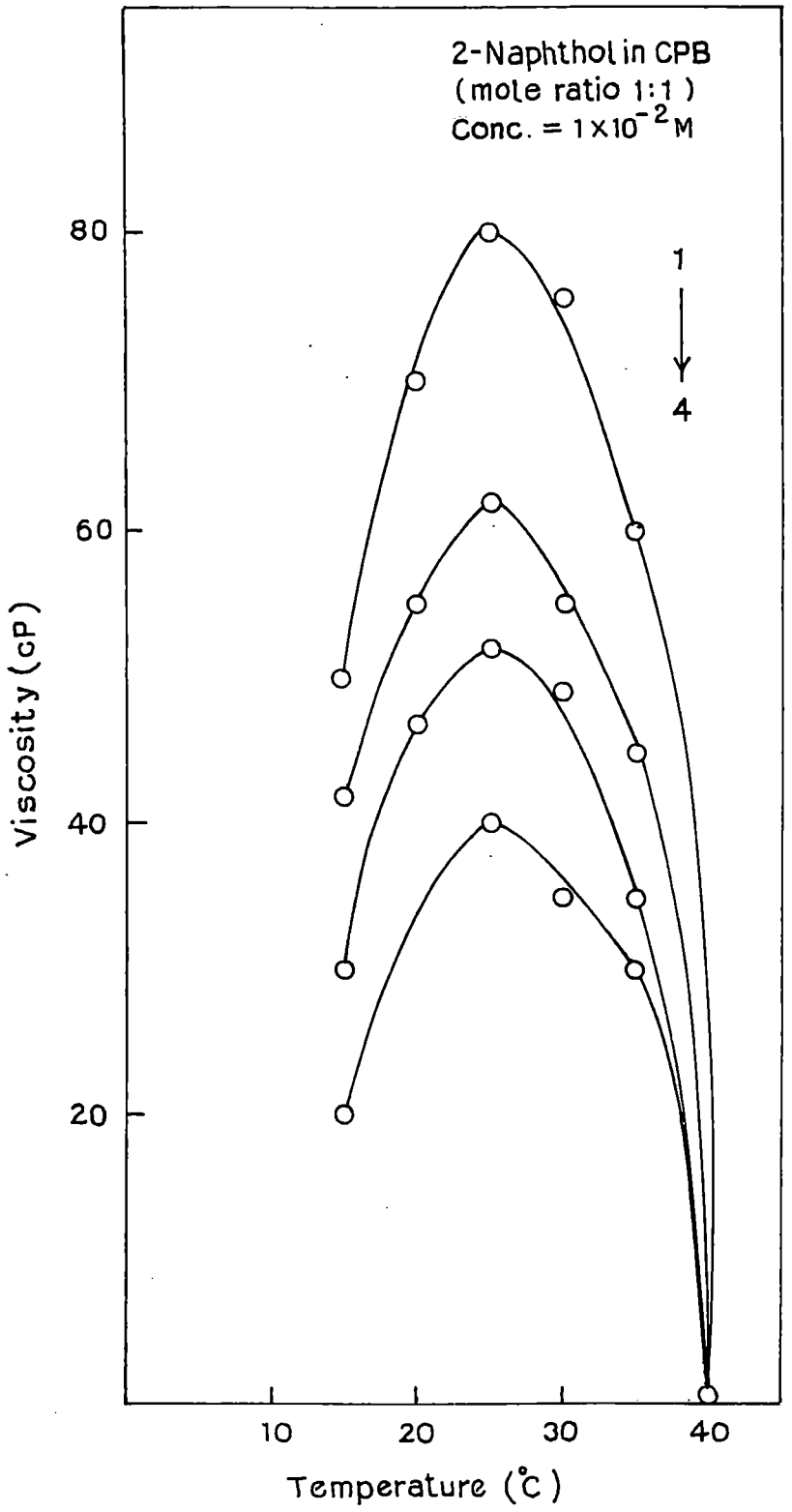

Fig. 23. Shear induced viscosity as a function of temperature. Applied shear (10 minutes): 36.71 s^{-1} (1); 73.42 s^{-1} (2); 122.36 s^{-1} (3); 244.72 s^{-1} (4).

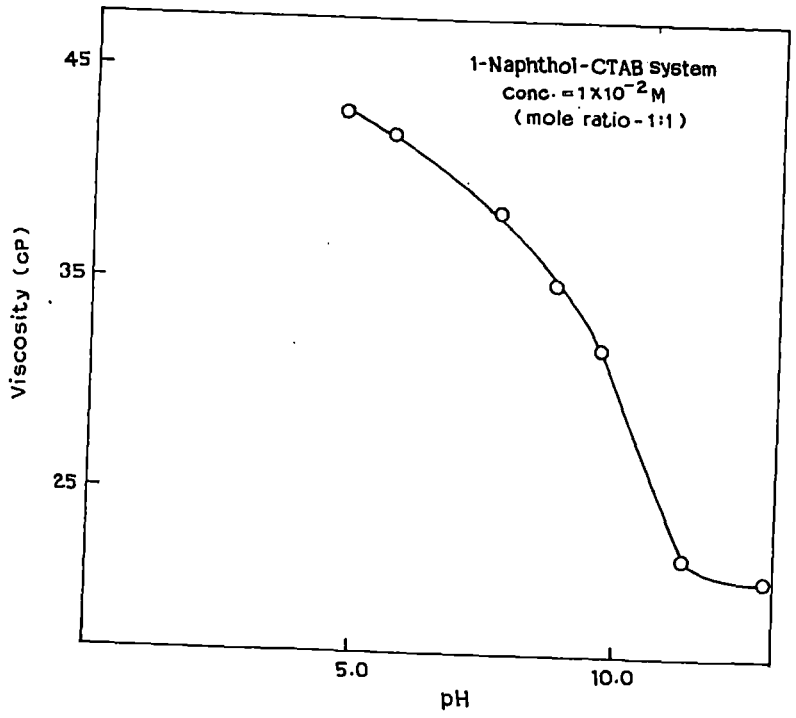

Fig. 24. Shear induced viscosity as a function of pH (applied shear = 36.71 s^{-1} for 10 minutes at 298K).

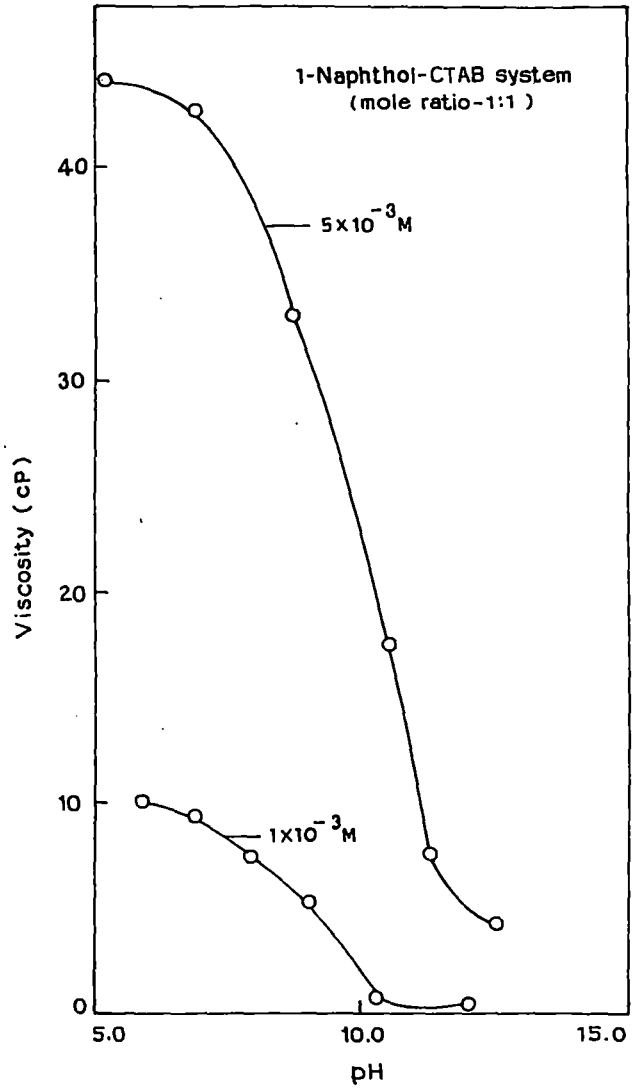

Fig.25. Shear induced viscosity as a function of pH (applied shear = 36.71 s^{-1} for 10 minutes at 298K).

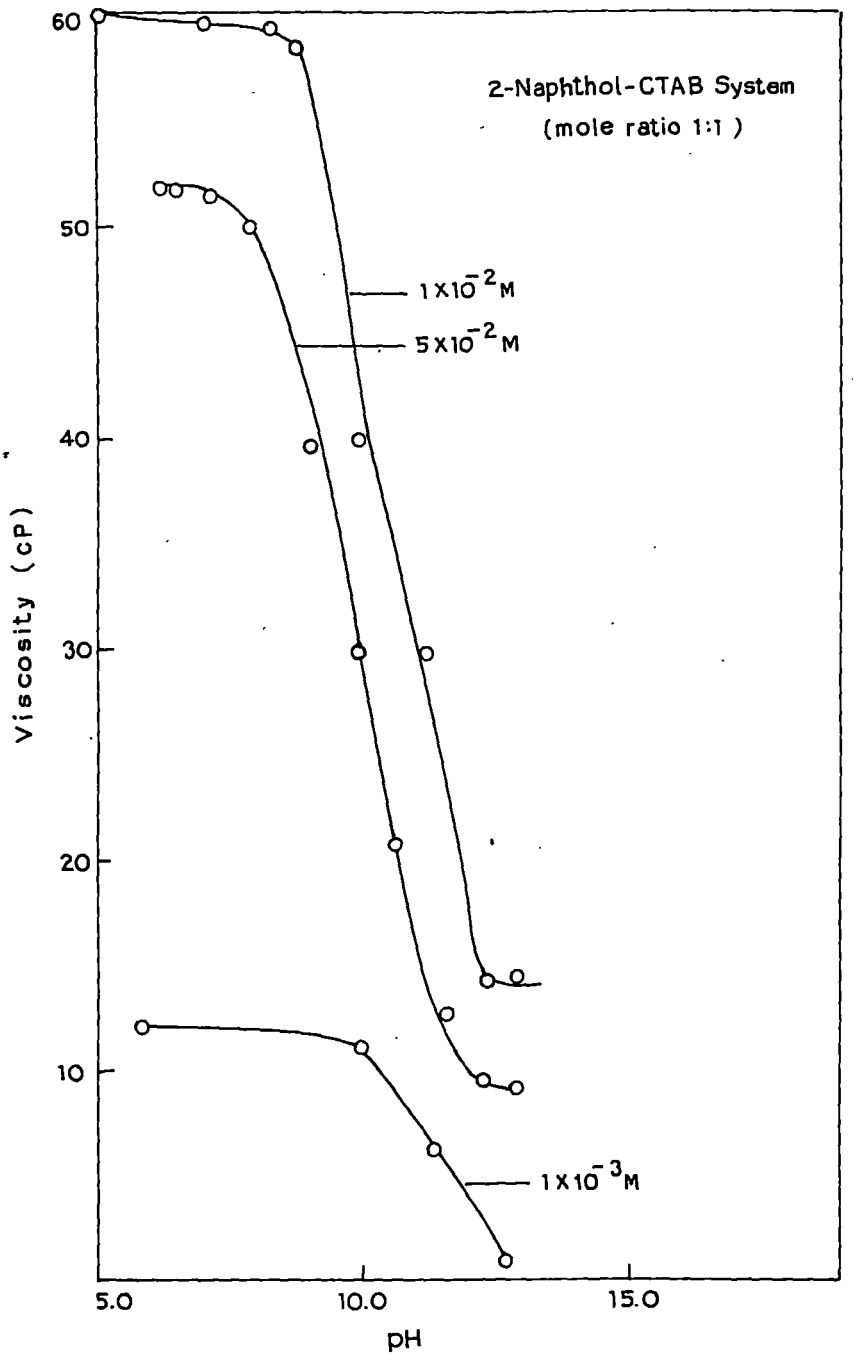

Fig. 26. Shear induced viscosity as a function of pH (applied shear = 36.71 s^{-1} for 10 minutes at 298K).

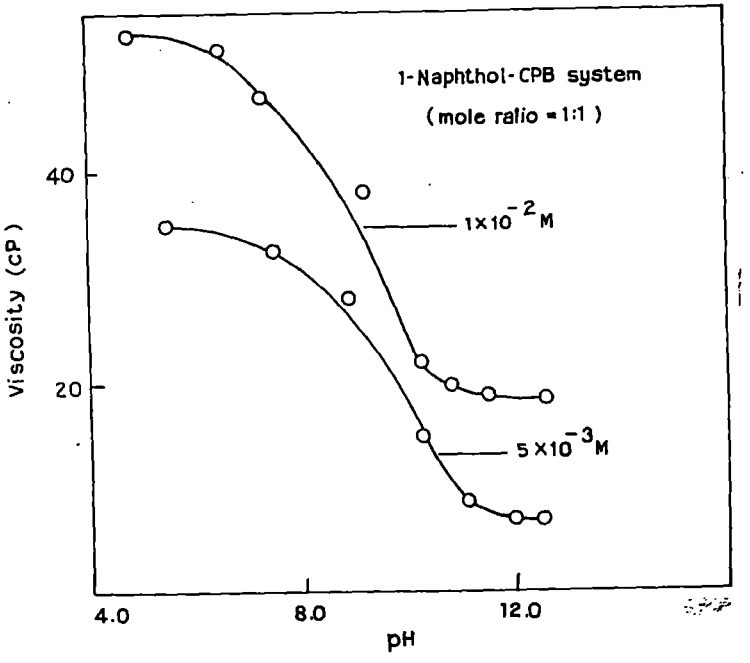

Fig. 27. Shear induced viscosity as a function of pH (applied shear = 36.71 s^{-1} for 10 minutes at 298K).

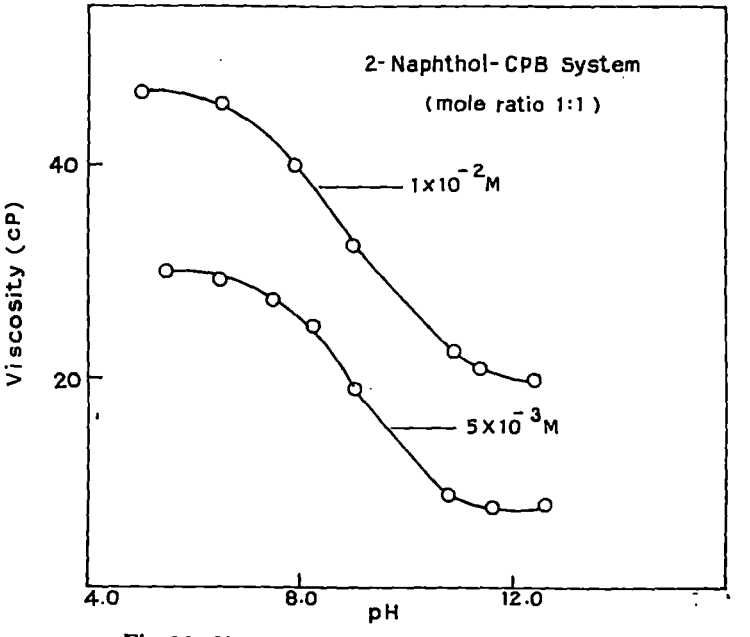

Fig. 28. Shear induced viscosity as a function of pH (applied shear = 36.71 s^{-1} for 10 minutes at 298K).

of charge density at the micellar interface promotes the growth of cylindrical micelles. However, any explanation emphasizing charge screening of micellar surface by the added salt anions as has been put forward in the above reference is again not applicable in the present system. Hydrophobic interaction between micellar core and the aromatic ring of the naphthol molecules seems to be important factor which impart thermoreversible viscoelasticity in the present systems also. But, as the temperature is increased, naphthol molecules (mostly protonated) become more and more soluble and perhaps are partitioned more strongly in the micellar hydrocarbon core. This favours the formation of longer wormlike micelle upto the critical temperature, above which the increased kinetic energy allowing surfactant unimers to hop more frequently between the body and the end cap results in the breaking up of the same.

Figs. 24-28 illustrate steady state viscosity of (1-10) mM equimolar CTAB/Naphthol and CPB/Naphthol solutions and as a function of bulk pH. Dependence of SIV on pH is also intriguing. Although SIV in most of the present systems remains virtually steady within pH range of 4.5 to 6.5 it starts decreasing thereafter. The SIV again become constant, after pH 11.0, pK_a of 1- and 2- Naphthols in aqueous medium are 9.2 ± 0.2 and 9.5 ± 0.3 respectively. When the Naphthols are bound at the aqueous micellar interface, the pK_a value will be modified slightly. It is, however, interesting to note that in 1- and 2-Naphthols, more than 50% of the hydroxyl group are ionized above pH 9.2 to 9.5 respectively, i.e., SIV decreases significantly as the hydroxyl groups are ionized. This observation is clearly indicative of the involvement of hydroxyl group of Naphthols in entanglement and/or transitional networking of micelles.

NMR and FTIR characterizations

The molecular origin of worm like micellar growth is believed to be the adsorption or insertion of the hydrotropes into the micelle and thereby altering the packing parameter of the micelles. However, screening of the charges of

head group facilitates the transition. Therefore, the location and orientation of the promoter is important factor. To determine the efficiency of the promoter molecule, the nmr spectroscopy is an ideal probe of the average position and orientation of the additives on the micellar surface. Past nmr studies of aromatic counter ions on cationic micelles showed an upfield shift in proton resonance of the aromatic moiety, from which it was inferred that the aromatic rings are inserted into the micelles.[98] In the present study, ^1H nmr spectra of pure Naphthols and CTAB and CPB in D_2O were measured. Fig.29 (inset a) shows that the spectra of 2-Naphthol in D_2O give clusters of signals centered at δ value of 7.850 and 7.382, due to the resonance of the aromatic ring proton. These two sets of signals are shifted upfield, broadened and merged to give two broad (signal) peaks at δ value of 7.337 and 6.991 respectively when 10 mM Naphthols are mixed with 10 mM CTAB in D_2O (Fig. 29; 1b). Thus large shift of aromatic proton resonance to low δ values clearly indicates the location of naphthol rings in the less polar environment than that of water. This means that the aromatic rings of the naphthols penetrates to some extent inside the non polar micellar core. On the other hand, ^1H resonance signals of Me_3N^+ head group of CTAB appears at δ value of 3.132 and the signals from $-CH_2$ group adjacent to head group appear at 3.313 and 3.289 (almost merged together)in D_2O (Fig.29; inset C). Although both of the protons signals shifted upfield, the protons of $-CH_2$ group adjacent of the tetramethyl ammonium $N(CH_3)_3$ head groups of CTAB are affected most due to the presence of naphthols (above two signals are shifted to 2.746 and 2.379 respectively, (Fig. 29; 1d). Signal from $-CH_2$ protons emerge on the other side of the $N(CH_3)_3$ peak. This identification is important because it indicates the presence of aromatic ring of the additive resides near the head groups but it is more close to the $-CH_2$ group, which are at immediate vicinity of the head group. This feature in conjunction with corresponding shifts of the aromatic protons of the solubilisate molecule conclusively proves that the solubilized molecule sits near the surface of the micelle with a well-defined orientation. The spectral feature is also suggestive

of the fact that the naphthol molecules are not penetrated deep inside the micellar core but present near the surface with hydroxy probably protruded from the micellar surface and screen the surfactant head group charges. Fig. 29; 2 shows spectra at high concentration of naphthol and CTAB. Due to stronger gel formation, the signals broadened.

Because FTIR is also a powerful tool to investigate the microstructures of gel system, we have used this technique also to investigate the structure of micellar entanglement. Fig. 30 and 31 show IR spectra of 1-Naphthol in presence and in absence of CTAB and CPB respectively. During sample preparation, naphthols and CTAB or CPB were mixed together at 1:1 mole ratio and shear was applied (200 rpm for 10 mins). The aqueous gel then dried at 25^0C temperature under vacuum for 24 hours or until the drying was found complete (since gel melts at high and low temperatures). Fig. 30 illustrates spectral feature of –OH stretching band in absence of CTAB (A) and that in presence of CTAB (B). It is observed that the gelation leads to a significant change in IR spectra. The broad band at 3354 cm^{-1} associated with –OH stretching of 2-Naphthol shifts to 3163 cm^{-1} (not sharp) upon micellar entanglement. In CPB micelles, this shift is even much prominent (shifts to 3100 cm^{-1}, Fig. 31). This large shift to lower frequency clearly indicates that even though weak intermolecular hydrogen bonding may be present in naphthols, it is still very strong when they are involved in bridging a number of long wormlike micelles leading to three dimensional network. Thus, the microstructural diversity associated with the intermolecular H-bonding in napthol, which results in the diffused and broad energy states of the excited normal modes no longer exist in gel. A comparatively more well defined and specific H-bond is present in gel, which may bridge wormlike micelles together to form the network structure. The peak at 3050 cm^{-1}, which remains almost unchanged upon gelation, may be assigned to aromatic –CH stretch. The shear induced phase is highly entangled viscous, strongly aligned, and consists of structure much larger than individual micelles. Present study undoubtedly show

that naphthols embedded in different micelles bridge between the micelles resulting in the entanglement. This is perhaps the first direct proof of involvement of hydrogen bonding in mecellar entanglement. The micron-sized structures, which are much larger than individual worm like micelles and are formed on the application of shear are also formed probably via hydrogen bond networking (Fig. 32). These percolating superstructures are responsible for the increase in viscosity, consistent with the observed shear thickening.

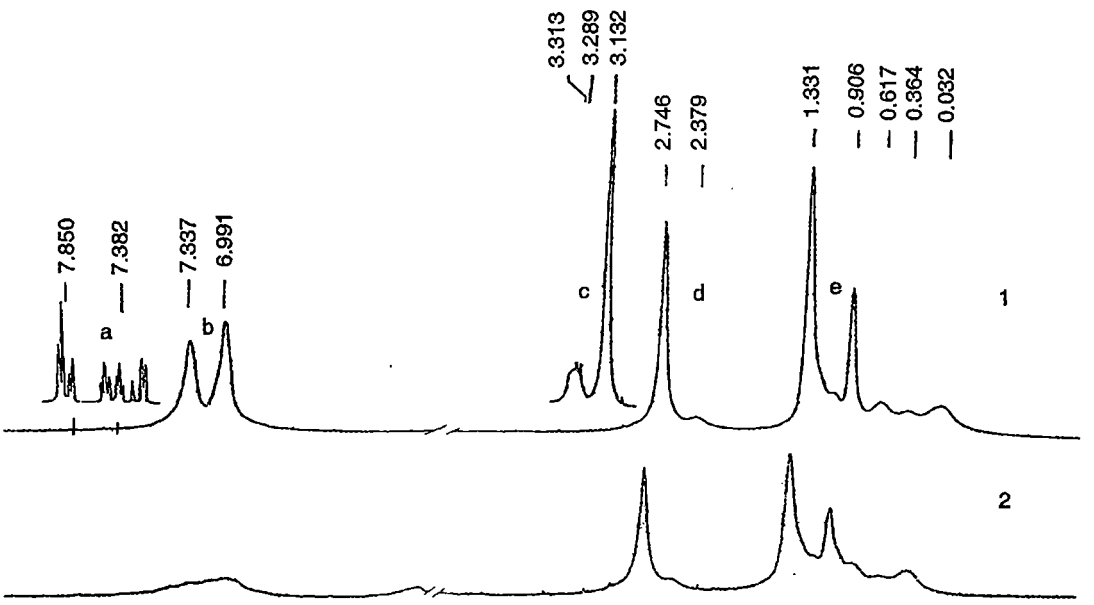

Fig. 29 ^{1}H nmr spectra of 2-Naphthol-CTAB system.

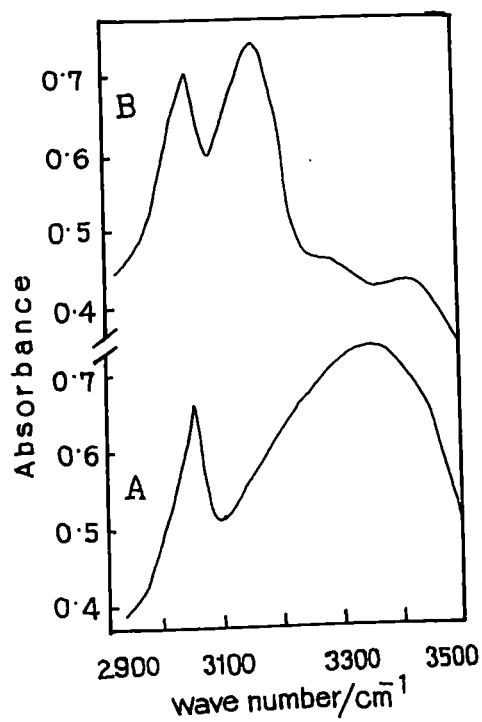

Fig. 30. FTIR spectra of 2-Naphthol in absence (A) and in presence of CTAB micelles (B).

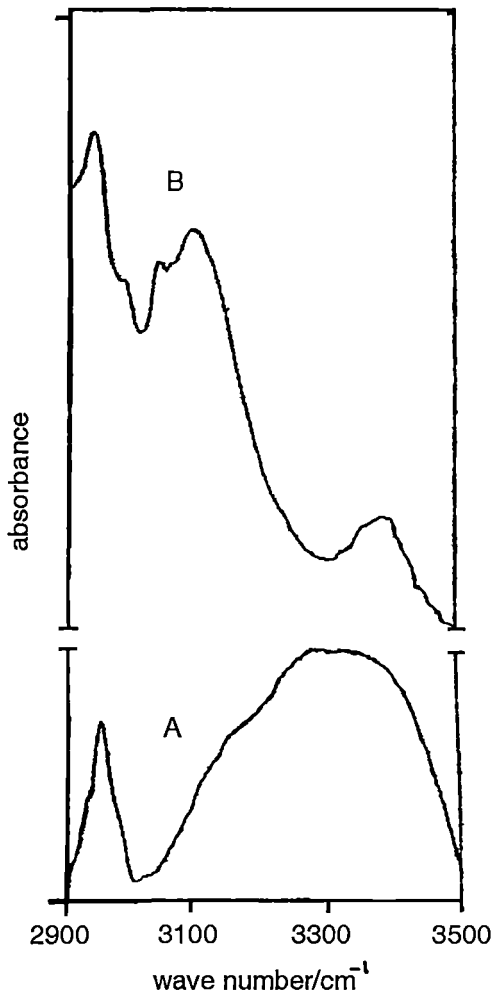

Fig. 31. FTIR spectra of 2-Naphthol in absence (A) and in presence of CPB micelles (B).

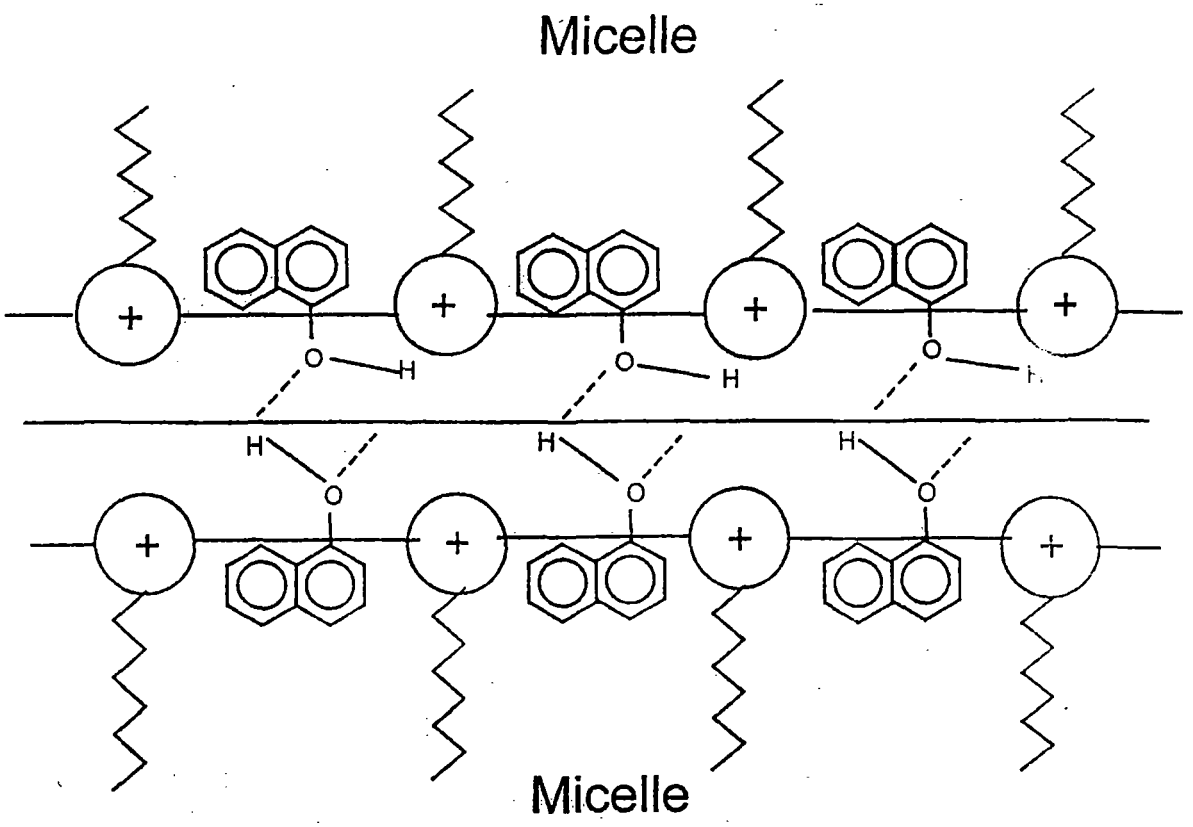

Fig. 32. Microstructure of transient network of micelles in presence of Naphthols.

References

1. Candau, S.J & Lequeux, F., *Current Opinion In Colloid and Interface* Science, **2**, 420 (1997).
2. Evans, D. F., and Wennerström, H., *The Colloidal Domain where Physics, Chemistry and Biology* Meet, Ed. Wiley-(1999).
3. Tanford, C. The Hydrophobic Effect, 2nd ed.; Wiley: New York,(1980).
4. Rehage, H., Hoffmann, H., *Mol. Phys.*, **74**, 933 (1991)
5. Cates, M. E., Candau, S. J., *J. Phys. Condens. Matter*, **2**, 6869 (1990).
6. Hoffmann, H., Munkert U.; Thunig, C.; Valiente, M., *J. Colloid Interface Sci.*, **163**, 217 (1994).
7. Shikata, T., Hirata, H.; Kotaka, T., *Langmuir*, **5**, 398. (1989).
8. Shikata, T., Hirata, H., Kotaka, T., *Langmuir*, **4**, 354 (1988).
9. Kern, F., Zana, R., Candau, S. J., *Langmuir*, **7**, 1344 (1991).
10. Kern, F., Lemarechal, P., Candau, S. J., Cates, M. E., *Langmuir*, **8**, 437 (1992).
11. Tornblom, M., Henriksson U., Ginley M., *J. Phys. Chem.*, 98, 7041 (1994).
12. Wang, S. Q., *J. Phys. Chem.*, 94, 8381 (1990).
13. Candau, S. J.; Hirsch, E.; Zana, R.; Adam, M., *J. Colloid Interface Sci.*, **122**, 430 (1988).
14. Hoffmann, H., Rauscher, A., Gradzielski, M., Schulz S. F., *Langmuir*, **8**, 2140 (1992).
15. Shikata, T., Morishima, Y., *Langmuir*, **12**, 5307 (1996).
16. Shikata, T., Imai, S., Morishima, Y., *Langmuir*, **13**, 5229 (1997).

17. Soltero, J. F. A., Puig, J. E., Manero, O.; Schulz, P. C., *Langmuir*, **11**, 3337 (1995).

18. Soltero, J. F. A., Puig, J. E., Manero, O., *Langmuir*, **12**, 2654 (1996).

19. Soltero, J. F. A., Bautista, F., Puig, J. E., Manero, O., *Langmuir*, **15**, 1604 (1999).

20. Hassan, P. A., Valaulikar, B. S., Manohar, C., Kern, F., Bourdieu, L., Candau, S. J., *Langmuir*, **12**, 4350 (1996).

21. Hassan, P. A., Manohar, C. J., *Phys. Chem. B*, **102**, 7120 (1998).

22. Wolff, T., Emming, C. S., von Bunau, G., Zierold, K., *Colloid Polym. Sci.*, **270**, 822 (1992).

23. Danino, D., Talmon, Y., Levy, H., Beinert, G., Zana, R., *Science*, **269**, 1420 (1995).

24. Israelachvili, J., *Intermolecular & Surface forces*, London: Academic Press (1992).

25. Majid, L. J., *J. Phys. Chem. B*, **102**, 4064 (1998) .

26. Cates, M. E., and Candau, S.J., *J. Phys : Condens. Matter*, **2**, 6869 (1990).

27. Hu, Y., Rajaram, C. V., Wang, and Jamieson, A. M., *Langmuir*, **10**, 80 (1994).

28. Hassan, P. A., Narayanan, J., Manohar, C., *Current Science*, **80**, 8 (2001).

29. Salkar, Hassan, R. A., *J. Chem. Soc., Chem. Comm.*, 1223 (1996).

30. Manohar, C., Rao, U. R., *J. Chem. Soc., Chem. Comm*, 379 (1986).

31. Turner, M. S., and Cates, M. E., *J. Phys: Condens. Matter*, **4**, 3419 (1992).

32. Cates, M. E., Candau, S. J., *J. Phys: Condens. Matter*, **2**, 6869 (1990).

33. Wunderlich, I., Rehage, H., Hoffmann, H., *Prog, Colloid Polimer Science*, **72**, 51 (1986).

34. Odijk, T., *J. Phys. Chem.*, **93,** 3888 (1989).

35. Lindman, B.; Wennerström, H., *Top. Curr. Chem.*, **87,** 1 (1980).

36. (a) Gravsholt, S. J., *Colloid Interface Sci.*, **57,** 575 (1976).

(b) Imae, T., Kamiya, R., Ikeda, S., *J. Colloid Interface Sci.* **108,** 215 (1985).

37. (a) Gamboa, C., Sepu´lveda, S. J., *J. Colloid Interface Sci.* **1986,113,** 566.

(b) Gamboa, C.; Rý´os, H.; Sepu´lveda, S. J., *J. Chem. Phys.*, **93,** 5540 (1989).

38. Hyde, A. J.; Johnstone, D. W. M., *J. Colloid Interface Sci.,* **53,** 349 (1975).

39. (a) Yatcilla, M. T., Herrington, K. L., Brasher, L. L., Kaler, E. W., Chiruvolu, S., Zasadzinski, J. A., *J. Phys. Chem.*, **100,** 5874 (1996).

(b) So¨derman, O., Herrington, K. L., Kaler, E. W., Miller, D. D., *Langmuir*, **13,** 5531 (1997).

40. Cates, M. E., Candau, S. J., J. *Phys. Condens. Matter*, **2,** 6869 (1990).

41. Rehage, H., Hoffmann, H., *Mol. Phys.*, **74,** 933 (1991).

42. Rao, U. R. K., Manohar, C., Valaulikar, B. S., Iyer, R. M., *J. Phys. Chem.*, **91,** 3286 (1987).

43. Bijma, K., Rank, E., Engberts, J. B. F. N., *J. Colloid Interface Sci.*, **205,** 245 (1998).

44. Olsson, U., So¨derman, O., Gue´ring, P., *J. Phys. Chem.*, **90,** 5223 (1986).

45. Manohar, C., Rao, U. R. K., Valaulikar, B. S., Iyer, R. M., *J. Chem. Soc.*, 379 (1996).

46. Turner, M. S., Marques, C., Cates, M. E., *Langmuir*, **6,** 695 (1993)

47. (a) Shikata, T., Sakaiguchi, Y., Urakami, H., Tamura, A., Hirata, H. J., *Colloid Interface Sci.*, **119**, 291 (1987).

(b) Sakaiguchi, Y., Shikata,T., Urakami, H., Tamura, A., Hirata, H. J., *Electron Microsc.*, **36**, 168 (1987).

(c) Sakaiguchi, Y., Shikata, T., Urakami, H., Tamura, A., Hirata, H., *Colloid Polym. Sci.*, **265,** 750 (1987).

48. (a) Lin, Z., Scriven, L. E., Davis, H. T., *Langmuir*, **8**, 2200 (1992).

(b) Clausen, T. M., Vinson, P. K., Minter, J. R., Davis, H. T., Talmon,Y., Miller, W. G., *J. Phys. Chem.*, 96, 474(1992).

49. (a) Shikata, T., Hirata, H., Kotaka, T., *Langmuir*, **3**, 1081 (1987).

(b) Imae, T., *Colloid Polym. Sci*, **267**, 707 (1989).

50. Lin, Z., Chai, J. J., Scriven, L. E., Davis, H. T., *J. Phys. Chem.*, **98**, 5984 (1994).

51. Mishra, B. K., Samant, S. D., Pradhan, P., Mishra, S. B., Manohar, C., *Langmuir*, **9**, 894 (1993).

52. Hassan, P. A., Narajanan, J., Menon, S.V.G., Salkar, R. A., Samant, S. D., Manohar, C., *Colloids Surf.*, 117, 89 (1996).

53. Berr, S. S., Caponetti, E., Johnson Jr., J. S., Jones, R. R. M., Magid, L. D., *J. Phys. Chem.*, **90**, 5766 (1986).

54. Salkar, R.A., Hassan, P.A., Samant, S.D., Valaulikar, B. S., Kumar, V. V., Kern, F., Candau, S. J., Manohar, C., *J. Chem. Soc. Chem. Commun.*, 1223 (1996).

55. Horbaschek, K., Hoffmann, H., Thunig, C., *J. Colloid Interface Sci.*, **206**, 439 (1998).

56. Menon, S. V. G., Manohar, C., Lequeux, F., *Chem. Phys. Lett.*, **263**, 727 (1996).

57. (a) Mendes, E., Narajanan, J., Oda, R., Kern, F., Candau, S. J., Manohar, S. J., *J. Phys. Chem. B*, **101**, 2256 (1997).

(b) Mendes, E., Manohar, C., Narajanan, J., *J. Phys. Chem. B*, **102**, 338 (1998).

58. Hassan, P. A., Valaulikar, B. S., Manohar, C., Kern, F., Bourdieu, L., Candau, S. J., *Langmuir*, **12**, 4350 (1996).

59. Hoffmann, H., *Viscoelastic Surfactant Solutions. In Structure and Flow in Surfactant Solutions*; Herb, C. A., Prud'homme, R. K., Eds.; *American Chemical Society*: Washington, DC, 2 (1994).

60. Yang, J., *Curr. Opin. Colloid Interface Sci.*, **7**, 276 (2002).

61. Cates, M. E., Candau, S. J., *J. Phys. Condens. Matter*, **2**, 6869 (1990).

62. Raghavan, S. R., Kaler, E. W., *Langmuir*, **17**, 300 (2001).

63. Makhloufi, R., Cressely, R., *Colloid Polym. Sci.*, **270,** 1035 (1992).

64. Ponton, A., Schott, C., Quemada, D., *Colloids Surf. A*, **145**, 37, (1998).

65. Rehage, H. and Hoffmann, H., *Mol. Phys.*, **74**, 933 (1991).

66. Bhattacharya, S. and De, S., *J. Chem. Soc., Chem. Comm.*, 651 (1995).

67. Bhattacharya, S. and De, S., *Langmuir*, **15**, 3400 (1999).

68. Bhattacharya, S., De, S. M. and Subramanian, M., *J. Org. Chem.*, **63**, 7640 (1998).

69. Bhattacharya, S. and De, S., *J. Chem. Soc., Chem. Commun.*, 1283 (1996).

70. Fukuda, H., Kawata, K., Okuda, H. and Regen, S. L., *J. Am.Chem. Soc.*, **112**, 1635 (1990).

71. Kobuke, Y., Ueda, K. and Sokabe, M., *J. Am. Chem. Soc.*, **114**, 7618 (1992).

72. Yatcilla, M. T., Herrington, K. L., Brasher, L. L., Kaler, E. W.,Chiruvolu, S. and Zasadzinski, J. A., *J. Phys. Chem.*, **100**, 5874 (1996).

73. Marques, E., Khan, A., de Graca Miguel, M. and Lindman, B., *J. Phys. Chem.*, **97**, 4729 (1993).

74. Brasher, L. L., Herrington, K. L. and Kaler, E. W., *Langmuir*, **11**, 4267 (1995)

75. Magid, L. J., Han, Z., Warr, G. G., Cassidy, M. A., Butler, P. D. and Hamilton, W. A., *J. Phys. Chem. B*, **101**, 7919 (1997).

76. Mishra, B. K., Samant, S. D., Pradhan, P., Sushama, B., Mishra and Manohar, C., *Langmuir*, **9**, 894 (1993).

77. Carver, M., Smith, T. L., Gee, J. C., Delichere, A., Caponetti, E. and Magid, L. J., *Langmuir*, **12**, 691 (1996).

78. Kreke, P. J., Magid, L. J. and Gee, J. C., *Langmuir*, **12**, 699 (1996).

79. Bachofer, S. J. and Simonis, U., *Langmuir*, **12**, 1744 (1996).

80. Long, M. A., Kaler, E. W. and Lee, S. P., *Biophys. J.*, **67**, 1733 (1994).

81. Zemb, T., Dubois, M., Deme, B. and Gulikkrzywicki, T., *Science*, **283**, 816 (1999).

82. Oda, R., Huc, I., Schmutz, M., Candau, S. J. and Mackintosh, F. C., *Nature*, **399**, 566 (1999).

83. Edwards, K., Gustaffson, J., Almgren, M. and Karlsson, G., *J. Colloid. Int. Sci.*, **161**, 299 (1993).

84. Friberg, S. E., Campbell, S., Fei, L, Yang, H., Patel, R. and Aikens, P. A., *Coll. Surf. A*, **129**, 167 (1997).

85. Kaler, E. W., Herrigton, K. L., Murthy, A. K. and Zasadzinski,J. A. N., *J. Phys. Chem.*, **96**, 6698 (1992).

86. Cohen, D. E., Thurston, G. M., Chamberlin, R. A., Benedek, G. B. and Carey, M. C., *Biochemistry*, **37**, 14798 (1998).

87. Pedersen, J. S., Egelhaaf, S. U. and Schurtenberger, P., *J. Phys. Chem.*, **99**, 1299 (1995).

88. de la Maza, A. and Parra, J. L., *Langmuir*, **11**, 2435 (1995).

89. Egelhaaf, S. U. and Schurtenberger, P., *Phys. Rev. Lett.*, **82**, 2804 (1999).

90. Egelhaaf, S. U. and, Schurtenberger, P., *Phys. B*, **234**, 276 (1997).

91. Oda, R., Bourdieu, L. and Schmutz, M., *J. Phys. Chem. B*, **101**, 5913 (1997).

92. Inoue, T., Motoyama, R., Miyakawa, K. and Shimozawa, R., *J. Colloid Interface Sci.*, **156**, 311 (1993).

93. Cariontaravella, B., Chopineau, J., Ollivon, M., Lesieur, S., *Langmuir*, **14**, 3767 (1998).

94. Forte, L., Andrieux, K., Keller, G., Grabiellemadelmont, C., Lesieur, S., Paternostre, M., Ollivon, M., Bourgaux, C. and Lesieur, P., *J. Thermal Analysis Calorimetry*, **51**, 773 (1998).

95. Dubachev, G. E., Polozova, A. I., Simonova, T. N., Borovyagin, V. L., Demin, V. V. and Barsukov, L. I., *Biol. Membr.*, **13**, 100 (1996).

96. Keller, S. L., Bottenhagen, P., Pine, D. J., Zasadzinski, J. A., *Phys. Rev. Letters*, **80**, 2725 (1998).

97. Kalur, G. C., Frounfelker, B. D., Cipriano, B. H., Norman, A. I., Raghavan, S. R., *Langmuir*, **21**, 10998 (2005).

98. Rao, U. R. K., Manohar, C., Valaulikar, B. S., Iyer, R. M., *J. Phys. Chem.*, **91**, 3286 (1987).

CHAPTER - 6

SUMMARY AND CONCLUSION

Summary and Conclusion

In Chapter 1, a general introduction covering the description of various organised molecular assembly, viz., micelles, microemulsions, vesicles, lipid bilayers etc. and their importance are presented. The physico-chemical properties of the organised assemblies are generally studied by introducing a probe molecule (e.g., pH indicators) and monitoring the change in the properties of the probe in the new environment. For example, investigations of acid-base equilibria of amino acids, their interaction with metal ions in media of varied ionic strength, temperature and dielectric constant throw light on the mechanism of enzymes catalyzed reaction. Although it is known that the polarity of the active site cavities in proteins is lower than that of the bulk, a direct measurement of dielectric constant is not possible. A method wherein comparison of formation constants obtained from acid-base and/or metal complex equilibria with the corresponding values observed at the biological centre offers a way to estimate an effective dielectric constant for the cavity has been invoked.

(Page 1-11)

Chapter 2 describes the scope and object of the present investigation. The importance of interfacial region between aqueous and non-polar part of the self-assembled lipid phase is very well recognized in biological membranes. For the measurement of the electrical potential at the surface of a charged membrane or a similar interface one requires a probe of molecular size which does not disturb the system itself. It has been suggested that the use of pH indicators can act as probes for charged micelles and attributed the "apparent" shift of pK_a detectable in the micellar solution, as compared to pure aqueous solutions, to a change of the "local interfacial" proton activity at the surface of charged micelles as compared to that in bulk water. The equilibrium of an indicator, bound to a surface, may be affected not only by an electrostatic

potential, but in addition by a different local environment, e.g., by a lower dielectric constant as compared to bulk water and also by specific interactions of the indicator at the surface, if any. Although different types of organic indicator molecules have been applied as spectroscopic probes for studying above properties, surprisingly, two important uv active aromatic amino acids e.g., tyrosine and tryptophan have not been used so far. However, there are certain class of molecules which are biologically quite important but their spectral properties are quite insensitive to the surroundings. It has been found that while the protonation-deprotonation equilibrium of hydroxy group of tyrosine and 5-Hydroxytryptophan influence their electronic spectra to a great extent, the spectral profile of tryptophan is insensitive to acid or base. Thus sometimes, the spectral characteristics, specially fluorescence spectra, are very sensitive to the environments of the systems. Because of this, fluorescence spectroscopy has become one of the fundamental methods for the study of the structure and dynamics of the microheterogeneous systems. The photophysics of probe molecules, therefore, are studied in those systems. Physical gelation of surfactant micelles and their stimuli responsive behaviour are interesting from biology as well as chemical technology points of view. It is particularly interesting that while a wide variety of worm-like ionic micellar solution display identical rheological responses, a common element in all of these systems is the presence of salt anions like sodium salicylate. This limitation has perplexed the scenario to some extent and impeded the development of an acceptable theory which may explain micellar shape transition under dilute condition. It has been found in the present work that molecules like 1- and 2-Naphthols with a strong hydrophobic aromatic ring and a polar hydroxy group support shape transitions of surfactant micelles very efficiently.

Keeping the above aspects in view, a number of biologically important organic molecules and their hydroxy derivatives and also 1- and 2-Naphthols are chosen as indicator (probe) molecules for studying the protonation-deprotonation equilibria at the micellar surface of different ionic and non-ionic

micelles as well as in aqueous-organic medium. These indicator molecules are, 5-Hydroxyindole, 5-Hydroxy-L-tryptophan, L-Tyrosine, L-Tyrosine-methylester, 1-Naphthol and 2-Naphthol. A detail study on the protonation-deprotonation equilibrium of these probes in micellar media has been undertaken. Fluorescence spectroscopic properties of these molecules have been studied in different solvents to understand the photo-physics of the systems.

Moreover, the role of 1- and 2-Naphthols in developing stimuli sensitive properties of surfactant solutions has been studied. The physicochemical aspects of micellar shape transition, rheological behaviour have been investigated and the microstructure of the system is proposed.

(Page No. 12-16)

In chapter 3, results of the study on protonation-deprotonation equilibrium of OH groups of biologically important indicator molecules in micellar media as stated above have been presented. The surfactants which have been employed in the present study are Cetyltrimethylammonium bromide (CTAB; cationic surfactant), Sodium dodecylsulfate (SDS; anionic surfactant), Sodium bis (2-ethylhexylsulfo-succinate) (Aerosol-OT or AOT; double tailed anionic surfactant), Polyoxy-ethylenesorbitan monopalmitate (Tween – 40; non-ionic surfactant) and Polyoxyethylenelauryl ether (Brij-35; non-ionic surfactant).

In section 3.1, an introduction and review of previous works is given. Organic compounds are generally soluble in micellar media although they may or may not be soluble in water or organic solvent alone. This solubilization leads to a change in the acid-base equilibrium of the solubilisate organic acid. Two established models, viz., thermodynamic model and pseudophase ion exchange model explain the observed pK_a shifts of the acid-base equilibrium. A brief discussion on both of the models are included. In theoretical discussion on

acid-base equilibrium of a indicator, which has its prototropic moiety residing within the interfacial region of a self-assembled surfactant can be represented as

$$HIN \underset{}{\overset{K_a}{\rightleftharpoons}} H^+ + IN^-$$

where HIN, IN, H^+ denote the protonated (acid), deprotonated (base) forms of the solute organic molecule and the proton respectively.

For the organic indicators in aqueous micellar solution, the apparent pK_a values were obtained from the change in the ultraviolet absorption spectrum of each indicator with bulk aqueous pH by means of the expression

$$pK_a^{obs} = pH - \log\frac{[IN]}{[HIN]}$$

with $$\frac{[IN]}{[HIN]} = \frac{\alpha}{1-\alpha}$$

and $$1-\alpha = \frac{A_{IN} - A}{A_{IN} - A_{HIN}}$$

where A represents the uv absorbance at the uv wave length band maximum of the deprotonated form of the indicator, λ_{max}, at a given pH, A_{HIN} the absorbance at λ_{max} when all the indicator molecules are protonated and A_{IN} the absorbance at λ_{max} when all the indicator molecules are deprotonated. Representative ultraviolet absorption spectra for 5-Hydroxyindole, 5-Hydroxy-L-tryptophan, L-Tyrosine, L-Tyrosinemethylester, 1-Naphthol and 2-Naphthol, as a function of bulk aqueous pH are presented.

The thermodynamic acid-base equilibrium constant for the reaction in 1,4-dioxane-water mixtures is given by :

$$pK_a^m = B + \log U_H^\circ - \log\frac{[IN]}{[HIN]} - \log\frac{\gamma_{IN}^m}{\gamma_{HIN}^m}$$

where γ_{IN}^{m} and γ_{HIN}^{m} denote the activity co-efficient of the base and acid forms of the indicators, respectively, referred to the particular 1, 4 dioxane-water mixture at infinite dilution. It is not completely clear how one should approximate the activity co-efficients of large complex organic ions such as the present indicator molecules. Consequently, the pK_a^m values given in this work neglect the activity co-efficient term.

In the present work following points have been considered during the study of the acid-base equilibrium of interfacially located indicator molecules:

(i) Variations of pK_a's, which appear in the study of an interfacial acid-base equilibrium, are characterized.

(ii) Titration of all indicators (molecular probe) in charged and uncharged micelles is described.

(iii) The observable shifts of "apparent" pK_a which is partitioned explicitly into a component due to the electrical potential and a component caused by a change of polarity for a charged micelle is described.

(iv) By comparing the shift of the interfacial intrinsic pK_a^i to the pK_a shift measured in non-polar non-aqueous solvents, an attempt has been made to estimate the effective interfacial dielectric constant wherever possible, exhibiting the indicators as probes of interfacial polarity in same systems.

The theoretical background to the forthcoming analysis of the interfacial protonation-deprotonation equilibrium of the present indicator (probe) molecules has been given in this chapter. Provided there is no significant contribution to the apparent acid-base equilibrium constant of an interfacially located organic molecules from specific solute-solvent interactions, the following relationship hold:

$$pK_a^i = pK_a^m - \log m\gamma_H^+$$

$$pK_a^0 = pK_a^i + \log \frac{\gamma_{IN}^i}{\gamma_{HIN}^i}$$

$$pK_a^0 = pK_a^{obs} + \frac{F\psi_0}{2.303RT}$$

where $m\gamma_H^+$ is the medium effect on the proton, γ_{IN}^i and γ_{HIN}^i denote the activity co-efficients of the deprotonated and protonated forms of the indicator molecules respectively referred to the interfacial phase at infinite dilution, and F, R, T, Ψ_0 represent the Faraday constant, the universal gas constant, the absolute temperature and the electrostatic surface potential respectively.

In addition, it is convenient to define:

$$\Delta pK_a^m = pK_a^m - pK_a^w$$

$$\Delta pK_a^i = pK_a^i - pK_a^w$$

$$\Delta pK_a^0 = pK_a^0 - pK_a^w$$

The nature of variation of ΔpK_a^m and ΔpK_a^i as a function of the dielectric constant of 1,4 dioxane-water mixtures are studied. In calculating pK_a^0 for charged micelles, surface potential ψ of CTAB, SDS and AOT micelles were taken as +141 mv, -140 mv and, -140 mv respectively.

(Page No. 18-35)

In 3.2, experimental aspects have been presented.

(Page No. 35-39)

In section 3.3.1, ultraviolet spectral profile of 5-Hydroxyindole and 5-Hydroxy-L-tryptophan at different pH have been presented. This spectra have been taken in water as well as in various concentrations of CTAB, SDS, AOT,

Tween-40 and Brij-35 in order to study protonation-deprotonation equilibria in micellar microenvironment of above surfactants. Protonation-deprotonation equilibria of hydroxy groups of the two indicators are also studied in 1,4 Dioxane-water mixture. pK_a^{obs}, pK_a^0, ΔpK_a^0 values are calculated for the indicators solubilized in interfacial region of the micelles and ΔpK_a^m and ΔpK_a^i of the indicators are measured in 1,4 Dioxane-water mixture of different compositions. Result shows that ΔpK_a^0 is a function of concentration of the surfactants and both the indicator molecules perhaps undergo specific interaction with the surfactant headgroups of anionic surfactant, viz., SDS and AOT. On the other hand, most probably 5-Hydroxyindole and 5-Hydroxy-L-tryptophan are protonated weakly in non-ionic micelles and values of ΔpK_a^0 is small. However, these indicators are partitioned in the interfacial position of CTAB to a greater extent and D_{eff} value of 38.8 to 52.2 is obtained for 5-Hydroxyindole depending on the concentration of CTAB. This value of inter-facial polarity, D_{eff} is measured by comparing ΔpK_a^0 of the indicators in the interfacial region of the micelle with ΔpK_a^i's of the same in organic-water mixtures. On the other hand, a value of ~ 55 is obtained for 5-Hydroxy-L-tryptophan for the same micelle and indicates that both the molecules are partitioned in the interfacial region and distributed around upto certain distance from the micellar surface.

(Page No. 40-45)

uv spectral profile of L-Tyrosine and L-Tyrosinemethylester have been presented in section 3.3.2. Like 5-Hydroxyindole and 5-Hydroxy-L-tryptophan, spectra of these indicator probe molecules were taken in water and in various concentrations of different surfactants including organic-water medium as mentioned in section 3.3.1 to study the protonation-deprotonation equilibria in these systems. However, the spectral profiles of these indicator molecules become complicated by giving more than one isobestic points. The values of λ_{max} of deprotonated form of L-Tyrosine is found to undergo a red shift in 1,4-

Dioxane-water mixture of low dielectric constant. Due to the existence of an isoelectric point of L-Tyrosine near 5.66, the protonated form remain closer to SDS micellar interphase than those of deprotonated form due to electrostatic repulsion at high pH. The spectral properties do not show any observable effect of the easterfication of carboxylic acid group in L-Tyrosinemethylester. From the pK_a^{obs} values of both the indicators in Tween-40 and Brij-35 micelles, it is apparent that the deprotonated forms of the indicators are stabilized more in micelles than in water.

Values of ΔpK_a^i and ΔpK_a^m for both the indicators are consistently positive in 1,4- Dioxane-water mixtures. On the other hand, ΔpK_a^0 values are positive for both the non-ionic micelles but negative in anionic micelles. The results once again show that while the indicator molecules are weakly partitioned by non-ionic micelles, there is specific interaction between indicator molecules and anionic micelles. The effective dielectric constant (D_{eff}) values for CTAB micellar interface observed from the acid-base equilibrium of both the indicators are more or less same, i.e., 49 ± 1. The result once again shows that the indicator molecules are distributed in the interfacial region of the micellar surface upto a certain distance.

(Page No. 45-48)

Section 3.3.3 describes uv spectral study of protonation-deprotonation equilibrium of 1- and 2- Napthols. While spectral profile 1-Napthol in different media under investigation provides interesting result, the uv spectra of 2-Napthol is insensitive to solution pH. Therefore, attempt has not been made to study the acid-base equilibrium of 2-Napthol in micellar media by the present spectroscopic technique. From the results of foregoing investigation for 1-Napthol shows that the deprotonated form of indicator is stabilized in interfacial region of the micelle. The deprotonated form of 1-Napthol probably interacts with SDS and AOT headgroups and not efficiently partitioned in the micelles. However, 1-Napthol is probably partitioned more efficiently than all

other indicators under investigation, as is evident from high ΔpK_a^0 values. The interfacial polarity of CTAB micelle (D_{eff}) observed from the present study yield a value of ~ 45, indicating a distribution of indicator molecules surrounding the interfacial region.

(Page No. 48-49).

Chapter 4 deals with the study in photophysical properties of indicator organic molecules when they are in a variety of organic solvent of different dielectric constant, viz., different alkanols and 1,4-dioxane-water mixtures. An introduction and a brief review have been illustrated in section 4.1. Mainly, there are two types of solvent effects, one is the general solvent effect and the other is the specific solvent effect. All of these were discussed in this section.

(Page No. 71-79)

In section 4.2, the experimental procedure involved in the study was illustrated.

(Page No. 79)

In section 4.3, i.e., in the results and discussion section, all of the spectral shifts are tabulated. The high frequency polarizability, which is a function of refractive index of the solvent and low frequency polarizability, a function of dielectric constant of the medium are considered to probe the effect of solvent on solutes. The orientation polarizability or the polarity index function, which is a difference of the above two functions are also taken into account. Variation of Stokes' shift with Kosower-Z values, orientation polarizability etc. are studied and interpreted. It was also found that beside the general solvent-fluorophore interaction, there is also the specific solvent-fluorophore interaction, which arises due to hydrogen bonding.

(Page 79-83)

Chapter 5 of the thesis deals with the study on the role of 1- and 2-Napthol in promoting micellar shape transition under salt free condition. In section 5.1, an introduction and a brief review of the previous works have been presented. Physical gelation of surfactant micelles and their stimuli responsive behaviour are interesting from biology as well as chemical technology points of view. Unlike simple halides, sodium salicylate promotes sphere to worm like micellar transition at the cmc of CTAB. The flexible and elongated worm like micelles show complex and unusual rheological phenomena. Although it is generally believed that micellar entanglement and transient network formation are responsible for developing shear induced viscoelasticity, precise knowledge regarding the nature of interaction is still lacking. It is particularly interesting that while a wide variety of worm like micellar solution display identical rheological responses, a common element of all these systems is the presence of salt anions like salicylate. This limitation has perplexed the scenario to some extent an impeded the development of an acceptable theory for micellar shape transition. In the present work we have demonstrated for the first time that due to the presence of strong hydrophobic aromatic rings and polar hydroxy groups in their molecular architectures 1- and 2-Napthols can promote micellar shape transition in CTAB and CPB (Cetylpyridinium bromide) efficiently.

(Page No. 98-105)

In section 5.2, i.e., in the experimental section of this chapter, detail experimental procedure has been presented.

(Page No. 105-106)

Section 5.3 deals with the results and discussion of the present study. It is observed that at low concentration of CTAB-Napthol and CPB-Napthol systems, shear thinning property is displayed, which is common for a non-Newtonian fluid. On the other hand, at high concentration the system shows interesting rheological properties. Upto the applied shear of 30 rpm shear thinning is observed above which shear thickening takes lace. The effect of

temperature on the viscoelasticity of the present system is intriguing. Typically when a worm like micellar solution is heated the micellar contour length decays exponentially with temperature. At higher temperature surfactant unimers can hop more rapidly between the cylindrical body and the hemispherical end cap of the worm (the end cap is energetically unfavourable over the body by a factor equal to the end cap energy). Thus, because the end cap constraint is less severe at higher temperature the worms grow to a lesser extent. However, CTAB-Napthol and CPB-Napthol systems display an opposite trend. In this case hydrophobic interaction between the micellar core and the aromatic rings of the Napthol molecules are important. As the temperature is increased Napthol molecules are more and more soluble and partitioned more strongly in the micellar hydrocarbon core. This favours the formation of longer worm like micelle upto the critical temperature above which the increased kinetic energy allowing surfactant unimers to hop more frequently between the body and the end cap of the worm results in the breaking of the micelles. NMR and FTIR spectral study shows that Napthol molecules are embedded inside the surfactant micelles near the surface whereas OH groups are protruded above the surface of the micelles and screen the surfactant headgroup charges. Spectral study shows that the Napthol molecules which are embedded in different micelles bridge between the micelles via H-bonding resulting in the entanglement. The micro-structural diversity associated with intermolecular H-bonding in Napthols, which results in the diffused and broad energy states of the excited normal modes, no longer exists in gel. A comparatively more well-defined and specific H-bond is present in gel, which bridge worm like micelle together to form the network structure.

(Page No. 106-113)